

META-HEURISTIC APPROACHES FOR RESERVOIR
OPTIMISATION OPERATION AND INVESTIGATION OF
CLIMATE CHANGE IMPACT AT KLANG GATE DAM

VIVIEN LAI MEI YEN

DOCTOR OF PHILOSOPHY (ENGINEERING)

LEE KONG CHIAN
FACULTY OF ENGINEERING AND SCIENCE
UNIVERSITI TUNKU ABDUL RAHMAN
JULY 2023

**Meta-Heuristic Approaches for Reservoir Optimisation Operation and
Investigation of Climate Change Impact at Klang Gate Dam**

By

VIVIEN LAI MEI YEN

A thesis submitted to the Department of Civil Engineering,
Lee Kong Chian Faculty of Engineering and Science,
Universiti Tunku Abdul Rahman,
in partial fulfillment of the requirements for the degree of
Doctor of Philosophy (Engineering)
July 2023

ABSTRACT

META-HEURISTIC APPROACHES FOR RESERVOIR OPTIMISATION OPERATION AND INVESTIGATION OF CLIMATE CHANGE IMPACT AT KLANG GATE DAM

Vivien Lai Mei Yen

Due to the extraordinarily rapid growth in population and development, the demand for energy and water has increased to critical demanding levels, globally. Thus, the reservoir, the essential infrastructure for water storage during extreme events such as intense rainfall or drought periods, is indeed crucial to ensure availability of potable water. With the right reservoir functioning, society can achieve hydrological resilience, water sustainability, relief from and control of urban flooding, and sustainable energy. Over the years, dam operators, stakeholders, and scholars have shown their commitment to sustaining reservoir operations and doing their best to gain knowledge on how to manage reservoir operations, in order to maximise benefits while minimising the drawdowns in water supplies or overcoming poor performance. In 1998, a severe water crisis in the Klang Valley, Malaysia, due the El Niño phenomenon, had the water level at the Klang Gate Dam (KGD) dropped dramatically. This intricately added to the reservoir and dam issues in Malaysia, particularly the frequent intense rainfall within short periods of time, which made it difficult for the reservoir and dam operator to monitor and maintain the storage level of the reservoir and discharge water downstream to prevent overflow and flooding. Consequently, seeking

managing of reservoir optimisation operations had always been at the forefront and to improve managing, algorithms have had been presented over the past few decades, beginning with conventional algorithms, followed by heuristic algorithms, and finally, the meta-heuristic algorithms (MHAs). However, due to the drawbacks of the conventional algorithm as well as the heuristic algorithms handling complicated and multi-objective reservoir optimisation, the advantages of the strategy of simultaneous exploration and exploitation led to the decision to utilise meta-heuristic algorithms in this study. The original idea of this study was to investigate the climate impact onto the KGD current and future operations. By preserving the equilibrium between the proposed MHAs and reservoir risk analysis indices, the stakeholder can select or control the optimal KGD operation by referring to the summary of findings for the observed period assessments. The Whale Optimisation Algorithm (WOA), Harris Hawks Optimisation (HHO) Algorithm, Lévy Flight WOA (LFWOA) and the Opposition-Based Learning of HHO (OBL-HHO) were proposed to simulate the initial model's response and optimise the Klang Gate Dam (KGD) release operation with observed inflow, water level (storage), release, and evaporation rate (loss). There were two observed periods of timeline: (a) for year 2001-2019 and (b) for year 1987-2008 (compared with past studies). The results obtained from the proposed meta-heuristic algorithms of this study were then evaluated for reservoir risk analysis, for the observed period assessment and the climate assessment. In addition, extreme climate change occurrences have impacted the future reservoir operation, and this is something that previous KGD studies have yet to investigate. Thus, the continuing investigation of the optimisation of the future KGD operation

under various climatic scenarios by leveraging on the proposed MHAs, was conducted for the climate assessment for year 2020-2099. The comparison between the reservoir simulation (ANN) and reservoir simulation-optimisation (MHAs) were carried out in terms of examining the reservoir climate assessments, as well as the monthly storage capacity. In addition, a few scenarios of the future water demand were developed and estimated based on a close proximity of real condition: (i) Temperature Scenarios and (ii) Forecasted Population Growth. Scenario 1 was developed for the base period and the water demand was identical to the observed period assessment. Scenario 2: Maximum Temperature, Scenario 3: Mean Temperature and Scenario 4: Minimum Temperature; were developed for the water demand conditions. The results obtained for year 1987 - 2008 assessments showed the proposed MHAs as an optimistic conclusion for the dam operator to consider based on the trade-off between reliability and resilience or other reservoir risk indices. The proposed MHAs were next compared to past studies and it was shown that the GA binary had the lowest reliability and the Artificial Bee Colony (ABC) in the past studies, had the most vulnerability and sensitivity in data interpretation, especially with limited observed datasets. The LFWOA showed the highest level of periodic reliability, with 69.70%, while the HHO exhibited a slightly lower percentage of 63.26%. The ABC and PSO algorithms exhibited lower periodic reliability percentages of 61.36% and 59.47%, respectively. The OBL-HHO and WOA algorithms showed periodic reliability with percentages of 56.44% and 56.06%, correspondingly. The GA-RC algorithm showed a periodic reliability percentage of 55.65%, whereas the GA algorithm exhibited the lowest periodic reliability percentage of 23.5%.

For the year 2001-2019 assessments, the algorithms varied in the ranking of reservoir risk assessments for all the three inflow magnitude types (low, medium and high). For the high inflow category, the LFWOA exhibited the highest periodic reliability in terms of meeting exact demand with a value of 15.35% whilst the WOA had achieved a reliability of 14.47%. At the same time, the HHO and OBL-HHO algorithms resulted in lower levels of periodic reliability, with values of 13.16% and 9.21% respectively. The HHO model was still inspired to be the model to perform the reservoir optimisation operation even though it had obtained the highest sequence for the vulnerability in the high inflow category. Within the medium inflow category in terms of meeting precise demand, the LFWOA exhibited the highest level of periodic reliability with a percentage of 42.54%. This was closely followed by the WOA with 39.91%, the HHO with 38.60%, and then, the OBL-HHO with 20.54%. The resilience metric associated with the medium inflow category exhibited performances that align with the periodic reliability in a similar sequence. Regarding the medium inflow category for the vulnerability metric, it has been observed that the algorithms of OBL-HHO, HHO, WOA, and LFWOA exhibited significant robustness. For the 2020-2099 climate assessments, the sequence of the respective algorithms in terms of individual reservoir risk analysis assessment in accordance with RCP 2.6 of Scenario 2, Scenario 3, and the forecasted population growth of future water demand showed that the WOA was extremely vulnerable and sensitive. The monthly storage capacity fails in 2077, substantially earlier than the other three algorithms in Scenario 2. The LFWOA was used in this study to improve the efficacy of the algorithms by delivering a more accurate monthly storage

capacity and reservoir risk assessment for Scenario 2 of RCP 2.6. In Scenario 4, the lowest ranking of vulnerability showed that the LFWOA was the most vulnerable and sensitive whereby the month storage capacity failed in 2077, but it was able to recover, as LFWOA gained the second-highest resilience index ranking. In RCP 4.5, Scenarios 3, Scenario 4, and forecasted population growth had no monthly storage failures. However, the LFWOA had the lowest vulnerability sequence for Scenario 2, which occurred in 2062 and after. On the other hand, the monthly storage failure occurred too rapidly in the near future for Scenario 3, Scenario 4, and future population growth since RCP 8.5 is called "High emissions". To retain the balance of trade-offs at the KGD operation, the best reservoir operation decision must be aware of the storage failure event when an extreme event occurs. From the above-mentioned, the major findings of this study were on the investigations of the climate assessments during KGD operations under the scope of the different climate change scenarios, using an ensemble of GCMs with the purpose of equally distributing the uncertainty accuracy of the downscaled as compared to previous studies which were then using the single GCM approach. Few recommendations of future work direction such as by hybridisation or utilising other algorithms (with a similar strategy of exploitation and exploration) to further examine the critical events obtained in this study, were suggested further improvements. Aside from that, it is also recommended that with the implementing of the most recent GCMs (ensemble) of CMIP 6 to analyse and compare with the current studies conducted at KGD using ensembles GCMs of CMIP 5, should pave the way for more intense forward research.

ACKNOWLEDGEMENTS

My sincere heartfelt appreciations to Ir. Dr. Huang Yuk Feng, my main supervisor, who has always imbued within me, competent advice, patience, and support throughout the many stages and trials and tribulations of my research. Many thanks to Ir. Dr. Koo Chai Hoon, my co-supervisor; her input and insightful criticism encouraged me to embark on the kind of efforts I have intended to make in this research, with originality as the prime motivating factor. My sincere gratitude goes out to Dr. Al Mahfoodh Ali Najah Ahmed, my co-supervisor who has continuously encouraged me to focus on publications with high impact factors and has offered his invaluable assistance and support whenever I have needed it. I would like to thank all my supervisors for helping me complete this PhD research in a challenging and enjoyable manner.

My heartfelt thanks go to my parents, sister, and friends, who have always in one way or another, provided me with blessings and support, whether directly or indirectly, during my research journeys.

In closing, I am thankful to Universiti Tunku Abdul Rahman, Malaysia, for sponsoring my PhD study with the project grant of IPSR/RMC/UTARRF/2020-C1/H01. The contributing data relating to this study area at Klang Gate Dam were provided by the Malaysian Meteorological Department (Malaysia), Lembaga Urus Air Selangor (LUAS), Department of Irrigation and Drainage (DID), and Puncak Niaga (M) Sdn Bhd.

LEE KONG CHIAN FACULTY OF ENGINEERING AND SCIENCE

UNIVERSITI TUNKU ABDUL RAHMAN

Date: 12/9/2023

SUBMISSION OF THESIS

It is hereby certified that VIVIEN LAI MEI YEN (ID No: 20UED05661) has completed this thesis entitled “Meta-Heuristic Approaches for Reservoir Optimisation Operation and Investigation of Climate Change Impact at Klang Gate Dam” under the supervision of Ir. Prof. Dr. Huang Yuk Feng from the Department of Civil Engineering, Lee Kong Chian Faculty of Science and Engineering, and Ir. Dr. Koo Chai Hoo Department of Civil Engineering, Lee Kong Chian Faculty of Science and Engineering.

I understand that University will upload softcopy of my thesis in pdf format into UTAR Institutional Repository, which may be made accessible to UTAR community and public.

Yours truly,



(Vivien Lai Mei Yen)

APPROVAL SHEET

This dissertation/thesis entitled “**META-HEURISTIC APPROACHES FOR RESERVOIR OPTIMISATION OPERATION AND INVESTIGATION OF CLIMATE CHANGE IMPACT AT KLANG GATE DAM**” was prepared by VIVIEN LAI MEI YEN and submitted as partial fulfillment of the requirements for the degree of Doctor of Philosophy (Engineering) at Universiti Tunku Abdul Rahman.

Approved by:



(Ir. Prof. Dr. Huang Yuk Feng)

Date:.....07/07/2023.....

Professor/Supervisor

Department of Civil Engineering

Lee Kong Chian Faculty of Engineering and Science

Universiti Tunku Abdul Rahman



(Ir. Dr. Koo Chai Hoon)

Date:.....07/07/2023.....

Associate Professor/Co-supervisor

Department of Civil Engineering

Lee Kong Chian Faculty of Engineering and Science

Universiti Tunku Abdul Rahman



Dr. Al Mahfoodh Ali Najah Ahmed
Senior Lecturer
Dept. of Civil Engineering
College of Engineering
Universiti Tenaga Nasional

(Dr. Al Mahfoodh Ali Najah Ahmed)

Date:.....07/07/2023.....

Senior Lecturer/Co-supervisor (External)

Department of Civil Engineering

College of Engineering

Universiti Tenaga Nasional

DECLARATION

I hereby declare that the dissertation is based on my original work except for quotations and citations which have been duly acknowledged. I also declare that it has not been previously or concurrently submitted for any other degree at UTAR or other institutions.

Name ___ VIVIEN LAI MEI YEN ___

Date ___ 05/07/2023 _____

TABLE OF CONTENTS

	Page
ABSTRACT	i
ACKNOWLEDGEMENTS	vi
SUBMISSION OF THESIS	vii
APPROVAL SHEET	viii
DECLARATION	ix
TABLE OF CONTENT	x
LIST OF TABLES	xiv
LIST OF FIGURES	xvii
LIST OF ABBREVIATIONS	xxi
CHAPTER	
1.0 INTRODUCTION	1
1.1 Background	1
1.2 Problem Statement	4
1.3 Research Gap	6
1.4 Objectives	8
1.5 Scope of Study	9
1.6 Contributions of the Study	10
1.7 Outline of the Thesis	11
2.0 LITERATURE REVIEW	13
2.1 Introduction	13
2.2 Reservoir Optimisation Techniques	13
2.2.1 Conventional Optimisation Techniques	14
2.2.2 Linear Programming	15
2.2.3 Non-Linear Programming	16
2.2.4 Stochastic Dynamic Programming	17
2.2.5 Heuristic Algorithms	18
2.2.6 Meta-Heuristic Algorithms (MHAs)	22

2.2.7	Hybridisation Technique	32
2.2.8	Summary	38
2.3	Climate Change Impact on Reservoir Optimisation	39
2.4	Downscaling of GCMs	53
2.4.1	Statistical Downscaling Method	54
2.4.2	Dynamical Downscaling Method	59
2.4.3	Summary of Downscaling Approaches	61
2.5	Hydrological Process Involved in a Reservoir	63
2.5.1	Rainfall-Runoff Relationship	63
2.5.2	Evaporation in Reservoir and its Approaches	65
2.6	Future Water Demand Estimation	70
2.7	Review on Reservoir Assessment Metrics	73
2.8	Summary	73
3.0	METHODOLOGY	76
3.1	Introduction	76
3.2	Flow of Methodology	77
3.3	Study Area	82
3.4	Datasets	85
3.4.1	Datasets from Year 2001 to 2019	85
3.4.2	Datasets from Year 1987 to 2008	88
3.4.3	Datasets for Future Climatic Investigation	90
3.4.4	Selection of GCMs in CMIP5	97
3.4.5	Missing Data in Future Projected Climatic Scenario	99
3.5	Data Preparation Stages for Climate Assessment	100
3.5.1	Computation of Rainfall-Runoff Relationship	101
3.5.2	Estimation Method for Evaporation	103
3.5.3	Estimation of Future Water Demand	105
3.5.4	Statistical Model Performance Evaluations	114
3.6	Metaheuristic Algorithms (MHAs)	116
3.6.1	Whale Optimisation Algorithm (WOA)	116
3.6.2	Lévy Flight WOA (LFWOA)	120
3.6.3	Harris Hawks Optimisation Algorithm (HHO)	122
3.6.4	Opposition-Based Learning HHO (OBL-HHO)	128

3.6.5	Evaluation of Exploration and Exploitation Capabilities in Benchmark Functions Testing	129
3.6.6	Parameters Setting for the Respective Proposed MHAs	132
3.6.7	Design of Experiment (DoE)	136
3.7	Problem Formulation	139
3.7.1	Objective Function	140
3.7.2	Handling of the Thresholds or Constraints	141
3.7.3	Penalty Functions	142
3.8	Reservoir Risk Assessments	144
3.8.1	Reliability	144
3.8.2	Resilience	144
3.8.3	Vulnerability	145
3.8.4	Maximum Deficit	145
3.9	Summary	146
4.0	RESULTS AND DISCUSSION	148
4.1	Introduction	148
4.2	Execution of <i>EvoPy</i> Benchmark Test Functions	149
4.2.1	Statistical Model Performances	149
4.2.2	Ranking Assessment	153
4.3	Execution of Observed Period Assessments for Year 2001- 2019	155
4.3.1	Statistical Model Performances Evaluations	155
4.3.2	Monthly Release Curves Correspond with Inflow Categories by Utilising WOA versus LFWOA	178
4.3.3	Reservoir Risk Assessment for WOA and LFWOA	186
4.3.4	Monthly Release Curves Correspond with Inflow Categories by Utilising HHO versus OBL-HHO	189
4.3.5	Reservoir Risk Assessment for HHO and OBL-HHO	196
4.4	Execution and Validation of Reservoir Risk Assessment for year 1987 - 2008	199
4.5	Statistical Model Performances for Investigation of Future Climate Change Impact under Climatic Scenarios	203
4.5.1	For the Predictants	203
4.5.2	For the Estimation of Water Demand	209

4.5.3	For the Estimation of Evaporation	210
4.6	Climate Change Impact on Future Water Demand Based on Temperature Factor	212
4.6.1	Scenario 1: Base Period	213
4.6.2	Scenario 2: Maximum Temperature	215
4.6.3	Scenario 3: Mean Temperature	222
4.6.4	Scenario 4: Minimum Temperature	229
4.6.5	Reservoir Risk Assessment for all Scenarios	237
4.7	Execution of Future Climate Change Impact Based on Forecasted Population Growth	248
4.7.1	Monthly Release Operation under various RCPs	248
4.7.2	Monthly Reservoir Storage Capacity under various RCPs	253
4.7.3	Reservoir Risk Assessment	255
4.8	Summary	258
4.8.1	Relationship between Reservoir Risk Assessment and MHAs for Observed Period Assessments	258
4.8.2	Relationship between Reservoir Risk Climate Assessments and Monthly Storage Capacity via MHAs under various RCPs Based on Temperature and Forecasted Population Growth Factors	262
5.0	CONCLUSIONS AND RECOMMENDATIONS	267
5.1	Conclusions	267
5.2	Limitations and Recommendations	272
	REFERENCES	275
	LIST OF PUBLICATION	307

LIST OF TABLES

Table		Page
2.1	Studies under variety of categories based under MHAs	28
2.2	Benefits and Drawbacks of the algorithms	31
2.3	Similarities between RCP projections and SRES	47
2.4	Summary of the case studies on climate change impacts	48
2.5	Summaries of the downscaling approaches	61
3.1	KGD features	84
3.2	Monthly Descriptive Statistics in MCM unit	86
3.3	Inflow Categories	86
3.4	KGD Storage Conditions (MCM)	87
3.5	Range of the Lt (MCM)	87
3.6	Monthly targeted Demand at KGD	88
3.7	Monthly Descriptive Statistic of Rainfall Data	89
3.8	Monthly average hydrological variables for the base period (1991–2005) under CMIP 5	92
3.9	Monthly average hydrological variables for climatic scenarios (2020 to 2099) under CMIP5	93
3.10	CMIP5 GCMs (IPCC-AR5) for Predictant Variables	95
3.11	Resolution for the selected GCMs	98
3.12	Conceivable combinations of predictant-predictor variables under CMIP5	99
3.13	Summaries of three estimation procedure for rural catchment recognised by DID, Malaysia	102

3.14	Population Growth at Kuala Lumpur from year 1988 to 2019	108
3.15	LULCC Detection Maps during 1899 vs 2010 and 2010 vs 2021	110
3.16	Characteristic of <i>EvoPy</i> Test Functions	131
3.17	Parameter Setting for proposed MHAs	135
3.18	Response Table	138
3.19	ANOVA analysis	139
4.1	Statistical results for benchmark testing for year 2001 to 2019	151
4.2	Friedman ranks	154
4.3	Summary of Statistical Performance Evaluations	177
4.4	Periodic Reliability performance via WOA and LFWOA	187
4.5	Reservoir Risk Assessment	188
4.6	Periodic Reliability performance via HHO and OBL-HHO	197
4.7	Reservoir Risk Assessment	198
4.8	Comparison of the Periodic Reliability performance	200
4.9	Comparison of the Reservoir Risk Assessments	203
4.10	Summary of the Base Period Statistical Performance for the Predictants - Predictors	205
4.11	Summary of the Climatic Scenarios for the Statistical Performance for year 2020 - 2099 (Poly Kernel Functions)	206
4.12	Average Proportion (%) of Predictants Corresponded to RCPs and Base Period	207

4.13	Statistical model performance for predicted of future water demand based on temperature factor under climate change scenarios	209
4.14	(a) Performance of statistical models for empirical methods	211
4.14	(b) Performance of statistical models for prediction-based method	211
4.15	Comparison between simulation vs simulation-optimisation for reservoir risk analysis evaluation in base period	214
4.16	Periodic Reliability by utilising WOA	239
4.17	Periodic Reliability by utilising LFWOA	240
4.18	Periodic Reliability by utilising HHO	241
4.19	Periodic Reliability by utilising OBL-HHO	242
4.20	WOA vs LFWOA comparison of the reservoir risk assessments under various RCPs based on temperature water demand	245
4.21	HHO vs OBL-HHO comparison of the reservoir risk assessments under various RCPs based on temperature water demand	246
4.22	Extensive assessment in terms average water storage resilience (<i>WSRavg</i>) indicator under various RCPs reservoir optimisation based on temperature water demand	247
4.23	Comparison of Periodic Reliability under several RCPs	256
4.24	Comparison of the Reservoir Risk Assessments under various RCPs	257
4.25	Comparison of the Reservoir Risk Analysis Assessment for Observed Period for year 2001-2019 and for year 1987-2008	261
4.26	Comparison of Reservoir Risk Assessments under various RCPs Based on Temperature and Forecasted Population Growth	266

LIST OF FIGURES

Figures		Page
2.1	Simple flow charts of GA	20
2.2	WOA model structure - Spiral bubble (Ghamrawy and Hassanien, 2020)	36
2.3	HHO model structure (Heidari et al., 2019a)	36
2.4	Summary of Optimisation Techniques Reviewed	37
2.5	ANN structure	58
2.6	SVR structure	59
3.1	(a) Overall flow of the study	80
3.1	(b) Reservoir Optimisation Procedure and Conceptual flow of the proposed algorithms	81
3.2	Case Study Area	83
3.3	Illustration of the KGD's reservoir (Lai et al., 2021)	84
3.4	LULCC Detection Map from year 1988 to 2021	111
3.5	LULCC Detection Map at downstream of KGD During 1988 to 2010	112
3.6	LULCC Detection Map at downstream of KGD During 2010 to 2021	113
3.7	Flow Chart of the WOA	119
3.8	Denotes the conceptual idea of the Lévy flights (Houssein et al., 2020)	120
3.9	Flow chart of the LFWOA	122
3.10	Flow chart of the HHO	127
3.11	OBL-HHO	129

3.12	Response Graph of the (a) WOA and (b) LFWOA	133
3.12	Response Graph of the (c) HHO and (d) OBL-HHO	134
3.13	Main effect plot for Taguchi Method	137
4.1	(a) Monthly RMSE (MCM) for different inflow categories in WOA	156
4.1	(b) Monthly PBIAS (MCM) for different inflow categories in WOA	157
4.1	(c) Monthly MAE (MCM) for different inflow categories in WOA	158
4.2	R ² evaluation (a) in High Inflow, (b) in Medium Inflow; (c) in Low Inflow for WOA algorithm from 2001 to 2019	159
4.3	(a) Monthly RMSE (MCM) for different inflow categories in LFWOA	161
4.3	(b) Monthly PBIAS (MCM) for different inflow categories in LFWOA	162
4.3	(c) Monthly MAE (MCM) for different inflow categories in LFWOA	163
4.4	R ² evaluation (a) in High Inflow, (b) in Medium Inflow, (c) in Low Inflow for LFWOA algorithm	164
4.5	(a) Monthly RMSE (MCM) for different inflow categories in HHO	166
4.5	(b) Monthly PBIAS (MCM) for different inflow categories in HHO	167
4.5	(c) Monthly MAE (MCM) for different inflow categories in HHO	168
4.6	R ² evaluation in (a) High Inflow, (b) in Medium Inflow, (c) in Low Inflow for HHO algorithm	169

4.7	(a) Monthly RMSE (MCM) for different inflow categories in OBL-HHO	171
4.7	(b) Monthly PBIAS (MCM) for different inflow categories in OBL-HHO	172
4.7	(c) Monthly MAE (MCM) for different inflow categories in OBL-HHO	173
4.8	R ² evaluation in (a) High Inflow, (b) in Medium Inflow, (c) in Low Inflow for OBL-HHO algorithm from 2001 to 2019	174
4.9	(a) January release curve - (l) December release curve by utilising WOA and LFWOA	180
4.10	(a) January release curve - (l) December release curve by utilising HHO and OBL-HHO	190
4.11	Monthly mean inflow (MCM) corresponded to RCPs and Base Period	208
4.12	Inflow variation corresponded to RCPs and Mean Base Period (MCM)	208
4.13	Comparison of base period releases (1991-2005)	213
4.14	WOA vs LFWOA for the comparison of simulation vs simulation-optimisation of optimal reservoir releases in Scenario 2 (a) RCP 2.6, (b) RCP 4.5 and (c) RCP 8.5	216
4.15	HHO vs OBL-HHO for the comparison of simulation vs simulation-optimisation of optimal reservoir releases in Scenario 2 (a) RCP 2.6, (b) RCP 4.5 and (c) RCP 8.5	218
4.16	Monthly storage capacity (MCM) for Scenario 2 (a) – (c)	221
4.17	WOA vs LFWOA and for the comparison of simulation vs simulation-optimisation of optimal reservoir releases in Scenario 3 (a) RCP 2.6, (b) RCP 4.5 and (c) RCP 8.5	223

4.18	HHO vs OBL-HHO for the comparison of simulation vs simulation-optimisation of optimal reservoir releases in Scenario 3 (a) RCP 2.6, (b) RCP 4.5 and (c) RCP 8.5	225
4.19	Average monthly storage capacity (MCM) for Scenario 3 (a) RCP 2.6, (b) RCP 4.5 and (c) RCP 8.5	227
4.20	WOA vs LFWOA for the comparison of simulation vs simulation-optimisation of optimal reservoir releases in Scenario 4 (a) RCP 2.6, (b) RCP 4.5 and (c) RCP 8.5	231
4.21	HHO vs OBL-HHO for the comparison of simulation vs simulation-optimisation of optimal reservoir releases in Scenario 4 (a) RCP 2.6, (b) RCP 4.5 and (c) RCP 8.5	233
4.22	Average monthly storage capacity (MCM) for Scenario 4 (a) – (c)	236
4.23	WOA vs LFWOA for the comparison of simulation vs simulation-optimisation of optimal reservoir releases in forecasted population growth factor (a) RCP 2.6, (b) RCP 4.5 and (c) RCP 8.5	249
4.24	HHO vs OBL-HHO for the comparison of simulation vs simulation-optimisation of optimal reservoir releases in forecasted population growth factor (a) RCP 2.6, (b) RCP 4.5 and (c) RCP 8.5	251
4.25	Average monthly storage capacity (MCM) for forecasted population growth of water demand (a) – (c)	253

LIST OF ABBREVIATIONS

ABC	Artificial Bee Colony
ACO	Ant Colony Optimisation
AI	Artificial Intelligence
ANN	Artificial Neural Network
CCLP	Chance-constrained linear programming
CS	Cuckoo Search
CMIP5	Coupled Model Intercomparison Project 5
DCSA	Developed Crow Search Algorithm
DE	Differential Evolution
DID	Department of Irrigation and Drainage
DP	Dynamic Programming
ESGF	Earth System Grid Federation
ESO	Explicit Stochastic Optimisation
GA	Genetic Algorithm
GCMs	Global Climatic Models
GWO	Grey Wolf Optimisation
HHO	Harris Hawks Optimisation
ISO	Implicit Stochastic Optimisation
KGD	Klang Gate Dam
LFWOA	Lévy Flight Distribution Whale Optimisation Algorithm
LP	Linear Programming
LSA	Lion Swarm Algorithm
LUAS	Lembaga Urus Air Selangor

MFO	Month-flame optimisation
NLP	Non-linear programming
NSGA-II	Non-dominant sorting GA II
OBL-HHO	Opposition-Based Learning Harris Hawks Optimisation
OF	Objective Function
PF	Penalty Functions
PKF	Polynomial Kernel Functions
PSO	Particle Swarm Optimisation
RBF	Radial Basic Function
RCP	Representative Concentration Pathways
SA	Shark Algorithm
SDP	Stochastic Dynamic Programming
SLP	Stochastic Linear Programming
SVM	Support Vector Machine
SVR	Support Vector Regression
SI	Swarm Intelligence
TS	Tabu Search
MHAs	Meta-heuristics Algorithms
WOA	Whale Optimisation Algorithm
WCA	Water Cycle Algorithm
R_p	Reliability
Vul	Vulnerability
R_s	Resilience
$WSR_{avg}(t)$	Water storage resilience
$Max\ Deficit_{annual}$	Annual Maximum Deficit

CHAPTER 1

INTRODUCTION

1.1 Background

The global demand for energy and water has reached critical and demanding levels due to the incredibly fast increase in population and development (Wang et al., 2009; Yan et al., 2017; Feng et al., 2019). The reservoir is widely considered one of the key infrastructure strategies for increased water quality sources (Yang et al., 2016; Zhang et al., 2017; Niu et al., 2018a; Feng et al., 2020a). The reservoir is also the important infrastructure for storing, stocking, and supplying fresh surface water for many purposes. Effective reservoir maintenance will inevitably provide society with hydrological resilience, water sustainability, urban flood control and the generation of safe, sustainable electricity. Over the past century, dam owners, decision makers and scientists have made a great deal of effort to understand the operations of the reservoir better and build optimal reservoir operating techniques (Yang et al., 2017).

Many countries have taken much aggressive measures in recent years to mitigate the harmful impacts of reservoirs and protect the health of the river habitats. In order to achieve all forms of reservoir functions and prevent danger to humans and the river ecosystems, science-based estimates, simulations and

forecasts on reservoir storage or release and designing proper plans of reservoir service are necessary (Loucks and Sigvaldason, 1982). Similar attention has been granted to several hydro power ventures (Hui et al., 2016; Pang et al., 2018; Xu et al., 2020). For example, the Three Gorges is the world's biggest water supply inter-base network (Liu et al., 2015; Zhao et al., 2015; Wang et al., 2018a) and China's most esteemed water reservoir supported by huge turbine reservoirs (Chen et al., 2013; Ming et al., 2017; Feng et al., 2020b). But the reservoir operations and maximum storage capacities are challenging for policy makers, as they require numerous decision criteria and physical constraints, such as top and bottom reservoir storage limits, discharged turbine limits and upstream water levels, etc. Therefore, the main priority is the optimum function of the water supply and release from the dam. More focus and consideration are also given to this topic by several academics and engineers (Bai et al., 2017; Xie et al., 2018).

Of utmost importance, climate change has led to inevitable drastic hydrological globalisation changes: - processes such as ice melting, rising sea levels and deterioration of living environments are immediate examples (Sun et al., 2013). The phenomenon of climate change was an added dimension challenge to the reservoir and dam problems in Malaysia. The intense rainfall conditions and severity pose obstacles to the workings of the reservoir and dam while managing storage of the reservoir and discharge water downstream to deter floods and runoff is in progress. These phenomena have influenced the trend towards water supply and it is important to reduce these problems for

decision-makers. Temperature and precipitation mainly exhibit the effect related to climate change on water sources (Zaman et al., 2018).

Therefore, a suitable optimisation method for managing the reservoir is essential for guiding and advising decision-makers, on the effectiveness of present and future climatic scenarios. Scientists from all over the world have successfully founded and developed numerous experiments, including conventional approaches, dynamic programming, network-based methods and swarm intelligence approaches, in attempts to solve this optimisation problem. Traditional mathematical models such as non-linear programming struggle to adjust to multi-objective concerns and to run the optimisation process in a suitable time frame. There is a need for additional research due to the fact that these traditional approaches have limitations in solving real-world functional engineering challenges (Feng et al., 2018a; Liu and Luo, 2019;). In addition, the optimisation process has never before being influenced by the factors like climate change conditions (climate variables) or uncertain reservoir inflows (Wan et al. 2017).

Optimisation algorithms capable of gathering and analysing massive data under various climate change conditions has also useful for managing reservoirs as efficient methods of preparing and tracking water supplies. Problems with planned reservoirs have several boundary conditions caused by climate change conditions (Afshar, et al., 2011). In addition, to adequately supply downstream water needs, the releases from the dams must be controlled in order to minimise the over-supply and waste that can contribute to floods. On

this note, the first and second objectives of this study are to simulate initial model's response, and optimise the Klang Gate Dam (KGD) release operation, by utilising metaheuristic algorithms with observed datasets of inflow, water level (storage), release, and evaporation rate (loss). The results obtained are then evaluated in the reservoir risk performance analysis, which forms the third objective of this study.

1.2 Problem Statement

In many regions of the globe, socioeconomic growth were impacted by water resource management, which was a key of hydrological field topic. For those concerned with dam or reservoir management, particularly stakeholders, have seen the worldwide water shortage or deficit as a key concern (Haddad et al., 2008; Haddad et al., 2011). Recently, there have been many discussions about and technological advancements made in relation to the problem of water consumption viz a viz, to river regulations and operations. One of the most innovative approaches to address water scarcity is optimising the operations of the reservoir or dam. In addition, the fundamental and primary function of the Klang Gate Dam, (KGD, the chosen study area of this research) was to meet the most urgent potable water needs and also to serve as the safety reason for the downstream communities to alleviate flooding by saving up the water during the rainy season.

Climate change undoubtedly, will alter the rhythm of the water cycle and the hydrological variables of precipitation and temperature, and subsequently,

will thus affect the reservoir's performance. In 1998, a severe water crisis in Klang Valley had led to the water level at the KGD to drop dramatically due to the El Niño phenomenon (Latif et al., 2020; Latif et al., 2021). The major issue is that the operation of the reservoir depends on the time of the inflow, which is dependent on precipitation, making it one of the most susceptible hydrological variables in the era of climate change.

The effect of concern is on the inflow to the reservoir in order for it to function properly and to meet the downstream KGD's water supply needs. Several heuristic algorithms, namely the Particle Swarm Optimisation (PSO), Genetic Algorithm (GA), and Artificial Bee Colony (ABC), were implemented at the KGD to develop the optimal operation rules (Hossain and El-Shafie, 2014a). However, this investigation was generally retrieved from observed inflows to reservoirs using optimised algorithms and was rarely interpreted using anticipated hydrological variables such as projected rainfall and temperature in the context of including climate change scenarios. Aside from this, these algorithms were troubled with the following disadvantages: such as their rapid collapse through the local optimum in high-dimensional space and; their poor or premature convergence rate during the iterative process due to the nature of the algorithms.

While considering research gaps and objectives, there is very little comprehensive information available on the impacts of the reservoir at the KGD. By adding the predicted hydrological variables to the proposed models in this analysis, it is possible to investigate future inflows resulting from future

reservoir operations to achieve optimal operating conditions. Incidentally, determining whether the current reservoir operation rules are capable of addressing the future period with optimal operating conditions is all the more important for efficient management strategies. The reservoir should be operated optimally to obtain an acceptable level of release and storage volume, taking into consideration prospective inflows and the requirement to resolve climate change scenarios in order to solve this issue. Thus in this study, the meta-heuristic algorithms, namely Whale Optimisation Algorithm (WOA), Harris Hawks Optimisation (HHO) algorithm, and their respective enhancement methods are proposed for simulation and optimisation of the KGD reservoir operation.

1.3 Research Gap

In previous studies, three distinct optimisation techniques namely the particle swarm optimisation (PSO), the genetic algorithm (GA), and the artificial bee colony (ABC) were deployed to handle the reservoir release optimisation problems located at the study area of this study. Several studies that mentioned in problem statement showed the disadvantages of these algorithms, such as their rapid collapse through the local optimum in high-dimensional space and their poor or premature convergence rate during the iterative process due to the nature of the algorithms. As a result, meta-heuristic algorithms that are proposed to overcome the drawbacks of existing methods ought to be sought out for development, by applying the strategy of exploitation and exploration simultaneously.

In Malaysia, dams are also vulnerable to environmental challenges such as the ubiquitous climate change calamities. According to the Department of Irrigation and Drainage (DID), wet, hot or dry weather causes severe water crises, and as a result, practically all significant dams across the country are either drying up or swollen from intense runoff at particular times of the year. For instance, the standard height of Klang Gate Dam had decreased from 94 metres to 90.26 metres, considering the sedimentation over the years. This action will likely affect the water supply-demand balance and violate the dam's traditional designed operational guidelines. Despite very limited systematic research has been conducted in Malaysia, dam operations under various climate change scenarios are now mandatorily having been examined to optimise release and mitigate any risks.

In addition, the earlier problem statement emphasised the importance of investigating the influence of climate change on reservoir operations for effective water resource management. In Malaysia, however, there is a limitation of organised data regarding the impact of climate change scenarios on optimal future reservoir operations, simply due the fact that no study has ever being made in this direction as yet. Infrequently too, are projected hydrological variables being used to interpret the standard investigation, which is often derived from observed reservoir inflows using optimised methods.

The hydrological factors that affect the volume of water held in a reservoir are precipitation, temperature, and evaporation. However, anticipated precipitation is the most important hydrological variable when taking

cognizance of the climate change vagaries. Therefore, it would be more useful and reliable to assess the reservoir optimisation operating rules using more useful hydrological variables, such as anticipated rainfall, as these are more practical and closely related to the real approximation of the future reservoir operations as determined by research carried out under various climate change scenarios provided by the UN IPCC (Bates et al., 2008). The objectives of this study is to simulate the initial model's response by analysing the current KGD's operation and providing the optimal release policy in order to address the future reservoir performance with the proposed meta-heuristic algorithms (MHAs):- (i) Whale Optimisation Algorithm, WOA; (ii) Lévy flight WOA, LFWOA; (iii) Harris Hawks Optimisation Algorithm, HHO; (iv) Opposition-Based Learning HHO, OBL-HHO.

1.4 Objectives

- i. To simulate the initial model's response using the observed inflow, water level(storage), release, and evaporation rate located at Klang Gate Dam through implementing the Meta-heuristic Algorithms (MHAs) such as Whale Optimisation Algorithm (WOA), Lévy Flight WOA (LFWOA), Harris Hawks Optimisation (HHO) Algorithm, and Opposition-Based Learning HHO (OBL-HHO) by generating the current reservoir release operation
- ii. To optimise the simulation results reservoir release operation with the WOA, LFWOA, HHO, and OBL-HHO in respect of

observed inflow, water level(storage), release, and evaporation rate at the KGD.

- iii. To evaluate the model performance of the WOA, LFWOA, HHO and OBL-HHO in terms of the metrics for reliability, vulnerability, and resiliency.
- iv. To investigate the impact of the climate change at the KGD under the scope of the different climate change scenarios using an ensemble of GCMs considering the CMIP5 scenario.

1.5 Scope of Study

The most critical problem faced by decision-makers in reservoir management is the water release operations to downstream that would be influenced by climate change and also the constraint of the hydrological elements. Therefore, defining an appropriate optimisation algorithm by considering the influential variables is essential to provide effective operation guidance and information to decision-makers for comprehensive planning in current and future times. Furthermore, due to the nature of the algorithms, the problem related to previous studies such as the PSO, ABC, and GA had resulted in the rapid collapse through the local optimum in high-dimensional space and their poor or premature convergence rate during the iterative process. Hence, with these problems arising, the motivation to conduct the current study has proposed the optimisation algorithms by considering climatic and hydrological variables and the constraint of the reservoir. In order to verify and validate the optimal reservoir water release algorithm, the proposed approaches have

compared with other previous algorithms carried out at the KGD. The outcome of the current study has examined and evaluated the optimal optimisation algorithm for the reservoir release operation to ease the complexity of the multi-purpose reservoir and maximise its operations and also minimise the wastage of water release to downstream. Additionally, by anticipating various climate change scenarios, to take into account how future climate change may impact future reservoir release operations. Few future water demand scenarios have been suggested to a near approximation of realistic circumstances which is based on the temperature factors and forecasted population growth. The scope of this study does not extend to the sustainability and water quality downstream of the reservoir during or after reservoir release operations.

1.6 Contributions of the Study

The aim of this study was to prioritise which reservoir risk analysis index that would correspond best to the present climate event and which that should be implemented to achieve optimal KGD release operations, and as a result, to provide the dam operator or stakeholder with alternatives of the recommended MHAs. In addition, by implementing the proposed MHAs, it has expected that they are capable of closing the gap of this research and overcoming the problems mentioned in this study.

The novel aspects of this research are categorised into three subcategories. First, the outcome of this research has believed to be beneficial for other scholars, researchers or universities to consider and examine at other

dams around the world, particularly on the aspect of the impact under future emission scenarios in reservoir optimisation, as very little comprehensive knowledge on the impacts of climate change under different climate scenarios has been discussed, especially about the reservoir at the KGD. Next, it has been anticipated that the novelty of this study has a significant impact on policymakers, particularly dam operators under the Lembaga Urus Air Selangor (LUAS – Selangor Water Management Board) to maximise the operational benefits of the KGD simultaneously to reduce the water scarcity. Aside from that, the findings of this study can help alleviate the risk of flooding the downstream of the KGD, which has been always under the authority of the Department of Irrigation and Drainage (DID), Malaysia. Finally, the novelty of this study has also included the benefit of the socio-economic aspects by adopting the flow of this study to investigate the impact of climate change on future reservoir operation and management across many climate change dimensions using data mining and meta-heuristic approaches with the concern of the National Fourth Industrial Revolution (4IR) Policy to facilitate more sustainable development projects throughout Malaysia.

1.7 Outline of the Thesis

Chapter 1 provides a concise overview of the research issue. Begin with the background of the study, followed by the problem statement and then the elaboration on the research gap of this study. The research questions are addressed in accordance with the study's objectives.

Chapter 2 includes past reviews of the literature in relation to the limitations of the traditional algorithms and modern evolutionary algorithms integrated with various reservoir operations to obtain an optimisation strategy. The introduction of the recent meta-heuristic algorithms has the capability of overcoming the limitation of the previous studies. Followed by climate change investigations on the future operation of the reservoir under different climate scenarios. Prior research employing various global climatic models (GCMs) and the method for downscaling GCMs has been discussed. In addition, this chapter elaborates on prior knowledge regarding the computation of rainfall-runoff, estimation of evaporation, and future water demand.

The reservoir formulations, statistical uncertainty evaluation, and reservoir risk analysis in terms of metrics reliability, resilience, and vulnerability have described in Chapter 3. Additionally, this chapter includes the flow of methodology.

In Chapter 4, the observed period results for the years 2001-2019 and 1987-2008 have presented and discussed. In addition, this chapter discusses the future KGD's operations under climate change scenarios.

Chapter 5 concludes the investigation conducted throughout the study. In addition, some future recommendations and study limitations have been given.

CHAPTER 2

LITERATURE REVIEW

2.1 Introduction

Reservoir system operation and optimisation, is a critical area of study for both, water resource management and hydrology. To operate a reservoir system optimally, numerous researchers have developed various modelling processes that would more conveniently represent the operating system. These advancements include progressions in calibrating decision-making policies, optimisation processes, or both. This study is primarily concerned with intelligent optimisation processes and this chapter will discuss previous modelling approaches and optimisation techniques used in this field.

2.2 Reservoir Optimisation Techniques

In the next sub-sections, the sequence of reservoir optimisation techniques or models implemented in previous decades is described.

2.2.1 Conventional Optimisation Techniques

According to past studies, the performance of the existing reservoirs can be elevated by employing the models based on the mathematic concepts to mimic the pattern of the observed data and to optimise reservoir operations. The very first original and traditional dam design was based on Rippl's method, which was efficient on the small-scale reservoir capacity in order to ensure the release met the demand in the event of a worst-case drought (Rippl, 1883; Hazen, 1914; Loucks and Van Beek, 2017). It is hard to use this method on the reservoirs with multiple objectives and some other operations that are more complicated than an isolated operation (Lee et al., 1963). As reported by Dobson et al. (2019), adaptable strategies for addressing these disadvantages have been suggested and addressed (Vogel and Stedinger, 1987;1988; Douglas et al., 2002; Celeste, 2016). Conventional optimisation techniques have been recommended over Rippl's method in order to determine the optimal reservoir capacity that meets the objective functions under a diverse range of hydrological conditions. Using these design techniques, a simulation of the reservoir system versus an extensive period of the inflow time series data was conducted. There are two main categories for conventional stochastic optimisation (SO) techniques: which are the implicit (ISO) and the explicit (ESO) optimisation.

ISO implicitly accounts for forcing input variability by utilising a long and varied realisation, particularly one that is represented by a statistical model of the reservoir systems based on the time series of historical observations (Dobson et al., 2019). A deterministic optimisation approach is used by ISO,

also known as the Monte Carlo optimisation, to identify the best reservoir releases for a range of inflow ensembles (Celeste and Billib, 2009; Liu et al., 2014). However, the deterministic model is hinged on observed data and easily affected by extreme conditions.

Instead, during the optimisation process, the ESO incorporates the statistical model directly. Labadie (2004) showed that this method is more established for reservoir operation optimisation. The ESO is only useful for the most straightforward scenarios involving reservoir systems with a single input because it can typically characterise the full range of inflow uncertainty using probability distributions. To increase clarity and understanding, it is also vital to take into account the significance and size of these trade-offs at both the geographical and temporal dimensions (Derepasko et al., 2021). Thus, the invention of model efficiency in reservoir optimisation is advanced through the application of linear programming.

2.2.2 Linear Programming

In both the standard and modified forms, linear programming (LP) has been widely used in reservoir optimisation problems (Loucks, 1969; Houck et al., 1980). The stochastic approaches integrated with the LP in the modified category include stochastic linear programming (SLP) and chance-constrained linear programming (CCLP). In the SLP, inflows are thought to follow a single Markov chain. Several studies have been conducted to assess the efficacy of the SLP in reservoir systems. Loucks (1969) created a SLP to represent an unified

reservoir operating policy. Houck et al. (1980) proposed a linear decision rule for calibrating a release policy to maximise the hydropower reservoir's benefits. Furthermore, various recent studies have used the CCLP in various fields of study (Stuhlmacher and Mathieu, 2020a;2020b; Yuan et al., 2021). While developing the release policy in the CCLP, violations of constraints were kept within allowable limits. The constraints are created by taking into account the storage capacity or release limits. Feng et al. (2020a) presented an integration of the dynamic programming and the linear programming, to investigate power generation in a cascaded hydropower reservoir in China. Though the LP is very useful for developing operating rules, the accuracy of the results may not always meet the researchers' expectations because most reservoir problems are highly non-linear. As a result, the chronological order for the optimisation topic on the reservoir has moved forward to nonlinearity and stochastic dynamic programming.

2.2.3 Non-Linear Programming

The benefits terms (to achieve the objective function of the specific reservoir) and the operational cost as the non-linear formation are sometimes included in the objective functions. Non-linear programming (NLP) is commonly used in these situations because the water or hydrology studies are predominantly non-linear. As a result, there were some previous studies that involved the optimisation of the water distribution system (Samani and Taghi, 1996; Benli and Kodal, 2003). According to Lansey Mays (1989), the utilisation of the existing simulation model for the water distribution purpose was

hybridised with the non-linear programming techniques and this hybridisation can achieve and provide better optimal water allocation and management purposes compared to the stand-alone simulation model on water distribution. However, the results of this study's solution may not be an integer for the pumps and pipes. Another disadvantage perceived is that the model required a significant amount of computer time. Carini et al. (2018) proposed a non-linear least-cost optimisation model that was applied to a real-world case study in the province of Croton, Southern Italy. However, the studies showed the output by minimising the cost of total water transportation, which includes piping, distribution, and labour, rather than just the energy cost.

2.2.4 Stochastic Dynamic Programming

Numerous works utilised dynamic programming to improve water resource systems (Yakowitz, 1982; Chaves et al., 2004). Stochastic dynamic programming (SDP) is among the most widely utilised techniques for reservoir operations (Loucks et al., 1984). In order to achieve the maximisation of the economic value for the cascaded hydropower reservoir, the water volume and head must be taken into account in the objective function of the reservoir optimisation (Lund and Guzman, 1999). Wu et al. (2018) investigated multiple local optima cascaded hydropower reservoir operations. The authors proposed a two-stage solution algorithm to enhance the accuracy of the outcome with the integration of the traversing and search functions. Starting with the feasible region, finding one or more promising points near local optima via local search algorithm. However, the objective values and simulation results showed no

significant improvement. Due to the dimensionality and complexity of a multi-reservoir system, Zeng et al. (2019) proposed a rule-based improved DP (RIDP) and rule-based SDP. Stochastic programming was used to optimise the joint operation of multiple reservoirs in the Pi River Basin (China) during flood seasons (Xu et al., 2020). In a multi-reservoir system of the Pi River Basin, Lu et al. (2021) proposed a risk-based aggregation-decomposition method for to inspect the floodwater. As compared with the deterministic model, the results showed no significant difference in floodwater usage. All these studies mainly improved the basic DP application approaches in the reservoir optimisation problem.

2.2.5 Heuristic Algorithms

The existence of optimisation methods may be traced back to the days of Newton, Bernoulli, Lagrange, and others when the mathematical analysis was formed on the basis of calculus or variations (Rao, 2019). A real-world problem that needs to be solved must first be modelled mathematically. As a result, utilising this mathematical formula as a criterion seeks to identify the optimal answer in the shortest amount of time. The heuristic algorithm's drawback is that it does not guarantee the best outcome. The algorithm is considered effective depending on how rapidly it arrives at a decent result.

Genetic Algorithm (GA) is a subcategory of heuristic algorithms. It is inspired by the theory of evolution with features such as mutations, crossover, and selection, as presented in Figure 2.1. A further brief description of the GA

can be found in Holland (1992). Due to its ease of use and problem-independent applicability, the GA is one of those major EAs used in reservoir optimisation (Li et al., 2020; Tegegne and Kim, 2020). Wang et al. (2011) examined the Shihmen Reservoir via GA in order to optimise the irrigation basis. However, the authors find that the GA often fails to simplify complex reservoir problems to accelerate and improve the search for answers. The authors proposed a multi-tiered interactive GA (MIGA) to determine the optimal reservoir operation plan and the results showed there was an increase proportion of 25% and a reduction proportion of 80% of the performances in terms of fitness value and the computation time, respectively. In addition, Liu et al. (2020a) showed an improved GA technique named as non-dominant sorting GA II method (NSGA-II) by optimising the multi-objective problems in reservoir operation. Deb et al. (2002) provide a more thorough description of the NSGA-II. A limited quantity of information was provided regarding dam releases to strike a compromise between fish habitat preservation (ecology) and electricity generation (Cioffi and Gallerano, 2012; Ren et al., 2019). The authors discovered the best Pareto front for this trade-off issue using the NSGA-II and ϵ -constraint approaches. The robustness results in the ϵ -constraint approach were computed in a faster manner and provided a straightforward solution under constraint via sensitivity analysis, according to a comparison of the two methods. Meanwhile, the NSGA-II can be useful for learning about the more complete space solution. Additionally, Feng et al. (2018a) highlighted a concatenation for the GA called the parallel multi-objective GA (PMOGA), which was carried out at the Wu Hydropower in China and had the similar advantages of trade-off in ecology. The PMOGA was meant to make solutions more likely to work and to speed up the time it takes for the

stand-alone GA to converge. The authors suggested this research strategy to optimise real reservoirs using heuristic techniques. Additionally, Li and Qiu (2016) leveraged the NSGA-II to optimise the hydropower or PV hybrid power system in Qinghai, China. By segregating hydropower and PV generation, the NSGA-II yielded findings that were both computationally accurate and reasonably priced. In addition to these common GA blending techniques, the originality of the multi-objectives GA provided to enhance simulation and optimisation in streamflow and reservoir operation (Srivastav et al., 2011). This strategy, however, is too simplistic to be used in real-world situations, showing that it lacks concepts of consistency and is susceptible to sample size.

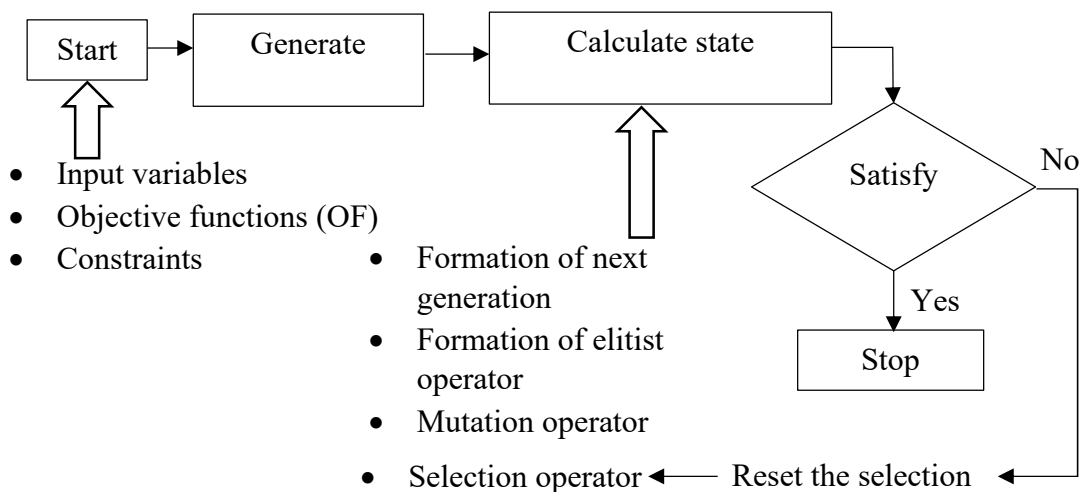


Figure 2.1: Simple flow charts of GA

Apart from the GA, Tabu search (TS) is also part of the heuristic algorithm. The mechanism of the TS is to avoid repeating movements during the preceding steps, solving is forbidden again in the following steps. As a result, a regional search is undertaken to study solutions to reach the optimum solution. A detailed explanation of the TS can be found in (Glover and Laguna, 2013). There were relatively few TS researches in the reservoir optimisation field.

However, the TS was shown to be popular in the water distribution network. Da Conceição et al. (2004) used the TS to determine the lowest-cost design of water distribution networks. However, because of the limited number of studies conducted, this study could not conclude that the TS was a promising algorithm in this subject field. As a result, the authors proposed that additional study and exploration be conducted on various algorithms applied in this field to compare more complete research works. After a 17-year hiatus, there was a new update on TS with the same topic of study work as De Macêdo et al. (2021). Due to the disadvantage of the PSO being readily caught in local optima, the authors showed the integration of the TS with the PSO. This integration was then evaluated with three distinct benchmark networks, with the results compared to the stand-alone Particle Swarm Optimisation (PSO). The results revealed that the integration models gave superior solutions than the PSO by minimising the computation of the water distribution cost design and executing in a suitable time frame due to the efficiency of the exploration in the search space. In addition, the blending approach with the conditional TS and the conditional GA was ultimately implemented in reservoir operation (Thongwan et al., 2019). This study was carried out at Thailand's Ubolrat Reservoir for both past and future B2 scenarios. The results revealed that the rule curves developed from both reservoir models corresponded to the real rule curves with the condition of maintaining the water at the end of the rainy season (November), as the dry period needed a sufficient amount of water to be released to the downstream area.

Besides, the GA and TS, the Simulated Annealing is an estimate that is feasible for a function with a broad search space. The location determines whether there is a chance of survival or return to a previous state. This will optimise the system's energy use. Electronic circuit design is frequently utilised to solve problems such as image processing and navigation. There are few studies that utilised the Simulated Annealing in reservoir optimisation operation. However, the Simulated Annealing has been implemented in hydrometric network topics (Chebbi et al., 2017) and landslide (Ferreiro-Ferreiro et al., 2020). After that, the temporal order proceeded to change into algorithms that drew inspiration from nature. The knowledge of nature-inspired algorithms has the strategy of exploitation and exploration, making it difficult to get stuck in a local optimum while also searching for global optimal solutions.

2.2.6 Meta-Heuristic Algorithms (MHAs)

The transition was then moved to the most successful and well-known swarm-based MHAs, namely the Particle Swarm Optimisation (PSO), Ant Colony Optimisation (ACO), Firefly Algorithm, and etc, which are inspired by the movements of the swarms in nature. After that, more advanced fields in MHAs such as multimodal and multi-objective optimisation, hybrid MHAs, constraints or penalty function handling were developed. In order to conduct thorough space searches, nature-inspired MHAs often go through two unique phases of search: exploitation and exploration. There are a variety of categories based on the MHAs such as evolutionary, swarm, physics, human, biology, system, math, and music. These research works is tabulated in Table 2.1 by

segregating them into different categories. Following this are the benefits and drawbacks of these reservoir algorithms which are tabulated in Table 2.2. However, in this chapter, the elaboration will focus on the swarm-based studies and its enhancement techniques that have been conducted in earlier studies to support the selection of reservoir models in Chapter 3 - Methodology. It begins with a swarm-based algorithm, then an insect-based algorithm, and finally an animal-based algorithm.

Below are the case studies implemented under the swarm based algorithms in reservoir optimisation. Al-Aqeeli and Mahmood Agha (2020) investigated the reservoir operation by finding the optimum operation between maximising hydropower and flood control in Iraq (Mosul and Badush Dams) via the PSO. He et al. (2014) suggested using the enhancement strategy namely the chaotic PSO (CPSO) to decrease the standard deviation of the discharge flow and a piecewise linear interpolation function (PLIF) was employed to deal with the restrictions for solving the objective function (OF). Following that, the findings gained showed that the CPSO outperformed than the GA, DE, and PSO. For more effective scheduling, multi-objective flood control actions should be taken into account. Bai et al. (2019) showed the equilibrium ecology system of the Yellow River in China by conducting a compensation element between water and sediment process. The authors utilised the PSO and the feasible search space to minimise disasters and maximise the advantages of the water storage capacities of the two cascade reservoirs. Furthermore, the PSO and GA both used the same execution principles from the parallel multi-objectives (PMO) for the cascade hydropower reservoir in China (Niu et al., 2018b). Aside from that,

to solve the multi-objective problems, Chen et al. (2020) established a new blending reservoir model namely the adaptive random inertia weight (ARIW)-PSO algorithm to optimise the dispatch of the Panjiakou Reservoir, and the flood control operation at China's Luanhe River. The probability distribution function led to the blending, while the inertia weight was randomly generated. To begin with, global optimisation favours inertia weights that are higher. As evolution proceeds, however, the inertia weights progressively decrease, benefitting local search optimisation. Then, the authors showed that the blending reservoir model obtained the objective function with the value of 0.8514, which was outperformed by other algorithms such as the GA and stand-alone PSO, at 0.9651 and 0.8876, respectively. The authors claimed that this blending model could effectively solve the real-time optimisation problem. The Cuckoo Search (CS) is the most used strategy for enhancement after the PSO. There are numerous strategies for enhancing population initialisation. Meng et al. (2019) suggested an improved multi-objective cuckoo search (IMOCS) to alleviate one drawback of the MOCS.

The Klang Gate Dam (Hossain and El-shafie, 2014a) and the Aswan High Dam (AHD) (Hossain and El-Shafie, 2014b) with the PSO, were used as examples of the other application of the swarm-based reservoir models' popularity to provide optimal release policy for reservoir systems. Next, the past studies were based on insect -based algorithms. The water distribution system design challenges were solved using the ant-colony algorithm, which was then verified using a few test functions (Zheng et al., 2017). However, this study showed the model's performance in terms of convergence rate; no actual

optimisation problem was presented. The same is true of the firefly optimization, which is solely used as an algorithmic test function in mathematics (Aydilek, 2018). The Moth-flame Optimisation (MFO) was created by Mirjalili (2015). In order to prevent settling into a local optimum, the new strategy for the flame population has to be enhanced by using the moth's linear flying path. This process is known as the improved MFO (IMFO). The inadequacies of the traditional Pareto domination led Zhang et al. (2020) to propose a new blending technique based on the R-domination (R-IMFO) to address the trade-off between the ecology and navigation of the cascade reservoir operation. The following paragraph briefly described the case studies utilising animal-based algorithms.

Animal-based algorithms consist of the Bats, Sharks, Lion Swarms, Grey Wolf, and more. Ehteram et al. (2017a) has attempted to reduce the reservoir water scarcity with a demonstration of the shark algorithm (SA) and the other standalone method (GA and PSO) to evaluate based on the reservoir risk assessments. The results revealed that the SA surpassed the other two standalone algorithms in respective with reservoir risk assessment and model performance. The SA continues to have the lowest vulnerability (31%) and the highest reliability (96%). Dehghani et al. (2019) suggested integrating the Grey Wolf Optimisation with the ANFIS for the development of the hydropower generation at the Dez basin. The output of this study showed that the integration of the GWO-ANFIS managed to forecast and optimise hydropower production and successfully facilitate policymakers. There is little information available on the Lion swarm algorithm employed in the optimisation procedure especially in

reservoir field. In their demonstration of the LSA in cascade hydropower, Liu et al. (2020b) examined the robustness of the LSA via various of model performances.

The hybridisation under MHAs is the main topic of the current paragraph. Allawi et al. (2019a) suggested the SVR and RBF as AI models for forecasting inflow and evaporation of the reservoir as the Scenario 1. By hybridising the machine learning in the SA (SMLA), GA and PSO were utilised and optimised where inflow and evaporation as observable deterministic variables (Scenario 2). SMLA outperformed GA and PSO for optimisation, whereas SVR exceeded RBF for projected hydrological parameters. Scenario 2 leveraged expected deterministic factors to optimise existing unreal conditions to lower the water shortage. In addition, the blending algorithms of PSO, Differential evolution (DE), WOA, and crow search algorithm was formed a Master-slave model strategy in order to identified and attained best reservoir policy at the AHD (Turgut et al., 2019). This method's advantage is that it is extremely competent at identifying and perceiving the considerable stochastic character and non-linearity of the reservoir system. Yaseen et al. (2019) suggested a commonly used hybridisation technique in reservoir control, called as the bat-swarm algorithm, the HB-SA, in order to reduce irrigation shortfalls at the respective dam of the Golestan and Voshmgir. One of the advantages for the hybridisation techniques was capable to speed up the convergence rate whereby it is necessary for a workable real-time dam and reservoir to provide optimal solution. The HB-SA was compared to the other stand-alone algorithms and outperformed, attained the highest reliability readings in the range between 94% to 96%.

However, Turgut et al. (2019) has also been mentioned in this study by suggesting for the future research to examine and determine if the existing reservoir policy can continue to be applied in future climatic and hydrological circumstances at dam scales.

Table 2.1: Studies under a variety of categories based on MHAs

Categories	Objective of study	Method adopted	Findings and Limitation	Reference
Evolutionary based	To solve the climate uncertainty in reservoir management	<ol style="list-style-type: none"> 1. Coral reefs algorithm (CRO) 2. Constrained CRO 3. Reinforcement learning CRO 	<p>The acquired findings were then compared to LP. To summarise, the reinforcement learning CRO outperforms others in terms of convergence and accuracy to the problem of a four-reservoir system. Due to the CRO being easily trapped in local optimum, two enhanced methods were introduced for the equilibrium tradeoff between exploration and exploitation.</p>	(Emami et al., 2021)
Physic based	To solve the large-scale Dez reservoir operation optimisation problem	<ol style="list-style-type: none"> 1. Gravitational search algorithms (GSA) 2. Partially Constraint GSA (PCGSA) 3. Fully constraint GSA (FCGSA) 4. Unconstrained GSA (UCGSA) 	<p>FCGSA was very efficient in resolving this optimisation issue, resulting in a substantial decrease in the search area. It obtained 7.377 cost values in Dez hydropower. As the GSA is slow with convergence speed and trap in local minima, the hybrid GSA were conducted in different months of operation in order to validate among the models.</p>	(Moeini et al., 2017)

Table 2.1 (continued): Studies under variety of categories based under MHAs

Categories	Objective of study	Method adopted	Findings and Limitation	Reference
Physic based	To solve the hydropower optimisation problem in karon4 and four-reservoir optimisation problem	1. GSA 2. GA	The GSA standard deviations for Karon4 and four-reservoir optimisation were 0.0009 and 0.277, respectively, whereas the GA standard deviations were 0.161 and 0.705. As a consequence, the GSA outscored GA in terms of reliability and its tuning parameters were easier and faster.	(Bozorg-Haddad et al.,2016)
Physic based + Swarm based	To solve the multiple hydropower reservoirs and solar photovoltaic plants optimisation problem	1.GSA 2. Neighbourhood search strategy GSA 3. Adaptive mutation strategy GSA 4. Constraint handling technique GSA 5. GA 6. PSO 7. DE	The simulation results show that the improvement technique can overcome the early convergence problem in GSA. Furthermore, GSA enhancement methods have proven that dynamically scheduling both hydropower and solar PV facilities may produce higher-quality scheduling schemes.	(Niu et al., 2021)
Physic based + Swarm based	To examine the effectiveness of the methods	Integration of PSO and GSA (HGSPSO)	This method integrates the local search skills of GSA with the global best skills of PSO. The HGSPSO was satisfied for optimising reservoirs.	(Khan and Ling, 2021)

Table 2.1 (continued): Studies under variety of categories based under MHAs

Categories	Objective of study	Method adopted	Findings and Limitation	Reference
System based + Swarm Based	1. To minimise the water deficit at Klang Gates Dam 2. To investigate the efficiency of CSS	1. Charged System Search (CSS) 2. ABC 3. PSO 4. GA	CSS was verified and compared to other algorithms; the findings showed that CSS was accurate in simulating, and the release policy excelled other algorithms. CSS can achieve the overall reliability of 96% compared to the other algorithms.	(Latif et al., 2021)
System based + Swarm Based	To derive the water-supply and hydropower operating policies in Dez reservoir	1. CSS 2. GA 3. ACO 4. PSO 5. NLP	CSS had faster and more exact convergence. The result was employed in Dez reservoir optimization. CSS proved to be an efficient strategy for improving reservoirs. Uncertainty may affect policy due to the study's known river inflow.	(Asadiéh and Afshar, 2019)
Math based	To balance global exploration and local exploitation in a cascade hydropower reservoir in China	1. Sine Cosine Algorithm (SCA) 2. Adaptive SCA	At Wu hydropower in China, ASCA can improve scheduling in different runoff cases. ASCA demonstrated strong performance and global search capability when compared to SCA.	(Feng et al.,2020a)

Table 2.2: Benefits and Drawbacks of the algorithms

Algorithm	Benefits	Drawbacks
GA	<ul style="list-style-type: none">• It can manage complexity problems and constraints in non-linear conditions.• It is easy to implement.• It can be utilised on its own to address a particular problem.• It does not rely on any additional algorithms or heuristics.	<ul style="list-style-type: none">• Uncertainty of achieve global maxima, easily stuck in local maxima, and loses population density.• Due to the numerous factors involved, it can be time-consuming and lacks common termination criteria.
DE	<ul style="list-style-type: none">• It is competent at exploration and diversification.• It can handle both unimodal and multimodal situations.	<ul style="list-style-type: none">• The convergence rate is unstable.• The local optimum is reached quickly.
PSO	<ul style="list-style-type: none">• The computation is easy.• It is perfect for dynamic applications due to its rapid response.	<ul style="list-style-type: none">• Population density is declining, therefore premature convergence is unusual.
ABC	<ul style="list-style-type: none">• It has a flexible tuning range and few parameters.	<ul style="list-style-type: none">• Less parameter adjustment is needed, which reduces accuracy.
Ant-colony	<ul style="list-style-type: none">• It avoids early premature convergence and is essentially parallel because the solutions can be found independently and concurrently.	<ul style="list-style-type: none">• It ensures the convergence aspect, but the time is not specified.

Table 2.2 (continued): Benefits and Drawbacks of the algorithms

Algorithm	Benefits	Drawbacks
Firefly & Moth flame	<ul style="list-style-type: none"> • Because it naturally separates the population into various groups, it has strong diversity. 	<ul style="list-style-type: none"> • It can become stuck in local optima when faced with complex multi-objective.
Bat, Shark, Lion, and grey wolf	<ul style="list-style-type: none"> • Simultaneously searching of exploration stages and exploitation stages. • It is simple to implement and adaptive. 	<ul style="list-style-type: none"> • It cannot handle discrete problems. • Enhancement techniques, data-driven techniques, or MHA hybridisation help solve this problem.

2.2.7 Hybridisation Technique

Numerous hybridisation studies have been conducted. The hybridisation is divided into three kinds in this sub-section: (i) hybridisation under EA, (ii) integration of EA and SI, and finally, (iii) MHAs inspired by nature. The following lines begin with hybridisation under EA. The shortcomings of the standalone algorithms can be overcome by the hybrid algorithm. Hybrid algorithms' consistency may be helpful in research on multi-objectives trade-offs. Ibrahim et al. (2021), for instance, showed how to combine optimisation modelling and data-driven methodologies to forecast streamflow. At the Vanderkloof Dam, efficient optimisation (Pareto multi-objective DE) and precise reservoir inflow predictions (artificial neural networks) can increase daily hydropower production (Olofintoye et al., 2016). To achieve the optimal reservoir policy, investigations of combining NN and EAs were undertaken (Feng et al., 2019). To show how trade-off of the water distribution system, (i.e.,

costs and design size) were made, the EPANET water distribution model and EAs were merged (Kurek and Ostfeld, 2013). Additionally, because they are simple and effective, multi-objectives optimisation reservoir procedures like the DE (Yazdi and Moridi, 2018) and the PSO (Sedki and Ouazar, 2012) are well-liked hybrid EAs. Additionally, the multi-objectives EAs were employed for purposes other than reservoir optimisation, such as a method for experiment design (Li et al., 2021), and they also serve as a radiation detecting system (Holland et al., 2021). The PSO had two flaws: inertia weight and poor variety. The DE can lead to premature convergence, whereas the PSO is capable of looking for local optimum solutions. In order to improve the fundamental composition of the DE and PSO algorithms, respectively, Ahmadianfar et al. (2020) suggested an adaptive (A-DEPSO) method. Modern technology is used by A-DEPSO to enhance both local and worldwide search. A four-reservoir hydroelectric facility in southwest Iran is being used to test the suggested method. Because it accounted for 57% of the decrease variance in the hydropower plant, this method performed better than previous stand-alone approaches. Ehteram et al. (2017b) have established the GA and the krill algorithm as a hybrid approach for a multi-purpose reservoir systems. The fundamental drawbacks of the present GA algorithms, weak convergence and local optimum, are overcome through integration. The suggested hybrid algorithm was compared to identify and assess the algorithm's effectiveness based on reservoir risk assessments. For each situation, the suggested hybrid algorithm discovered the overall best value. Reservoir optimisation, a formula for the greatest possible control of a dam or reservoir, however, necessitates realistic simulation. In essence, hybrid EAs deal with challenging problems in water resource management. However, a different

method is used to balance the weakness of the stand-alone EAs and strengthen or improve them. Next is the combination of EA-SI. Hossain et al. (2018) developed the passive congregation theory in particle movement, the PC-PSO at the Klang Gate Dam. Although the PSO was an excellent optimizer, the PC-PSO performed slightly better than the PSO, in terms of reservoir risk analysis assessment. When an extreme weather event occurs, the vulnerability and the resilience index (heavy-rainfall or extreme draught), respectively are vital as is life threatening to the residents at the downstream. Moeini and Babaei (2020) showed the original concept of an improved PSO to a constrained version (CIPSO) in order to deal with uncertain inflows. The explicit satisfaction of the CIPSO requirement limits the search space and lowers the computing expense. According to the findings, SVM-CIPSO2, performed better than expected in terms of reservoir risk analysis and raised the sustainability index by 11.27% with the observed data loaded into the CIPSO, and the outputs were then transmitted to the SVM, a data-driven model that may duplicate an earlier optimised data pattern which generated a smaller search space. Then, a 10-cascaded hydro plant using this approach was implemented in a multi-objectives reservoir system. Performance indicated that the MGPSO had a lesser energy deficit than the DE and PSO (Zhang et al., 2013). The estimation of distribution algorithm, EDA and the PSO were also integrated to address the multi-objectives reservoir activities in order to alleviate the flood at Ankang Reservoir (Luo et al., 2015). Yang et al. (2015) established a non-linear global evolutionary optimisation by concatenating with principal component analysis, PCA and crowding distance operation to solve the multiplex objectives at California hydroelectric dam. The immune algorithm-based PSO is another illustration. It

combines the PSO and the idea of an immune information processing mechanism to provide good global optimal capability (Fu et al., 2011). However, these conjunction techniques were not the most well-liked SI techniques for enhancing reservoir operations. Finally, the hybridisation of MHAs with nature inspiration. To determine if the existing reservoir policy can continue to be successful, scholars must take the initiative to examine the future climatic scenarios and hydrological circumstances. Besides, the same suggestion made by Turgut et al. (2019) has also been mentioned in this study, namely that the insufficient climatic data and the effect of climate effects on reservoir operations should be taken into cognizance in future studies.

As a result, it is suggested in this study to utilise the meta-heuristic algorithms, namely the Whale Optimisation Algorithm, Harris Hawks Optimisation Algorithm, due to their strategy of exploration and exploitation during the search simultaneously and their respective enhancement approach, which will be described in the Methodology section. Thus far, both meta-heuristic algorithms (MHAs) been not be performed at the KGD operation, leading to their selection algorithms in this study. In Chapter 3.6, will be further elaborate the equations involved in WOA and HHO. The model structures of WOA (spiral bubble attacking method) and HHO are depicted in Figure 2.2 and Figure 2.3, respectively. Figure 2.4 depicts the summary of reviewed optimisation techniques utilised in reservoir optimisation operation in this study. A few categories have been mentioned and classified under the traditional approach, heuristic algorithms, and meta-heuristic algorithms. In short, most of the hybridisation case studies in this section were executed in swarm-based

intelligence and this included the benefits and drawbacks of the algorithms, as seen in Table 2.2.

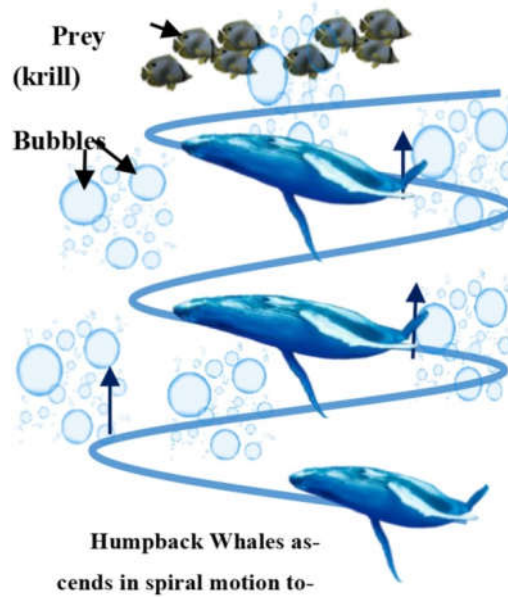


Figure 2.2: WOA model structure - Spiral bubble (El Ghamrawy and Hassanien, 2020)

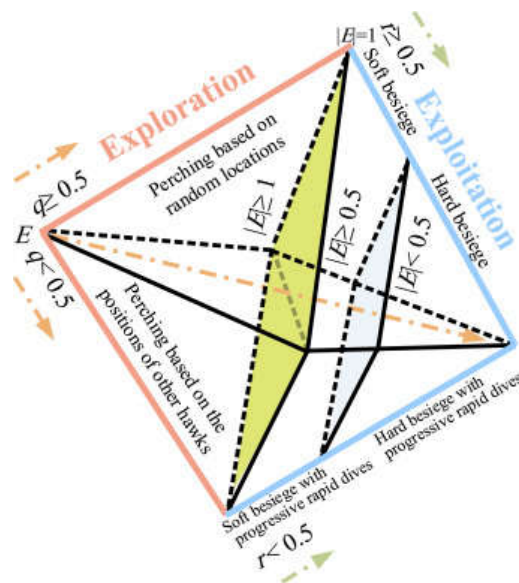


Figure 2.3: HHO model structure (Heidari et al., 2019)

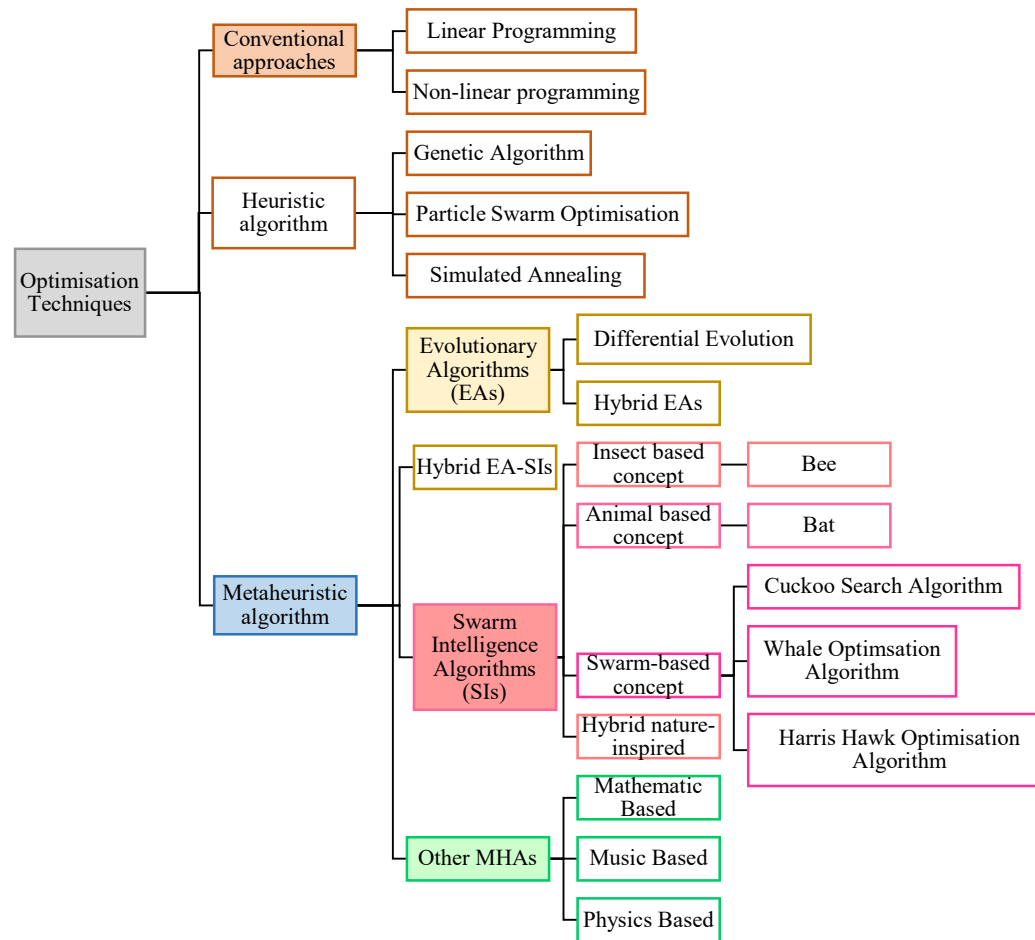


Figure 2.4: Summary of Optimisation Techniques Reviewed

2.2.8 Summary

The purpose of this section is to provide a comprehensive overview of all the sub-sections contained within section 2.2. In summary, the limitations of Rippl's method, as outlined in section 2.2.1, have been addressed through the integration of conventional optimisation techniques. This was necessary due to the limited capacity of the reservoir design and the challenges associated with its adoption in the context of multiplex objective functions. Subsequently, the ISO and ESO were implemented, both of which were classified as conventional optimisation techniques. Nonetheless, the ESO exhibited similar behaviour to Rippl's approach in that its capacity was limited to addressing only the simple optimisation problem of reservoirs. The ISO, also referred to as the Monte Carlo optimisation, has been found to have limitations due to its dependence on observed data and susceptibility to extreme conditions. Despite the frequent applications of LP in various studies, where it has been incorporated with other methodologies to enhance the development of operating rules, its limitations have been brought out to the forefront. Specifically, the accuracy of the results obtained through LP has been adjudged into question due to the prevalence of non-linear reservoir problems. With regards to the NLP characteristic, it is observed that it does not exhibit the dual characteristics of exploitation and exploration that are typically associated with meta-heuristic algorithms. Consequently, as the complexity of reservoir operation problems increases, the computational time required for NLP and heuristic algorithms (presented in Table 2.2) increases. The complexity of reservoir problems pertaining to trade-off operation necessitated an integration of commonly employed approaches from basic dynamic programming (DP), namely the stochastic programming

(SDP) and the rule-based improved DP. Table 2.2 has shows the limitations associated with the corresponding meta-heuristic algorithms (MHAs) were found to exhibit both exploitation and exploration characteristics. However, minor adjustments in terms of convergence and the challenge of being trapped in local optima when dealing with multi-dimensional trade-offs, necessitated the introduction and proposal of hybridization techniques to enhance the applications of MHA

2.3 Climate Change Impact on Reservoir Optimisation

The transition of the climate is undoubtedly caused by human activities as a result of more sophisticated lifestyles that place a higher priority on energy demand, resulting in increases in greenhouse gases (Akbari et al., 2019). The increase in global temperatures is causing these gases to rise (Terzi and Manolis, 2020). Greenhouse emissions are the primary source of global warming. Greenhouse gases are significant in climate change. Other factors that affect climate change include variations in sunlight intensity and the Earth's direction (Coelho et al., 2020). It also caused temperature, rainfall, and wind speeds turn into more extreme. This also impact the reservoir operations. These dramatic developments also significantly affect human health, poverty, and the wellbeing of people (Yalew et al., 2020).

The likelihood of experiencing severe weather will ascend as a result of climate change (Katelaris, 2021). If climate change intensifies, heat waves are predicted to intensify. This will trigger many droughts and calamities. These

occurrences pose a threat to the current designed system for delivering the water in different climatic regime. The transition of the extreme climate affects planning, design, and execution of water projects. The major contribution factors especially temperature and precipitation (rainfall) which reflect the potential and influence to the water supplies (Manzanas et al., 2020). Therefore, effective water management approaches should include and focus on integrating in all of its dimensions that is from the impacts of climate change.

One of the most crucial pieces of a climate change impact assessment is using the global climate models (GCMs). The models were, however, limited in their ability to be applied on a local scale due to their coarse horizontal spatial resolution (100 to 200 km) (Solomon, et al., 2007). As a result, coarse resolution GCMs output is downscaled to a finer regional resolution in order to ensure logical readings display for projected future data (Teutschbein and Seibert, 2010).

The output of a GCM can also be downscaled statistically or dynamically (Fowler et al., 2007). According to Jakob Themeßl et al. (2011), a large-scale lateral boundary circumstances from GCMs is utilised for the dynamic downscaling process in order to encourage better resolution outputs from a regional climate model (RCM). Although more costly and introducing additional biases due to increased uncertainties in local forcing, the RCMs do offer a more accurate physical depiction than the lateral bounds of the GCMs (Rowell, 2006). In Malaysia, a tropical nation with a highly variable precipitation pattern,

statistically downscaled GCMs are utilised for the vast majority of studies in this region.

The climate projections from CMIP 5 showed good performance in historical rainfall simulation in the Malaysia region, as claimed by Tan et al. (2017). For validation purposes, from the year 1991 to 2005 was chosen as base period; whilst for the future timeline are sub-divided into the near future year (2020-2039), mid future year (2040 – 2069), and the far future years (2070 – 2099). The selection of the GCMs mainly from Queensland Climate Change Centre (CSIRO-Mk 3.6) and University of Tokyo (MIROC-ESM-CHEM, MIROC-ESM and MIROC 5) due to the acceptable and tolerable resolution at this study region than the other GCMs in the CMIP 5. In this study, three RCP scenarios will be examined, which include the RCP 2.6 as the low emission path scenario, the RCP 4.5 scenario act as the intermediate level and lastly the RCP 8.5 scenario as a very high and excessive greenhouse gas emission scenario. The respective radiative forcing pathway can be referred to in Table 2.3.

According to Yaseen et al. (2019) and Turgut et al. (2019), climate change uncertainties or scenarios can have a significant impact on how reservoirs operate in future reservoir policies. Therefore, this would make determining optimal reservoir operation rules in the future more feasible and reliable. General circulation models (GCMs) resulting from the fifth phase of the Coupled Model Intercomparison Projects, CMIP 5 (Taylor et al., 2007), were used for future climate scenarios, as part of the Intergovernmental Panel on Climate Change's, IPCC Fifth Assessment Report, AR5 (Stocker et al., 2013). Each GCM in AR5

disclosed various representative concentration pathways (RCPs), which represent various ways of greenhouse gas concentrations resulting in radiative forcing by 2100, depending on human activity mitigation (Meinshausen et al., 2011). The listing characteristics of RCPs are presented in Table 2.3. RCP 2.6 is known as the most optimistic scenario for maximum mitigation; RCP 4.5 and RCP 6.0 are known as intermediate level of emissions in which there is increased radiative forcing, but it stabilises; and RCP 8.5 is known as the most pessimistic scenario or highest emissions in which higher levels of radiative forcing and temperature increase do not stop.

However, there were some case studies still had adopted the Special Report on Emission Scenarios (SPRES), which was reported based on the IPCC-Fourth Assessment Report (AR4). In AR4, the emission scenarios were built based on a more economic focus and a more environmental or sustainable development. The radiative forcing in RCP 8.5 is roughly similar to A2 scenario in AR4; the RCP 4.5 is roughly similar to B1 scenario in AR4. Then RCP 6.0 and RCP 8.5 are corresponded to A₁B and A₁F₁ in AR4, respectively. Table 2.3 presents the RCPs corresponding to the SRES. The investigation carried out by Ahmadi et al., (2014) segregated the periods of the estimated precipitation and temperature with early, middle, and late periods of 21st century under the emission scenario of A2.

Estimated precipitation and temperature parameters were used to simulate reservoir inflow at the Karoon-4, Iran. NSGA-II was then utilised to

optimise Karoo-4's operation rules. Considering the impact of climate change on the future reservoir, this study determined that activities are required. According to Ehteram et al. (2019), climatic change impacts reservoir discharge activity. Climate change affects rainfall-runoff, which affects river input. This research analysed temperature and precipitation trends as an indicator for decreasing the gap between water supply and demand. Iran's Aydoughmoush Dam was the research site. This investigation used the HAD-CM3 model for climate change backdrop based on the A₁B scenario with two primary predictors (precipitation and temperature) for 2046-2065. IHACRES calculated runoff. The novel nature-inspired optimisation algorithm, the shark algorithm, utilised climate change results to generate an optimum operating rule for reservoir release operation. The performance and operating rules currently in place may be impacted by climate change and escalating the maintenance requirements for ageing reservoirs (Desiree et al., 2020). This study showed the integration reservoir's operational performance for the SOP and climate scenarios under RCP 8.5 via ResSim. However, it can be improved using ensembled GCMs and other factors affecting future reservoir operation. Besides, global climate change puts pressure on resources management, specifically for reservoirs, as fluctuating precipitation due to rising global average temperature which also increased evapotranspiration rates. This study conducted by Mandal et al. (2019) utilised four downscaling climate models (CanESM2, CCSM4, CSIRO-MK3-6-0, and GFDL-ESM2G) for future reservoir simulation release policies via system dynamics simulation model, SDM. However, this analysis does not address reservoir optimisation or other factors affecting hydropower generation (e.g., population growth). Zhang et al. (2017) conducted a comprehensive analysis of

the reservoir release policy with various operating rules (i.e., conventional, fixed and adaptive) in order to maximise the utilisation of water resources and avoid profits sharply decreasing for agriculture development via two-dimensional dynamical programming under future scenario (2015-2040). However, the study lack consideration of the perspective of population growth or socioeconomic land use land cover change (LULCC).

Apart from that, there were several studies conducted under investigation of climate change based on RCPs in IPCC-AR5 for the future reservoir optimisation operation. Nourani et al. (2020) suggested an integration approach to examine the dam operation in order to adapt the climate change at the Shahrchay reservoir in Iran. Among the immense number of possible large-scale climate variables of the General Circulation Models (GCMs), the model M5 tree was introduced to pick the most appropriate predictors. Furthermore, an Artificial Neural Network (ANN) preparation was used for the observed temperature and precipitation time series. RCP 4.5 and RCP 8.5 have been implemented to obtain insight into potential changes in rainfall and temperature. Finally, the GA was used to refine the reservoir system's operational rule curves using the annual estimated evaporation and inflow of precipitation, considering water supply and municipal targets, and minimising possible overall square deficiencies. Aside from this, Thomas et al. (2021) presented the adaption policy in Narmada basin, India for the future RCPs, such as RCP 4.5 and RCP 8.5 scenarios in reservoir optimisation operation. Huangpeng et al. (2021) showed the hydropower production at Jinanqiao Dam in Chiana's Yunnan Province. The authors considered three scenarios, namely RCP 2.6 (low), RCP 4.5 (medium)

and RCP 8.5 (high) which have been developed by the IPCC-AR5 (Rogelj et al., 2012). Besides, this study was then implemented by metaheuristic algorithms (MHAs) for the future reservoir optimisation operation in RCP 2.6, RCP 4.5, and RCP 8.5. The study was intended to forecast the future hydropower production (2021–2050) under RCP2.6, RCP4.5, RCP 8.5. Hydropower plants can be susceptible to changes in the amount of precipitation to the reservoir. A method has been used that improves the accuracy of flow estimation. The new version of the Developed Crow Search Algorithm (DCSA) was used to solve the problem. It improves precision by overcoming the drawbacks of the optimisation: trapped in optimal location, imbalances between exploitation and exploration of ANN. This study was conducted under climate change scenarios of RCP2.6, RCP4.5 and RCP8.5. The result notes that the amount of electricity production should escalate in the coming years. These findings will support managers in controlling water and energy resources.

With all these case studies mentioned above and summarised in Table 2.4, however, there is very little information of the Klang Gate Dam (Case Study location) being investigated with the climate change scenarios and implementing MHAs approaches by following the AR5 climate scenarios. Under the Coupled Model Intercomparison Project (CMIP3 and CMIP5), researchers have continuously assessed the simulated surface temperature for climatic variable projections. The most recent version of CMIP5, which is also a component of the IPCC-AR5, incorporates relatively higher resolution and a variety of experiments. In their study, Jourdain et al. (2013) compared the performance of models available under CMIP5 to CMIP3. Additionally, Sperber et al. (2013)

claimed that the multi-model mean produced in CMIP5 is more accurate than CMIP3. However, the CORDEX-SEA in Asia domain region, namely the WAS-44 or WAS-44i was not in the finer resolution of the GCM and the data availability in the Earth System Grid Federation (ESGF) portal for the RCPs do not have complete sets. Hence, CMIP5 was selected as the GCM in this study to further the investigation into future reservoir optimisation operation.

According to Table 2.3, the RCP 2.6 act as the most optimist condition for maximum mitigation, RCP 4.5 and RCP 6.0 both considered as stabilisation scenarios, and RCP 8.5 as the worst-case scenario. The predictor variables for RCP 6.0 were insufficient for inclusion in this study simply because there were inadequate CMIP 5 data available for this study region. Additionally, using an unfair combination of predictors and predictor variables due to the inaccessibility of the RCP 6.0 predictor data will increase the degree of uncertainty regarding the results. Hence, the executions of the RCPs scenarios implemented in this study are the RCP 2.6, RCP 4.5, and RCP 8.5 at Klang Gate Dam (KGD) while utilising MHAs to investigate the climate change impact on the future reservoir operation. Based on the observation in Table 2.4, it shows the climatic variables involved in and how future reservoir operations will be affected by climate change.

In short, the review of the past studies made in section 2.3 have highlighted several points, especially the model involved in SDSM, where it certainly has constraints on the climatic variables as it is only operated on a daily time frame and could be analysed and solely in a single GCM. Hence, the

uncertainty of the model itself was high as compared to the other model (data-driven or weather-classification model) where ensembled GCMs can be involved in the downscaling process and have equally distributed onto the uncertainty manner. The selection of the GCMs or the ensemble of GCMs are also significant for future climate impact investigations. In addition, some regions of study area may have difficulties in the aspect of quality of the data (missing data in majority) or insufficient predictor variable criteria in order to downscale the GCM, which could lead to the high uncertainty in terms of accuracy for the downscaled output.

Table 2.3: Similarities between RCP projections and SRES

Fifth	Radiative Forcing (W/m^2)	Forth
Assessment		Assessment
Report		Report
RCP 2.6	From $3 \text{ W}/\text{m}^2$ then decreases to $2.6 \text{ W}/\text{m}^2$ (by 2100)	Not available
RCP 4.5	4.5 (post 2100)	SRES B1
RCP 6.0	6 (post 2100)	SRES A ₁ B
RCP 8.5	8.5 (post 2100)	SRES A ₁ F ₁

Table 2.4: Summary of the case studies on climate change impacts

Author(s), Year	RCP/SRES	GCMs Involved	Downscaling Method	Climatic Variables	Future Periods	Study Area	Approaches for Reservoir Optimisation
Huangpeng et al. (2021)	RCP 2.6 RCP 4.5 RCP 8.5	GFDLCM3	LARC-WG	Minimum Temperature Maximum Temperature Precipitation	2021-2050	Jinanqiao Dam, China	Crow Search algorithm
Thomas et al. (2021)	RCP 4.5 RCP 8.5	CSIRO CCAM ACCESS1.0 CNRM-CM5 CCSM4 GFDL-CM3 MPI-ESM-LR NorESM-M	-	Temperature Precipitation	2006-2040 2041-2070 2071-2099	Narmada Basin, India	NSGA-II + MOGA
Yaghoubi et al. (2020)	A2	HadCM3	SDSM	Daily temperature Daily precipitation	2026-2036 2048-2058 2081-2091	Gaverood River Basin, western Iran	Quantitative-Qualitative model

Table 2.4 (continued): Summary of the case studies on climate change impacts

Author(s), Year	RCP/SRES	GCMs Involved	Downscaling Method	Climatic Variables	Future Periods	Study Area	Approaches for Reservoir Optimisation
Nourani et al. (2020)	RCP 4.5	CGCM3	ANN	Precipitation	2020-2060	Shahrchay Dam, western Iran	GA
	RCP 8.5	ACCESS1.0		Temperature			
	A1B B1	MIROC-ESM- CHEM					
Fallah- Mehdipour et al. (2020)	RCP 2.6	CanESM2	SDSM	Daily precipitation	2009-2059	Karkhe Basin, Iran	NSGA-II
	RCP 4.5			Daily maximum			
	RCP 8.5			temperature Daily minimum temperature			
Ahmadianfar & Zamani (2020)	RCP 8.5	CSIRO-Mk 3.6	LARC-WG	Daily precipitation	2025-2054	Jarreh reservoir, southwestern Iran	Two-dimensional hedging rule
		MIROC-ESM		Daily maximum			
		GFDL-ESM2M		temperature			
				Daily minimum temperature			

Table 2.4 (continued): Summary of the case studies on climate change impacts

Author(s), Year	RCP/SRES	GCMs Involved	Downscaling Method	Climatic Variables	Future Periods	Study Area	Approaches for Reservoir Optimisation
Ehteram et al. (2019)	A ₁ B	HadCM3	LARC-WG	Minimum Temperature Maximum Temperature Precipitation	2046-2065	Aydoughmoush Dam, Iran	Shark algorithm
Abera et al. (2018)	RCP 4.5 RCP 8.5	Ensembled CORDEX- AFRICA	-	Precipitation Temperature	2011-2040 2041-2070 2071-2100	Tekeze reservoir, eastern Nile	Hec-ResPRM
Ashofteh et al. (2017)	A2	HadCM3	-	Precipitation Temperature	2026-2039	Aidoghmoush Basin, East Azerbaijjan, Iran	MO-GP
Shukla et al. (2016)		HadCM3	SDSM	Daily precipitation Daily temperature (maximum & minimum)	1961-2099	Indira Sagar Canal, India	-
Ashofteh et al. (2015)	A2	HadCM3	-	Precipitation Temperature	2026-2039	Aidoghmoush Basin, East Azerbaijjan, Iran	GP

Table 2.4 (continued): Summary of the case studies on climate change impacts

Author(s), Year	RCP/SRES	GCMs Involved	Downscaling Method	Climatic Variables	Future Periods	Study Area	Approaches for Reservoir Optimisation
Zamani et al. (2017)	A2 B1	BCM2 CGCM3 CNRM-CM3 CSIRO-Mk3 ECHAM5-OM ECHO-G GFDL-CM2 GISS-E-R HadCM3 INM-CM3 IPSL-CM4 MRI-CGCM2.3.2 CCSM3 PCM	LARS-CF combination	Mean Precipitation Mean Temperature	2025-2054	Jarreh reservoir, southwest of Iran	Differential evolution algorithm

Table 2.4 (continued): Summary of the case studies on climate change impacts

Author(s), Year	RCP/SRES	GCMs Involved	Downscaling Method	Climatic Variables	Future Periods	Study Area	Approaches for Reservoir Optimisation
Ashofteh, et al. (2016)	A2	HadCM3 CCSR-NIES CSIRO-Mk2 CGCM2 GFDL-R30 NCAR-PCM ECHAM4	Proportional method	Precipitation Temperature	2026-2039	Aidoghmoush Basin, East Azerbaijain, Iran	Simulation
Ahmadi et al. (2014)	A2	HadCM3	Proportional method	Precipitation Temperature	2025-2039 2055-2069 2085-2099	Karoon-4, Iran	NSGA-II
Jahandideh- Tehrani et al. (2014)	A2	HadCM3	Proportional method	Precipitation Temperature	2025-2039 2055-2069 2085-2099	Karoon-4, Iran	Non-linear programming
Ashofteh et al. (2013)	A2	HadCM3	Proportional method	Precipitation Temperature	2026-2039	Aidoghmoush Basin, East Azerbaijain, Iran	Non-linear programming

2.4 Downscaling of GCMs

Generally, climate change has enormous effects on natural and human systems. Droughts and heat waves pose a high threat of causing irreversible damage to the terrestrial and maritime ecology, fresh water resources, food production, and human health under medium and high emission scenarios for this century (Field et al., 2014; Ali Khan et al., 2014). The climate at the upstream of the KGD is influenced by the rainy season from the southwest monsoon which approximately begins from May or June to September or early October and the second inter monsoonal phase (October to November). In addition, the location of the case study is situated in Peninsular Malaysia, which is significantly impacted by extreme precipitation events (Tan et al., 2017) and consequent flooding (Durumin Iya, 2014). The recorded precipitation over Peninsular Malaysia over the past 40 years demonstrates a significant upward trend in the yearly total precipitation (Mayowa et al., 2015). Peninsular Malaysia has likewise experienced an escalating trend in the frequency of extreme precipitation occurrences (Mayowa et al., 2015). Despite existing trends, given the possible effects of increased possibility of the extreme precipitation on the community and the ecosystem, it is imperative to examine the anticipated future changes in precipitation in the area. Climate models are an important tool for examining the potential risks of the changing hydrological extreme from a scientific standpoint, strengthening disaster prevention and adaptation measures in the face of a changing climate.

According to Bates et al. (2010), GCMs are the most advanced methods to project global scale climate change using hydroclimatic data. Furthermore, Earth system models (ESMs) are also used to simulate historical and future climatic change (Li et al., 2018). GCMs are constrained to generate future global climate scenarios based on predicted future GHG emission scenarios. Due to the coarse spatial scale of GCMs and ESMs, they are less effective in resolving the Earth's topography, cloud physics, and land surface processes (Bao et al., 2015). As a result, the catchment/station application does not readily utilise the climatic scenario variables. Numerous downscaling strategies have been developed to reduce the coarse-scale climatic scenario variables to the catchment or station level (Wilby and Wigley, 1997). In addition, downscaling techniques are divided into two major categories: dynamical and statistical downscaling, described in the following sub-section. Also, a detailed comparison between dynamic downscaling and statistical downscaling techniques can be found in (Zhang et al., 2020a).

2.4.1 Statistical Downscaling Method

To close the gap between them, statistical correlations between GCM outputs and catchment or station-scale hydroclimatic variables are constructed. It also requires less computational work than dynamic downscaling, thus it is the most popular downscaling technique. The statistical downscaling approaches can be further sub-divided into a few categories: the most common statistical method applied was the statistical downscaling models (SDSMs) (Wilby et al., 2002), weather classification-based approaches (Lu et al., 2017), weather

generators-based approaches (Semenov and Barrow, 1997), and non-linear regression or artificial intelligence models. However, the SDSM model is only applicable to execute the daily data and predictor-predictants for future investigation on climatic impact in the study area. It may be problematic for the user as the data availability and limitation source is somewhat, a hindrance.

Weather classification-based methods need a local variable whose forecast depends on the "states" of the atmosphere on a large scale. Due to their local or hidden weather patterns, the states can be considered as a complicated system. A GCM compares the predicted future state of the atmosphere to its most similar past state. The historical state of the atmosphere that was chosen is linked to a value or set of values for the local variable. These are then replicated based on what the weather will be like. These methods are perfect for downscaling non-normal distributions, like the amount of rain that falls daily. To look at all possible meteorological situations, though, require a lot of daily observational data, like 30 years of daily observational data for the area of interest. Moreover, these methods are more computationally intensive than regression because of the vast amount of daily data that is analysed and created. Subsequently, in order to better comprehend this method, some previous studies utilising weather classification in engineering matters will be discussed. The weather classification approach was used to provide accurate solar power estimates for 21 solar photovoltaic (PV) installations in Germany (Amarasinghe et al., 2020). The authors recommended comparing the accuracy of solar PV forecasting with several single machine learning techniques, including [deep belief network (DBN), support vector regression (SVR), and random forest (RF) regression

models] and proposed ensemble models of weather classification using deep learning. The results obtained for the suggested ensemble models were then analysed by RMSE error, revealing the declines RMSE error by 10.49%, 7.78%, and 7.95%, respectively, for the DBN, SVR, and RF. In order to outperform other strategies, however, this ensemble approach with deep learning may necessitate GPUs rather than CPUs due to its reliance on massive amounts of data. Consequently, the cost to the end user increased because of implementing this strategy. Other than that, convolutional neural networks were the most used approach for integrating with weather classification (CNN). This integration is evident in the research (Villarreal Guerra et al., 2018) and in the literature (Elhoseiny et al., 2015). Similar to the DBN, the limitation of the CNN increases the complexity of its development because it requires a significant quantity of data, which can only be processed by GPU settings. Despite the fact that, regardless of how reliable the methods or approaches have been studied in the past, there were still uncertainties in the practical implementation. When the model forecasts over a longer time horizon, by the rule of thumb in terms of inaccuracy, may increase even more. Consequently, other standard single ML approaches may still be an alternative for the statistical downscaling topic. The weather generators approach, which is an alternative to weather classification, is discussed in the next paragraph.

Weather generators (WG) are also commonly employed in temporal downscaling (Schoof, 2013). For example, these methods make daily sequences of weather variables like precipitation, the maximum and minimum temperatures, humidity, and other variables either in monthly or annual mean basis. It also used

to maintain the physical coherence between the downscale climate variable, for instance, precipitation and temperature, also known as inter-variable dependence. Also, some impact models need local spatial data with a daily resolution that cannot be dependably obtained from GCMs. This is where temporal downscaling comes in. Moreover, hydrological modelling requires an accurate depiction of inter-site dependency. For instance, the absence of spatial connection for precipitation downscaling would mislead the streamflow extremes at the catchment outlet. This would result in the possibility of higher runoff in one sub-basin and lower runoff in the other sub-basin. WG are data-intensive, need long series of daily data, and can be affected by missing or wrong calibration data (Wilby et al., 2009). Li and Babovic (2019a) developed a multi-multivariate WG based on Empirical Copula (EC) approach (MMWG-EC), wherein meteorological time series were simulated from a single-site multivariate WG in the first stage. Then the EC approach was used to overcome the limitations of conventional WG in the second stage. Thus, some enhancement of weather generators has been shown in (Li and Babovic, 2019b) as multivariate WG to address the limitation. A few additional studies were conducted by including the WG in multivariate two-stage techniques, as indicated by Li et al. (2017) and Chen et al. (2018). Due to the temporal persistence (low-frequency variables) discovered in (Chen et al., 2018) and the Iman shuffling applied in (Li et al., 2017) to rebuild and overcome the limitations of WG. However, neither study could replicate the post-processed series' temporal persistence and inter-annual variability.

The non-linear regression techniques were widely used in statistical downscaling which include the Multi Linear Regression (Sachindra et al., 2014), Artificial Neural Network (Nourani et al., 2014; Ahmed et al., 2015), Support Vector Machine (Sachindra et al., 2013; Moazenzadeh et al., 2018; Danandeh Mehr et al., 2019), Genetic Programming etc (Sachindra et al., 2018a). All these techniques also known as machine learning techniques (Sachindra et al., 2018b; Xu et al., 2020). Among these non-linear regressions or AI or machine learning techniques, there is a massive ability on the characteristic of the ANN whereby, to derive the correlation between predictor and predictants (Nourani et al., 2013). There were also some other successful studies that implemented ANN in downscaling. In addition, Campozano et al. (2016) performed a comparison of the SDSM, ANN, and least square SVR (LS-SVR) approaches for the monthly downscaled precipitation on a watershed scale in southern Ecuador. The authors concluded that the ANN and LS-SVR were both more resilient than the SDSM, despite the SDSM matching the mean and standard deviation of the observed monthly precipitation for some months. Table 2.5 depicts the reason for the selection in the machine learning statistical downscaling method (ANN and SVR) in this study. The model structures for ANN and SVR are depicted in Figure 2.5 and Figure 2.6, respectively.

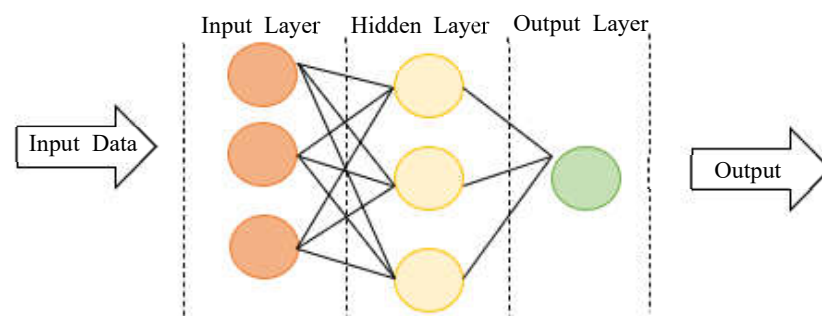


Figure 2.5: ANN structure

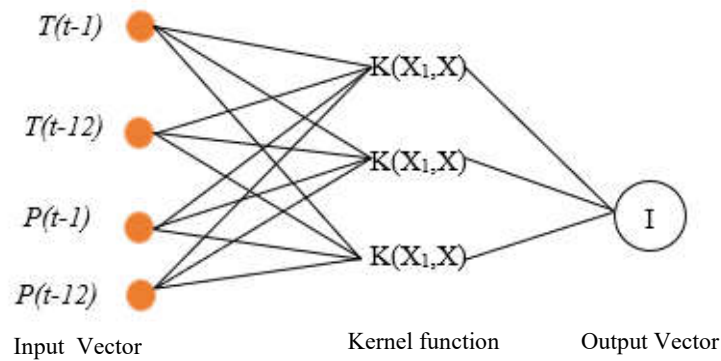


Figure 2.6: SVR structure

2.4.2 Dynamical Downscaling Method

Dynamical downscaling techniques are used in conjunction with physically based regional climate models, RCMs which are numerical models in which the GCM findings serve as the boundary conditions for the local climate domain (Guo and Wang, 2016; Wang, et al., 2017; Liang et al., 2019). RCMs can fine-tune physical atmospheric processes and simulate regional climatic characteristics at higher resolutions than GCMs given the same computational resources (Demory et al., 2020). Ensemble downscaling simulations using various RCMs and GCMs can deliver a more accurate estimation of the climate change and an uncertainty range (Xu and Yang, 2015). However, RCMs demonstrate considerable uncertainty in predicting precipitation over Southeast Asia, as their performance depends on the RCM configuration and the lateral boundary conditions derived from GCMs (Tangang et al., 2020; Nguyen-Thuy et al., 2021). In order to generate a more accurate regional climate projection, further research has applied bias correction techniques to the GCM data before

dynamical downscaling. There were various bias correction techniques applied in regional climate projection. For example, the latest studies that conducted by Rocheta et al. (2017) and Dai et al. (2020), utilised the bias correction of a multi-GCM ensemble and nested bias correction , respectively. Apart from that, mean bias correction (Holland et al., 2010) also known as linear bias correction, bias correction with physical consistent constraint (Meyer and Jin, 2016), mean and variance bias corrections (Xu and Yang, 2012), and Quantile-quantile correction (Colette et al., 2012). The further explanation of these methods by showing the advantages and limitation of respective methods was investigated by Xu et al. (2019). The comparison of the linear bias correction approach and the quantile bias correction method in monthly basis time frame has been shown in White and Toumi (2013). However, the quantile bias method has the substantial drawback of introducing spurious fluctuations to the GCM fields, increasing the variance in the RCM downscaled variables and harming the domain interior. The authors also noted that it is challenging to simulate extreme values using either method accurately. The climatological mean and the inter-annual fluctuations of the GCM were corrected using reanalysis data prior to RCM downscaling by utilising an improved linear bias correction approach. According to Xu and Yang (2012), this bias correction strategy considerably enhances downscaled temperature and precipitation extremes.

However, the complex design, massive computation, high computing cost of RCMs and manpower involved in the ensemble downscaling are significant disadvantages. Multimodal data resources were provided by the global Coupled Model Intercomparison Project (CMIP). Due to the limitations

of their coarse resolution and intermodal uncertainty, GCMs have been shown to be lacking the ability of resolving the specifics of localised climate change aspects (Moise et al., 2015; Ning and Bradley, 2016; Marotzke et al., 2017). For such reasons, in this study, the statistical downscaling method has been chosen. However, there are various groups under statistical downscaling, thus the following sub-section explains briefly which group should be selected for the implementation of the GCMs.

2.4.3 Summary of Downscaling Approaches

The following table summarises and compares the various aspects of dynamical and statistical downscaling.

Table 2.5: Summaries of the downscaling approaches

Aspects	Dynamic downscaling	Statistical downscaling
Provides	<ul style="list-style-type: none"> • Data from 20-50km grid cells • Data from sites with no observed data • Daily time-series • Time-series data on a monthly basis • Extreme event scenarios 	<ul style="list-style-type: none"> • Information at any scale, right down to the station level • Time series on a daily basis (SDSM method) • Time series on a monthly basis • Scenarios for any variable that is consistently observed

Table 2.5 (continued): Summaries of the downscaling approaches

Aspects	Dynamic downscaling	Statistical downscaling
Requires	<ul style="list-style-type: none"> • a large volume of data inputs 	<ul style="list-style-type: none"> • Computational resources that are required in medium to low level • A moderate volume of data inputs • A sufficient amount of observed data
Advantages	<ul style="list-style-type: none"> • Addresses both atmospheric and surface processes that happen at a relatively small grid scale than a GCM. • Not constrained by historical precedent, allowing for the simulation of novel scenarios. 	<ul style="list-style-type: none"> • The same method can be applied to other comparisons across different case studies regions, allowing for • Uses observed climate to drive future projections • Has the ability to supply point-scale meteorological variables for GCM-scale output
Disadvantages	<ul style="list-style-type: none"> • Uncertainty analysis is now possible with experiments involving an ensemble of RCMs • Computationally demanding • Limited number of RCMs available, with no model results for many regions • Various RCM assumptions generate different results. 	<ul style="list-style-type: none"> • Tools are widely available and simple to use • For many areas or variables, high-quality observed data may be unavailable. • Assumes that the relationships between large and small-scale processes will remain constant in the future (assumptions)

2.5 Hydrological Process Involved in a Reservoir

The following subsection briefly describes the variables involved in the hydrological process of a reservoir for the future climate scenario, as well as the approaches that have been used in prior studies that are also suited for the topography and climate of this study area.

2.5.1 Rainfall-Runoff Relationship

This sub-topic will introduce the rainfall-runoff relationship by providing a simple definition, describing the alternative approach available and supported by the Malaysian Department of Irrigation and Drainage (DID) for computing the rainfall-runoff relationship, also the difficulties and purpose of the procedure for selecting the appropriate method to use throughout this study.

Rainfall-Runoff is a relationship of the complex natural system that divides rainfall into surface runoff, evaporation, and moisture that is stored in the soil or groundwater (Peel and McMahon, 2020). The choice of rainfall-runoff approach or method is critical throughout the design flood estimating process if streamflow and rainfall records are available, as the objective of this study is to maximise the benefits of reservoir operation while minimising reservoir constraint. Additionally, an excessive flow of water to the downstream might result in a flooding incident. In addition, issues occurred when no such comprehensive records of rainfall are available, it can be done by setting up the instrument on the physical site for the period required to gather the hydrological data necessary to derive the design flood. However, the rain gauge was not 100%

found in complete records throughout the year. Besides, some records are not reliable as all the data present a similar value for a long period. These may be due to human error or failure of the instrument during the data collection or data download period. Also, it is significantly more time-consuming and generally more expensive in terms of liaising with numerous departments in order to acquire the entire dataset. Other than that, the mean area precipitation can be calculated with three methods, namely the station average method (Arithmetic Mean method), Thiessen polygon method, and isohyetal method. The details of these methods are not in the scope of this study as the aim of this study is the reservoir optimisation operation at KGD. Every method has its own pros and cons (Zhao et al., 2015). For instance, the arithmetic mean method can be straightforward and does not require a large amount of data or equipment to compute rainfall-runoff relation. However, its use is limited, and it rarely applies in real life scenarios. In addition, there are other aspects to consider (e.g., the area of the drainage basin not permitted to be large, the topographic inequality is small and rainfall station distribution must be homogenous). On the other hand, the Thiessen polygon method can be applied broadly, particularly in locations with an unequal distribution of rainfall stations. However, there were a few assumptions underlying this method: (a) the rainfall dataset is stable; and (b) the mean absolute percentage discrepancy increases when the catchment becomes smaller and rain gauge density becomes lesser. Finally, the isohyetal method is applied to a large-area region with obvious topographic variation and numerous rainfall stations. Unfortunately, this strategy is challenging to implement at KGD due to the limited availability of rainfall stations and topographic information. Besides the demerits mentioned, Hwang et al. (2020) have further examined the

other effects or limitations corresponding to the interpolation methods. Apart from that, the historical development of rainfall-runoff relationship models consists of various models which can be found in detail in (Peel and McMahon, 2020) including the brief elaborate of bottom-up and top-down approaches. The transition of rainfall-runoff relation development models, begin in the past few decades, there were studies conducted by utilising Artificial Intelligence (AI) approach (Daniell, 1991), followed by recent studies in AI methods for rainfall-runoff relation studies (Poonia and Tiwari, 2020; Safari, et al., 2020; Tikhamarine et al., 2020).

Hence, with all the above description which leaving the researcher the only option is to use a flood estimation procedure, to determine the design flood. Thus, this alternative is obviously more relevant, it must be employed in the absence of a complete hydrological record. There were four estimating procedures available in DID, Malaysia for computing rainfall-runoff relations. The detail of the various procedures by comparing each by catchment type and area will be further elaborated in Chapter 3.

2.5.2 Evaporation in Reservoir and its Approaches

When it comes to maintaining the water and heat balance of reservoirs/dams, evaporation is one of the most important processes involved. It is responsible for transporting enormous volumes of water and energy to the atmosphere through latent heat flow. Understanding the loss due to evaporation is extremely important when it comes to implementing water resource

management policies, as well as the operation and sizing of reservoirs, respectively. Furthermore, evaporation in tropical reservoirs has a significant impact on water quality, which can be adversely affected by increased concentrations of contaminants, and this must be taken into consideration while managing these assets. It is also necessary to have an accurate understanding of evaporation in reservoirs in order to discover the impact of climate change on society (Xu et al., 2020).

The escalating of the temperature threaten to reduce accessible surface water through increased evaporation, the evaporation process becomes even more critical. The studies conducted in Brazil in the context of climate change impact on the hydropower reservoirs in Brazil, by providing the current and future perspectives (Dias et al., 2018). The authors provided the overview and highlighted the main point of this study that the hydropower reservoir was an essential element in generating electricity in Brazil and shall be managed wisely. The intensity and length of rainfall are affected by climate change, as well as river discharge volume and the increased evaporation rate of reservoirs (Jahandideh-Tehrani et al., 2014). As a result, these factors interfere with the availability of water for energy generation and may result in indirect consequences such as changes in land usage and an increase in the demand for irrigation water (Sample et al., 2015). The rate of evaporation is influenced by a wide range of meteorological factors, such as the temperature differential between water and air, disparities in condensation pressure between water and air, wind speed, and solar radiation (Bhatt and Hossain, 2019; Yan et al., 2019) as well as the relative humidity of the surrounding air. However, estimating

evaporation rates in humid regions and other bodies of water is extremely hard due to the nonlinear behaviour of the different physical processes that drive vaporisation. Evaporation rates are also a sensitive indication of climate change (Wang et al., 2018b). Thus, more precise estimates of evaporation losses are critical for developing efficient water resource management plans and regulations (Kang and Park, 2014; Tinoco et al., 2016). Actual evaporation can be determined indirectly using empirical equations such as water balances, hydrometeorological, and energy balances, or experimentally via weighing lysimeters and remote sensing (Rana and Katerji, 2000). Compared to other experimental approaches, the lysimeter provided the most consistent method for determining the evaporation rate (Tao et al., 2018). However, the lysimeter approach is costly and time demanding, and it should only be used by highly qualified professionals (Jensen and Allen, 2016) also subject to significant uncertainties. As a result, empirical methods are devised for calculating the rate of evaporation.

The approaches to estimate the evapotranspiration rate varies according to the climatic variable's availability which were based on temperature, radiation and combination methods which being the most commonly applied. The initial way to estimate the evapotranspiration rate was by the use of FAO56 Penman-Monteith standards; some previous reviews utilising this approach can be obtained in (Allen, 1998; Valiantzas, 2018; Adnan et al., 2021). According to Muhammad et al. (2021), the proficiency of the FAO56 Penman-Monteith (PM) approach was evaluated across different regions, and the output of this shown the method's capability up to a certain level of reliability. However, the pitfall of

this method is the need for multiple meteorological characteristics as well as a large data span. Long-term data availability is critical for this method; however, not all developing nations have such long-term data availability (Lang et al., 2017; Shiri, 2017) .

The Thornthwaite model was the first temperature-based model, assuming an exponential relationship between average consumption and average temperature in a monthly basis (Thornthwaite, 1948). Blaney and Criddle (1950) established the temperature-based Blaney-Criddle model to have an approximate evapotranspiration rate in 1950; the most recent elaboration is available at (Blaney, 2017). This approach needs the meteorological data input of daylight hours and mean monthly temperature to determine the evaporation rate. Hargreaves and Samani (1985) devised the Hargreaves-Samani model for evapotranspiration rate estimation, which uses just the maximum and lowest temperatures, as well as radiation, as meteorological input factors. Makkink (1957) developed the Makkink model, which used just solar radiation as input factors to compute the evapotranspiration rate during a 10-day period in the Netherlands under a cold climatic condition. Turc (1961) introduced the Turc model for estimating evapotranspiration rate, with mean temperature, solar radiation, and relative humidity as needed meteorological parameters. Priestley and Taylor (1972) proposed the approach of estimating the evapotranspiration rate simply using the radiation parameter as an input.

Numerous studies have been conducted to compare the performance of various empirical estimate approaches. Kisi and Heddam (2019) investigated

evaporation in Turkey using solely temperature as input data and heuristic regression. Nourani et al., (2020) estimated evaporation using the Kharuffa approach, which is a temperature-based approach that requires only monthly mean temperature and monthly daytime hours used out of the yearly daytime hours of the year. However, this approach was discovered to be more appropriate for arid regions. Tukimat et al. (2012) concluded that the radiation-based technique beat the temperature-based approach in estimating the evaporation rate. The authors remarked that Turc model was suggested because of its simplicity and fewer input parameters. Muhammad et al. (2019) evaluated empirical evaporation conducted in Peninsular Malaysia using a compromise programming approach.

According to the analysis, the most appropriate estimation approach was the FAO-56 PM model, followed by Priestly and Taylor. However, because meteorological data may be challenging to get, the authors propose substituting Priestly and Taylor for FAO-56 PM. In general, it is quite difficult to determine the most appropriate approach for estimating the evapotranspiration rate since data availability and the topography of the study locations may make the approaches subjective. Chapter 3 will discuss the methodology used to estimate the evaporation rate at KGD in this study.

2.6 Future Water Demand Estimation

Climate is widely regarded as the most important determinant of a region's water balance (Middelkoop et al., 2001; Wang et al., 2015; Anang et al., 2017; Payus et al., 2020; Chan et al., 2021). As a result, changes in temperature caused by global warming could have a wide range of consequences for water resources. Climate change would likely result in significant temperature increases, which will affect evaporation and water demand (Xiao-jun et al., 2014). Besides, temperature is a key factor that is well-established, also the least uncertainties in GCM outputs (Liu et al., 2017). Numerous studies have been conducted to ascertain the effects of climate change on irrigation water demand across a range of geographical and climatic locations (Shahid, 2011; Al-Najar and Ashour, 2013; Wada et al., 2013). Näschen et al. (2019) developed a method named soil and water assessment tool (SWAT) for quantifying the impact of land use and climate change. The outcome of this study can be further utilised and improved by correlating with climatic models under few scenarios and developed a future reservoir optimisation operation policy

Water demand comes in a variety of forms and may affect the ecosystem as a result of climate change. They are categorised as agricultural, residential, and industrial. A critical piece of information given in Huang et al. (2018) whereby the authors did not transform and separate livestock water demand from irrigation water, despite the fact that irrigation water occupied for more than 90% of the overall agricultural water demand. With the preceding line, Du et al. (2021) showed that agricultural water demand in the future is determined by varying the

number of cropland and the amount of irrigation per unit of cropland. As a result of their lack of expertise on this complex subject, the authors made the decision to exclude the effect of climate change on irrigation rate per unit cropland area. For this reason, this would not be included in the scope of this study. The majority of KGD's downstream demand was and is for residential water demand. Sunil et al. (2021) investigated the future irrigation water demands for agricultural crops in India in the context of climate change using RCP 4.5 and RCP 8.5 climatic scenarios, respectively. The results indicated that irrigation demand for Kharif crops was greater under RCP 4.5 than under RCP 8.5, owing to the increased intensity of the forecasted rainfall values under RCP 8.5. This suggested that there is a greater likelihood of a flooding incident occurring under RCP 4.5. For Rabi crops, the average irrigation demand was lower under RCP 4.5 than under RCP 8.5, owing to the temperature increase under RCP 8.5. This phenomenon results in an increase in evaporation and a corresponding increase in water demand. Besides, residential water demand could be affected by many factors, such as population growth and climate change. Du et al. (2021) mentioned that there were few past studies by assuming the future residential water consumption will rise by 1% as daily maximum air temperature rises by 1°C in accordance to Al-Zubari et al. (2018).

In addition, a detailed review of integrating the effects of climate change and land-use can be found in (Pokhrel et al., 2018) at Mekong River Hydrology. Besides, a case study was conducted in Gauteng Province, Republic of South Africa (Zubaidi et al., 2020) to examine the historical trend of urban water demand using Artificial Neural Networks and Backtracking Search Algorithms

in order to forecast monthly water demand in the future under climate and population growth variability. The outcome of this case study assists the decision-makers and managers to improve the management of the current municipal water system and reservoirs, as well as to develop a more comprehensive plan for extension in response to the increased consumption in the downstream of study area. However, this case study relied solely on historical water demand trends to forecast future water demand due to a lack of thorough climate and demographic data. Nevertheless, the authors recommend that researchers to investigate other AI approaches in order to apply them to other study areas.

Apart from that, several studies have shown that land-use and land cover changed (LULCC) has an effect on the future trend of water demand, specifically in the area of cropland water demand using a dynamical downscaling approach (Näschen et al., 2019), biodiversity (Trisurat et al., 2019), and domestic water demand (Chishugi et al., 2021). With comprehensive studies, this study will apply climatic scenarios in terms of temperature as the major factor to generate a few scenarios for the future water demand trend. Also, by employing LULCC and population to generate various scenarios for future water demand at the KGD. Chapter 3 will go over the scenarios' application and a more detailed presentation of the formula.

2.7 Review on Reservoir Assessment Metrics

The three most common indices for measuring the levels of performance for a reservoir system are namely; reliability, resilience, and vulnerability (RRV). This set of evaluations were introduced by Hashimoto et al. (1982) and Fowler et al. (2003). Based on the past studies that were conducted by Hossain and El-Shafie (2013; 2014a) and KGD Hossain et al. (2018), similar reservoir assessment metrics had also been invoked. A review paper by Allawi et al. (2018) showed that one of the essential metric, periodic (R_p) to be applied for the reservoir optimisation operation correspond with the algorithms application and parameter involved is shown in Equation (3.59). The conventional approach to assessing reservoir performance includes the utilisation of resilience metrics, as discussed in the study was conducted by Asefa et al. (2014). Nevertheless, a novel metric was incorporated in this research. Shin et al. (2018) presented an extensive analysis of various indicators of resilience. In this study, the Water Storage Resilience (WSR) metric serves as a supporting measure of resilience. The final metric, the maximum annual deficit, is determined through a commonly used mathematical expression and is calculated by dividing it with the annual water demand.

2.8 Summary

Chapter 2 begins with an introduction that discusses the operation of reservoir systems and the optimisation techniques used in previous research. The methods for reservoir optimisation outlined and explored in previous studies include conventional optimisation, linear, non-linear, and stochastic dynamic

programming which were discussed and tallied. These approaches were justified in the text by describing their constraints and limitations, which resulted in the novel methods used in reservoir optimisation operations using heuristic methods. By careful identification of all these prior studies utilising the conventional optimisation and heuristic algorithms, it is crucial to further examine this topic by utilising MHAs. This was because MHAs have gained popularity in recent decades for their use in reservoir optimisation operations and are yet to explore at KGD. In addition, the nature of the strategy of these proposed MHAs in this study obtained the unique equilibrium strategy of the exploration and exploitation which is not found in conventional algorithms and heuristic algorithms that had been used in the previous studies conducted at KGD. Hence, the MHAs are proposed in this study to fill up one of the research gaps. Additionally, the impact of climate change on future reservoir operation and activities in prior studies were briefly discussed. However, majority of the climatic influence on future reservoir operations in prior studies were carried out via single GCMs. Furthermore, some of the studies used the SDSM approach as the downscale approach which is constrained to the daily time frame climatic variables. However, some portions of the research area may have data quality issues (missing data in majority) or insufficient predictor variable criteria to downscale the GCM, resulting in substantial uncertainty in the downscaled output's accuracy. In terms of dynamical downscaling, the pitfall was the limited number of RCMs available, with no model results for many regions and computationally demanding. Besides that, other than the common reservoir assessment metrics, the additionally support Water Storage Resilience (WSR) used to evaluate the resilience aspect in order to address the performance of the

reservoir system against climatic or hydrological variability. Thus, these motivates to fill up the other research gap of this study by investigating the impact of climate change on future KGD operation via ensembled GCMs in CMIP5 under various climate scenarios by utilising statistical downscaling approach.

CHAPTER 3

METHODOLOGY

3.1 Introduction

This chapter describes the metaheuristic algorithms (MHAs) that were used to simulate and optimise the current operation at the KGD for the base period data, also referred to as observed data, spanning the years 2001–2019. Additionally, the suggested metaheuristic algorithms were applied to the second observed timeline of 1987–2008 for the main purpose of comparing and validating them against previous studies that had been conducted at the KGD. The generated results are then analysed and evaluated using reservoir risk assessments that are typically used in reservoir optimisation topics. The subsequent segment of this investigation scrutinises the potential repercussions of climate change on KGD's operations, taking into account the stated three different climate change scenarios. (RCP 2.6, RCP 4.5, and RCP 8.5). Three time periods of the future climate scenarios are named as: (a) Near Future (2020-2049); (b) Mid Future (2050-2079); and (c) Far Future (2080-2099). As stated in Chapter 2, the merits and drawbacks of various optimisation techniques were briefly covered. However, not all approaches can be used and practised in similar optimisation problems because they are dependent on the sensitivity of the datasets and also due to their availability in each case study. This study was aimed to develop metaheuristic models capable of simulating and optimising reservoir operation at KGD, as well as determining whether the current reservoir

optimisation policy can cope with future climate change events and water demand. The flow of this chapter begins with the description of the case study site location, followed by the variables involved in this study, as well as the concept of the proposed algorithms, and lastly the problem formulation for the reservoir optimisation and reservoir risk assessments.

3.2 Flow of Methodology

The sequential order of reservoir operation optimisation began with conventional optimisation models, dynamic programming, and heuristic algorithms which included several studies as outlined in the previous chapter, where some of the algorithms performed inconsistently and took an exceptionally long time to convergence. Additionally, a tremendous computation burden was discovered in the reservoir operation optimisation. As a result, the diversity of metaheuristic algorithms (MHAs) has increased significantly during the last decade. However, further investigation is required due to the scarcity of knowledge regarding reservoir optimisation at the KGD via metaheuristic algorithms (MHAs). Figure 3.1(a) illustrates the overall flow of the study.

The data required for reservoir optimisation operation were then managed, and it consisted of two sections of historical datasets spanning the years (A) 2001–2019 and (B) 1987–2008. The first set of historical data from (A) 2001 to 2019 was utilised to optimise the current operation of KGD to

determine the robustness of the proposed MHAs and the reservoir risk assessments. The second set of historical data from (B) 1987 to 2008 was used in the proposed meta-heuristic algorithms to evaluate reservoir risk assessments, for comparison with previous prior studies as presented by Hossain and El-Shafie (2013; 2014a) and Hossain et al. (2018). The summary findings of these investigations were extensively utilised to compare with the proposed MHAs for this time frame. The historical variables were recorded in monthly intervals, and the variables involved, namely input, losses, release, demand, and storage, may be related and found in the continuous equation of the common reservoir. The flow of this analysis was then continued and depicted in Figure 3.1(b) by using the reservoir optimisation procedure in conjunction with the initialisation of the conceptual flow of the proposed MHAs until the objective function value reached the optimal value. The following sections further elaborate on the datasets used in this study. The flow of the analysis proceeds to the design of experiments (DoE), which utilised the Taguchi model to generate the response graph and ANOVA results. The intention of this DoE is to examine the effect of observed variables on the response graph to obtain the optimal reservoir release operation. The final stage before concluding observed reservoir optimisation operation analyses, was to conduct a reservoir risk analysis (observed period assessment).

Subsequently, the analysis acquired future climatic data from 2020 to 2099 for study on impact of future climate. The GCM data was then statistically downscaled. The Hydrology Procedure No. 11 (DID Technical Publications), gives the guidelines to the rainfall-runoff relationship that is used to compute the

inflow into the KGD. Also, the estimation of evaporation was through prediction with existing methods given in the literature and with measured temperature and radiation. The future downstream demand is also a vital variable in water supply reservoirs. The temperature and population growth factors were used in this study to anticipate future water demand. Once the reservoir simulation was satisfied, then the reservoir optimisation procedure was carried out in accordance with the proposed MHAs, and finally, the flow was completed with a reservoir risk analysis (climate assessment).

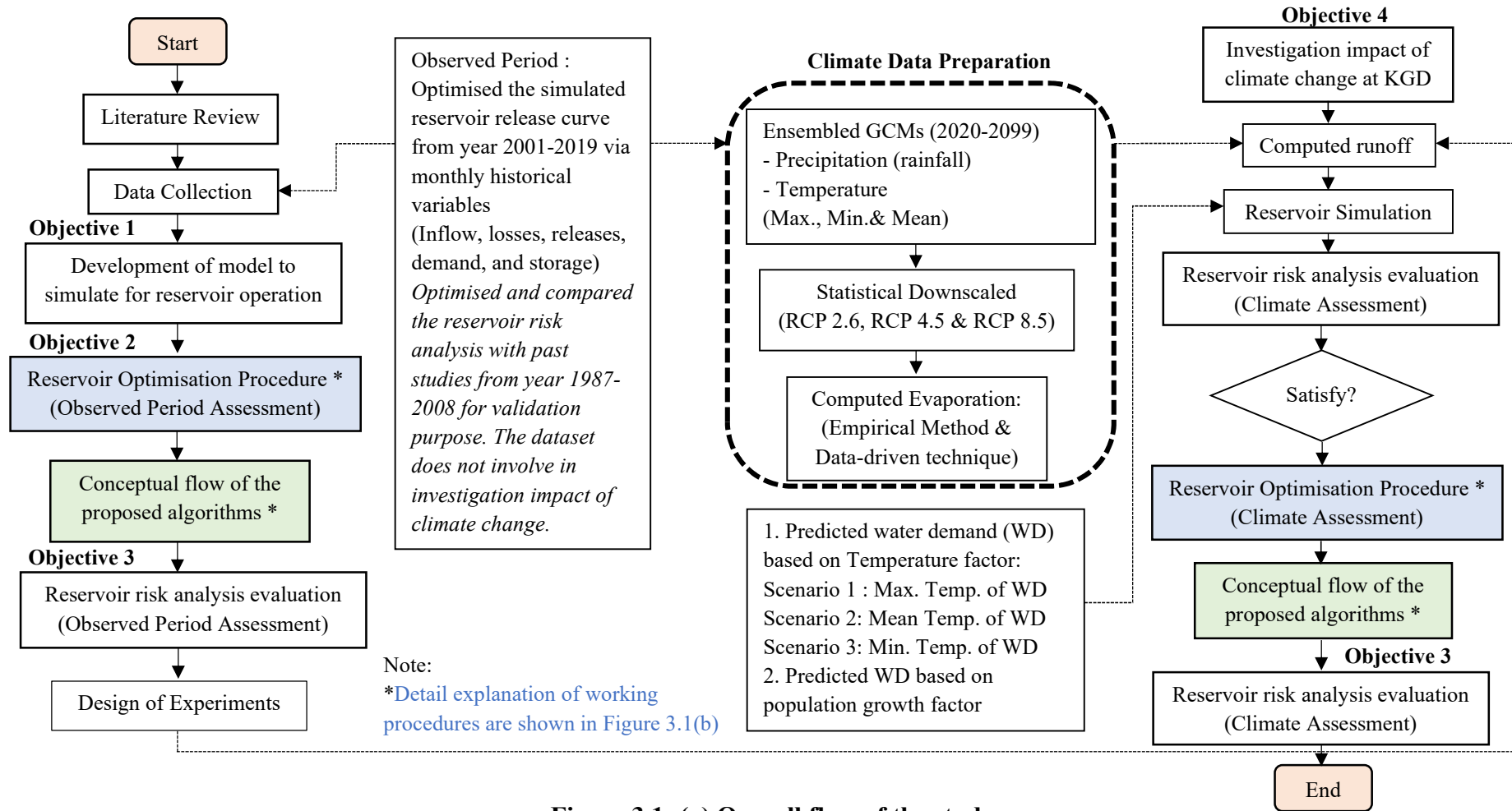


Figure 3.1: (a) Overall flow of the study

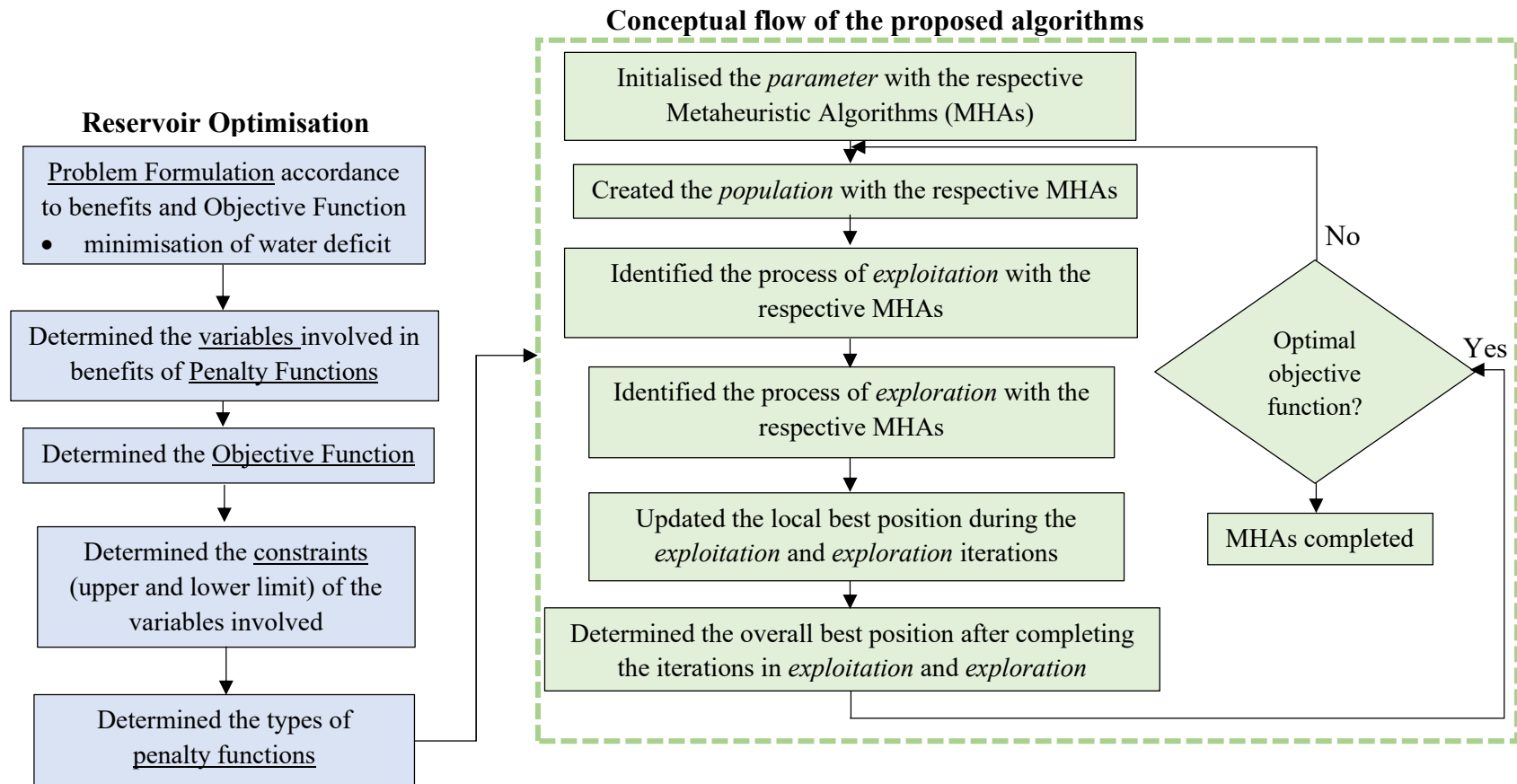


Figure 3.1: (b) Reservoir Optimisation Procedure and Conceptual flow of the proposed algorithms

3.3 Study Area

The study area is the KGD dam situated in the the heart of Kuala Lumpur, the Capital of Malaysia, and is located in the Gombak neighbourhood of Taman Melawati. The Bukit Tabur Dam is another name for it, and the rainfall station numbers are 3217002 and 3217004 respectively (Source: JPS). Figure 3.2 shows the map index of the Klang Gate Dam (KGD). The main purpose of this KGD was and still is, to distribute the potable water supply to the downstream of the water treatment plants (WTP) named as Bukit Nanas and Wangsa Maju, but it also serves as a flood mitigation dam. The features of the reservoir is presented in Table 3.1. Figure 3.2 displays a representation of the KGD which consists of inactive zone, conservation zone, and flood control zone. The estimation of the total capacity of the KGD is given in Figure 3.3.

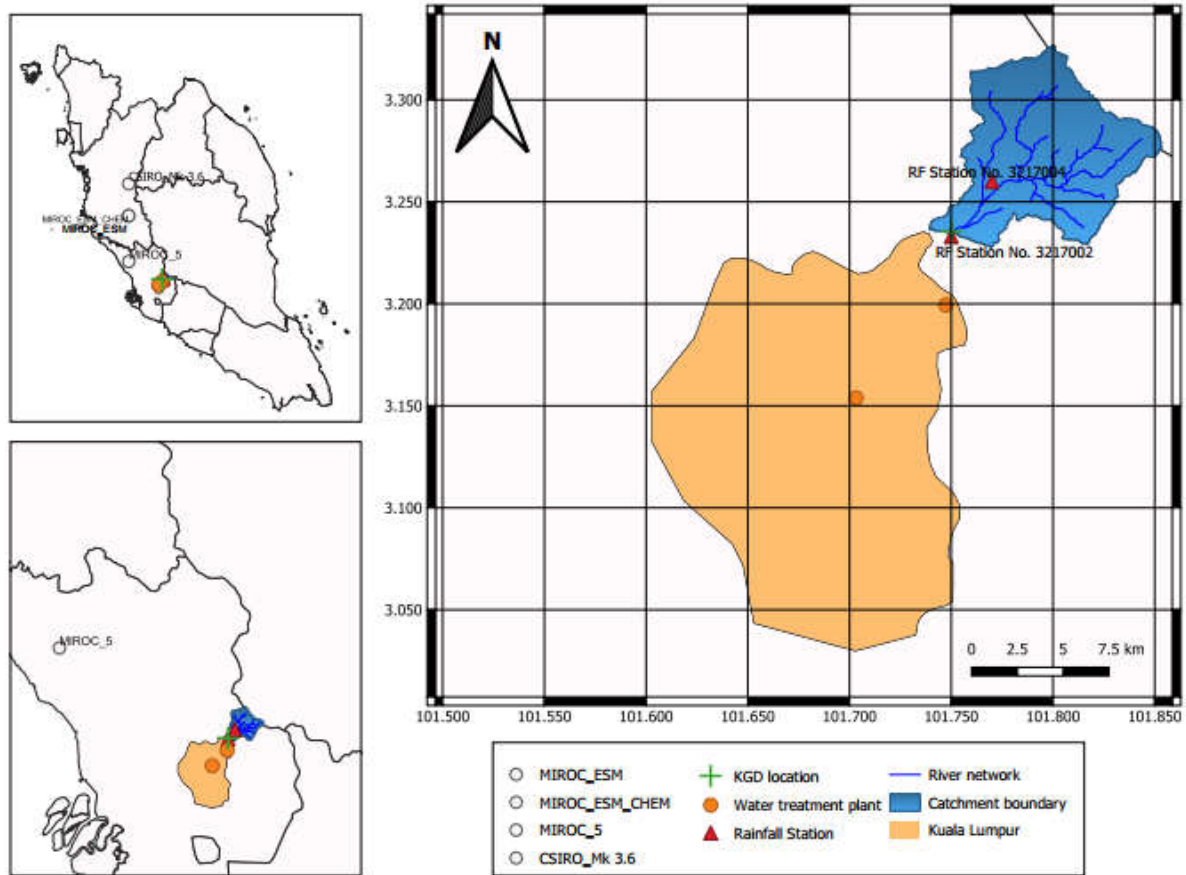


Figure 3.2: Case Study Area

Table 3.1: KGD features

Element	Explanation
Objective	Water supply and flood mitigation
Height	37.0metre
Length	138.7metre
Area of catchment	74.46km ²
Area of storage	2.70km ²
Overall capacity	32.02 million cubic metre (MCM)
Storage for inactive	3.2 million cubic metre (MCM)
Storage for flood control	6.2 million cubic metre (MCM)
Storage for conservation	22.6 million cubic metre (MCM)
Maximal Level	95.22metre ODL

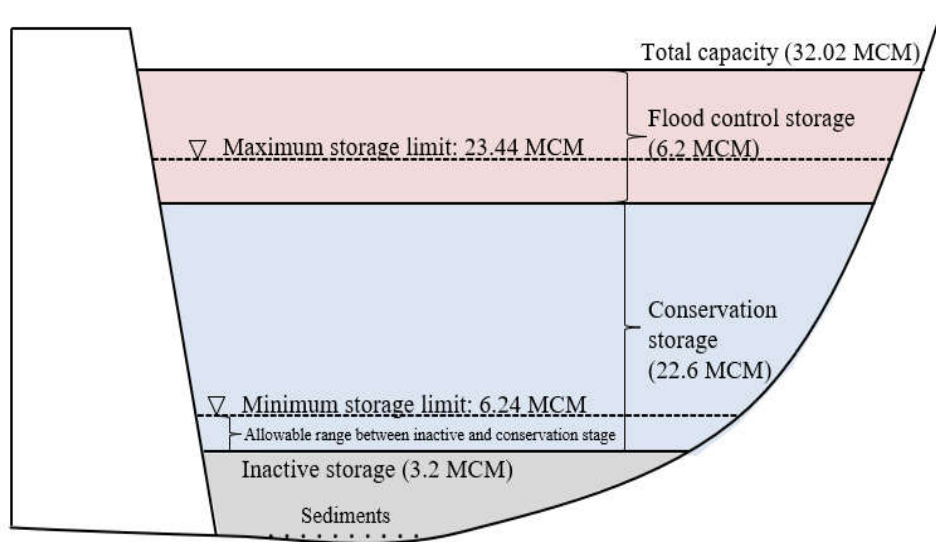


Figure 3.3: Illustration of the KGD’s reservoir (Lai et al., 2021)

3.4 Datasets

The datasets used for the observed period and the investigation of the impact of climate change (climate assessment) is outlined below.

3.4.1 Datasets from Year 2001 to 2019

The observed time data set comprised storage, inflow, evaporation rate, and discharge (Source: LUAS). The observed dataset is summarised in Table 3.2 with basic statistics presented in million cubic metres (MCM), were incorporated into the proposed algorithms for the purpose of the simulation and optimisation execution at the KGD. The inflow categories and KGD storage stages conditions are tabulated in Table 3.3 and Table 3.4, respectively. In addition, the monthly losses based on the range of the inflow to the KGD is tabulated in Table 3.5, and the respective months of the water demand is presented in Table 3.6.

Table 3.2: Monthly Descriptive Statistics in MCM unit

Variable/ Statistic	Inflow	Losses	Releases	Demand	Storage
Total Count	228	228	228	228	228
Mean	6.963	2.552	4.562	4.578	11.852
Stnd Dev	2.285	1.152	0.359	0.230	4.331
Sum	1,587.660	581.740	1,010.170	1,043.370	2,702.318
Maximum	17.790	5.000	6.013	4.920	23.932
Minimum	2.070	0.040	3.282	4.100	6.297
Median	6.785	2.430	4.563	4.565	11.111
Skewness	0.56	0.52	-0.70	-0.27	0.96
Kurtosis	1.45	1.13	4.81	-0.50	0.18

Table 3.3: Inflow Categories

Inflow Categories	Limits of Inflow (MCM)
High	More than 8.88 and above
Medium	3.88 – 8.87
Low	0.47 – 3.87

Table 3.4. KGD Storage Conditions (MCM)

Stage	Storage Conditions (MCM)
1	6.24
2	8.15
3	10.06
4	11.98
5	13.88
6	15.80
7	17.71
8	19.62
9	21.54
10	23.44

Table 3.5. Range of the L_t (MCM)

Inflow, I (million cubic metre, MCM)	Loss, L_t (million cubic metre, MCM)
Inflow from 1.89 and less than or equal to 3.78	0.04
Inflow from 3.79 and less than or equal to 5.68	1.78
Inflow from 5.69 and less than or equal to 7.57	2.43
Inflow from 7.58 and less than or equal to 9.46	2.80
Inflow from 9.47 and less than or equal to 11.35	5.00
Inflow more than or equal to 11.36	8.28

(Source: *Puncak Niaga (M) Sdn Bhd*)

Table 3.6: Monthly targeted Demand at KGD

Month	Targeted Demand (MCM)
January	4.92
February	4.10
March	4.36
April	4.44
May	4.54
June	4.81
July	4.76
August	4.57
September	4.39
October	4.56
November	4.59
December	4.89

(Source: Puncak Niaga (M) Sdn Bhd)

3.4.2 Datasets from Year 1987 to 2008

This sub-section elaborates on the base period study relying on 22 years of observed monthly rainfall data for the investigation of optimal release at the KGD from the year 1987 to 2008. The actual rainfall was converted into reservoir inflow. The monthly rainfall data are presented in millimetres and tabulated as a descriptive statistic in Table 3.7.

Table 3.7: Monthly Descriptive Statistic of Rainfall Data

Variable	Mean	StdDev	Sum	Minimum	Median	Maximum	Skewness	Kurtosis
1987	154.5	61.9	1853.9	72.5	145.5	256.1	0.29	-1.21
1988	144.6	67.8	1734.6	47.5	143.8	271.0	0.30	-0.67
1989	142.1	90.6	1704.8	20.5	116.9	311.3	0.64	-0.77
1990	137.6	65.7	1650.8	49.0	133.8	242.8	0.35	-1.01
1991	188.3	96.1	2259.2	16.8	189.2	308.2	-0.35	-0.88
1992	117.1	55.9	1404.8	17.0	138.5	192.4	-0.58	-0.83
1993	184.4	60.1	2212.8	103.6	167.7	296.7	0.75	-0.08
1994	201.1	125.9	2413.0	17.8	190.5	424.0	0.14	-0.72
1995	247.6	91.1	2971.0	85.5	255.9	359.7	-0.78	-0.31
1996	224.1	114.3	2689.0	22.5	239.5	411.5	-0.18	-0.75
1997	231.3	122.5	2775.7	119.9	194.3	521.0	1.52	1.88
1998	182.6	99.8	2191.5	53.0	152.6	412.5	1.12	1.29
1999	255.5	108.5	3065.8	104.5	260.5	399.3	0.04	-1.62
2000	285.0	102.2	3420.3	123.5	342.6	386.6	-0.49	-1.74
2001	234.0	131.0	2808.1	101.1	183.7	467.6	0.92	-0.47
2002	207.9	118.3	2494.5	16.0	215.3	421.7	-0.13	0.08

Table 3.7 (continued): Monthly Descriptive Statistic of Rainfall Data

Variable	Mean	StdDev	Sum	Minimum	Median	Maximum	Skewness	Kurtosis
2003	214.8	92.6	2577.3	99.2	215.6	394.0	0.44	-0.52
2004	221.6	137.9	2658.9	25.5	245.0	463.4	0.09	-1.03
2005	213.7	101.1	2564.9	9.6	233.0	334.0	-0.94	0.10
2006	253.6	78.9	3043.5	109.8	289.3	323.3	-0.85	-1.06
2007	245.4	100.1	2944.4	91.9	239.0	393.7	0.09	-1.22
2008	275.2	109.5	3302.8	72.3	302.9	431.5	-0.33	-0.67

Equation (3.1) elaborates on the inflow states utilised in Hossain (2013), in order to interpret the volume of the inflow whereby the rainfall flow into the catchment area of KGD during the month t .

$$I_t = 0.5 \times \text{catchment area} \times \text{rainfall}_t \quad (3.1)$$

which indicate I is inflow of the month t

Following that, the inflows were divided into three different states. The inflow benchmarking was the same as Table 3.3.

3.4.3 Datasets for Future Climatic Investigation

This section examined the impact of climate change on the optimal release of the KGD from 2020 to 2099, using future projection data. The monthly averages of the hydrological variables, reservoir demand, and temperature are

tabulated in Table 3.8 as parameters in the investigation of the impact of climate change for the base period (for year 1991- 2005). In addition, Table 3.9 tabulates the average values of the hydrological variables for various climatic scenarios (for year 2020-2099). Statistical downscaling methods were utilised in this study to determine the relationship between the predictants and predictor variables at the KGD via ANN and SVR: (i) radial basis function and (ii) polynomial kernel function. Table 3.10 contains the complete list of GCMs in the CMIP5 that correlate to the availability of RCPs for predictant variables. However, due to some predictor variables being unavailable, hence, to avoid any uncertainty during the downscaling, this study selected the RCPs with availability in both predictant-predictor variables. Next, the selection of climatic scenarios was based on the past implementation and execution of the majority of case studies. Additionally, the RCPs in each of the corresponding CMIP5 scenarios correspond to the data accessibility on the Earth System Grid Federation (ESGF) site.

The next step was to compute the rainfall-runoff relation and estimate evaporation for future periods using the *Kharuffa* Method, *Turc* Method, prediction-based of the data-driven techniques. Apart from that, the investigation of the climate assessment for the reservoir optimisation procedure based on temperature factor were classified into four Scenarios: Scenario 1: Base Period; Scenario 2: Maximum Temperature; Scenario 3: Mean Temperature; and Scenario 4: Minimum Temperature. Lastly, the execution of the climate assessment based on the forecasted population growth.

Table 3.8: Monthly average hydrological variables for the base period (1991–2005) under CMIP 5

Monthly average/ Description	1	2	3	4	5	6	7	8	9	10	11	12
Maximum temperature (°C)	32.8	33.2	33.3	33.3	33.2	33.0	32.5	32.5	32.7	32.6	32.6	32.6
Mean temperature (°C)	27.6	28.0	28.0	27.9	27.9	27.9	27.9	27.9	27.9	27.7	27.6	27.5
Minimum temperature (°C)	27.7	28.0	28.1	28.1	28.2	28.1	28.0	27.9	28.0	27.8	27.5	27.6
Precipitation (mm)	65.2	60.7	97.3	133.8	113.6	104.3	104.4	100.8	101.7	126.5	123.9	102.4
Inflow (Million cubic metre)	2.4	2.2	4.3	6.6	5.3	4.7	4.7	4.5	4.6	6.2	6.0	4.6
Evaporation (Million cubic metre)	0.5	0.5	0.5	0.5	0.6	0.6	0.6	0.6	0.6	0.5	0.5	0.5
Demand (Million cubic metre)	4.92	4.1	4.36	4.44	4.54	4.81	4.76	4.57	4.39	4.56	4.59	4.89

Table 3.9: Monthly average hydrological variables for climatic scenarios (2020 to 2099) under CMIP5

Monthly average/ Description	1	2	3	4	5	6	7	8	9	10	11	12
RCP 2.6												
Precipitation (mm)	189.45	193.30	209.41	236.31	253.67	259.00	252.92	254.71	254.96	253.14	234.60	210.03
Evaporation (MCM)	0.56	0.58	0.57	0.57	0.55	0.58	0.56	0.57	0.55	0.54	0.55	0.52
Maximum temperature (°C)	32.8	33.0	33.2	33.1	32.8	32.8	32.7	32.7	32.7	32.7	32.8	32.8
Mean temperature (°C)	25.5	26.1	26.3	26.0	25.6	26.0	25.8	25.8	25.7	25.5	25.5	25.3
Minimum temperature (°C)	26.7	27.1	27.2	27.1	26.8	27.0	27.0	27.0	26.9	26.9	26.9	26.6
RCP 4.5												
Precipitation (mm)	301.30	317.51	365.06	413.11	381.35	378.20	357.51	362.65	362.11	373.64	386.77	333.95
Evaporation (MCM)	0.57	0.59	0.59	0.58	0.58	0.59	0.57	0.57	0.56	0.56	0.57	0.54
Maximum temperature (°C)	32.5	32.5	32.42	32.4	32.4	32.4	32.4	32.5	32.5	32.5	32.5	32.5
Mean temperature (°C)	27.2	27.2	27.18	27.2	27.2	27.2	27.2	27.2	27.2	27.3	27.3	27.2

Table 3.9 (continued): Monthly average hydrological variables for climatic scenarios (2020 to 2099) under CMIP5

Monthly average/ Description	1	2	3	4	5	6	7	8	9	10	11	12
RCP 4.5												
Minimum temperature (°C)	26.6	26.8	26.9	26.8	26.7	26.8	26.7	26.7	26.8	26.9	26.8	26.5
RCP 8.5												
Precipitation (mm)	453.24	459.63	510.57	562.75	532.76	519.87	512.00	519.65	528.78	537.73	554.99	510.74
Evaporation (MCM)	0.56	0.59	0.58	0.58	0.58	0.58	0.57	0.57	0.56	0.55	0.54	0.53
Maximum temperature (°C)	32.5	32.5	32.4	32.4	32.4	32.4	32.4	32.5	32.4	32.5	32.5	32.5
Mean temperature (°C)	26.8	26.9	26.9	26.9	26.8	26.8	26.8	26.9	27.0	27.0	26.7	26.8
Minimum temperature (°C)	27.5	27.7	27.9	28.0	27.8	27.8	27.8	27.8	27.8	27.7	27.5	27.4

Table 3.10: CMIP5 GCMs (IPCC-AR5) for Predictant Variables

GCM	Institution/Modelling centre	RCP			
		2.6	4.5	6.0	8.5
BCC -CSM1.1	Beijing Climate Centre, China	O	O	O	O
BCC-CSM1.1(m)	Meteorological Administration	O	O	O	O
BNU-ESM	Beijing Normal University	O	O	X	O
CCCMA- CanESM2	Canadian Centre for Climate Modelling and Analysis	O	O	X	O
CESM1 -BGC	National Science Foundation,	X	O	X	O
CESM1 -CAM5	Department of Energy, National Centre for Atmospheric Research	O	O	O	O
CSIRO- ACCESS1.0	Commonwealth scientific and industrial Research Organisation (CSIRO) and	X	O	X	O
CSIRO- ACCESS1.3	Bureau of Meteorology (BOM), Australia	X	O	X	O
CSIRO-Mk3.6	Queensland Climate Change Centre of Excellence and Commonwealth Scientific and Industrial Research Organisation	O	O	O	O
EC - EARTH	European centre for medium range weather forecasts	X	X	X	O
FIO - ESM	The first institute of oceanography, State Oceanic Administration, China	O	O	O	O
GFDL - CM3	NOAA geophysical fluid dynamics	O	O	O	O
GFDL - ESM2G	Laboratory	O	O	O	O
GFDL - ESM2M		O	O	O	O

Table 3.10 (continued): CMIP5 GCMs (IPCC-AR5) for Predictant

Variables

GCM	Institution/Modelling centre	RCP			
		2.6	4.5	6.0	8.5
GISS-E2H	NASA Goddard Institute for Space	O	X	O	O
GISS-E2HCC	Studies USA	X	O	X	X
GISS-E2R		O	O	O	O
GISS-E2RCC		X	O	X	X
INM - CM4	Institute of numerical mathematics of the Russian Academy of Sciences	X	O	X	O
IPSL-CM5A-LR	Institute Pierre Simon Laplace	O	O	O	O
IPSL-CM5A-MR		O	O	X	O
IPSL-CM5B-LR		X	X	X	O
LASG-FGOALS- G2	Institute of Atmospheric Physics (LAGS) and Tsinghua University (CESS)	O	O	X	O
MIROC-ESM	University of Tokyo, National Institute	O	O	O	O
MIROC-ESM- CHEM	for Environmental Studies and Japan Agency for Marine-Earth Science and	O	O	O	O
MIROC-MIROC5	Technology	O	O	O	O
MOHC- HadGEM2-CC	UK Met Office Hadley Centre	X	O	X	O
MOHC- HadGEM2-ES		O	O	O	O
MPI-ESM-LR	Max Planck Institute for Meteorology	O	O	X	O
MPR-ESM-MR		O	X	X	O
MRI-CGCM3	Meteorological Research Institute	O	O	O	O

Table 3.10 (continued): CMIP5 GCMs (IPCC-AR5) for Predictant**Variables**

GCM	Institution/Modelling centre	RCP			
		2.6	4.5	6.0	8.5
NCAR - CCSM4	US National Centre for Atmospheric Research	O	O	O	O
NCC - NorESM1 -M	Norwegian climate centre	O	O	O	O
NIMR - HADGEM2 - AO	National institute of meteorological research and Korea meteorological administration	O	O	O	O

3.4.4 Selection of GCMs in CMIP5

As depicted in Table 3.11, the resolution of the four selected GCMs are in acceptable and finer resolution. The consideration of these modelling centre based in Asia and Australia is also depending on the availability of the RCPs data as shown in Table 3.10. Apart from that, there are also no specific rules or standard operating procedures for selecting how many GCMs can be implemented in the climate change assessment for the future reservoir optimisation operation and there are no fixed rules of the predictor variables selection for downscaling of GCMs (Chu et al., 2010). Thus, one to three predictors are frequently sufficient. For example, by analysing the downscale of GCMs for precipitation predictors, it is possible to determine that precipitation is dependent on and affected by gravity, winds, and temperature. On the other hand, there were prior studies conducted in this aspect by claiming that a single GCM execution in climate change assessment was discouraged (Tan et al., 2014;

Hussain et al., 2018). Further elaboration on this aspect corresponding to South Asia, East Asia, and South East Asia for GCMs in CMIP5 was reported by Hussain et al. (2018). Furthermore, there was a case study which investigated the future reservoir optimisation operation with three GCMs selection at Shahrchay dam, West of Iran (Nourani et al., 2020). The numbers of the GCMs selection chosen that were involved in climate change aspects for the respective case studies are presented in Table 2.4.

Table 3.11: Resolution for the selected GCMs

Model name/Country	Atmospheric Resolution (Degree; Lat x Lon)	Nearest Site to the Study Area (Degree; Lat x Lon)
CSIRO-Mk 3.6	1.9x1.9	4.7x101.3
MIROC 5	1.4x1.4	3.5x101.3
MIROC-ESM	2.8x2.8	4.2x 101.3
MIROC-ESM-CHEM	2.8x 2.8	4.2x 101.3

In view of the numerous predictors under the CMIP 5 that had been figured out that would match with the selected four GCMs as well as the RCPs, hence, first of all, the trial and error procedure was carried out to identify the overall best R^2 for the base period. Numerous researchers have utilised this method extensively (Nourani et al., 2020; Jaiswal et al., 2021) As a result, Table 3.12 presents the predictor and predictants variables that has been identified with the overall best combinations.

Table 3.12: Conceivable combinations of predictant-predictor variables under CMIP5

Predictants Variables	Predictor Variables
<i>Pr</i>	<i>Zg, Tas, Ua, Va</i>
<i>Ta</i>	<i>rsds, Zg, hus, Tas</i>
<i>Tas_Max</i>	<i>rsds, Zg, hus, Tas_Max</i>
<i>Tas_Min</i>	<i>rsds, Zg, hus, Tas_Min</i>
Solar Radiation	<i>Ta, Tas_Max, Tas_Min, rlds</i>

Note: Pr = Precipitation; Ta = Mean Temperature; Tas_max = Maximum Temperature; Tas_Min = Minimum Temperature; Zg = Geopotential Height; Ua = Eastward Wind; Va = Northward Wind; rsds = Surface Downwelling Shortwave Radiation; Tas = Near-surface Air Temperature; hus = Specific Humidity; rlds = Surface Downwelling Longwave Radiation

3.4.5 Missing Data in Future Projected Climatic Scenario

Missing data can seriously impact quantitative research, causing parameter estimates to be biased, information to be lost, statistical results to be reduced, standard errors to be increased, and finding generalisability to be weakened. The majority of early-stage studies used listwise, pairwise, or mean substitution methods to deal with missing data (Schafer, 1997). Despite their simplicity, these methods are notorious for producing biased and/or inefficient estimates (Myers, 2011).

Aside from that, there is another approach to dealing with missing data. To solve this issue, the interpolation method required more than two data stations. This interpolation method incorporates several techniques, including Arithmetic Average, Normal Ratio, and Inverse Distance. Some studies on these methods

have been conducted in climate change studies, particularly for predictors-predictants relationships in precipitation and temperature (Wan et al., 2017; Abdulla, 2020).

The Maximum likelihood (ML), expectation maximisation (EM), and multiple imputation are however, more statistically appropriate methods for dealing with missing data. Based on the available data, the ML procedures model the missing data and treat the accessible data as a sample that accurately represents a certain distribution. Basically, machine learning aims to create models that maximise the probability of discovering observed relationships in the data. Although the process is iterative, the EM is similar to the ML procedures for dealing with missing data. Finally, in this study, the multiple imputation technique with SPSS was used to fill in the missing data of the time series for the climate scenarios in precipitation and temperature.

3.5 Data Preparation Stages for Climate Assessment

The following sub-sections describe the stages involved in the investigation of climate assessment. It consists of rainfall-runoff relationship, estimation of evaporation, estimation of future water demand based on temperature factor and population growth. The last sub-section 3.5.4 is the description of the statistical model performances evaluation.

3.5.1 Computation of Rainfall-Runoff Relationship

In Table 3.13, the Regional Flood Frequency Method and the Rational Method in the Hydrological Procedures (HP) 4 and the HP 5, respectively, give a method for predicting the design flood peak. These approaches are adequate for engineering work involving the consideration of storage upstream of the structure (rural catchment type)., A more recent revised version in 2018 is the Design Flood Hydrograph, HP 11, which is acceptable for calculating the rainfall-runoff relationship was adopted for this study under a variety of climate conditions. In order to determine the inflow into the KGD from the rural catchment, the total storm rainfall was multiplied by the area of storage of KGD (Table 3.1). For Peninsular Malaysia, where P is the total storm rainfall in mm and Q is direct runoff in mm as shown in Equation (3.2) and Equation (3.3), respectively.

$$Q = 0.33 P; \quad P < 75mm \quad (3.2)$$

$$Q = P^2 / (P+150); \quad P > 75mm \quad (3.3)$$

Table 3.13: Summaries of three estimation procedure for rural catchment recognised by DID, Malaysia

Methods	HP No.	Year Published/ (Revised)	Area, km ²	Catchment Type	Variable involved
Regional Flood Frequency	4	1987	>20	Rural	Rainfall
Rational Method	5	1974	13-104	Rural	Rainfall
Design Flood Hydrograph	11	1980 (2018)	<518	Rural	Rainfall

3.5.2 Estimation Method for Evaporation

Evaporation or potential evaporation is a crucial component in hydrological and irrigation planning design. Despite the fact that this parameter is so crucial, there has not yet been created a practical, highly accurate way for determined it. Furthermore, no single strategy is universally reliable; instead, it is necessary to select the models that are most appropriate for a study area. This study therefore presented two empirical evaporation methods based on temperature and radiation for future RCPs. In order to validate the *Kharuffa* and the *Turc* methods, prediction-based of the data-driven strategies (SVR-PKF and SVR-RBF) were utilised to anticipate by employing temperature variables and by combining temperature and solar radiation variables which act similarly to the *Kharuffa* and *Turc* mathematical statements.

(a) Empirical Evaporation Method - *Kharrufa* Method

Nourani et al. (2020) utilised the *Kharrufa* Method to estimate the evaporation at Iran for both baseline and climatic scenarios in a monthly basis. The expression is represented by Equation (3.4).

$$E_d = 0.34 \times p \times T_{mean}^{1.3} \quad (3.4)$$

(b) Empirical Evaporation Method - *Turc* Method

A radiation-based evaporation method that averagely combined the variables as listed in Equation (3.5) and Equation (3.6) in order to estimate the evaporation rate for the various climatic scenarios.

For $RH < 50\%$,

$$E_d = 0.013 \left(\frac{T_{mean}}{T_{mean}+15} \right) (R_s \times 23.8846 + 50) \left(1 + \frac{50-RH}{70} \right) \quad (3.5)$$

For $RH > 50\%$,

$$E_d = \left(\frac{T_{mean}}{T_{mean}+15} \right) (R_s \times 23.8846 + 50) \quad (3.6)$$

where E_d is the depth of the reservoir evaporation in a month (mm/month); p is summation of the monthly daylight hours correlate to the summation of the yearly daylight hours (12 X 365) (Kharuffa, 1985; Xu and Singh, 2001); T_{mean} is the average temperature ($^{\circ}C$) in a monthly basis; RH denotes the relative air humidity in percentage; R_s represents of the solar radiation proportion to the surface of the crop (Wm^{-2}).

(c) Data-Driven Techniques for Prediction of Evaporation

Based on factors related to temperature and radiation empirical methods, the following equations show potential combinations for future evaporation prediction and is expressed in E_d (mm/month) and in order to get cubic metre per month, E_v (m^3 /month) is calculated by the production of the surface area of the KGD.

By employing temperature-based concept of prediction:

$$\begin{aligned} \text{Stnd Prediction of Evaporation}_{x,Temp.} = & \text{Stnd } T_{mean,x} + \text{Stnd } T_{max,x} + \\ & \text{Stnd } T_{min,x} \end{aligned} \quad (3.7)$$

By combining temperature and radiation-based concept of prediction:

$$\begin{aligned} \text{Std Prediction of Evaporation}_{x,Temp.+Radiation} &= \text{Std } T_{mean,x} + \\ \text{Std } T_{max,x} + \text{Std } T_{min,x} + \text{Std } T_{RS,x} & \end{aligned} \quad (3.8)$$

where x represents the three RCPs climate scenarios in this study; *Std* represents the variables undergo the standardisation before proceeding to the prediction.

3.5.3 Estimation of Future Water Demand

- (a) Estimation of Future Water Demand Based on Temperature-factor under various scenario of climatic variables

Anang et al. (2017) discovered that various parts of the water supply pattern are affected in some way by climate change in terms of water availability, quality, and quantity. For instance, during the dry season, the downstream resident needed higher water demand as such must increase its consumption and water supply. Consequently, this study examined on how meteorological parameters affected and the temperature as a key factor in determining water consumption by predicting the future water demand using ANN as presented in Equation (3.9) – Equation (3.11).

$$\begin{aligned}
& \textit{Stnd Prediction Max.Temperature of Water Demand}_x = \\
& \textit{Stnd Water demand}_{obs} + \textit{Stnd Inflow}_x + \textit{Stnd Evaporation}_x + \\
& \textit{Stnd Pr}_x + \textit{Stnd Max.Temp}_x
\end{aligned} \tag{3.9}$$

$$\begin{aligned}
& \textit{Stnd Prediction Mean Temperature of Water Demand}_x = \\
& \textit{Stnd Water demand}_{obs} + \textit{Stnd Inflow}_x + \textit{Stnd Evaporation}_x + \\
& \textit{Stnd Pr}_x + \textit{Stnd Mean Temp}_x
\end{aligned} \tag{3.10}$$

$$\begin{aligned}
& \textit{Stnd Prediction Min.Temperature of Water Demand}_x = \\
& \textit{Stnd Water demand}_{obs} + \textit{Stnd Inflow}_x + \textit{Stnd Evaporation}_x + \\
& \textit{Stnd Pr}_x + \textit{Stnd Min.Temp}_x
\end{aligned} \tag{3.11}$$

x indicated the RCP 2.6, RCP 4.5, and RCP 8.5; *Stnd* represents the procedure of the standardisation for the respective variables; *obs* stands for the observational data for water demand.

- (b) Estimation of Future Water Demand Based on Population Growth Forecasting and in conjunction with LULCC Detection Map as evidence

The design of water supply network at the downstream of KGD was completed considering the temperature factor under the climatic scenario given in section 3.6.2. The estimation of future water demand can be further refined into an idea by estimating the population growth as well as examining and

validating the forecasted population growth in conjunction with the LULCC detection map, as this would be more visual than a tabulated figure of the population changes in the city over the years. The current and historical population data for Kuala Lumpur were derived from census population records (Sources of data: Department of Statistics, Malaysia). Following the collection of these data, population forecasting can be estimated using a variety of techniques, as described in (Mohamad et al., 2020). In this study, geometrical increase method was chosen for the population growth technique, as presented in Equation (3.12). The population growth of Kuala Lumpur city by employing the geometrical increase method is tabulated in Table 3.14. Meanwhile, the LULCC detection maps from 1988 to 2021 are illustrated in Figure 3.3 to Figure 3.5, respectively.

$$P_n = P \left(1 + \frac{IG}{100} \right)^n \quad (3.12)$$

where P population at present ; n number of decades ; IG geometric mean (%)

Table 3.14: Population Growth at Kuala Lumpur from year 1988 to 2019

Year	Population ('000)	Increment ('000)	Growth (%)
1988	1169.6		
1989	1194.1	24.5	2.05
1990	1217.8	23.7	1.95
1991	1262.1	44.3	3.51
1992	1281.5	19.4	1.51
1993	1298.7	17.2	1.32
1994	1314.4	15.7	1.19
1995	1328.9	14.5	1.09
1996	1342.5	13.6	1.01
1997	1356.4	13.9	1.02
1998	1373	16.6	1.21
1999	1394	21	1.51
2000	1416	22	1.55
2001	1446.2	30.2	2.09
2002	1474.1	27.9	1.89
2003	1500.5	26.4	1.76
2004	1526.4	25.9	1.70
2005	1551.8	25.4	1.64
2006	1577.5	25.7	1.63
2007	1603.3	25.8	1.61
2008	1628.9	25.6	1.57
2009	1652.8	23.9	1.45
2010	1674.8	22	1.31
2011	1693	18.2	1.08
2012	1702.1	9.1	0.53
2013	1723.4	21.3	1.24
2014	1737.4	14	0.81
2015	1780.4	43	2.42
2016	1789.7	9.3	0.52
2017	1793.2	3.5	0.20
2018	1790	-3.2	-0.18
2019	1782.5	-7.5	-0.42
Total		612.9	41.76
Average		19.8	1.35

The geometrical increase method was used to calculate the population growth index each year. The average percentage of population growth in Kuala Lumpur city is shown in Table 3.14, with an average of 19,800 people per year or 1.35 percent of population growth. With the above average percentage growth index, thus the population forecasting results from year 2020 to 2099 can be determined as $P_{1988} = 1,169,600$, $r (\%) = 1.35$, $P_{2019} = 1,782,500$ and with the interval of $t = 31$.

The average projected population number in Kuala Lumpur city in 2099 is 4,673,800, which is nearly 60% of the current total population. The LULC for the years 1988, 2010, and finally 2021 has represented in Figure 3.4. The information in the figure shows that the built-up area was becoming increasingly being developed in 2021, but in 1988, the forest and grass areas landscape had remained the majority landuse in Kuala Lumpur then, which is downstream of the KGD. Figures 3.5 and Figure 3.6 depicted the detection maps from 1988 to 2010 and 2010 to 2021, respectively. However, it is difficult to see any substantial difference between the two figures. As a result, Table 3.15 was created for the purpose of detecting changes in the years 1988, 2010, and 2021 and was expressed in km^2/year . The LULC changes include Forest Area (FA), Green Area (GA), Water Bodies (WB), and Built-up Area (BA). Water bodies, forest area, grass area, and built-up area all remained constant at $187 \text{ km}^2/\text{yr}$, $546 \text{ km}^2/\text{yr}$, $613 \text{ km}^2/\text{yr}$, and $5,126 \text{ km}^2/\text{yr}$, respectively. However, FA-WB results reflect a change of $297 \text{ km}^2/\text{yr}$ between 1988 and 2010.

Table 3.15: LULCC Detection Maps during 1899 vs 2010 and 2010 vs 2021

	<u>1988 vs 2010</u>	<u>2010 vs 2021</u>
LULC Changes	km ² /year	km ² /year
Water Bodies, WB (No Change)	187	462
FA-WB	297	95
GA-WB	171	254
BA-WB	260	1,016
WB-FA	59	162
Forest Area, FA (No Change)	546	1,055
GA-FA	209	914
BA-FA	97	461
WB-GA	192	335
FA-GA	489	312
Grass Area, GA (No Change)	613	1,538
BA-GA	483	2,220
WB-BA	668	795
FA-BA	1,041	285
GA-BA	1,401	700
Built up Area, BA (No Change)	5,126	12,088

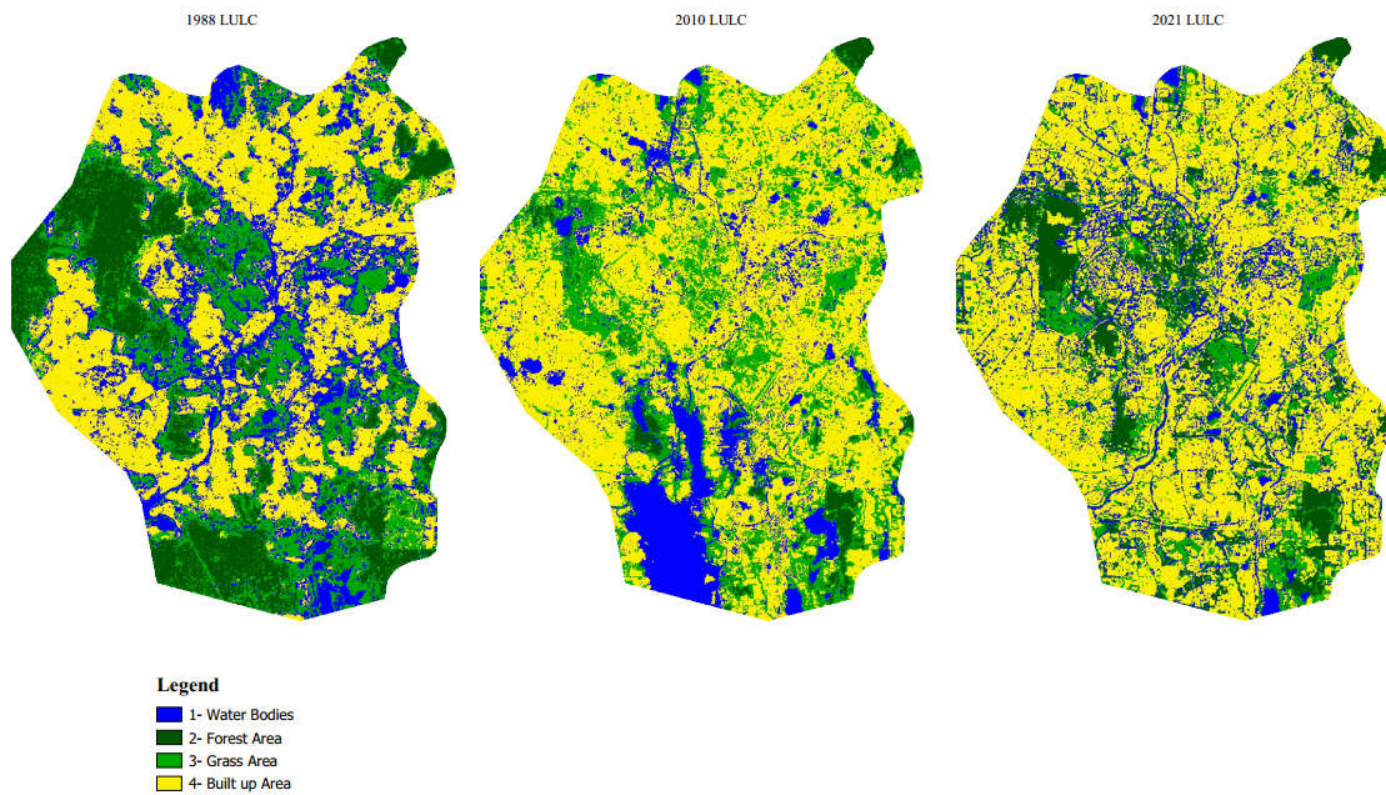


Figure 3.4: LULCC Detection Map from year 1988 to 2021

LULC Change Detection Map at downstream of KGD During 1988 to 2010

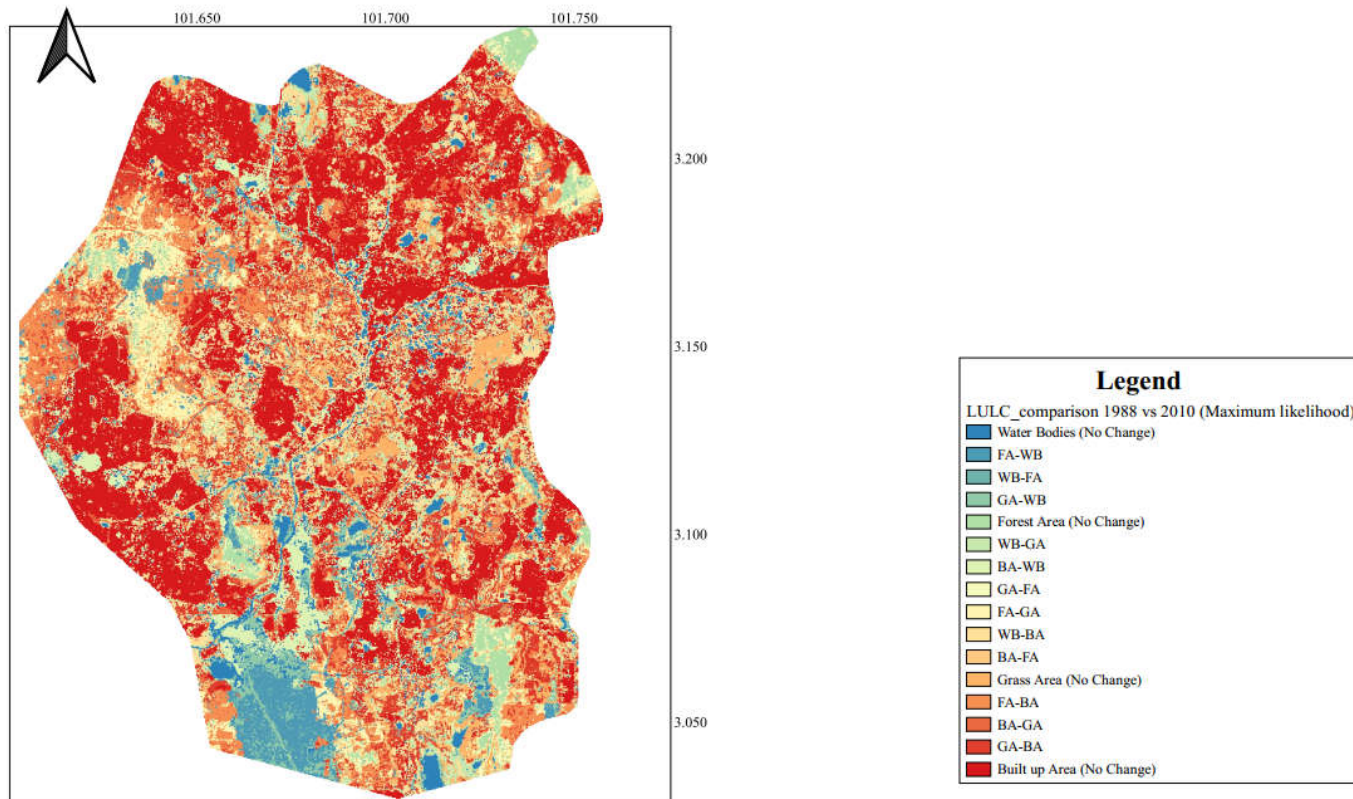


Figure 3.5: LULCC Detection Map at downstream of KGD During 1988 to 2010

LULC Change Detection Map at downstream of KGD During 2010 to 2021

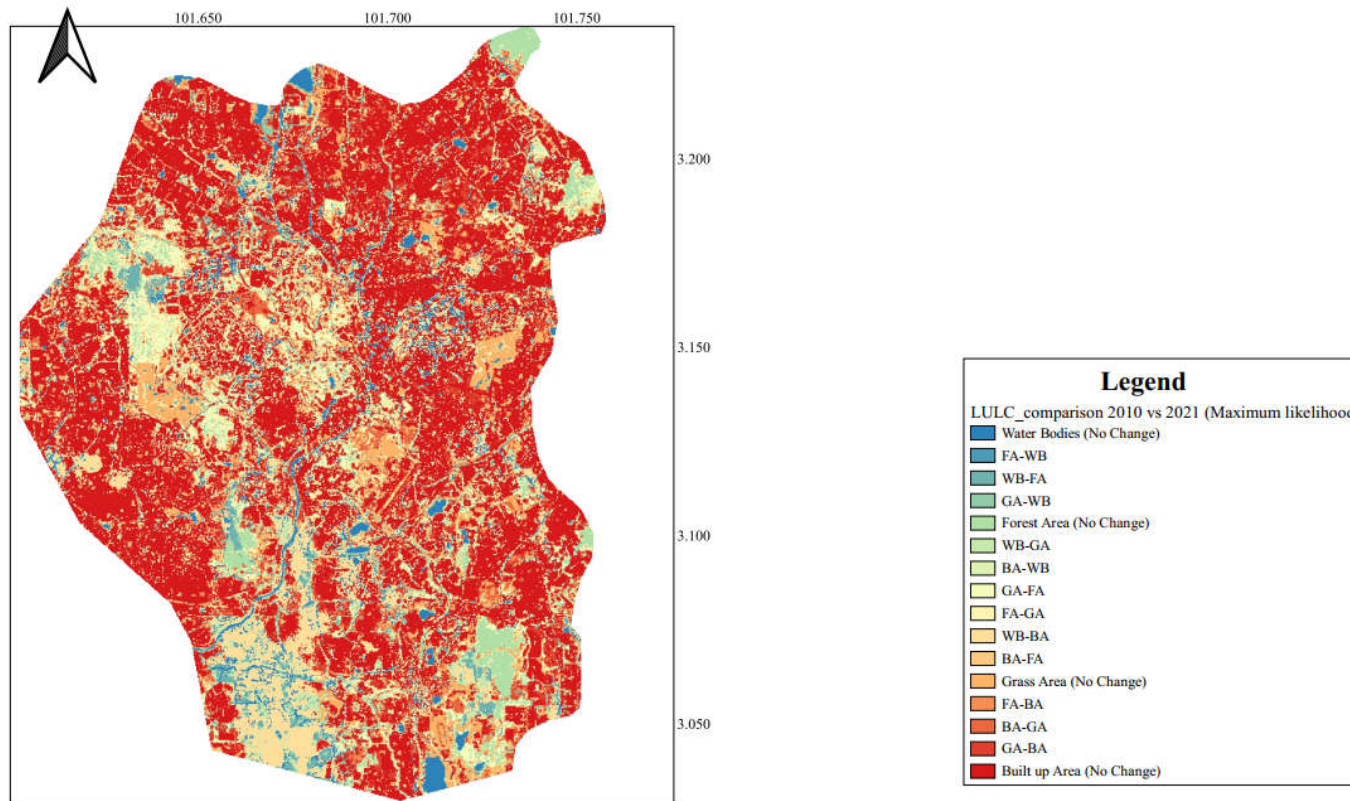


Figure 3.6: LULCC Detection Map at downstream of KGD During 2010 to 2021

3.5.4 Statistical Model Performance Evaluations

There are various indices employed for the purpose of evaluating the statistical model performances of the uncertainty in the climatic model. In this study, the Nash-Sutcliffe efficiency, the Percent Bias, and the Coefficient of Determination, were used and evaluated for the climate change impact. The additional statistical error performance such as RMSE and MAE were used to evaluate the model performance in future projected data and other which involved of the implementation data-driven techniques.

(a) Nash-Sutcliffe Efficiency (*NSE*)

The values range from $-\infty$ to 1, with a higher value indicating better model performance (Begou et al., 2016). It also determines how much the residual variance (also known as "noise") varies from the observed data variance. Equation (3.13) is used to calculate the *NSE*.

$$NSE = 1 - \frac{\sum_{i=1}^n (Y_i^{target} - Y_i^{sim})^2}{\sum_{i=1}^n (Y_i^{target} - \bar{Y}^{target})^2} \quad (3.13)$$

(b) Percent Bias (*PBIAS*)

As indicated in Equation (3.14), *PBIAS* examines the model's calculation bias. Positive and negative *PBIAS* values showed model underestimation and overestimation bias, respectively, whereas small magnitude values indicated more accurate model simulations (Begou et al., 2016).

$$PBIAS = \frac{\sum_{i=1}^n (Y_i^{sim} - Y_i^{target}) \times 100}{\sum_{i=1}^n Y_i^{target}} \quad (3.14)$$

(c) Coefficient of Determination (R^2)

The values ranges from 0 to 1 whereby the value closer to 1 indicates the error is low and vice versa, the values equal to or more than 0.5 are commonly considered acceptable in watershed scales, which is calculated using Equation (3.15) (Begou et al., 2016).

$$R^2 = \left(\frac{\sum_{i=1}^n (Y_i^{target} - \bar{Y}^{target})(Y_i^{sim} - \bar{Y}^{sim})}{\sqrt{\sum_{i=1}^n (Y_i^{target} - \bar{Y}^{target})^2} \sqrt{\sum_{i=1}^n (Y_i^{sim} - \bar{Y}^{sim})^2}} \right)^2 \quad (3.15)$$

(d) Root Mean Square Error ($RMSE$)

The root mean square error ($RMSE$) is a commonly used measure of the difference between the values simulated by a model and the actual observation data (targeted). The lower the value in this indicator represents better model performance with minimum error obtained. This can be evaluated using Equation (3.16) (Ahmadzadeh Araj et al., 2018).

$$RMSE = \left[\frac{\sum_{i=1}^n (Y_i^{sim} - Y_i^{target})^2}{n} \right] \quad (3.16)$$

(e) Absolute Error in Mean (MAE)

MAE is a measure of the difference in error between simulated and targeted. It can be calculated using Equation (3.17) (Atmaja and Akagi, 2021).

$$MAE = \frac{1}{n} \sum_{i=1}^n |Y_i^{sim} - Y_i^{target}| \quad (3.17)$$

where: Y_i^{sim} = i th simulated ; Y_i^{target} = i th targeted; $\overline{Y^{sim}}$ = simulated mean value ; $\overline{Y^{target}}$ = targeted mean value; n = total number of targets

3.6 Metaheuristic Algorithms (MHAs)

The following sub-sections describe the proposed MHAs in this study.

3.6.1 Whale Optimisation Algorithm (WOA)

The WOA defines how humpback whales approach prey by swirling above it in the water to form sphere-shaped bubbles that encircle it (Mirjalili and Lewis, 2016). Figure 3.7 illustrates the flow of WOA.

The initial step in the chasing ritual of humpback whales is to encircle the target, which is known as encircling the prey. It indicates that the target prey is the optimal option at the moment, and trying to improve its location toward the intended outcome. The following Equation (3.18) and Equation (3.19) are the expressions.

$$\vec{D} = \left| \vec{C} \cdot \vec{X}(t) - \vec{X}(t) \right| \quad (3.18)$$

$$\vec{X}(t+1) = \text{int} \left[\vec{X}^*(t) - \vec{A} \cdot \vec{D} \right] \quad (3.19)$$

\vec{A} and \vec{C} are calculated as:

$$\vec{A} = 2 \vec{a} \cdot \vec{r}_1 - \vec{a} \quad (3.20)$$

$$\vec{C} = 2 \vec{r}_2 \quad (3.21)$$

which \vec{D} indicates the separation between \vec{X} and \vec{X}^* ; \vec{a} represent decrease linearly from 2 to 0 through iterations; followed by the \vec{r}_1 and \vec{r}_2 shows vectors in [0,1] in randomly; \vec{A} and \vec{C} represent vectors in coefficient; t indicates on-going iterations; \vec{X} gives the vector with the best positions that obtained so far; \cdot is the multiplication of two vectors pairwise; and lastly int represents an integer number.

As indicated in Equation (3.22), the WOA search agents are correct to the closest integer for discrete issues. Next, the following techniques known as encircling the prey are shown by the Bubble-net idea in mathematical modelling of the attacking strategies: (a) By reducing the encircling process, the value of a can be decreased in Equation (3.20). The random value of \vec{r}_1 in the interval $[-a, a]$ and (b) The current best method for imitating whale spiral movement between the present position of the whale and the prey are shown in Equation (3.22) and Equation (3.23).

$$D^l = \left| \vec{X}^*(t) - \vec{X}(t) \right| \quad (3.22)$$

$$\vec{X}(t+1) = int \left[\frac{D^l}{e^{bl}} \cdot \cos(2\pi l) + \vec{X}^*(t) \right] \quad (3.23)$$

where $\vec{D}^l =$ distance of i^{th} whale to the prey; $b =$ the definition of the shape of the logarithmic spiral; $l =$ random number $[-1,1]$

When using a spiral equation, the assumption of the 50% probability of selecting between updating the whales' new position or reducing their encirclement is written as in Equation (3.24).

$$\vec{x}(t+1) = \begin{cases} \text{int} \left\{ \frac{\vec{x}^*(t) - \vec{A} \cdot \vec{D}}{A} \right\} & \text{if } p < 0.5 \\ \text{int} \left[\frac{\vec{x}}{D^l} e^{bl} \cdot \cos(2\pi l) + \vec{x}^*(t) \right] & \text{if } p \geq 0.5 \end{cases} \quad (3.24)$$

where $p =$ numerical number of $[0,1]$ randomly.

Instead of employing the best effective search agent throughout the process of discovery, humpback whales randomly explore for prey; this mechanism occurs when $\left| \frac{\vec{x}}{A} \right| \geq 1$; it is also known as exploration. These equations facilitate to select a random search agent and alter its location:

$$D^l = \left| \frac{\vec{x}_r - \vec{x}(t)}{A} \right| \quad (3.25)$$

$$\vec{x}(t+1) = \text{int} \left[\frac{\vec{x}_r - \vec{A} \cdot \vec{D}}{A} \right] \quad (3.26)$$

which \vec{x}_r indicates the vector position by randomly selecting a whale from the on-going iteration or population; When a random search yields a better result, \vec{x}_r , or the most recent search solution (\vec{x}^*), are modified by the searching patterns.

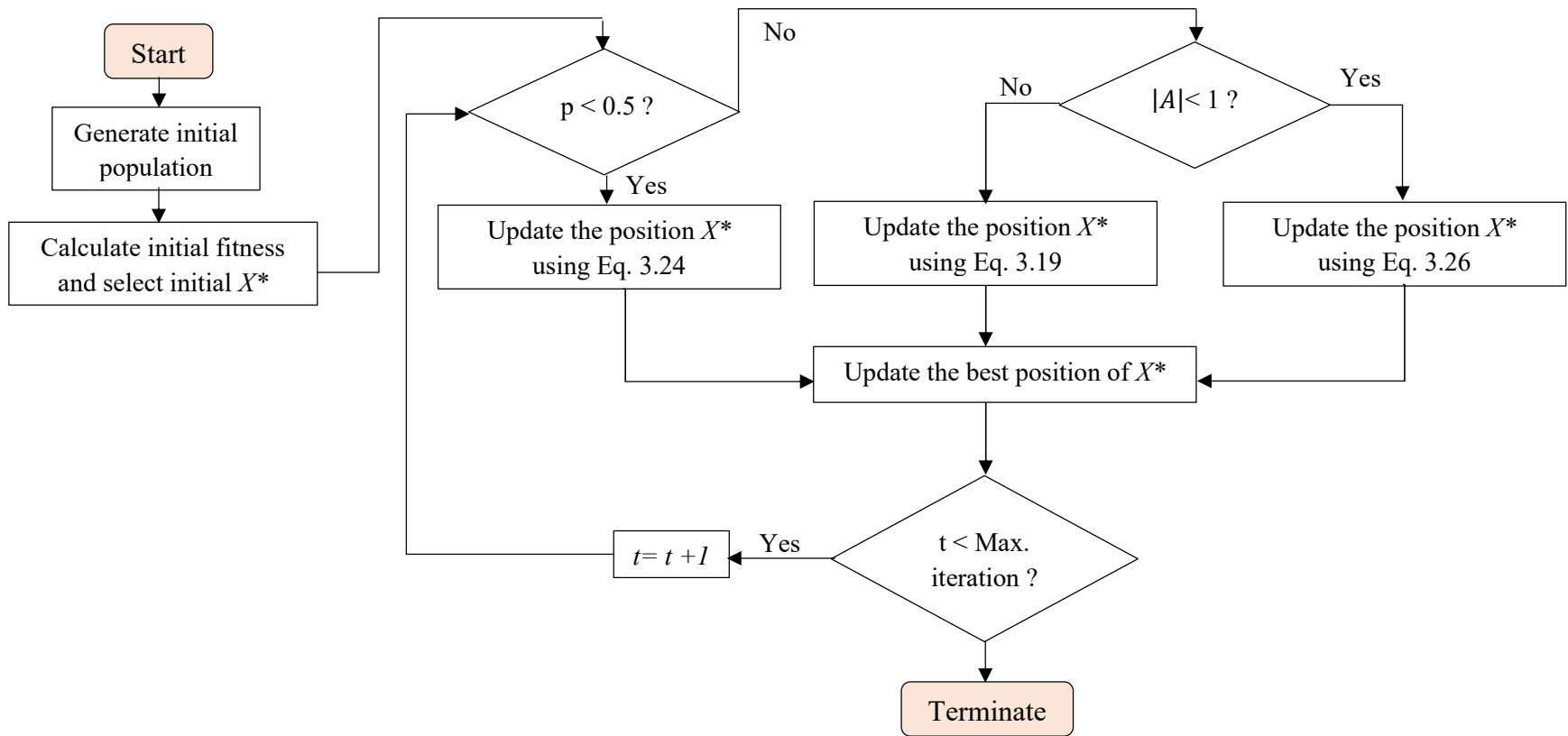


Figure 3.7: Flow Chart of the WOA

3.6.2 Lévy Flight WOA (LFWOA)

The most effective type of random walk to utilise is Lévy flight where the situation range widely, as shown in Figure 3.8. This concept allows the have a better global search. By applying Lévy flight in algorithms, Kamaruzaman et al. (2013) showed how the swapping between exploration and exploitation during the search process and trapping in local optima can be avoided. This was done by using the Lévy flight trajectory (Yang and Deb, 2009). The flow of LFWOA is presented in Figure 3.9.

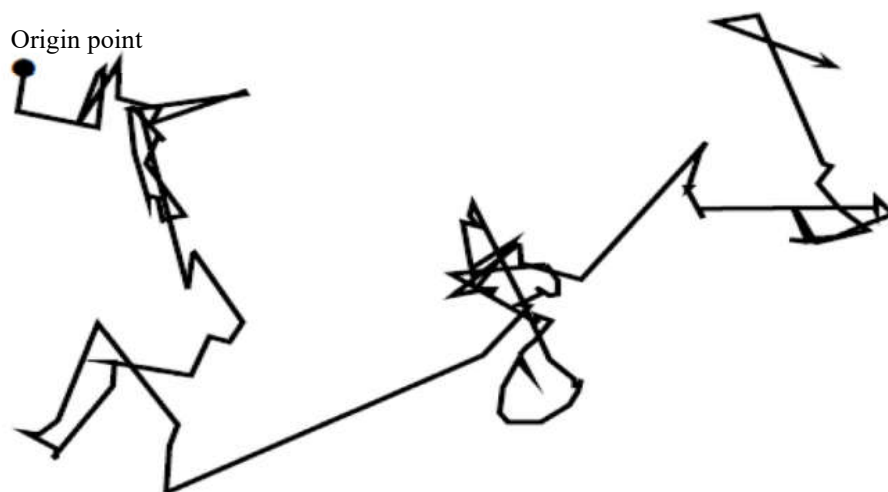


Figure 3.8: Denotes the conceptual idea of the Lévy flights (Houssein et al., 2020)

In this study, the WOA was integrated with the Lévy flight to speed up the convergence of the WOA, enhances efficiency and prevents the occurrence of local minimums (Zhou et al., 2018) via the simultaneously searching process of exploration and exploitation. The new positions of the humpback whale in the

form of random, which can be stated as Equation (3.27) is the length of the search step in the manner of stochastic version.

$$\vec{X}(t + 1) = \vec{X}(t) + \mu \left[rand - \frac{1}{2} \right] \oplus Levy \quad (3.27)$$

which $\vec{X}(t)$ indicates the vector \vec{X} located at the iteration of t ; μ is a stochastic variable that conforms to a uniform probability distribution ; product \oplus means entry wise multiplication; $rand$ denotes the numerical from the range 0 to 1 in random; $[rand - \frac{1}{2}]$ only has three possible values: 1, 0, and -1.

According to Yang and Deb (2009), the Lévy random walk provides the following distribution:

$$Levy \sim u = t^{-\lambda}, 1 < \lambda \leq 3 \quad (3.28)$$

$$s = \frac{\mu}{|v|^{1/\beta}} \quad (3.29)$$

where:

s = step length of the Levy flight, which is Levy(λ)

λ in Equation (3.28) obeys the formulation that $\lambda = 1 + \beta$, where $\beta = 1.5$,

$$\mu = N(0, \sigma_\mu^2)$$

$v = N(0, \sigma_v^2)$ are both normal stochastic distributions in Equation (3.30).

$$\sigma_\mu = \left[\frac{(1+\beta)X \sin(\pi X \beta/2)}{(1+\frac{\beta}{2})X \beta X 2^{(\beta-1)/2}} \right]^{1/\beta} \quad (3.30)$$

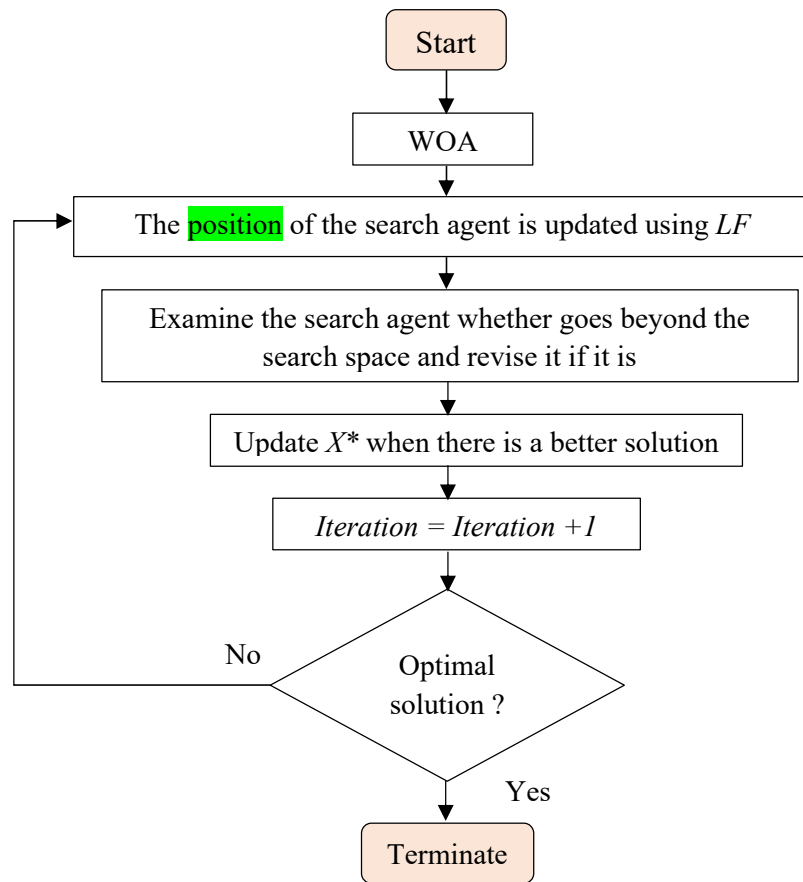


Figure 3.9: Flow chart of the LFWOA

3.6.3 Harris Hawks Optimisation Algorithm (HHO)

The harris hawk (HH) equipped with the characteristic of the intelligence and sharp observation, can pursue, encircle, hunting to the prey in cluster is a common strategy among this species. HHO algorithm employ various different hunting strategies to target rabbit (optimal solution). The leader hawk will try to catch the prey at first in a random pace, but if the prey is dynamic and has a tendency to flee, the hawk will move to a different approach of the hunting strategies. The rest of the flock will continue to pursue and aim until the target rabbit is caught. Hawks can chase after fleeing prey by distorting and decimating

the prey. The targeted prey in HHO is the optimal or ultimately solution, whereas hawks are candidate solutions. Consequently, HHO undergoes exploration and exploitation stages (Heidari et al., 2019; Islam et al., 2020) whereby the details are elaborated as following paragraphs. Also, the detail of the HHO is depicted in Figure 3.10.

During this exploration stage, the surveillance and detection process is carried out by the Harris Hawks. The majority of the time, Harris Hawks often fly to higher level to stalk their prey. Equation (3.31) is the statement that starts the searching process of Harris Hawks. The Harris Hawks will perch close to the hunting area if $q < 0.5$, vice versa, and they often choose a tall tree and stay on it.

$$X(iter + 1) \begin{cases} X_{rand}(iter) - r_1 X_{rand}(iter) - 2r_2(iter) \dots \dots \dots \text{if } \dots q \geq 0.5 \\ X_{rabbit}(iter) - X_m(itter) - r_3(LB + r_4(UB - LB) \dots \text{if } \dots q < 0.5 \end{cases} \quad (3.31)$$

where q is a positive integer from 0 to 1.

$$X_m = \frac{1}{N} \sum_{i=1}^N X_i(iter) \quad (3.32)$$

Equation (3.32) depicts the stage of transition from exploration-exploitation. Iteration E fluctuates randomly between -1 and 1, then shifts from -2 to 2, but it decreases throughout the process. HHs are in the stage of seeking for prey if $|E|$ is bigger than one, and when $|E|$ is less than one the HHs are most likely hunting rabbits, which is a likely exploitation stage. Exploration and exploitation potentially transform the energy flow.

$$E = 2 E_0 \left(1 - \frac{iter}{T}\right) \quad (3.33)$$

X_{iter} represents the present hawks position; X_{rand} represents the hawk is selected randomly from the available population; $iter$ is for the current repetition; X_{rabbit} stands for the position of the rabbit; $r_1, r_2, r_3,$ and r_4 stand for random numbers from 0 to 1; X_m denotes the current median location of the hawks; LB denotes lower boundary values; UB indicates upper boundary values; N is the number of hawks in the population; X_i represents the position of each hawk; T denotes the maximal repetitive runs; E_0 represents the preliminary stage of the energy.

Based on multiple hawk surveillance techniques and evasion from rabbit environments schemes in the exploitation stage, four feasible solutions have been attained, which explained in the next paragraph Technique (a)-(d) (Heidari et al., 2019). A better and straightforward flow chart of these techniques is depicted in Figure 3.10 associated to the equations that were involved in the HHO.

Technique (a) act as the hawks encircle the rabbit softly, the rabbit maintains sufficient energy and attempts to escape by making a series of random leaps. This is referred to as a soft siege. This innovation serves as a model for the following guidelines:

$$X(t + 1) = \Delta X(t) - E|JX_{rabbit}(t) - X(t)| \quad (3.34)$$

$$\Delta X(t) = X_{rabbit}(t) - X(t) \quad (3.35)$$

which $X(t)$ denotes the distance and the vector position of the rabbit during iteration t ; $J = 2(1 - r_5)$ indicates the random jump strength of the rabbit; r_5 represents a random number inside (0,1).

The rabbit has almost entirely exhausted itself and has reached its limits. This is referred to as a hard siege, Technique (b). The following description has been updated for this position:

$$X(t + 1) = X_{rabbit}(t) - E|\Delta X(t)| \quad (3.36)$$

Before the hawks can undertake a surprise attack, a soft siege must be established. The Soft siege with continuous quick dives, Technique (c) as illustrated in Equation (3.37) which is superior to Technique (a) due to the implementation of the Lévy flight idea.

$$Y = X_{rabbit}(t) - E|X_{rabbit}(t) - X(t)| \quad (3.37)$$

In order to establish several attempts based on Lévy flight (*LF*) whether was successful or unsuccessful is shown as follows:

$$Z = Y + S X LF(D) \quad (3.38)$$

D represents dimension of the problem; *S* denotes random vector of size 1 X *D* ; *LF* function can be indicated as statement:

$$LF(x) = 0.01 X \frac{u X \sigma}{|v|^{\frac{1}{\beta}}} \quad (3.39)$$

$$\sigma = \left(\frac{[(1+\beta)X \sin(\frac{\pi\beta}{2})]}{[(\frac{1+\beta}{2})X \beta X 2^{\frac{(\beta-1)}{2}}]} \right)^{\frac{1}{\beta}} \quad (3.40)$$

u and v are identical values in the interval $[0,1]$, and is a constant considered to equal 1.5. Thus, the ultimate rule for updating hawks in this Technique (c) is as follows:

$$X(t+1) = \begin{cases} Y & \text{if } F(Y) < F(X(t)) \\ Z & \text{if } F(Z) < F(X(t)) \end{cases} \quad (3.41)$$

which Y and Z are compute via Equation (3.37) and Equation (3.38).

This update rule for Hard siege with continual quick dives, Technique (d) is as follows:

$$X(t+1) = \begin{cases} Y & \text{if } F(Y) < F(X(t)) \\ Z & \text{if } F(Z) < F(X(t)) \end{cases} \quad (3.42)$$

$$Y = X_{rabbit}(t) - E|JX_{rabbit}(t) - X_m(t)| \quad (3.43)$$

$$Z = Y + S X LF(D) \quad (3.44)$$

Until the ideal solution is found, the Y and Z variables denote the positions for the subsequent iterations as presented in Equation (3.42) and Equation (3.43).

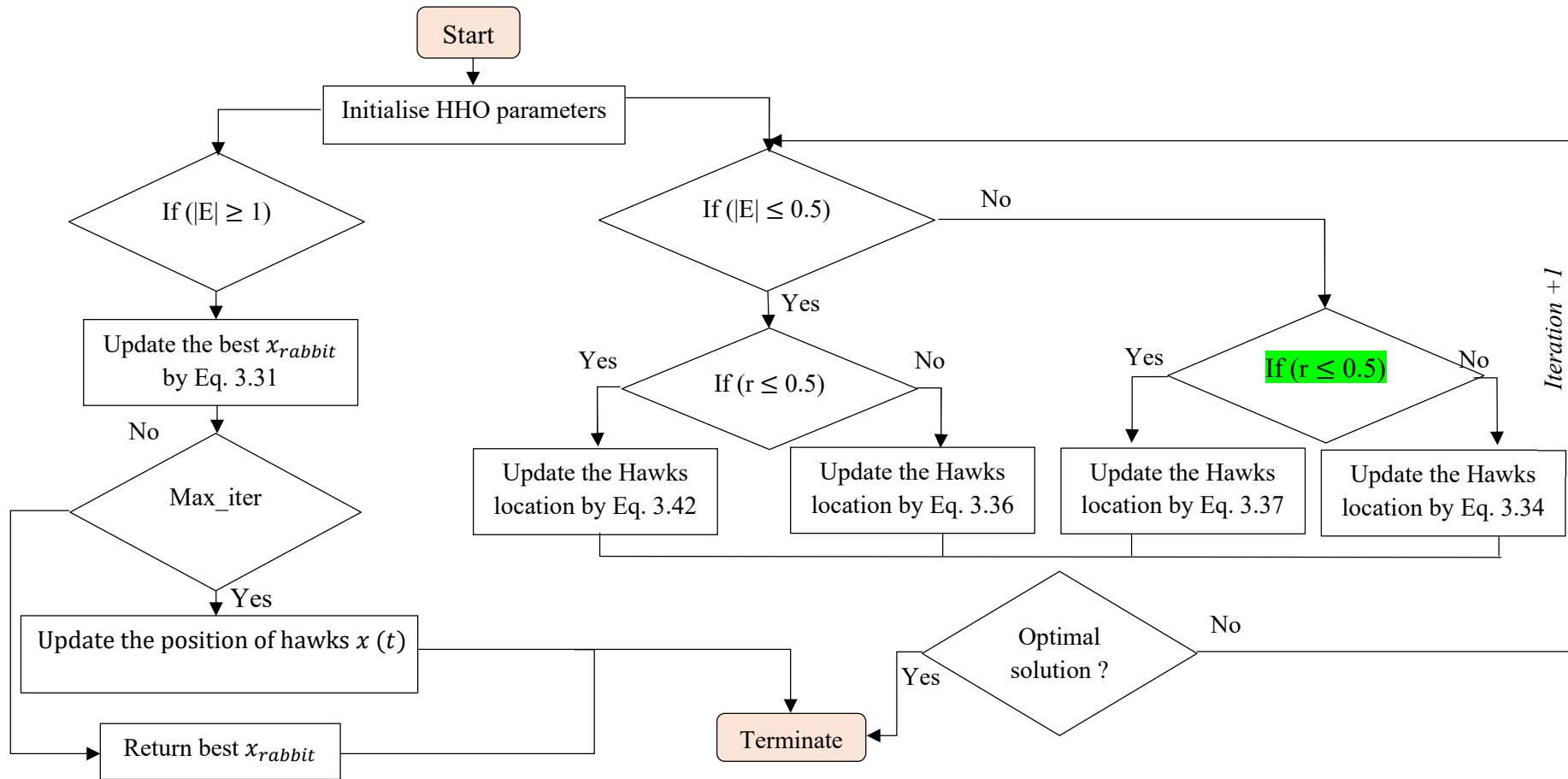


Figure 3.10: Flow chart of the HHO

3.6.4 Opposition-Based Learning HHO (OBL-HHO)

The study by Kelidari and Hamidzadeh (2020), applied Opposition-based learning (OBL) by concatenating with other techniques have been proposed as potential solutions for addressing real-world problems. The utilisation of OBL has been found to be a proficient approach in comprehensively examining the issue space. This approach can enhance efficiency by searching simultaneously for the solution and inverse. Although this approach imposes a greater computational burden on the algorithm, it substantially enhances the rate of convergence. The subsequent equation delineates the OBL methodical in a space of D dimensions. Also, Figure 3.11 shows the flow of OBL-HHO.

$$\tilde{x}_j = u_j + l_j - x_j \quad j = 1, 2, \dots, D \quad (3.45)$$

where x = The concept of habitat within a search space.; \tilde{x} = The contrary of a habitat that was produced during the timeframe of $[u, l]$; j = Every dimension of the additive inverse.

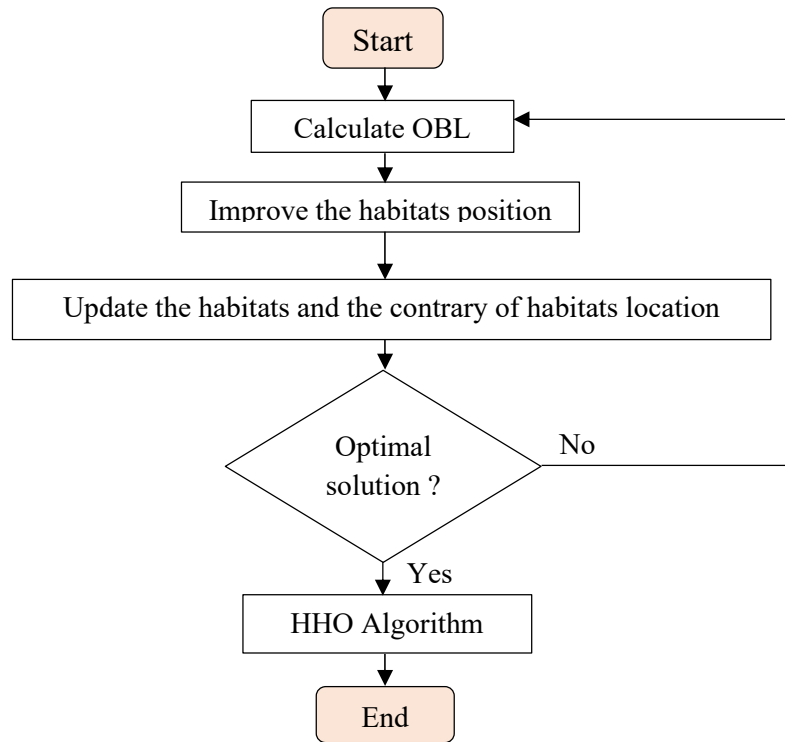


Figure 3.11: OBL-HHO

3.6.5 Evaluation of Exploration and Exploitation Capabilities in Benchmark Functions Testing

These six benchmark functions of *EvoPy* are proposed as shown in Equation (3.46) to Equation (3.51) (Faris et al., 2016). These benchmark functions were utilised to evaluate the efficacy and robustness of the proposed MHAs. The outcome of the performance measure based on the benchmark functions served as the comparison between the MHAs and datasets before applying it to reservoir optimisation. The characteristic of *EvoPy* test function has presented in Table 3.16 (Khurma et al., 2020; Qaddoura et al., 2020). Each function group performed an average of 20-runs for respective proposed MHAs to determine the optimal value of these functions. The tested results will be

further discussed in Chapter 4, in Table 4.1. The reason for an average 20-runs having been initially set as the optimal target iterations was mentioned in Chong et al. (2021). It has also achieved the optimal values after several trial-and-error attempts from the 6 difference benchmark functions of *EvolvoPy*, and it was found that was unnecessary to execute the extra runs as it takes up more time of execution.

$$F_1(x) = \sum_{i=1}^n (\sum_{j=1}^i x_j)^2 \quad (3.46)$$

$$F_2(x) = \sum_{i=1}^n |x_i| + \prod_{i=1}^n |x_i| \quad (3.47)$$

$$F_3(x) = \sum_{i=1}^n (x_i + 0.5)^2 \quad (3.48)$$

$$F_4(x) = ix_4^4 + random(0,1) \quad (3.49)$$

$$F_5(x) = \frac{\pi}{n} \{10 \sin^2(\pi y_1) + \sum_{i=1}^{n-1} (y_i - 1)^2 [1 + 10 \sin^2(\pi y_{i+1})] + (y_n - 1)^2\} + \sum_{i=1}^n u(x_i, 10, 100, 4)$$

$$y_i = 1 + \frac{x_i + 1}{4}, u(x_i, a, k, m) = \begin{cases} k(x_i - a)^m & x_i > a \\ 0 & -a \leq x_i < a \\ k(-x_i - a)^m & x_i < -a \end{cases} \quad (3.50)$$

$$F_6(x) = 0.1 \{ \sin^2(3\pi x_i) + \sum_{i=1}^n (x_i - 1)^2 [1 + \sin^2(3\pi x_{i+1} + 1)] + (x_n + 1)^2 [1 + \sin^2(2\pi x_n)] \} + \sum_{i=1}^n u(x_i, 5, 100, 4) \quad (3.51)$$

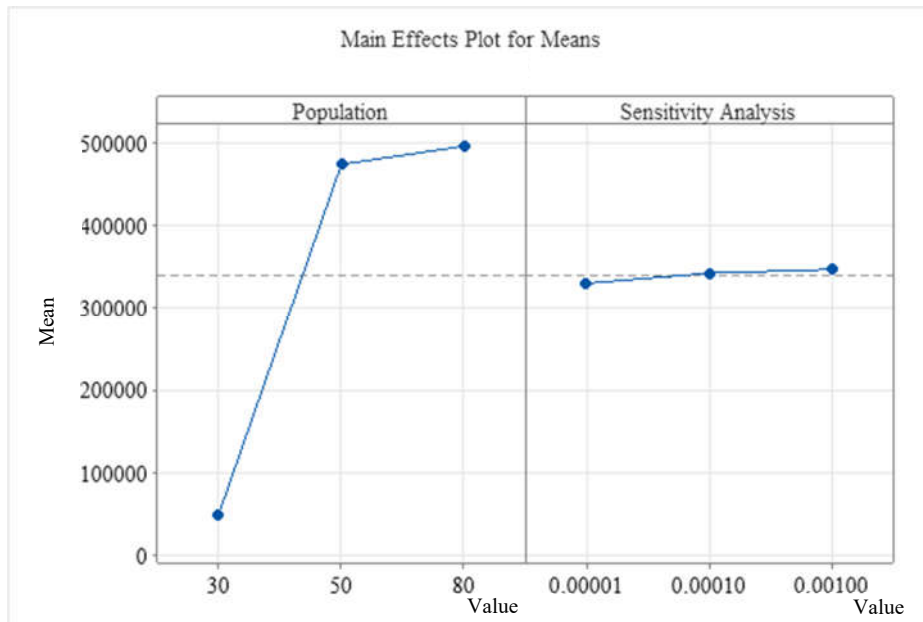
Table 3.16: Characteristic of *EvoLoPy* Test Functions

Description	F ₁	F ₂	F ₃	F ₄	F ₅	F ₆
Function group	Unimodal	Unimodal	Unimodal	Unimodal	Multimodal	Multimodal
Population	80	80	80	80	80	80
Minimum frequency (f_{\min})	-100	-100	-100	-1.28	-50	50
Maximum frequency (f_{\max})	100	100	100	1.28	50	50
Number of examination, m	10	10	10	10	10	10
Number of runs	20	20	20	20	20	20
Number of dimensions	30	30	30	30	30	30

3.6.6 Parameters Setting for the Respective Proposed MHAs

The Taguchi technique was built on orthogonal arrays, which explained how to do the minimum possible trials while obtaining adequate details on all parameter settings in MHAs likely to impact the resulting parameter. The execution of the orthogonal array in this sub-section of L9 (3^2) was used to investigate the influence of two factors using 9 experiment runs and 3 levels of values. The benchmark testing for the respective algorithms in terms of population was presented in Figure 3.12(a) to Figure 3.12(d), and the sensitivity analysis, also referred to as accuracy testing, was adjusted accordingly. As illustrated in Figure 3.12(a) to Figure 3.12(d), the x-axis (mean) represented of the steep (high) slope whilst for the y-axis represented the three initial target population values and their respective sensitivity (accuracy setting value) to be executed in trial-and-error in order to understand what were the most impacted parameter settings corresponded to the respective proposed MHAs. According to the respond graphs for respected proposed MHAs, the population's peak impact was 80, and the accuracy testing was 0.0001. Table 3.17 contains the parameter settings for the proposed MHAs.

(a) WOA



(b) LFWOA

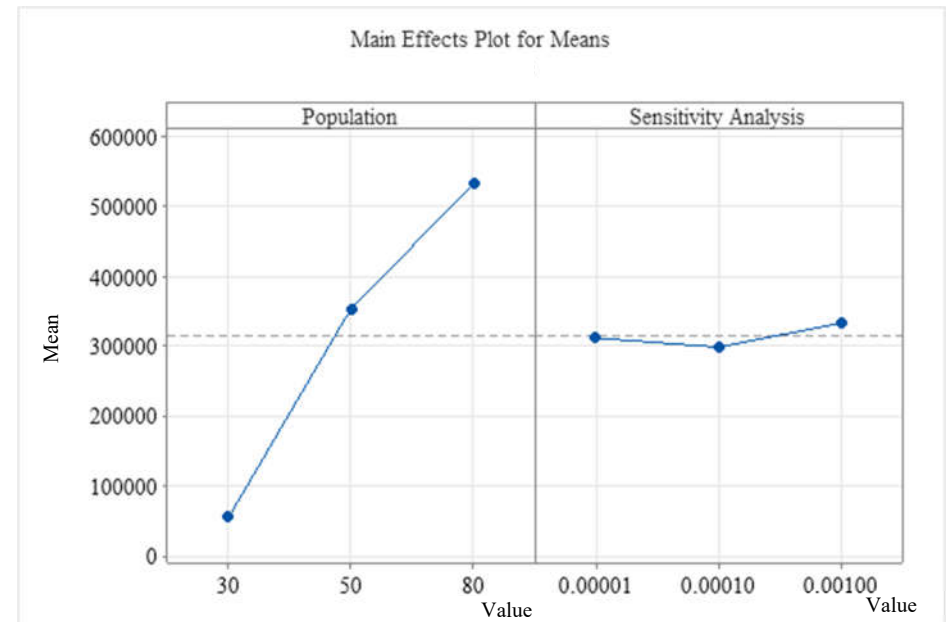
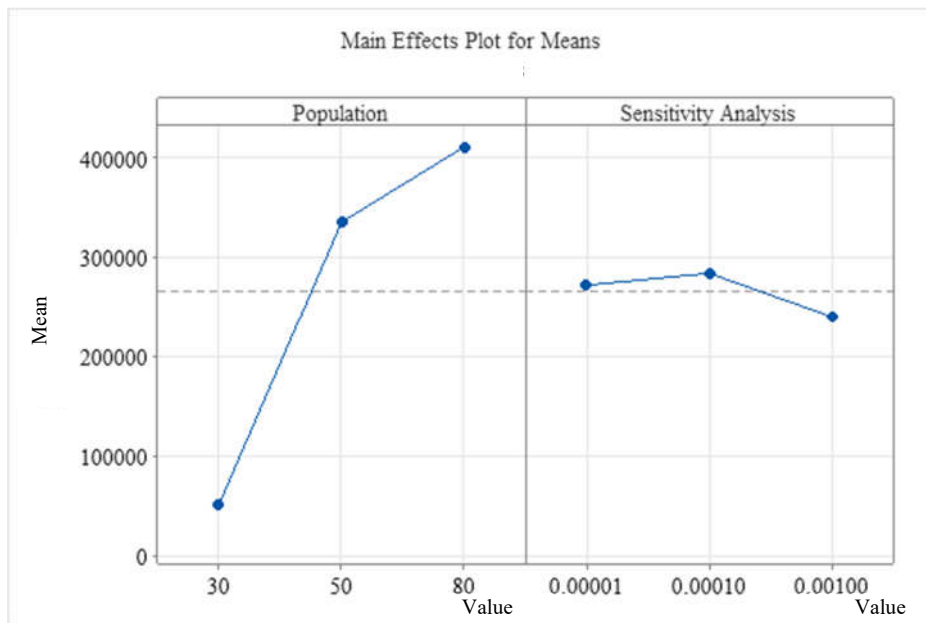


Figure 3.12: Response Graph of the (a) WOA and (b) LFWOA

(c) HHO



(d) OBL-HHO

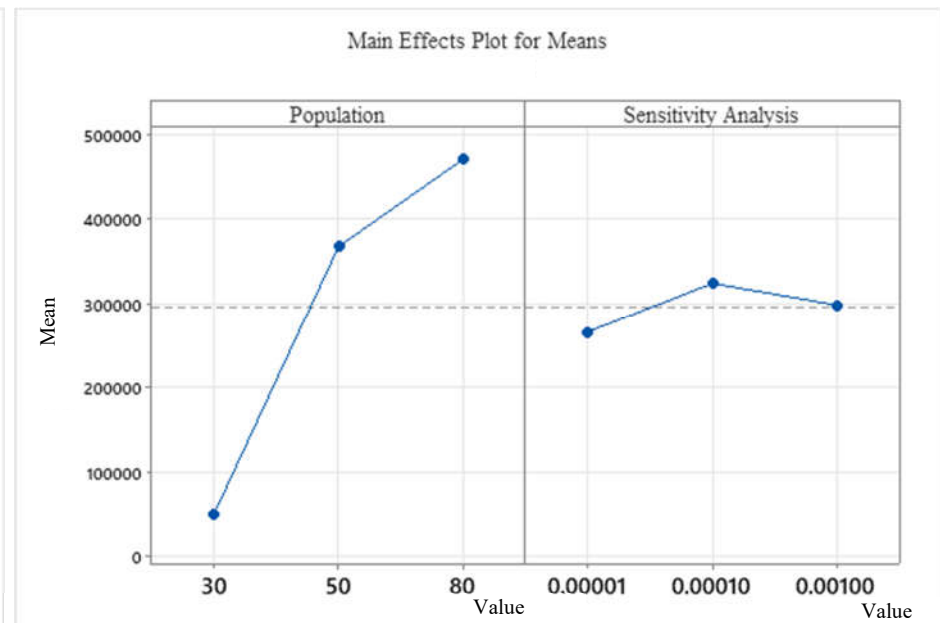


Figure 3.12: Response Graph of the (c) HHO and (d) OBL-HHO

Table 3.17: Parameter Setting for proposed MHAs

Algorithms	Parameters	Values
WOA	Whales number	35
*initial adjustment Epsilon and Dimension	a	$\epsilon [0,2]$
	a2	$\epsilon [-1,-2]$
	Search agent	35
	Threshold	2
	CSV	0.5
Lévy flight WOA (LFWOA)	β	1.5
*initial adjustment Stepwise and Dimension	a ₁	10
	a ₂	0.00005
	a ₃	0.005
	∂_1	0.9
	∂_2	0.1
HHO	Rabbit energy	[0,2]
*initial adjustment Epsilon and Dimension	β	1.5
OBL-HHO	Follow the LFWOA parameter setting	
*initial adjustment Dimension		

3.6.7 Design of Experiment (DoE)

The objective of this study was set to determine the optimal release at the KGD and minimise the water deficit without compromising the constraints. The details of comparing various designs of experiment (DoE) can be found in (Tanco et al., 2009). The DoE conducted for this study was the Taguchi Method which aims to investigate the main effects of the factors involved in the water demand reservoir and the parameter setting of the corresponding proposed MHAs.

The primary objective of the Taguchi method is to examine the main effects of variables (Heidari-Rarani et al., 2020). The Taguchi method yielded more consistent findings than factorial design DoE, when results from two factorial DoE cases in the same experiments might be different and not easy to interpret (Roy, 2010). Hence, the potential application for the DoE, Taguchi method, was introduced. Some past studies implemented the Taguchi method involved in real-engineering (Liao et al., 2008; Heidari-Rarani et al., 2020; Zhang et al., 2021). It was also found in the studies of reservoir operation optimisation (Chong et al., 2021). The DoE software package applied in this study is the Minitab (Minitab Inc.).

The present sub-section of L16 employs an orthogonal array with a 2^4 design to examine the impact of four factors, sixteen experimental runs were conducted, each featuring two levels that were defined by an upper and lower

boundary. Figure 3.13 illustrates the main effect plot for the simulated releases. The simulated release at the KGD was most significantly impacted by inflow, with storage, demand, and loss following in descending order of influence.

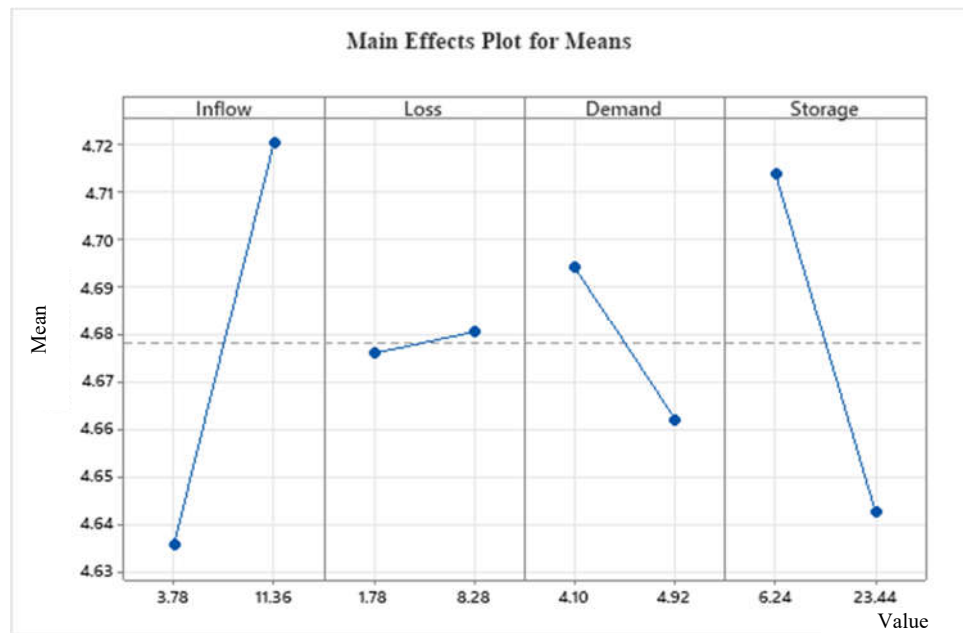


Figure 3.13: Main effect plot for Taguchi Method

The response table generated by the Taguchi method is summarised in Table 3.18. The delta value demonstrates the significant effects of inflows because it received the highest score, 0.085, and had the greatest influence on the main effects of the factors, whereas the delta value for the storage factor was 0.071, followed by demand with a delta value of 0.032, and lastly loss variable with a delta value of 0.005.

Table 3.18: Response Table

Level	Inflow	Loss	Demand	Storage
1	4.636	4.676	4.694	4.714
2	4.720	4.680	4.662	4.643
Delta	0.085	0.005	0.032	0.071
Rank	1	4	3	2

The present study employed a univariate analysis of variance (ANOVA) to examine the effects of various elements on the response parameters. The data used in the analysis were obtained from the Taguchi method analysis. Table 3.19 presents the results of the ANOVA, which examines the effects of different factors on the explanatory variables and their relations. The table also displays the pairwise interactions between the factors. The presentation of the effects of each factor on the explanatory variables does not include any statistically significant results with a significance level of less than 0.05. The study determined that the inflow factor had the greatest impact on the percentage of contribution (PC), as evidenced by the results presented in Table 3.19. Specifically, the PC value of 11.55% ranked first in the main effects plot, while the remaining PC values in Table 3.19 were consistent with those in Table 3.18 in terms of rank and delta value. The principal component with the highest percentage obtained for the interaction between the factors was demand*storage, which accounted for 32.07%. This was followed by inflow*demand and inflow*storage, which accounted for 19.72% and 12.10%, respectively.

Table 3.19: ANOVA analysis

Source	F-value	P-Value	Degree of Freedom	Sum of Squares	Mean of Sum Squares	Percentage of Contribution (%)
Inflow	5.4	0.07	1	0.0287	0.0287	11.6
Loss	0.02	0.91	1	0.000081	0.000081	0.03
Demand	0.78	0.42	1	0.0042	0.0042	1.7
Storage	3.8	0.11	1	0.0203	0.0203	8.2
Inflow*Loss	0.00	1.00	1	0.000	0.000	0.0
Inflow*Demand	9.2	0.029	1	0.0491	0.0491	19.7
Inflow*Storage	5.7	0.063	1	0.0301	0.0301	12.1
Loss*Demand	1.2	0.33	1	0.0062	0.0062	2.5
Loss*Storage	0.7	0.44	1	0.0037	0.0037	1.5
Demand*Storage	14.99	0.012	1	0.0798	0.0798	32.1
Total			15	0.2488	0.2488	100

3.7 Problem Formulation

The optimal release reservoir operation serves as a guide for decision-makers in achieving the reservoir's intended function (water supply, flood mitigation, and in some cases, hydropower generation, and so on). This section covers the features and considerations for a reservoir management system. The problem has been formulated in a straightforward manner that can be optimised using improved techniques, specifically meta-heuristic algorithms based on swarm intelligence. For the purpose of verifying the efficiency of the algorithms

and datasets in reservoir operation at the KGD, simulation was performed, and performance indices were introduced to analyse the output of the results obtained to determine whether the algorithm was able to achieve the target function.

For the purpose of addressing the best release for the KGD operation, the formulation of the problem in the reservoir at the Klang Gate Dam (KGD) consists of three considerations: (a) objective function, (b) threshold or constraints, and (c) penalty functions (Allawi et al., 2019b). The following subsections introduce these considerations and the equations of the performance indices involved in this optimisation release operation at KGD.

3.7.1 Objective Function

Minimising the water deficit or shortage is the objective function of this optimisation operation at KGD. In other words, is to minimise the disparity between the amount of water required and the amount of water discharged. as defined by Equation 3.52.

$$\text{Minimisation of function } Z = \sum_{t=1}^{12} (D_t - R_t)^2 \quad (3.52)$$

where t denotes the months within a calendar year; D_t denotes demand in monthly basis; R_t indicate release in monthly basis.

3.7.2 Handling of the Thresholds or Constraints

The most efficient and widely used method for dealing with constraints in optimisation algorithms is to impose a penalty for any violation of the thresholds or constraints. In general, for reservoir operation, decision-makers may face a few types of thresholds or constraints in determining the optimal release amount, boundaries of release, and storage level in order to ensure reservoir operation for the next period would be sufficient to supply and safe operational zone if there is an extreme weather event (i.e., heavy rainfall). This study introduces two types of thresholds, which are elaborated on below: -

(a) Equal Continuity:

Eq. 3.53 below gives the statement:

$$S_{t+1} = S_t + I_t - R_t - L_t \quad (3.53)$$

where:

S_{t+1} denotes ending of the storage;

S_t represents the starting of the storages;

t denotes months in a year;

I_t indicates the inflow to the KGD;

R_t denotes the release from the KGD;

L_t is tabulated as in Table 3.5.

(b) Inequality for:

(i) Storage Capacity, S_t :

Upper boundary ≤ 6.24 million cubic metre and lower boundary
 ≤ 23.44 million cubic metre (for $t = \text{Jan, Feb, \dots, Dec}$) (3.54)

(ii) Release, R_t :

Upper boundary ≤ 3.28 million cubic metre and lower boundary
 ≤ 5.22 million cubic metre (for $t = \text{Jan, Feb, \dots, Dec}$) (3.55)

3.7.3 Penalty Functions

This section briefly explains the penalty functions applied in the reservoir optimisation operation. For decades, penalty functions (PF) have been a component of the literature on restricted optimisation. There are two basic forms of PF: (a) external PF, which disguises infeasible solutions as feasible ones, and (b) internal PF, which penalises feasible solutions. A feasible solution is one that meets all the requirements, whereas an infeasible solution is the inverse condition. Static PF is a straightforward approach for penalising infeasible solutions by imposing a continuous penalty on solutions that violate feasibility in any way. Dynamic PF was used by enabling the exploration of infeasible regions while still requiring the ultimate solution to be feasible. Finally, while including distance and the time of the search into the PF has been usually beneficial, these penalties that disregard any other elements of the search is

known as the adaptive PF (Smith and Coit, 1997). In this study, the penalty function is to convert the infeasible to feasible solution. The threshold for the storage capacity can be resolved by utilising the following equation to penalise the objective function.

$$penalty\ 1 = \begin{cases} 0 & \text{if } S_t > S_{min} \\ C_1(S_{min} - S_t)^2 & \text{if } S_t < S_{min} \end{cases} \quad (3.56)$$

$$penalty\ 2 = \begin{cases} 0 & \text{if } S_t < S_{max} \\ C_2(S_{max} - S_t)^2 & \text{if } S_t > S_{max} \end{cases} \quad (3.57)$$

where:

C_1 and C_2 are the coefficients of the penalty;

S_t is expressed as storage;

S_{min} denotes the minimum storage;

S_{max} represents the maximum storage.

After applying the penalty functions, the ultimate objective function of the optimisation operation at KGD has been rewritten in Equation (3.58) for a monthly basis.

$$\text{Minimisation of function } Y = \text{Minimisation of function } Z + \text{penalty } 1 + \text{penalty } 2 \quad (3.58)$$

3.8 Reservoir Risk Assessments

After obtaining the results of simulations and optimisation, the performance is checked to determine the system's failure or success. The three most common indices for measuring the level of performance are reliability, resilience, and vulnerability (Hashimoto et al., 1982). The three indices are elaborated on below.

3.8.1 Reliability

For a model to be effective in achieving the objectives of a reservoir optimisation model, periodic reliability serves as one of the most important indicators. The system is more reliable when the R_p indices are higher.

$$\text{Periodic Reliability, } R_p = \left(\frac{n}{N}\right) \times 100\% \quad (3.59)$$

3.8.2 Resilience

Resilience is the likelihood of a scarcity to satisfy future demand. The correlation of the number of meeting the demand followed by the unfavourable events (shortage) occurred with the overall shortage period. An alternate definition of resilience is the capacity of a framework for overcoming a sequence of persistent setbacks. Resilience can be expressed mathematically as in Equation (3.60).

$$\text{Resilience, } R_s = \frac{NS}{NT} \quad (3.60)$$

The average WSR has been applied in this study as one of the indicators of reservoir system resilience to address the performance of the reservoir system against climatic or hydrological variability. The negative values denotes the failure of the reservoir system, and vice versa.

$$WSR_{avg}(t) = \frac{S_{avg}(t) + Q_{avg\ inflow}(t) - Q_{avg\ output}(t) - Q_{storage\ min.}(t) - Q_{total\ demand}(t)}{Q_{total\ demand}(t)} \quad (3.61)$$

3.8.3 Vulnerability

Is an index that depicts how catastrophic the failure conditions are which stated in Equation (3.62):

$$Vul = \frac{1}{m} \times \sum_{t=1}^N [\max(0, D_t - R_t)] \quad \text{for } t=1, 2, \dots, N \quad (3.62)$$

3.8.4 Maximum Deficit

This indicator is calculated by dividing the annual water deficit by the annual water demand which represents in Equation (3.63).

$$Max\ Deficit_{annual} = \frac{deficit_{annual}}{water\ demand_{annual}} \quad (3.63)$$

in which n is defined as overall times meeting the exact period; N represents the total number of time periods that were examined, NS represents the number of time periods that were considered satisfactory and followed by a shortage period, and NT represents the total number of failure periods. The defines of m as the

number of model failure periods when there is water deficit, given that N_v is the total time period considered for simulation in months, D_t is the targeted demand for any given month t , and R_t is the water release for that particular month t .

3.9 Summary

This chapter discussed the practical applications involving the problem formulations at the KGD to meet the objective function of the optimisation, along with the reservoir risk analysis assessment for both observed period and climate assessment. The characteristics of the KGD were highlighted and the overall flow path of the study was provided. This chapter also discussed the datasets involved for year 2001-2019, followed by the comparison of the proposed MHAs with the previous studies that had investigated at KGD for year 1987-2008. The more recent revised version (2018) of Design Flood Hydrograph, HP 11 has been utilised to compute the rainfall-runoff relationship. The estimation approaches for evaporation and future water demand have been briefly discussed by employing two empirical evaporation methods (a) *Kharuffa* and (b) *Turc*. In order to validate the *Kharuffa* and the *Turc* methods, prediction-based of the data-driven strategies were used to anticipate with temperature variables and by combining temperature and solar radiation variables. In addition, few future water demands have been developed via data-driven approaches and forecasted to a near approximation of realistic circumstances based on temperature factor and forecasted population growth before proceeding to the investigating the impact of the climate change. The most essential was the selection of the proposed MHAs with the simultaneous characteristic of

exploration and exploitation applied in this study and the respective parameter settings have been presented. Furthermore, the DoE was conducted using the Taguchi method and ANOVA to determine which of the variables have the greatest influence on the reservoir optimisation policy at the KGD. The Friedman test, also the part of the DoE which will be presented in section 4.2.2. An evaluation of the capabilities of the strategy of exploration and exploitation in proposed MHAs was examined by implementing the *EvoPy* benchmark test functions. The objective function at KGD has been set in order to minimise the water deficit by involving several thresholds of KGD as well as penalty functions. Lastly, the level of performances for the proposed MHAs in optimisation were evaluated using the common metrics (reliability, resilience, and vulnerability) in reservoir risk assessment. A new metric namely Water Support Resilience (WSR) implemented, is an extension of resilience metric to address the performance of the reservoir system against climatic or hydrological variability.

CHAPTER 4

RESULTS AND DISCUSSION

4.1 Introduction

This chapter discusses the results obtained from the reservoir optimisation at the KGD using the WOA, LFWOA, HHO, and the OBL-HHO. This chapter consists of two sections: (i) reservoir optimisation during the Observed Period; and (ii) investigating the future climate change impact for year 2020-2099 on the reservoir release operation under the different climate change scenarios at the KGD. The reservoir optimisation during the observed period consists of two timelines of the datasets. Firstly, the reservoir risk assessment for 2001- 2019 was examined, and the datasets for this timeline will be further utilised to investigate the impact of climate change under the different climate change scenarios. In the second sub-section of the observed period, a comparison was made between the proposed MHAs and published heuristic algorithms for year 1987 - 2008 on the reservoir's risk analysis. This is followed by the assessments including GCMs downscaling using the statistical downscaling method, and the future climate scenarios for RCP 2.6, RCP 4.5, and RCP 8.5 were determined in this study in order to investigate the climate change impact on the future KGD operations. The rainfall-runoff analysis was then computed. Several empirical evaporation methods have also been described and validated

with data-driven approach. In addition, the estimation of the future water demand for 2020 to 2099 was determined by analysing the temperature factors and the indirect relationship between population growth and land use and land cover change. Also, the impact of climate on reservoir operation at KGD was studied using data-driven techniques for reservoir simulation, and the results were compared to reservoir optimisation in respect of reservoir risk assessment. Finally, the efficacy of the proposed MHAs was identified and examined by conducting a ranking analysis of a non-parametric test.

4.2 Execution of *EvoPy* Benchmark Test Functions

This study tested the MHAs capabilities and efficacy using six *EvoPy* benchmark test functions mentioned in section 3.6.5. The following sub-section discusses the findings.

4.2.1 Statistical Model Performances

Table 4.1 indicates the obtained statistical results of the WOA, LFWOA, HHO, and the OBL-HHO for the unimodal functions (F₁-F₄) and multimodal functions (F₅-F₆), respectively.

Table 4.1 shows the overall optimal statistical results of the *EvoPy* Functions with the setting of the accuracy level of $\epsilon_f = 1.0e-04$ for WOA, HHO, and OBL-HHO, respectively whilst LFWOA applied $\epsilon_f = 1.0e-02$. The accuracy level setting was then applied to the subsequent reservoir optimisation. The

statistical criteria examined for the respective proposed MHAs in this benchmark test functions are the average, standard deviation (SD), worst, and best.

The purpose of these statistical findings from the benchmark testing as presented in Table 4.1 was to examine and validate the robustness of the algorithm as well as to show the statistical criteria obtained from the respective proposed algorithmic behaviour and datasets. The ranking of the respective proposed MHAs were also provided after the statistic criteria had been analysed from the benchmark test functions. According to the ranking based on the benchmark test function presented in Table 4.1, the HHO and OBL-HHO provided the optimal ranking in F_4 (in unimodal characteristic), respectively which anticipated both algorithms' behaviour are consistent and correlated to the datasets. Unlike the WOA and LFWOA, the optimal ranking for both algorithms fell in F_3 (in unimodal characteristic) and F_6 (in multimodal characteristic), respectively indicated both the algorithms presented the behaviour of sensitivity to the datasets.

Table 4.1: Statistical results for benchmark testing for year 2001 to 2019

Algorithms	Criteria	Functions					
		F ₁	F ₂	F ₃	F ₄	F ₅	F ₆
WOA	Average	2.01E-111	5.28E-62	1.11E-02	2.74E-04	1.13E-03	2.02E-02
$\epsilon_f = 1.0e-04$	SD	4.20E-111	1.05E-61	7.92E-04	1.54E-04	7.47E-05	6.27E-03
	Worst	1.30E-110	2.30E-61	1.26E-02	1.01E-04	1.09E-03	1.60E-02
	Best	6.64E-121	8.96E-65	1.05E-02	6.26E-04	1.22E-03	2.20E-02
	Ranking	6	5	1	4	3	2
LFWOA	Average	9.03E-59	1.04E-32	6.97E-03	1.80E-03	8.42E-04	2.61E-02
$\epsilon_f = 1.0e-02$	SD	1.36E-58	7.44E-33	2.49E-03	1.87E-03	2.82E-04	8.73E-03
	Worst	4.52E-59	1.09E-32	3.06E-03	1.04E-03	1.04E-04	4.7E-02
	Best	3.59E-62	3.96E-34	9.93E-03	7.55E-03	8.89E-04	1.5E-02
	Ranking	6	5	2	3	4	1

Table 4.1 (continued): Statistical results for benchmark testing for year 2001 to 2019

Algorithms/	Criteria	Functions					
		F ₁	F ₂	F ₃	F ₄	F ₅	F ₆
Accuracy							
Level							
HHO	Average	3.91E-88	8.96E-68	4.42E-06	8.56E-04	4.68E-06	0.00E+00
$\epsilon_f = 1.0e-04$	SD	1.17E-87	2.67E-67	2.29E-06	1.18E-03	1.76E-06	0.00E+00
	Worst	3.89E-87	8.91E-67	2.42E-06	1.09E-03	1.29E-06	0.00E+00
	Best	3.23E-117	8.46E-74	4.66E-06	4.48E-04	7.358E-06	0.00E+00
	Ranking	5	4	3	1	2	6
OBL-HHO	Average	2.58E-14	1.96E-11	1.71E-04	1.06E-02	4.09E-05	0.00E+00
$\epsilon_f = 1.0e-04$	SD	7.50E-14	3.94E-11	1.04E-04	1.19E-02	2.34E-05	0.00E+00
	Worst	2.51E-13	1.26E-10	1.24 E-04	3.84E-02	1.51E-05	0.00E+00
	Best	9.04E-24	7.07E-15	8.74E-05	4.43E-03	3.64E-05	0.00E+00
	Ranking	5	4	2	1	3	6

4.2.2 Ranking Assessment

This sub-section was the extension workflow under the DoE after Taguchi and ANOVA test been conducted in section 3.6.7. For data analysis in Computational Intelligence, non-parametric tests are incredibly valuable. The use of rank-based metrics allows for the analysis of both nominal and real data. To run a non-parametric test on a set of multiple issues, a result must be provided for each algorithm or pair of problems. Several previous studies have been undertaken and can be found in (Derrac et al., 2014; Ahmadianfar et al., 2020).

Before applying the test to the data, developing a null or no-effect hypothesis is essential. It frequently supports the equality or lack of discrepancies between algorithmic findings and allows alternate hypotheses to be formed that suggest the opposite. H_0 stands for the null hypothesis, whereas H_1, \dots, H_n stand for the alternative hypotheses. After conducting the tests, a statistic that can be used to reject the null hypothesis at a predetermined significance level, is calculated.

The Friedman test is utilised to assess and contrast the efficacy of the exploration and exploitation of the suggested MHAs, respectively. The validity of this claim can be ascertained by referring to the equations for the Friedman test and Chi-square, as presented below:

$$E(R) = \frac{N(k+1)}{2} \quad (4.1)$$

$$X^2 = \frac{12}{N \cdot k \cdot (k+1)} \cdot \sum R^2 - 3 \cdot N \cdot (k+1) \quad (4.2)$$

in which N = summation of rows ; k = summation of columns; R^2 = sum of the ranks.

Table 4.2 provides a summary of the Friedman test findings acquired utilising the different *EvolvoPy* functions and proposed algorithms. The HHO algorithm has been identified as the most efficient, with the WOA algorithm and its corresponding enhancement techniques, namely the LFWOA and the OBL-HHO, exhibiting comparable performance. The determination of a statistically significant difference involves consulting the Chi-Square distribution table, which yielded a value of 11.071, with a significance level of 0.05 while the computation of the degree of freedom (df) entails the subtraction of $k-1$, where k is equivalent to 5. Chi-square values of $X^2 = 1.142$ were found for F_1 through F_5 , whereas $X^2 = -0.2142$ was found for F_6 . Also, it was identified did not extend beyond the critical thresholds, thereby indicating the absence of any statistically significant difference. Consequently, the post-hoc analysis (Bonferroni-Dunn procedure) is not performed.

Table 4.2: Friedman ranks

Algorithms	Functions						Average rank	Rank
	F ₁	F ₂	F ₃	F ₄	F ₅	F ₆		
WOA	1	2	4	1	4	1	2.20	2
LFWOA	3	3	3	3	3	2	2.83	3
HHO	2	1	1	2	1	3	1.70	1
OBL-HHO	4	4	2	4	2	3	3.20	3
Sum of Rank, $\sum R$	10	10	10	10	10	9		

4.3 Execution of Observed Period Assessments for Year 2001- 2019

The proposed MHAs were utilised and investigated in these observed period datasets. The findings based on statistical model performance, optimal monthly releases curves via the proposed MHAs, optimal storage capacity, and reservoir risk analysis assessment are discussed in the next follow sections.

4.3.1 Statistical Model Performances Evaluations

(a) WOA

As shown in Figure 4.1 (a), the RMSE value for the medium inflow was the highest when compared to the other two inflow categories. In the category of the medium inflow, the month of January had the highest RMSE at 7.92, while the month of April had the lowest at 4.67. Aside from this, the second category with the highest RMSE was the high inflow, with the highest RMSE at 2.97 in June and the lowest RMSE in February, when there was no high inflow input. The maximum RMSE value for the low inflow reached was 1.63. The average RMSE attained for the high, medium and low inflow was 2.04, 5.94, and 0.49, respectively.

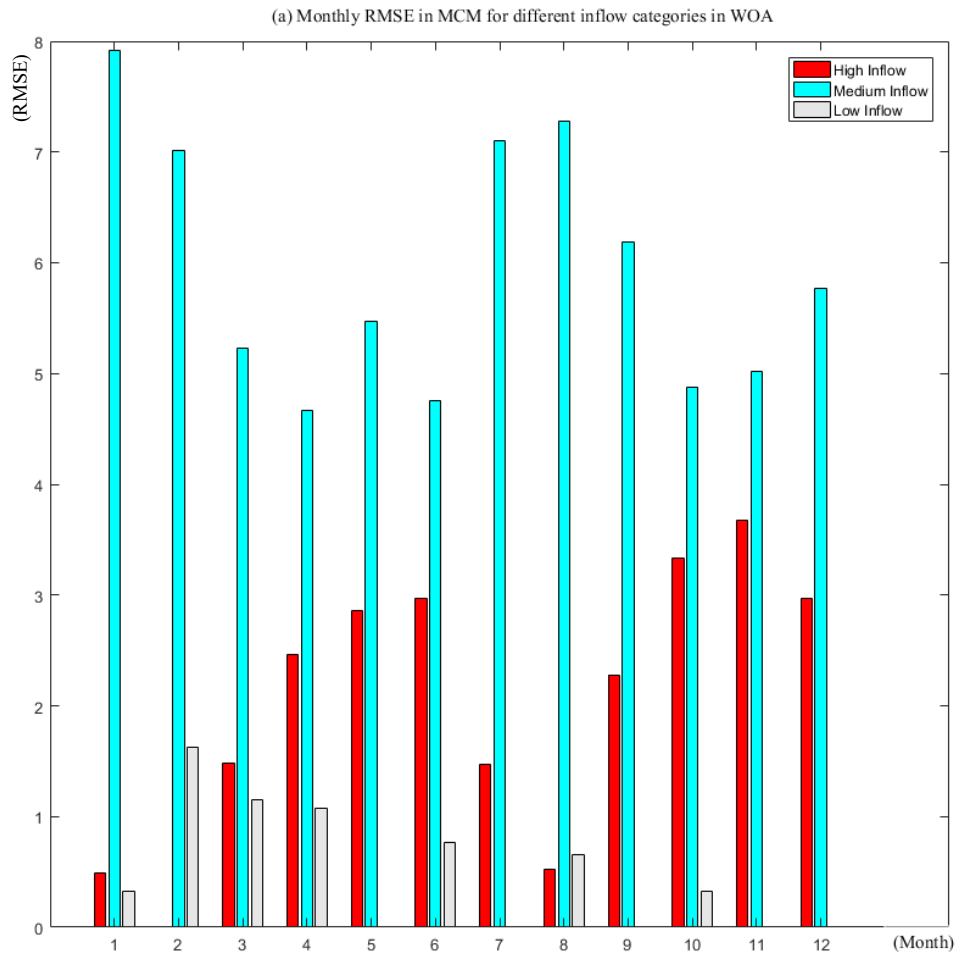


Figure 4.1: (a) Monthly RMSE (MCM) for different inflow categories in WOA

The monthly PBIAS for WOA is shown in Figure 4.1 (b). The leading value of PBIAS fell in the medium inflow category, reaching a peak of 120.3 in February and a lowest of 0.16 in November. In addition, the average PBIAS for medium inflow was 30.6. Despite the low inflow category, the average PBIAS was half the medium inflow category at 18.6, with August and January displaying the highest values at 72.1 and 54.3, respectively. The average PBIAS for the high inflow category was 6.4, whereas the highest PBIAS values were recorded in March and April, at 22,6 and 24,9, respectively.

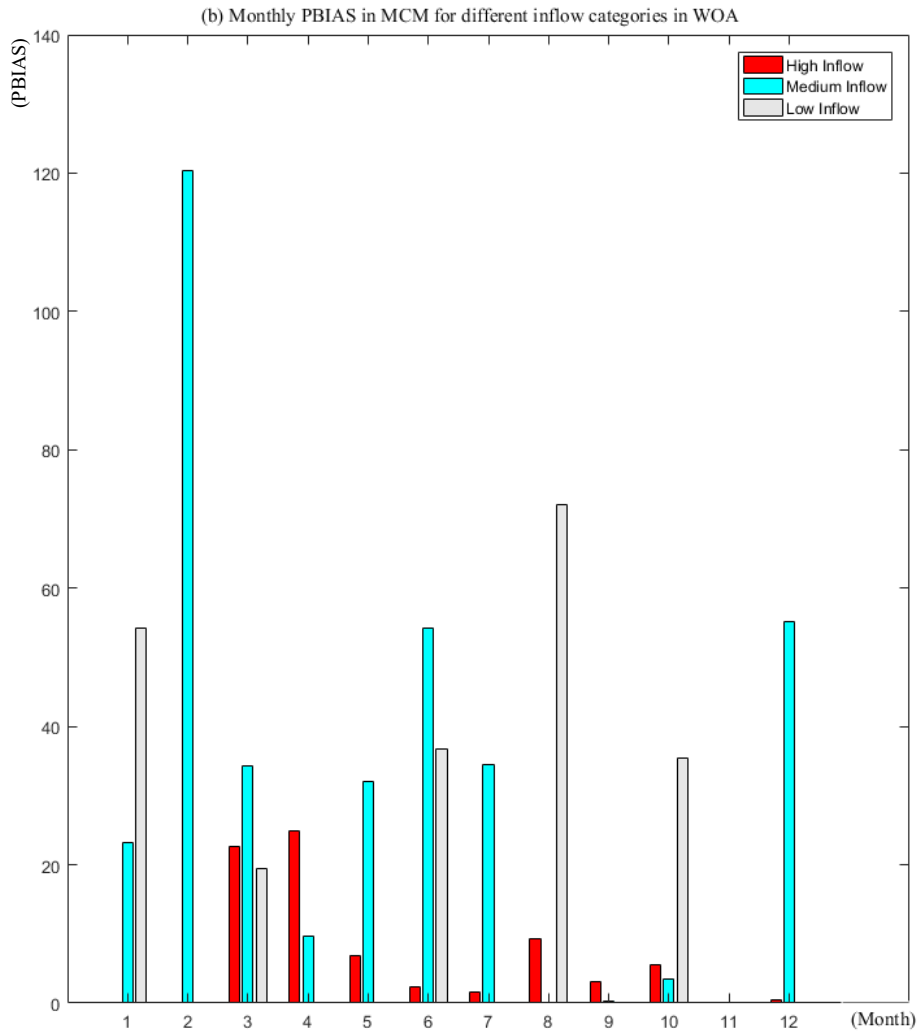


Figure 4.1: (b) Monthly PBIAS (MCM) for different inflow categories in WOA

By utilising the WOA, Figure 4.1 (c) depicts the monthly MAE in million cubic metre for three inflow categories. It shows the peak of the MAE in WOA fell within the medium inflow category, with a value of 0.86 in February, while the other months attained negative values of MAE ranging from -0.01 to -0.6. In April, the highest MAE values reached for the categories of high inflow (0.2) and low inflow (-0.2). The mean absolute error (MAE) for the medium inflow

group was -0.21. In contrast, for the high and low inflow groups, the MAE values were 0.08 and -0.09, respectively.

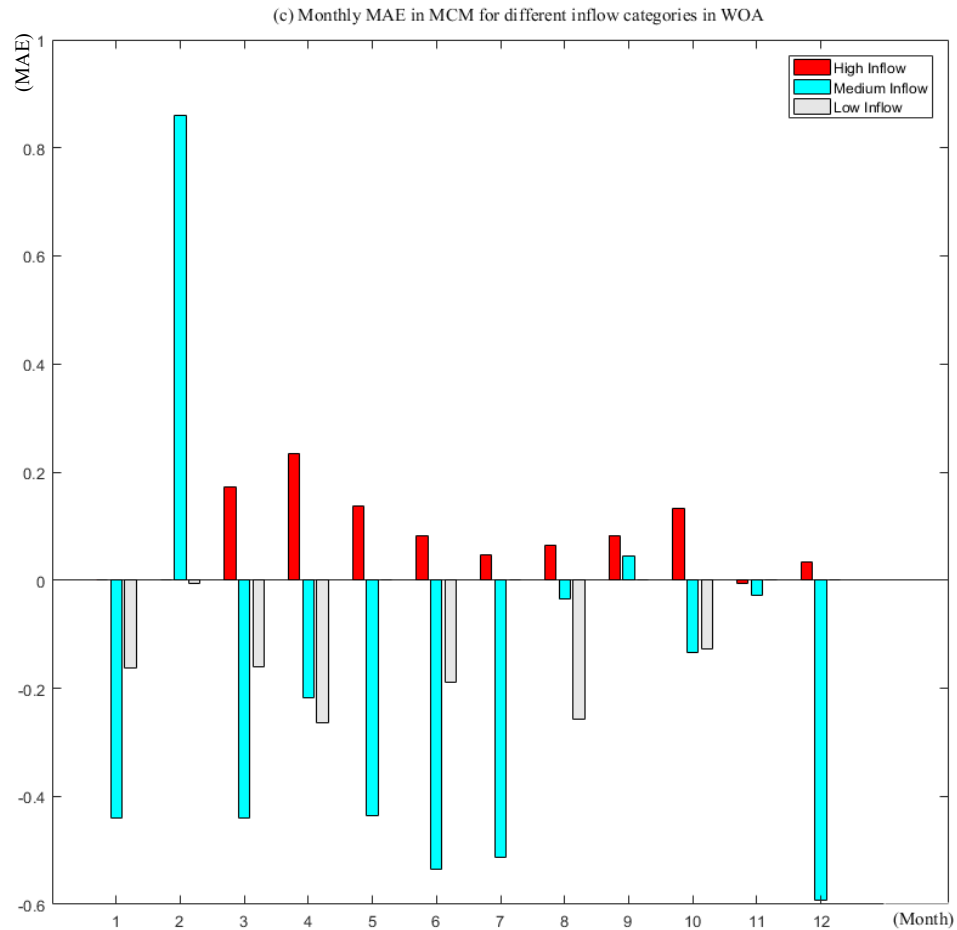
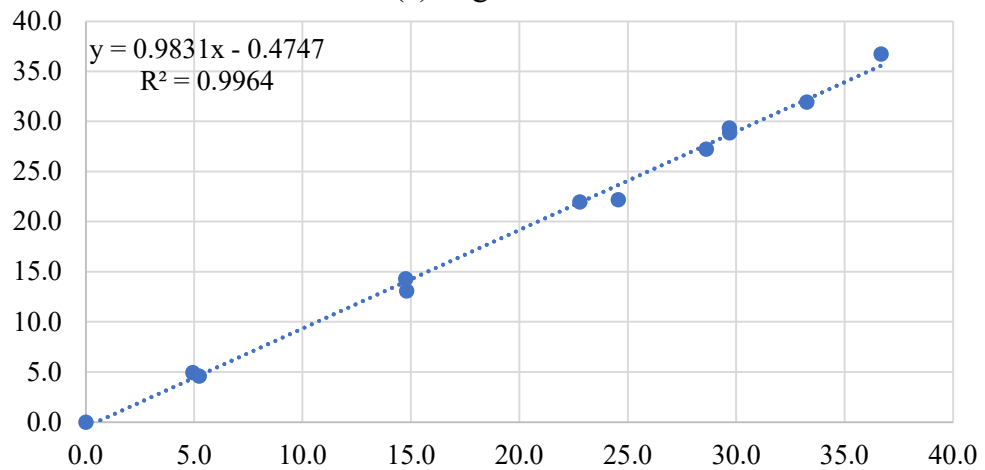


Figure 4.1: (c) Monthly MAE (MCM) for different inflow categories in WOA

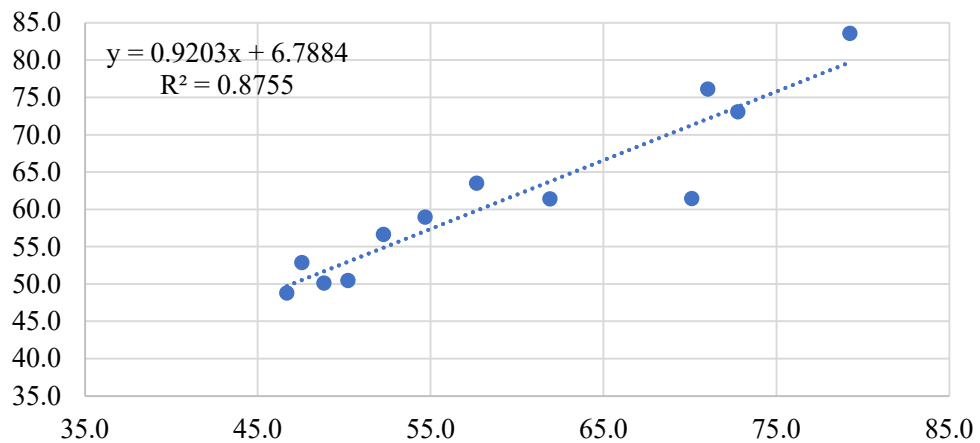
The R^2 values for the three different inflow categories are depicted in Figure 4.2(a)-(c). Using the HHO algorithm, the graphs displayed a high degree of precision between the simulated and targeted KGD demand. R^2 was found to be 0.9964 for the high inflow category, followed by $R^2 = 0.99763$ for the low inflow category and $R^2 = 0.8755$ for the category of medium inflow. Even though the category of the medium inflow had lower accuracy than the other two inflow

categories, evaluations with an accuracy of 0.85 or higher are still considered reliable. The NSE is the final component to be highlighted. The average NSE for the high and medium inflow categories were 0.9155 and 0.9083, respectively. The NSE for the low inflow category for January was, however, negative. As a result, the average NSE for the low inflow category was drastically distorted, but it was well obtained for R^2 . In addition, the months of April, May, July, September, November, and December showed no indications of low inflow.

(a) High Inflow



(b) Medium Inflow



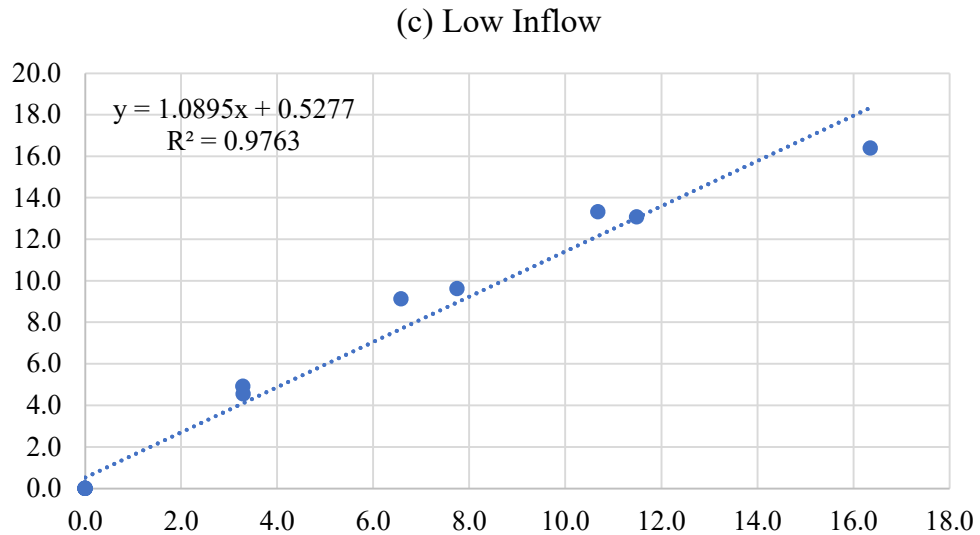


Figure 4.2: R^2 evaluation (a) in High Inflow, (b) in Medium Inflow (c) in Low Inflow for WOA algorithm from 2001 to 2019

(b) LFWOA

When compared to the other two inflow categories, the RMSE value for the medium inflow was the highest, as depicted in Figure 4.3 (a). The month of January had the highest RMSE of 8.13, while the month of April had the lowest RMSE of 4.77 in the category of medium inflow. Apart from that, the second highest RMSE category was the high inflow, with the maximum RMSE of 3.80 in November and the lowest RMSE in February, when there was no high inflow input. For the low inflow, the maximum RMSE value was 1.63. The average RMSE gained for high inflow (2.04), medium inflow (5.94), and low inflow (0.55).

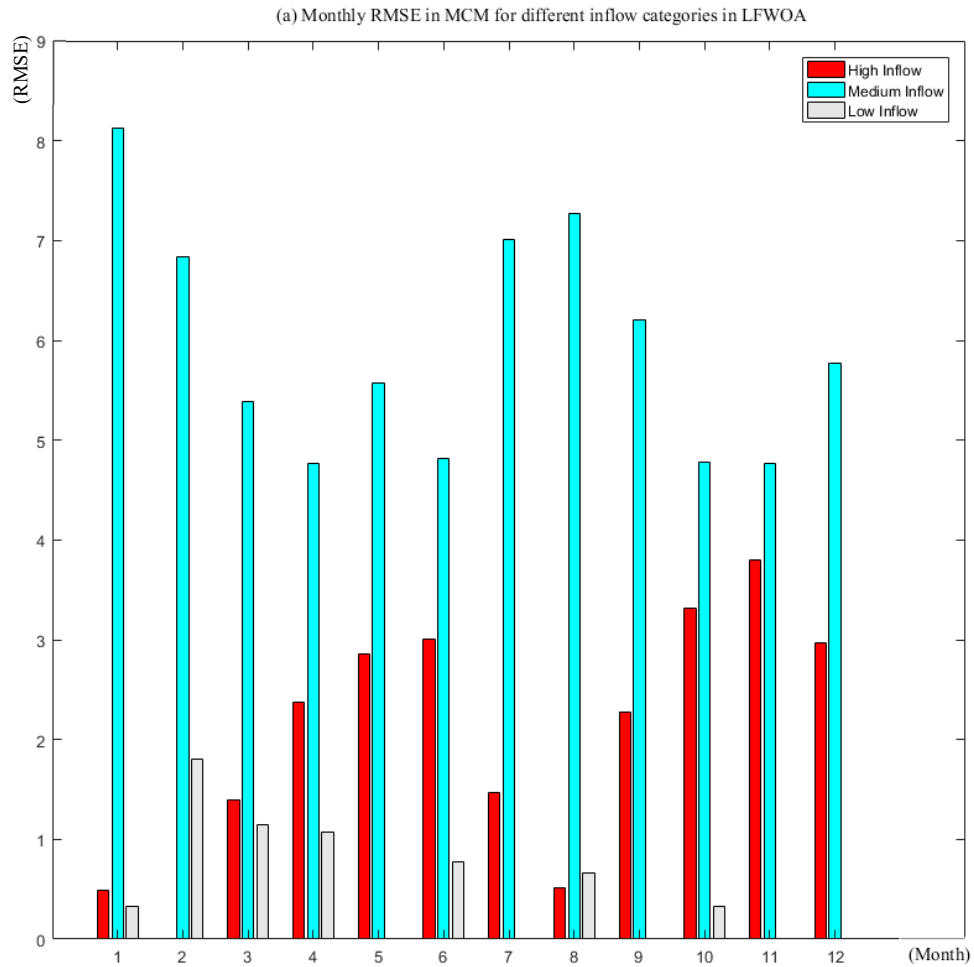


Figure 4.3: (a) Monthly RMSE (MCM) for different inflow categories in LFWOA

Figure 4.3 (b) presents the monthly PBIAS for LFWOA. The PBIAS's peak value fell into the medium inflow category, hitting a high of 78.44 in February and a low of 0.29 in August. Furthermore, for medium inflow, the average PBIAS was 24.5. Despite being in the low inflow category, the average PBIAS was marginally lower than the medium inflow category at 19.4, with the highest values of 71.8 and 54.5 in August and January, respectively. The average PBIAS for the high inflow category was 4.4, with the highest PBIAS values of 11.1 and 9.2, respectively, in April and August.

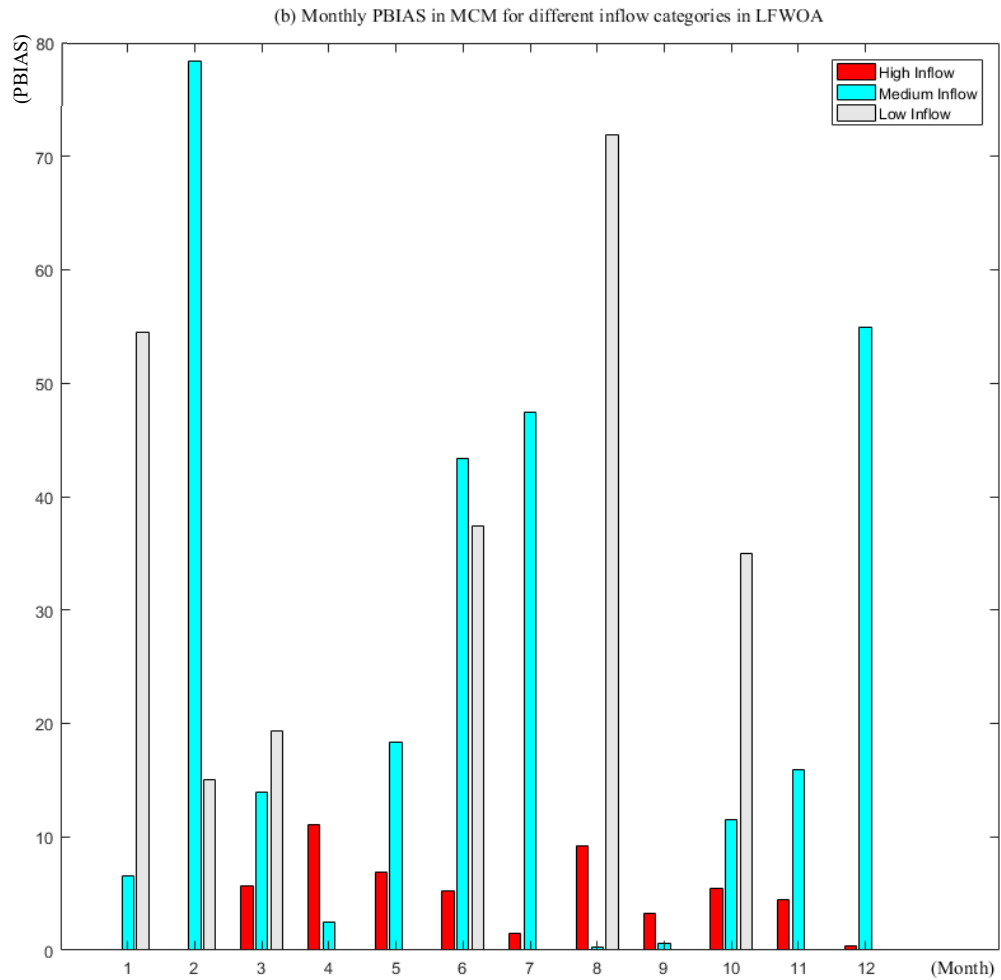


Figure 4.3: (b) Monthly PBIAS (MCM) for different inflow categories in LFWOA

Figure 4.3 (c) represents the monthly MAE for three different inflow categories using the LFWOA. Figure 4.3 (c) shows that the peak of MAE in the WOA occurred in the medium inflow category, with a value of 0.69 in February, whereas the other months had negative MAE values ranging from -0.04 to -0.6. The greatest MAE values in April were 0.15 and -0.26, respectively, for the categories of high inflow and low inflow. The average MAE attained for medium inflow (-0.21), whereas the high inflow (0.08) and low inflow (-0.09).

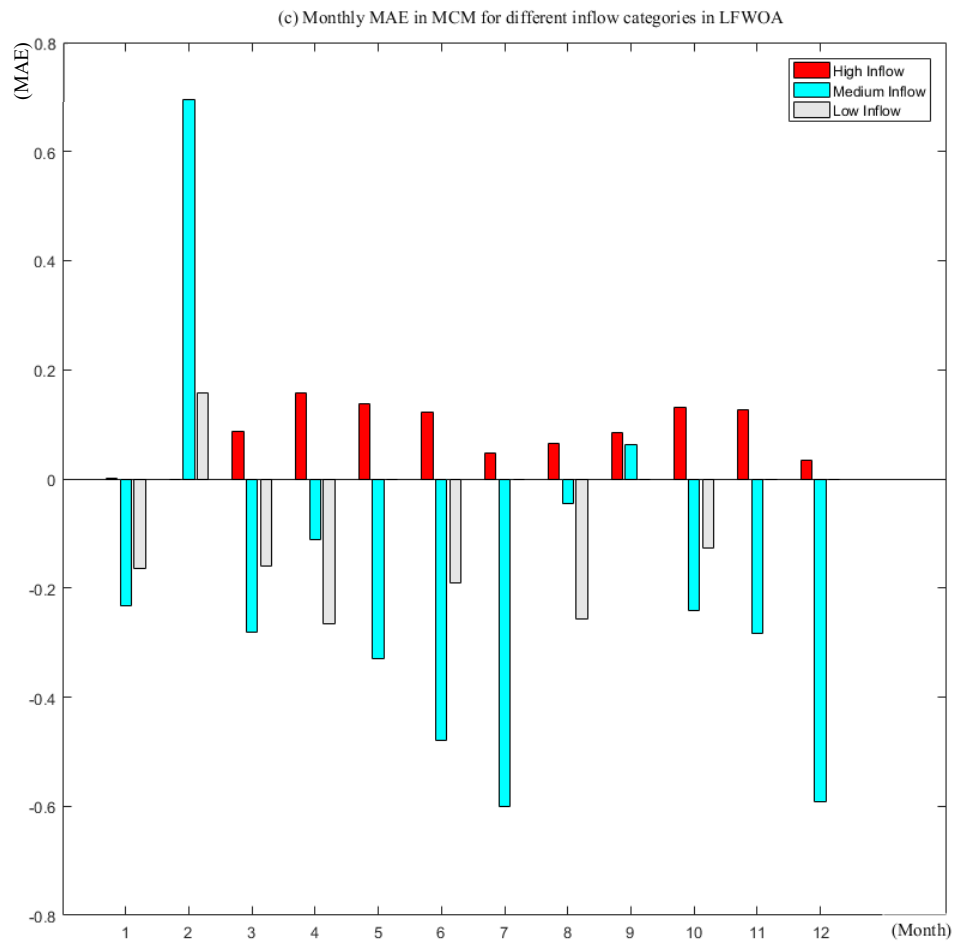
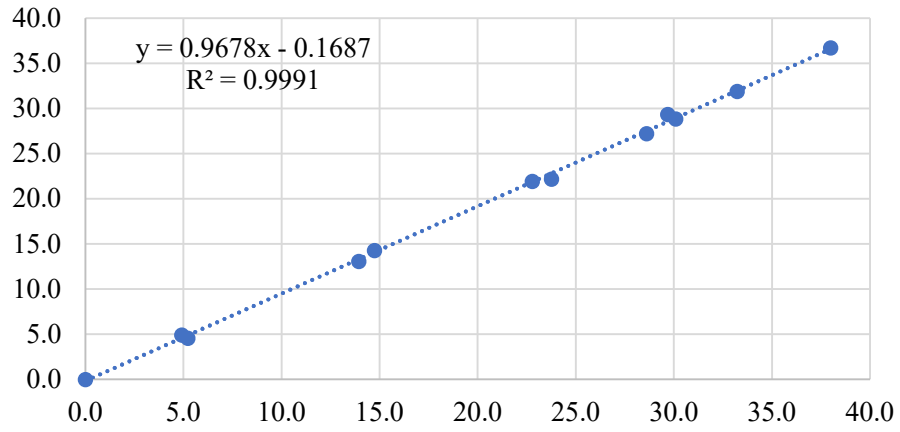


Figure 4.3: (c) Monthly MAE (MCM) for different inflow categories in LFWOA

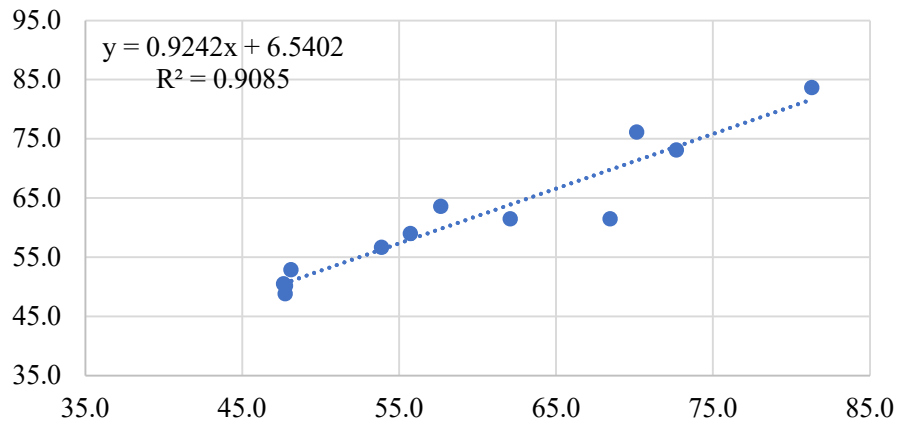
Using the LFWOA algorithm, the graphs in Figure 4.4(a)–(c) show that the simulated and targeted demand at KGD are very close. The category with the highest inflow had the highest R^2 , at 0.9991. The category with the lowest inflow had a value of 0.9572, and the category with the medium inflow was 0.9085. The average NSE for high inflow is (0.915) and for the medium inflow is (0.9114). The NSE achieved in the low inflow category, on the other hand, was a negative value, which is less ideal for evaluating uncertainty. Overall, the R^2 obtained in

LFWOA has shown a high correlation between simulated and targeted demand at KGD.

(a) High Inflow



(b) Medium Inflow



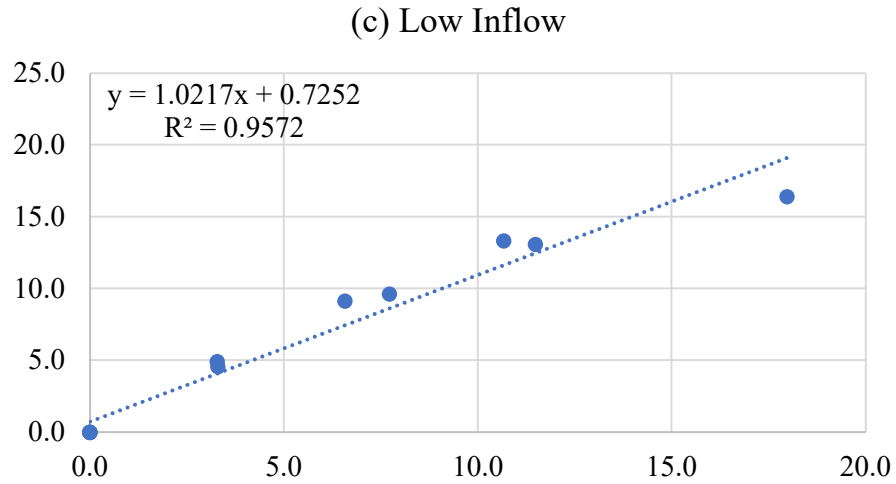


Figure 4.4: R^2 evaluation (a) in High Inflow, (b) in Medium Inflow, (c) in Low Inflow for LFWOA algorithm

(c) HHO

The statistical analysis of Root Mean Square Error (RMSE) on a monthly basis from 2001 to 2019 is presented in Figure 4.5(a) in respect of three different input categories. During the month of January, it was observed that the medium inflow category showed the highest root mean square error (RMSE) with a recorded value of 3.44(MCM). Nonetheless, no noteworthy distinction was detected between the categories of high and low inflow. Additionally, it is worth mentioning that in both high and low inflow categories, April showed the highest RMSE values, specifically 0.54 and 0.59, respectively. The root mean square error (RMSE) values for medium, low, and high inflow were 1.03, 0.19, and 0.17, respectively.

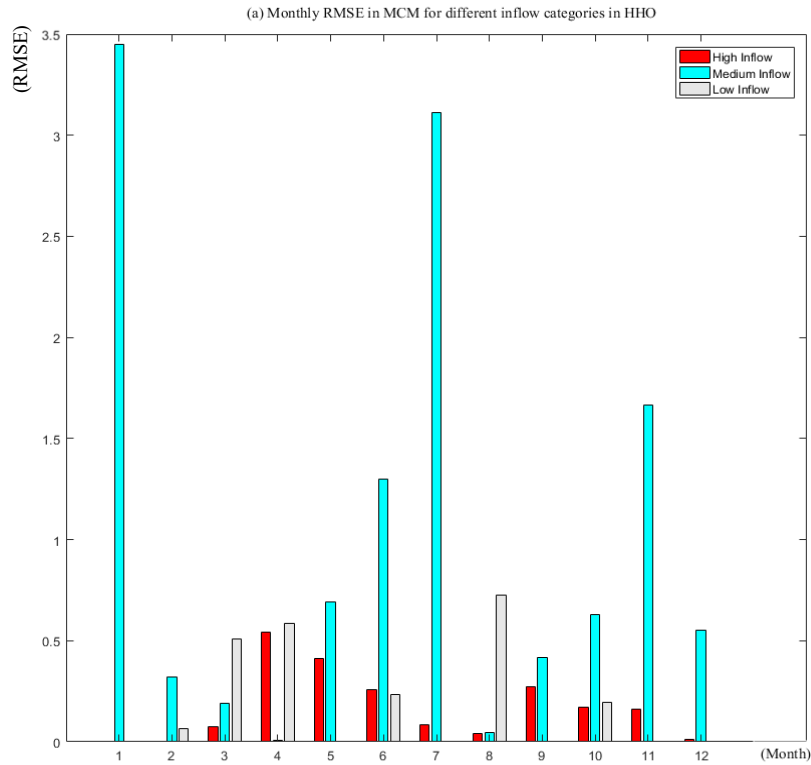


Figure 4.5: (a) Monthly RMSE (MCM) for different inflow categories in HHO

Figure 4.5(b) presents the uncertainty evaluation of the monthly PBIAS from 2001 to 2019 for three different inflow categories. In comparison to the medium and low inflow categories, which provided a greater average magnitude value for PBIAS, the high inflow categories obtained the lowest average magnitude range for PBIAS. As shown in Figure 4.1(b), the low inflow categories achieved the highest magnitude of PBIAS for August, with a value of 79.4, and an average PBIAS of 19.4. The highest magnitude for the medium inflow category was recorded in January and July, with 41.2 and 40.9, respectively, while the average PBIAS for the medium inflow category was 15.7. In addition, the average PBIAS for the high inflow category was 7.7, with April and May reporting the highest magnitudes at 24.4 and 15.1, respectively.

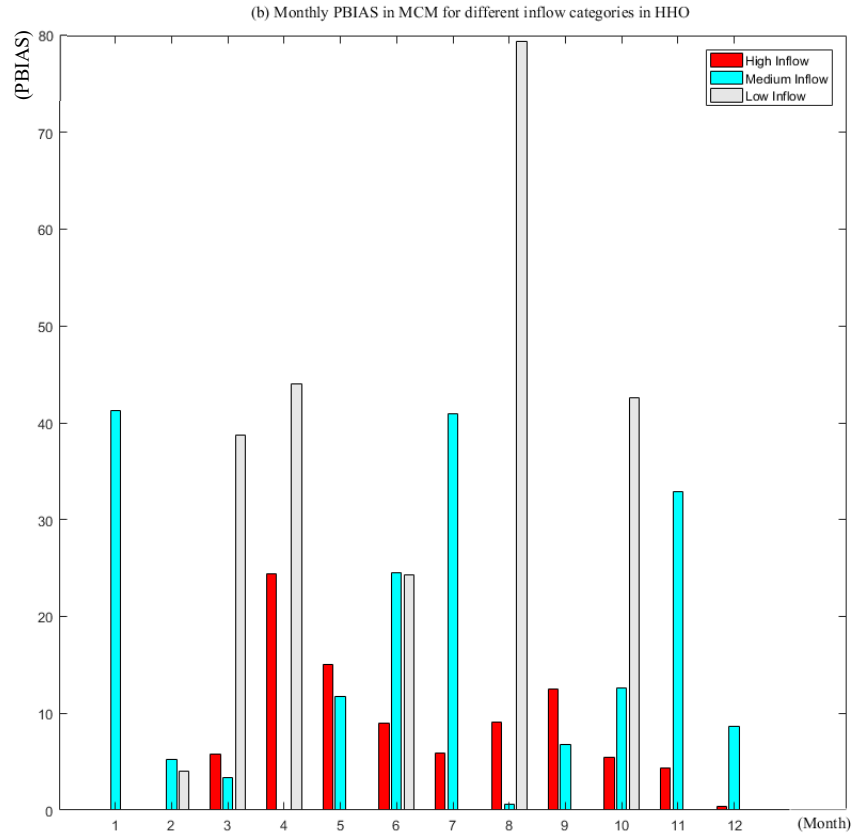


Figure 4.5: (b) Monthly PBIAS (MCM) for different inflow categories in HHO

Figure 4.5(c) displays the monthly MAE analysed by the HHO algorithm from 2001 to 2019 for the three distinct inflow categories. As seen from Figure 4.1(c), positive and negative values of MAE occur, with the high inflow category obtaining a positive MAE value of 0.11 on average. However, April and May had the highest MAE, with 0.23 and 0.20, respectively. In addition, the majority of MAE's negative fell into the medium and low inflow categories. The average negative value of MAE for medium inflow reached -0.21, with January and July recording the highest values, -0.58 and -0.558, respectively. Moreover, the average negativity of MAE for the low inflow category was -0.09, with the highest MAE occurring in August at -0.27.

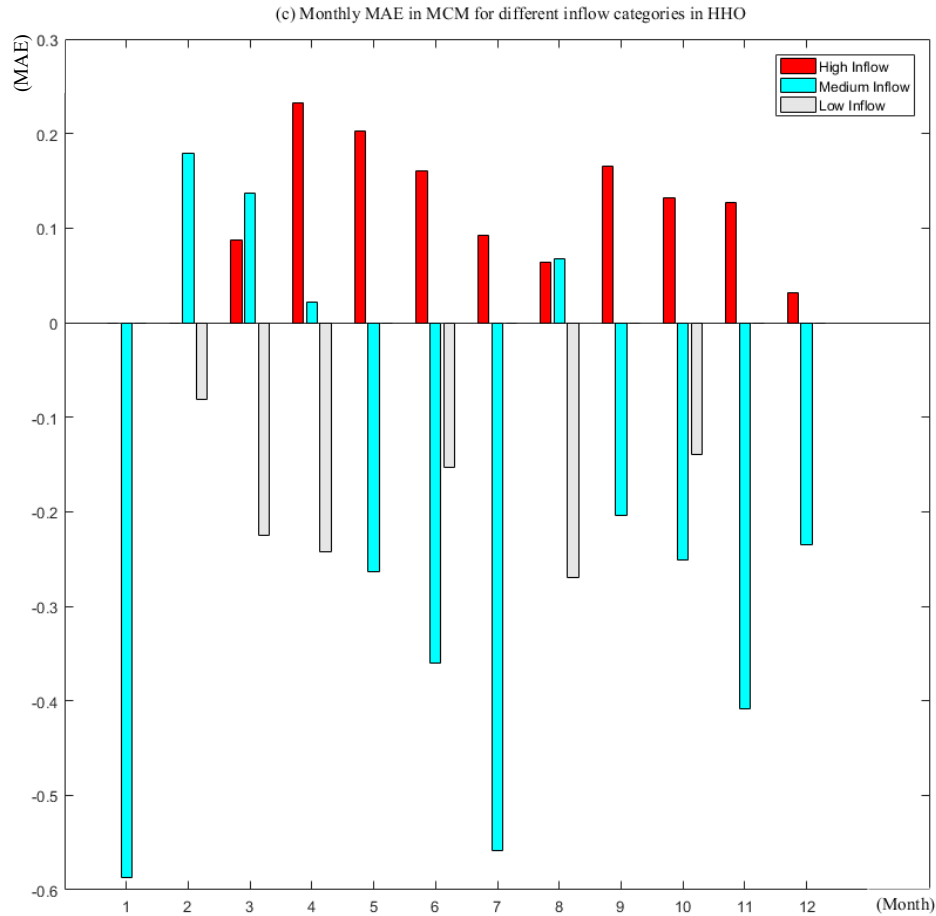
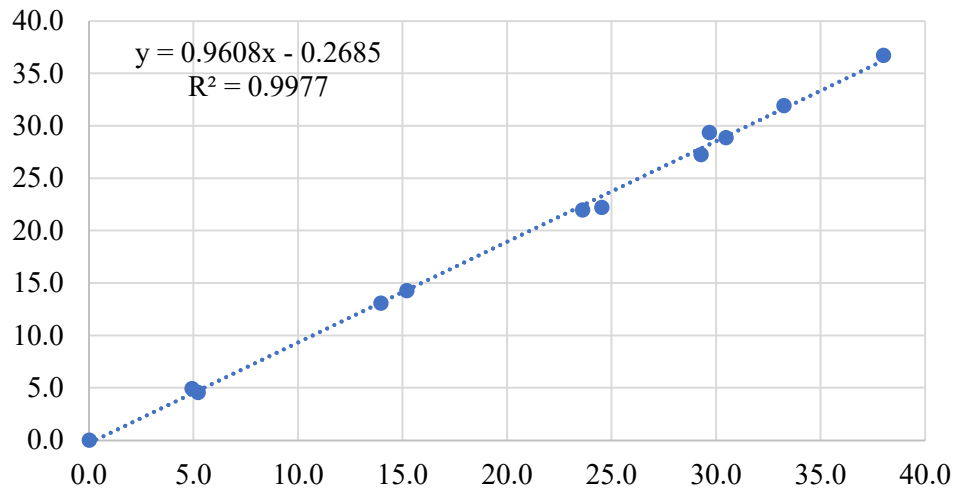


Figure 4.5 : (c) Monthly MAE (MCM) for different inflow categories in HHO

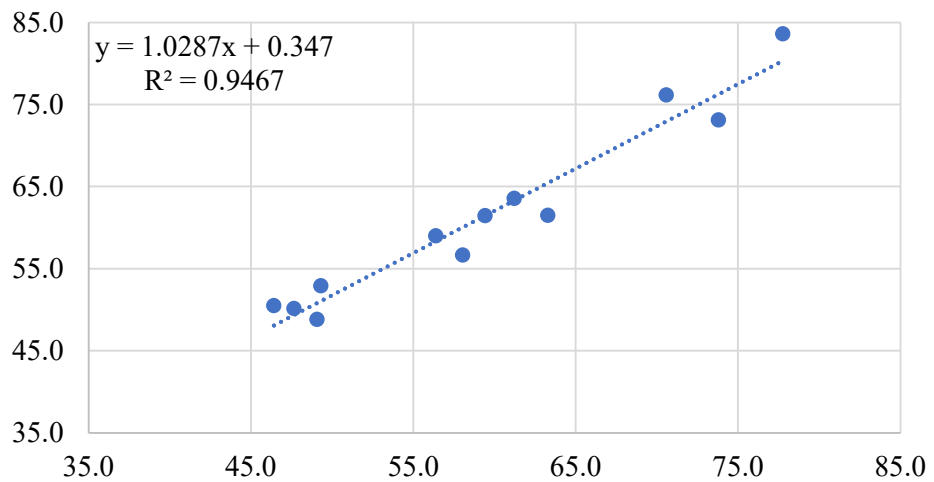
Figure 4.6(a) - (c) represented the R^2 values for the three distinct inflow categories. Utilising the HHO algorithm, the graphs displayed high accuracy between the simulated and targeted demand at the KGD. The highest R^2 was obtained for the high inflow category with 0.9977, followed by the low inflow category with $R^2 = 0.9825$ and the medium inflow category with $R^2 = 0.9467$. Even though the medium inflow category achieved a lower accuracy than the other two inflow categories, evaluations with an accuracy greater than 0.85 are still considered reliable. The final component to be highlighted is the NSE. The average NSE for the categories of high inflow, medium inflow, and low inflow

were 0.9149, 0.9082, and 0.56, respectively. However, the NSE for the low inflow category was low because several months (May, September, November, and December) exhibited no indication of low inflow.

(a) High Inflow



(b) Medium Inflow



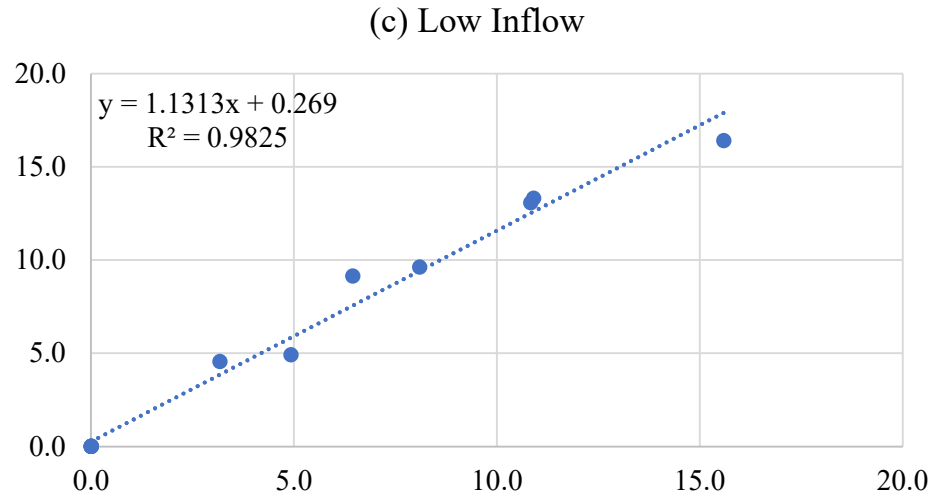


Figure 4.6: R^2 evaluation (a) in High Inflow, (b) in Medium Inflow, (c) in Low Inflow for HHO algorithm

(d) OBL-HHO

Fig. 4.7(a) depicts the statistical evaluations of RMSE (monthly) by the three input categories from 2001 to 2019. In January, the medium inflow exhibited the highest RMSE (million cubic metre) of 5.2, despite the fact that high and low inflow categories did not distinguish noticeably from one another. Aside from this, the RMSE values for the high inflow category reached 0.49 in April and 0.51 in August for the low inflow category. The average RMSE for medium inflow was 1.39, while for low and high inflow it was 0.14 and 0.2, respectively.

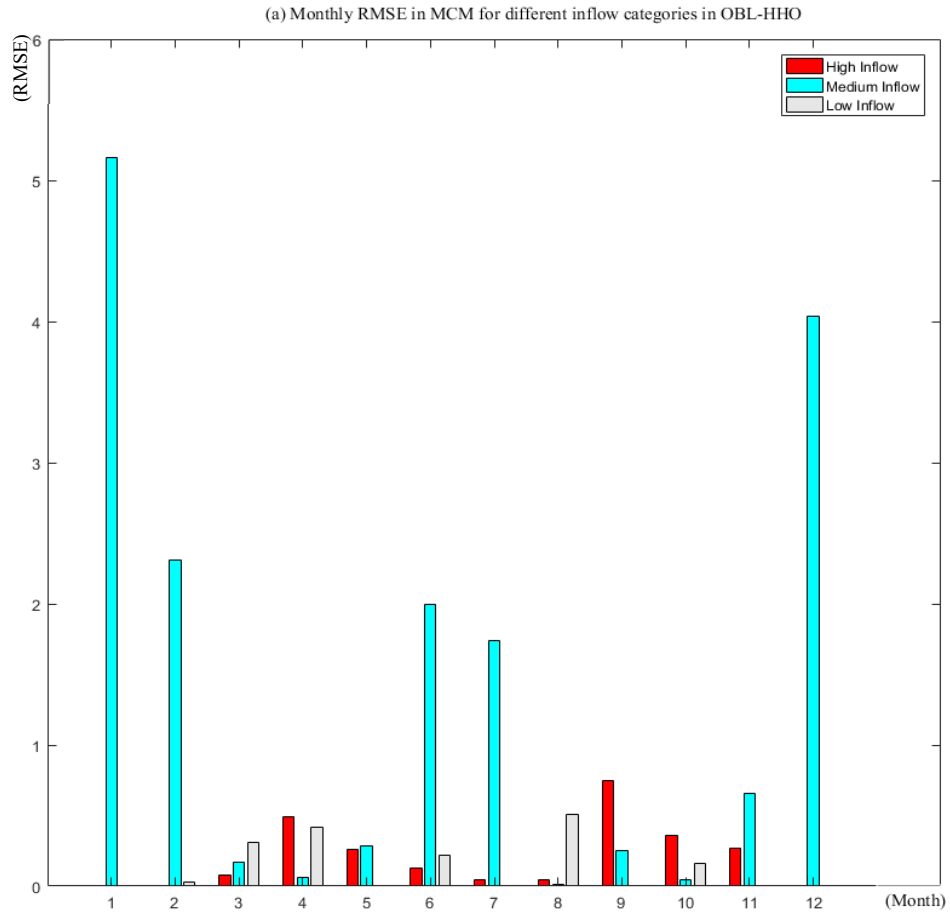


Figure 4.7: (a) Monthly RMSE (MCM) for different inflow categories in OBL-HHO

The uncertainty assessment of the monthly PBIAS from 2001 to 2019 for the three different inflow categories is shown in Figure 4.7(b). Figure 4.7(b) demonstrates that the low inflow category, with a value of 55.43 and an average PBIAS of 14.2, had the highest PBIAS magnitude for August. The highest magnitude for the medium inflow category was 61.7, and the average PBIAS for this category was 20.9 in January. The average PBIAS for the category of high inflow was 8.9, with the highest magnitudes observed in April and September at 22.3 and 34.03, respectively.

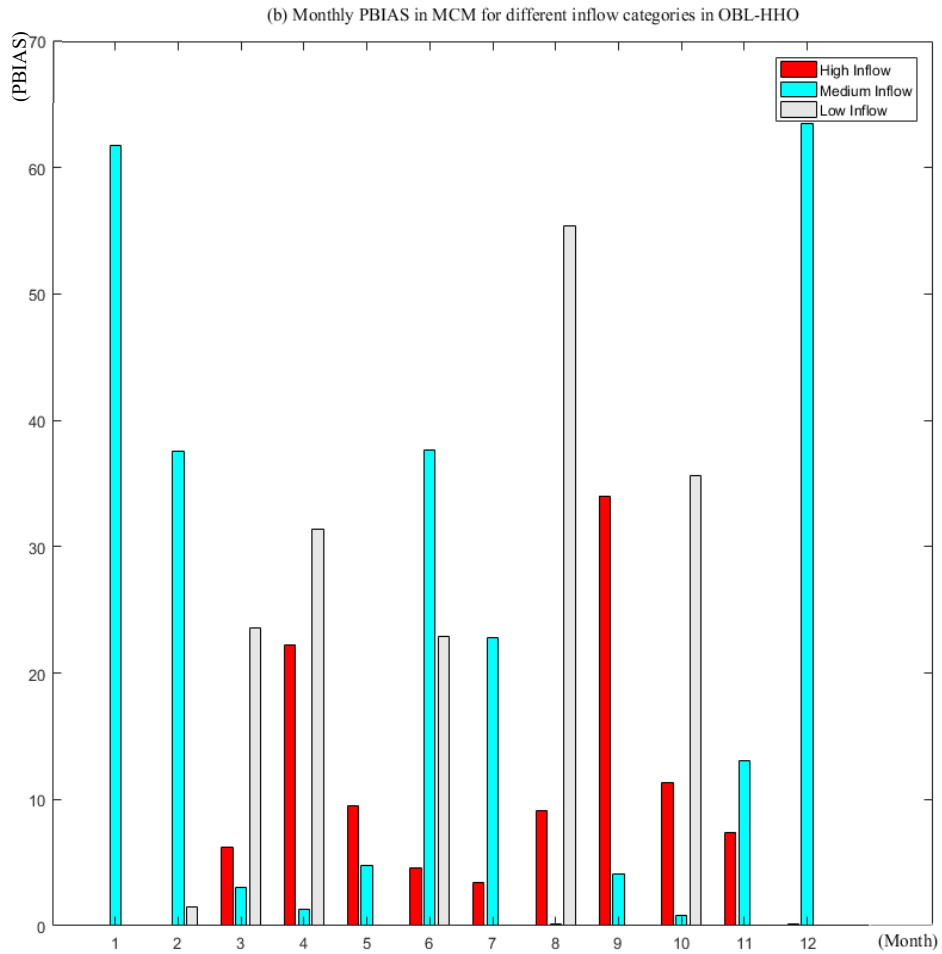


Figure 4.7: (b) Monthly PBIAS (MCM) for different inflow categories in OBL-HHO

The monthly MAE for each of the three different inflow categories from 2001 to 2019 is depicted in Figure 4.7 (c) that the MAE occurs in the high inflow category, with the maximum value of 0.22 recorded in April. The MAE achieved in the high inflow category on average was 0.11. Additionally, the majority of MAE's negativity was classified as having a medium or moderate inflow. The highest readings of -0.72 were recorded in January, with the average negative MAE for medium inflow reaching -0.19. Furthermore, the average MAE for the low inflow category was 0.08, with August having the highest MAE of 0.23.

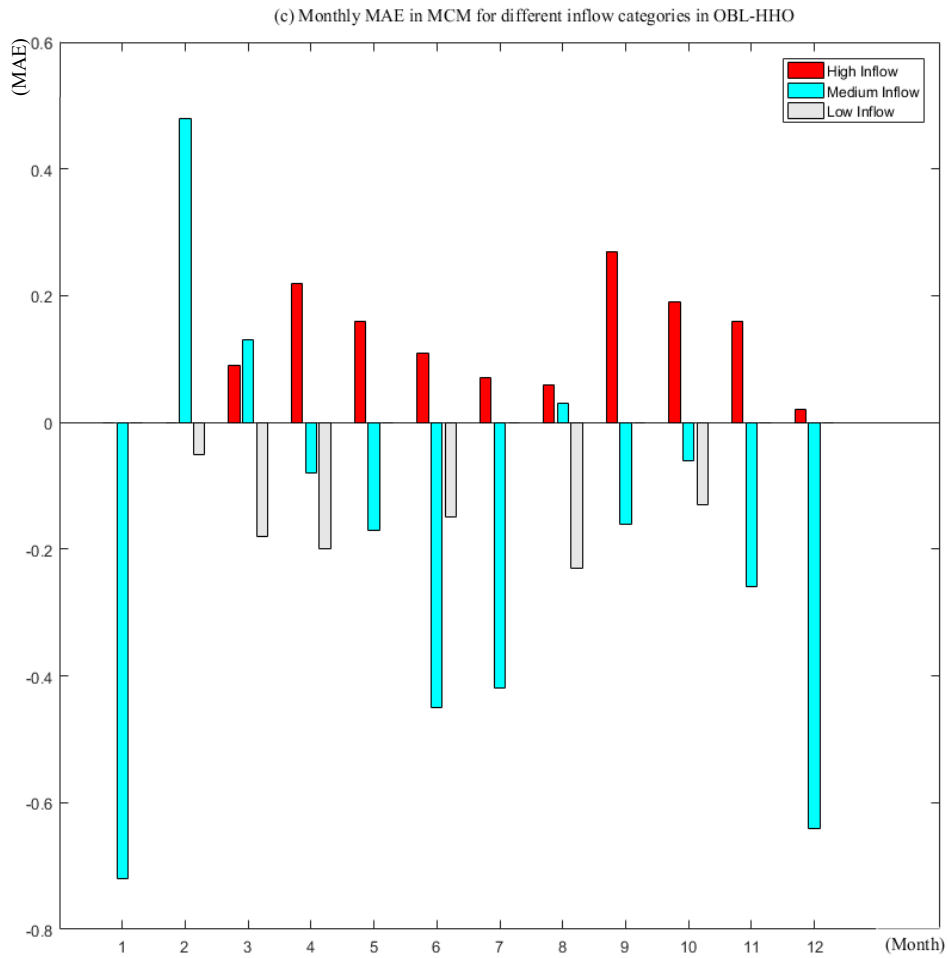
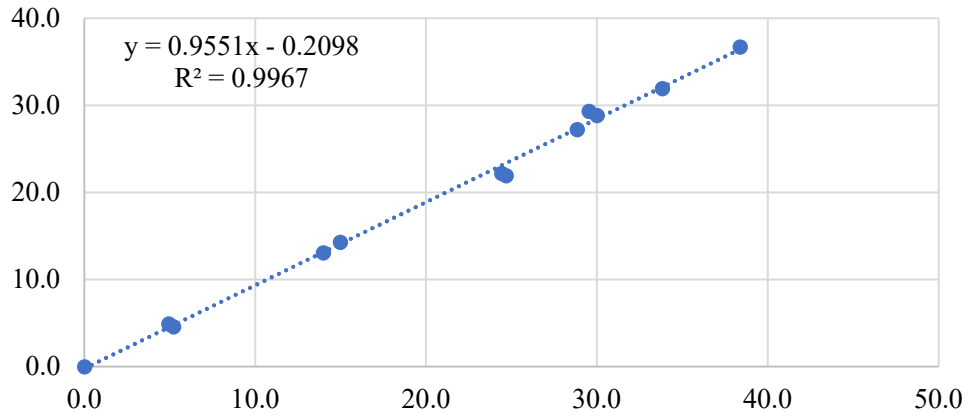


Figure 4.7: (c) Monthly MAE (MCM) for different inflow categories in OBL-HHO

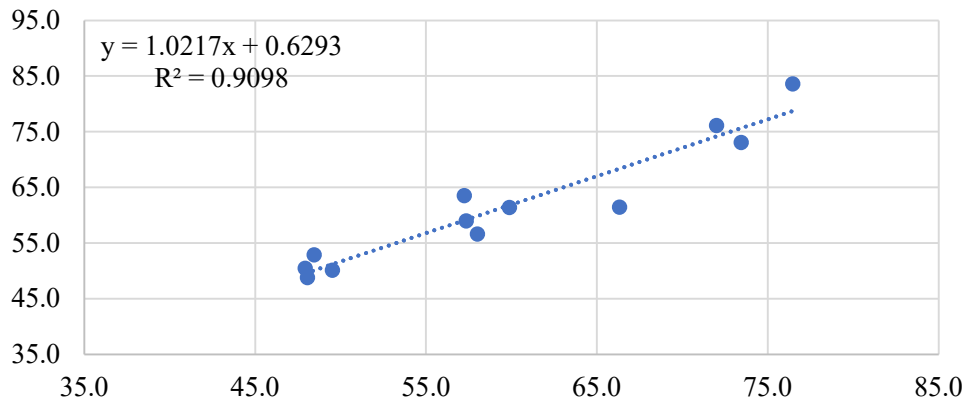
The R^2 values for the three different inflow categories are shown in Figure 4.8(a) - (c). The graphs showed the high accuracy between the simulated and targeted demand at KGD by using OBL-HHO algorithm. The high inflow category has the highest R^2 of 0.9967, followed by the low inflow category 0.9865, and the medium inflow category 0.9098. The mean NSE values for the categories of high inflow, medium inflow, and low inflow categories were 0.9151, 0.9051, and 0.5662, respectively. Despite of this, the NSE for the low

inflow category was low because May, July, September, November, and December showed no signs of low inflow.

(a) High Inflow



(b) Medium Inflow



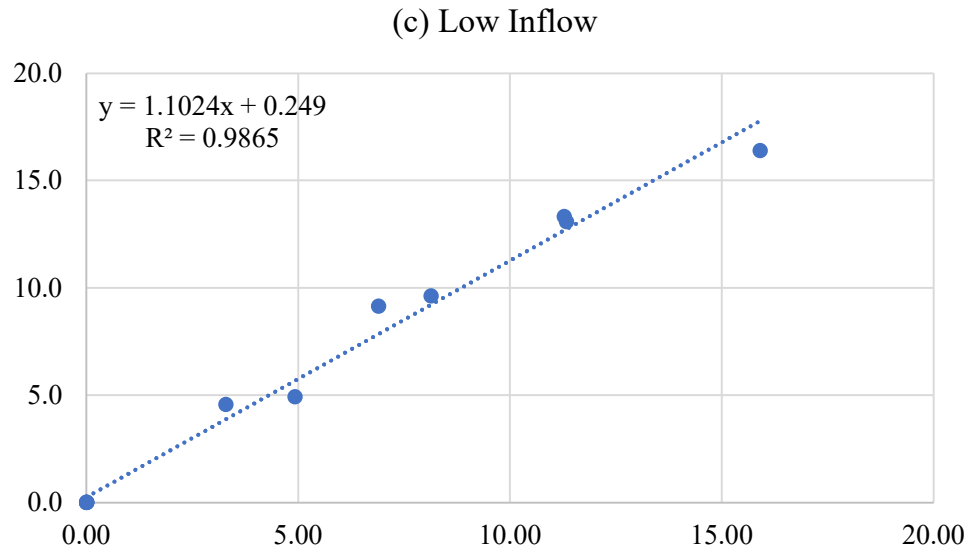


Figure 4.8: R^2 evaluation (a) in High Inflow, (b) in Medium Inflow (c) in Low Inflow for OBL-HHO algorithm

The summary of statistical model performance evaluations has been thoroughly examined and has tabulated in Table 4.3 according to the respective algorithms. Table 4.3 indicates that both HHO and enhancement of its model exhibited the lowest RMSE values in the high inflow category, as was also observed in the categories of medium inflow and low inflow. The LFWOA has the least PBIAS magnitude for the high inflow category. However, the results of PBIAS for the categories of medium inflow and low inflow increased significantly, ranging between 14.20 and 30.63, while the HHO and enhancement of its model achieved the lowest magnitudes, 15.72 and 14.20, respectively, for the categories of medium inflow and low inflow. The algorithms for high inflow were identical to those for medium inflow and low inflow for the MAE assessment, with no appreciable differences among the proposed algorithms. However, the MAE was negative for both categories of

inflow, resulting in an inability to draw conclusions regarding the MAE for medium inflow and low inflow. Additionally, the findings of R2's performances were above average, showing that the simulated and targeted demand was satisfied for all three categories. Similarly, the proposed algorithms achieved above-average outcomes, but because some months showed no trace of the low inflow category into KGD, there was a significant NSE difference between all three inflow categories. As a result, it gives an inconclusive summary for the overall ranking of the suggested algorithms, and further evaluation is necessary and must be examined in terms of how well those algorithms perform when it comes to reservoir risk analysis.

Table 4.3: Summary of Statistical Performance Evaluations

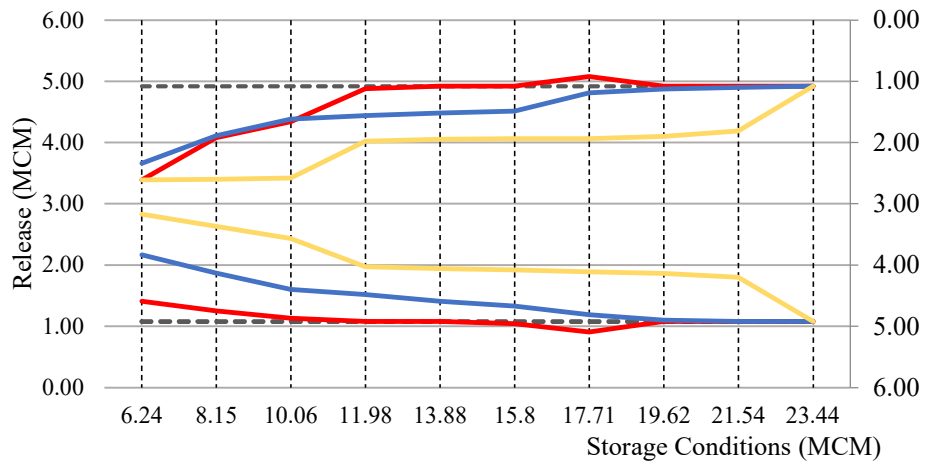
Average Statistical Evaluation/Inflow Categories/ Algorithms	RMSE			PBIAS			MAE			R ²			NSE		
	High	Medium	Low	High	Medium	Low	High	Medium	Low	High	Medium	Low	High	Medium	Low
WOA	2.04	5.94	0.49	6.39	30.63	18.16	0.08	-0.21	-0.09	0.996	0.876	0.976	0.916	0.908	0.26
LFWOA	2.04	5.94	0.51	4.42	24.50	19.44	0.08	-0.20	-0.08	0.999	0.909	0.957	0.915	0.911	0.26
HHO	0.17	1.03	0.19	7.65	15.72	19.41	0.11	-0.21	-0.09	0.998	0.947	0.983	0.915	0.908	0.56
OBL-HHO	0.20	1.39	0.14	8.99	20.88	14.20	0.11	-0.19	-0.08	0.997	0.910	0.987	0.915	0.905	0.57

4.3.2 Monthly Release Curves Correspond with Inflow Categories by Utilising WOA versus LFWOA

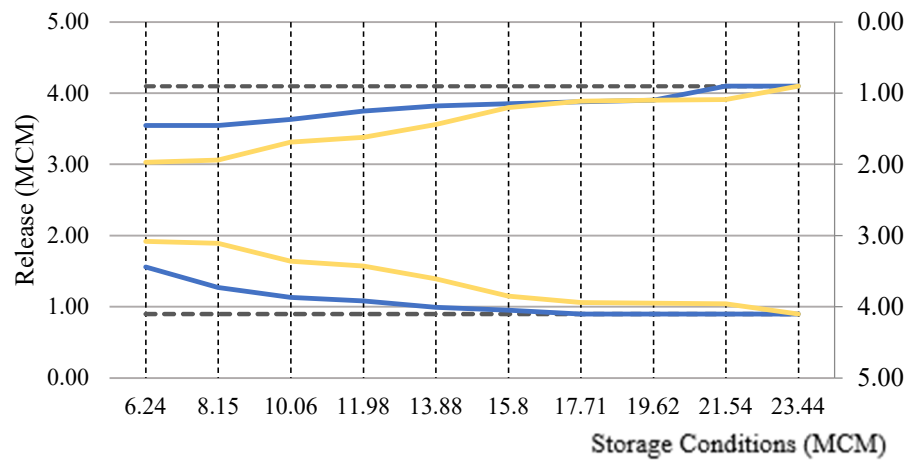
By implementing WOA and LFWOA, the observed period of the release curves presented in month for year 2001- 2019 was shown to correspond with the storage capacity as depicted in Figure 4.9 (a) - (l). As shown in Figure 4.9 (a) - (l), the upper graphs were plotted using the WOA whereas the lower graphs were generated using the LFWOA. The input data were processed by separating the inflow categories into three and splitting the storage represented on the X-axis into ten discrete storage, d . The maximum and minimum reservoir capacity S_{\min} and S_{\max} was calculated by utilising N as the state option and dividing the value by $N-1$ as the interval. Figure 4.9 (a) - (l) display the release curves presented for January to December by utilising the WOA and LFWOA under various storage condition limits. Figure 4.9 (a) and (b) display the January and February monthly release curves, respectively. For both months, the releases lines provide the ramp up trend towards the demand lines. As there was no significant high inflow during the month of February, the graph depicts only low and medium inflows. As depicted in Figure 4.9 (a) for WOA and LFWOA, respectively, during the storage level of 17.71 MCM, there was minor wastage during the high inflow in January. As depicted in Figure 4.9 (c) and (d) for March and April, there were a few instances in which the algorithms of LFWOA in March were oversupplied as the inflow within these storage boundaries at 10.06 MCM to 17.71 MCM was high, without jeopardising the KGD reservoir constraints and resulting in the wastage condition to occur. In addition, as shown in Figure 4.9 (d) for April, both the WOA and LFWOA algorithms exhibit a

comparable pattern for the release curves for the ten discrete storage locations. One scenario stands out, though, where both release curves intersect at a storage level between 6.24 MCM and 8.15 MCM, indicating that there was still sufficient reservoir storage to fill it up and fulfil the demand line. For May, July, September, November, and December, there were no low inflow categories indicated in Figure 4.9 (e),(g),(i), and (k) - (l). Figure 4.9 (a) - (l), which depict the plots of the release curves in the low and medium inflow categories, respectively, revealed that the releases have been increasing towards the demand lines. However, most of the plots display in these figures revealed that water surplus or oversupply typically occurred in the high inflow category, resulting in the excessive release of water back into the river or sea. Therefore, this incidence ought to be advised and recommended for future study. The optimal outcome is usually achieved by the demand versus release curve that exhibits the least amount of water deficit. The results of the reservoir risk analysis are tabulated in the subsequent section of sub-section 4.3.3.

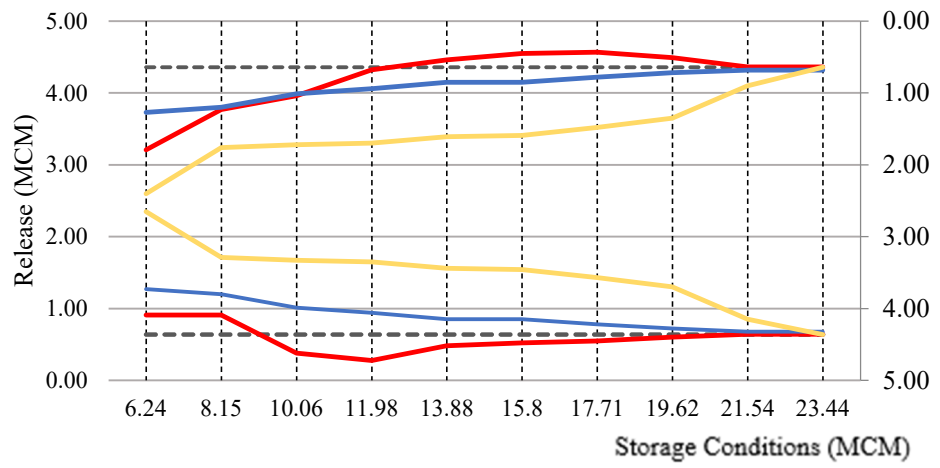
(a) January Release Curves



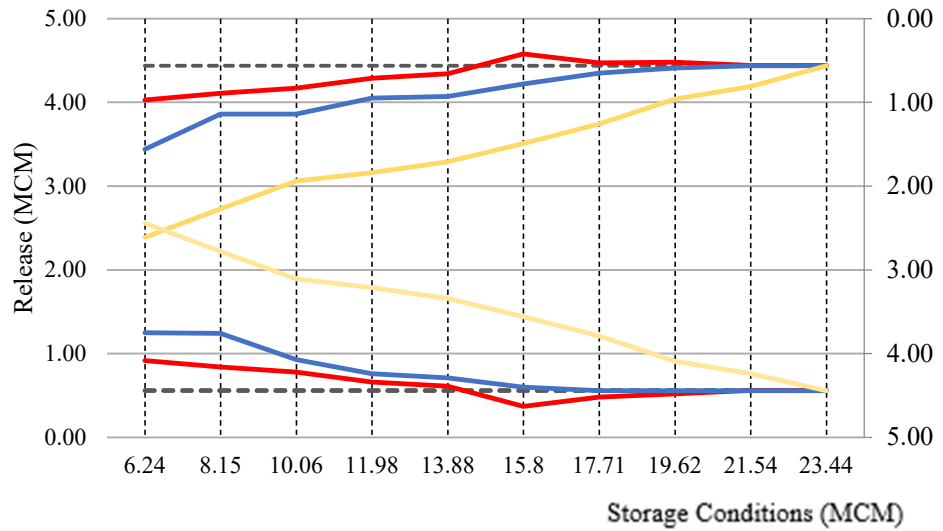
(b) February Release Curve



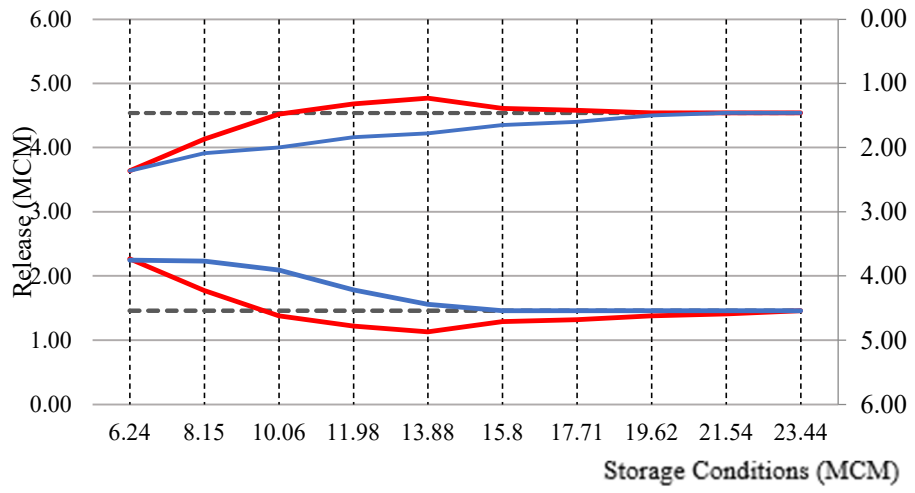
(c) March Release Options



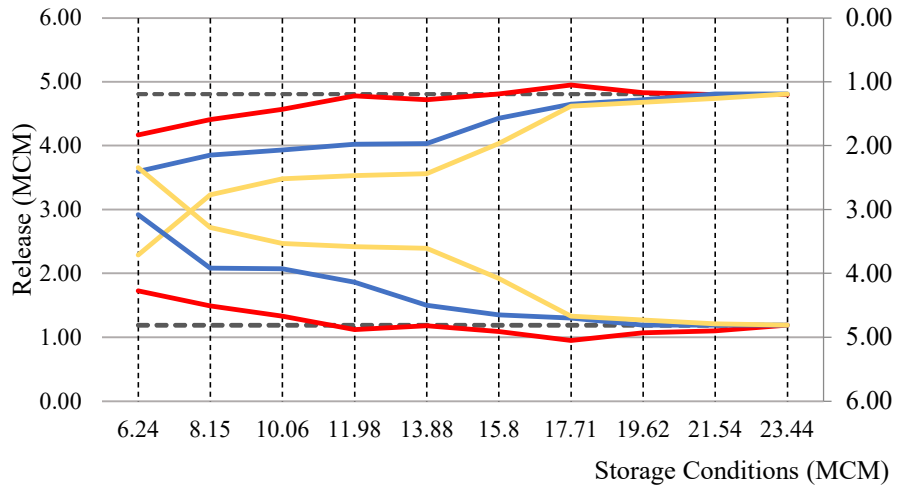
(d) April Release Options



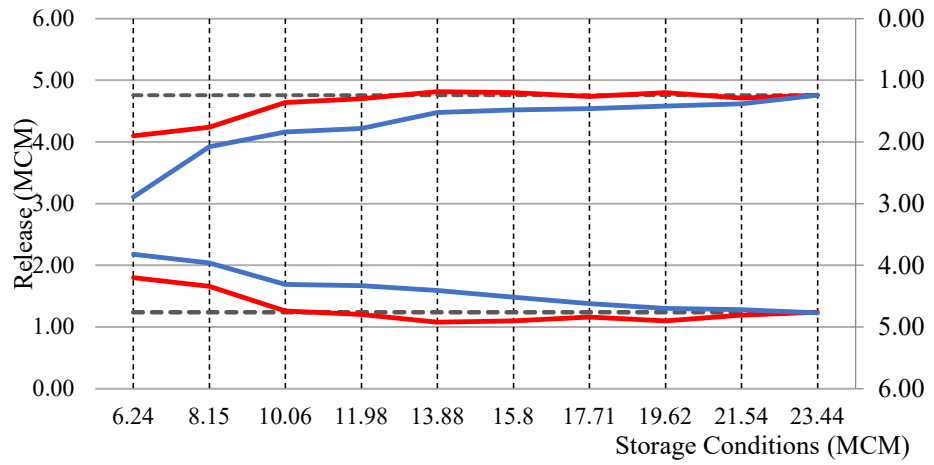
(e) May Release Options



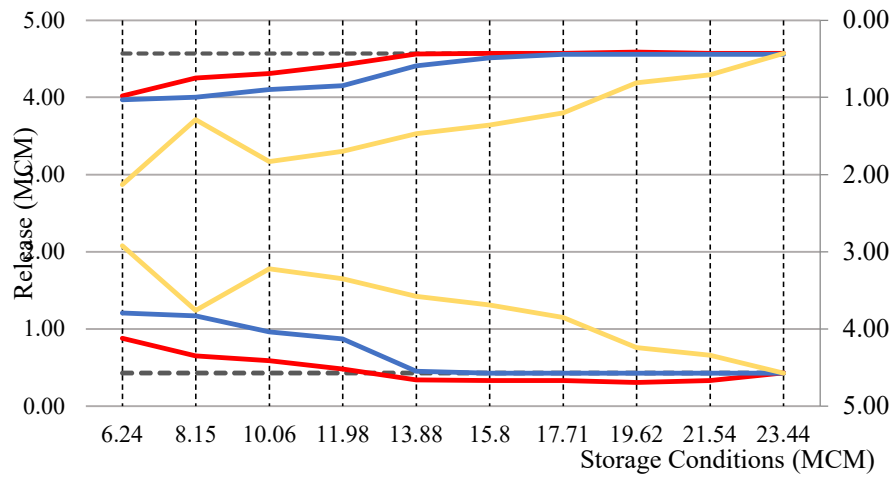
(f) June Release Options



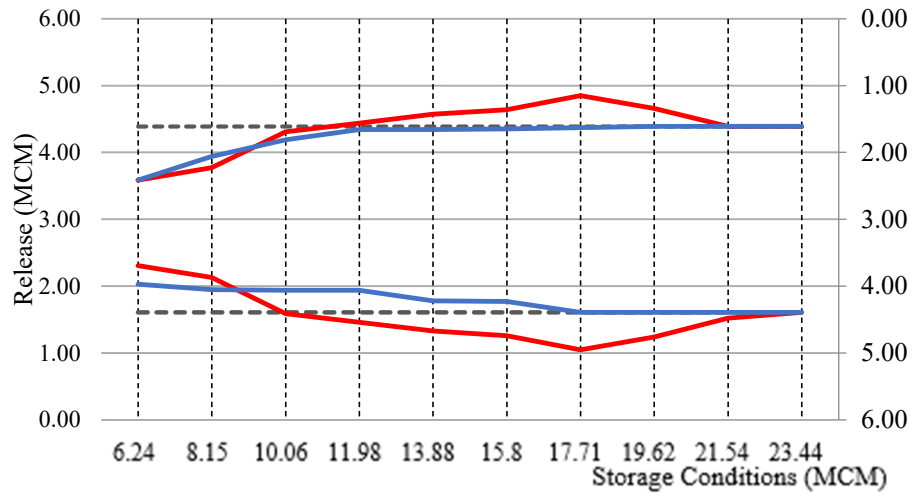
(g) July Release Options



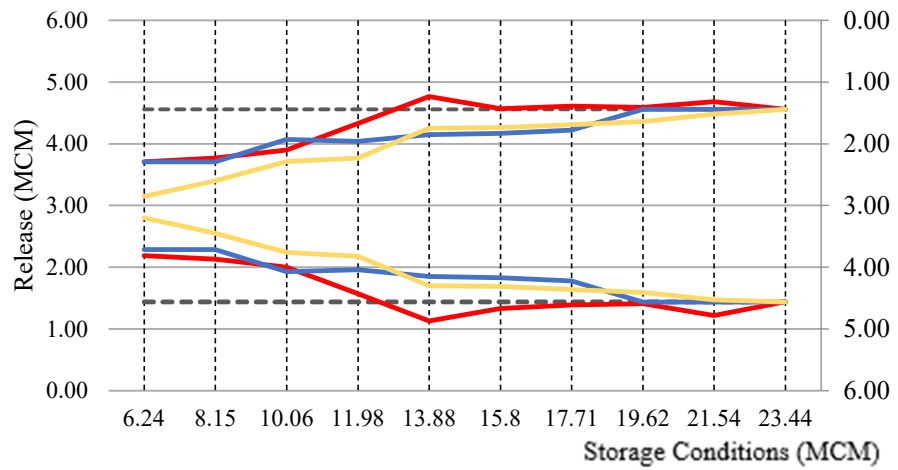
(h) August Release Options



(i) September Release Options



(j) October Release Options



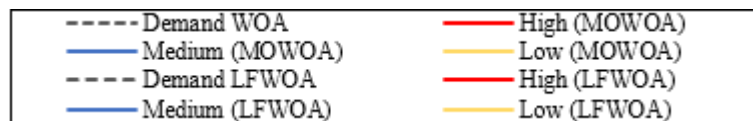
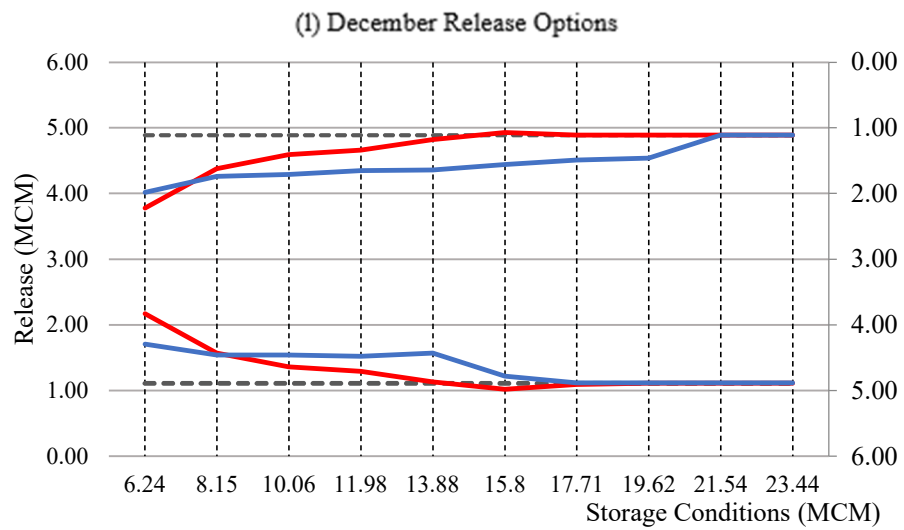
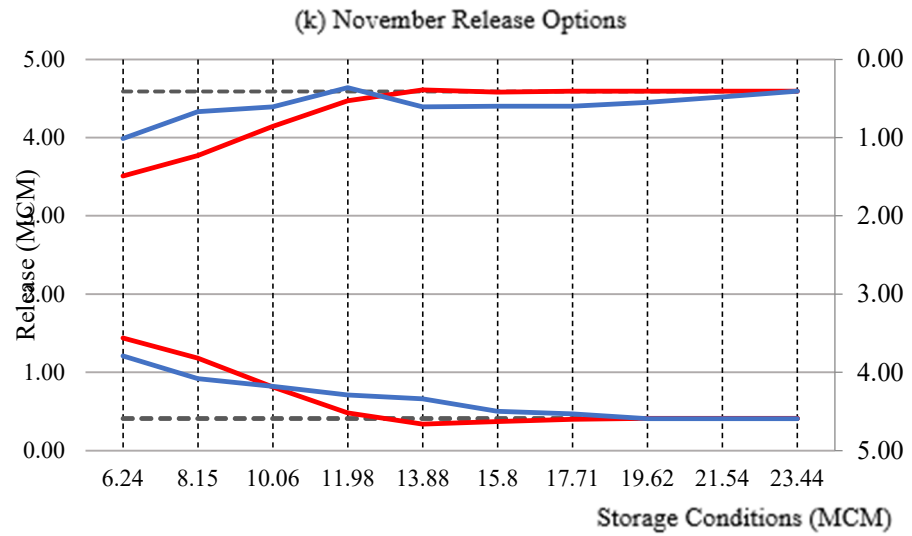


Figure 4.9: (a) January release curve - (l) December release curve by utilising WOA and LFWOA

4.3.3 Reservoir Risk Assessment for WOA and LFWOA

In this sub-section, the outcomes of the reservoir risk assessment from year 2001- 2019 are discussed. The periodic reliability between the WOA and LFWOA were compared in Table 4.4. Between 2001 and 2019, the three different inflow categories resulted in a total of 228 outcomes. No specific period of scarcity has been identified for optimising the high inflow category, given that the present inflow was adequated to meet the existing demand. For the WOA, excess periods happened 17 times (7.46%) and for LFWOA, 15 times (6.58%). WOA fulfilled demand 33 times (14.47 %) and LFWOA 35 times (15.35 %) during the periods of high inflows. The WOA satisfied 91 times (39.91 %) of the medium inflow demand, while the LFWOA satisfied 97 times (42.54 %), 2.63 % more than the WOA. During the excess period, the WOA and LFWOA produced 33 times (14.47%) and 29 times (12.72%), respectively. The WOA had delivered 38 times (16.67%) and LFWOA had obtained 35 times (15.35%) during the shortage with a medium inflow. The WOA attained 9 times (3.95%) and LFWOA gained 6 times (2.63%) in hitting the exact demands.

Table 4.4: Periodic Reliability performance via WOA and LFWOA

Inflow categories	Surplus period	Exact period	Shortage period
WOA (times, %)			
High	17,(7.46%)	33, (14.47%)	0, (0%)
Medium	33, (14.47%)	91, (39.91%)	38, (16.67%)
Low	0, (0%)	9, (3.95%)	7, (3.07%)
Total no. of release	50, (21.93%)	133, (58.33%)	45, (19.73%)
LFWOA (times, %)			
High	15, (6.58%)	35, (15.35%)	0, (0%)
Medium	29, (12.72%)	97, (42.54%)	35, (15.35%)
Low	0, (0%)	6, (2.63%)	11, (4.82%)
Total no. of release	44, (19.30%)	138, (60.52%)	45, (39.90%)

Table 4.5 summarises the WOA and LFWOA model performance for the KGD. According to the shortage index evaluation criteria, the LFWOA had a shortage index value of zero in the low inflow categories, while the WOA achieved a value of 0.00005, which is very close to zero. In contrast, for the category in medium inflow, the shortage index, the WOA achieved 0.00024 while the LFWOA achieved 0.00033, indicative the system might experience a water scarcity in the future. During medium and low input events, both algorithms could recover from failure; however, during high inflow events, neither algorithm could do so and would go beyond the storage capacity. Finally,

the vulnerability index produced the lowest value would be the more consistent way. The least value series begins with the WOA 0.35, 0.49, and 2.74 for medium, high, and low values, respectively. In contrast, the LFWOA obtained 0.12, 0.44, and 0.55 for the low, medium, and high inflow, respectively. Except for the high inflow category, the LFWOA is much more robust than the WOA in this vulnerability criteria of evaluation reservoir risk analysis.

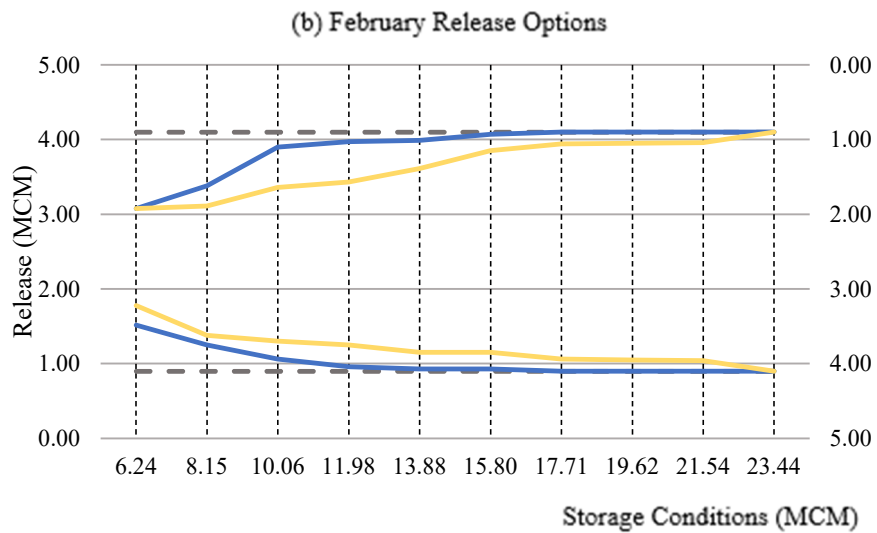
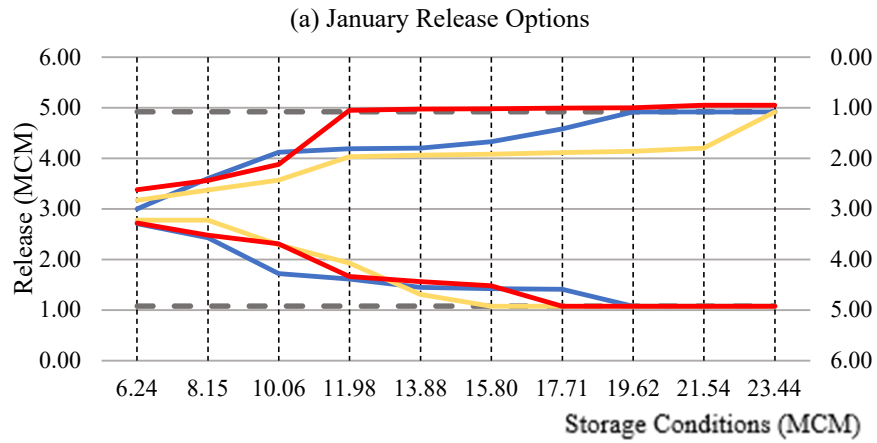
Table 4.5: Reservoir Risk Assessment

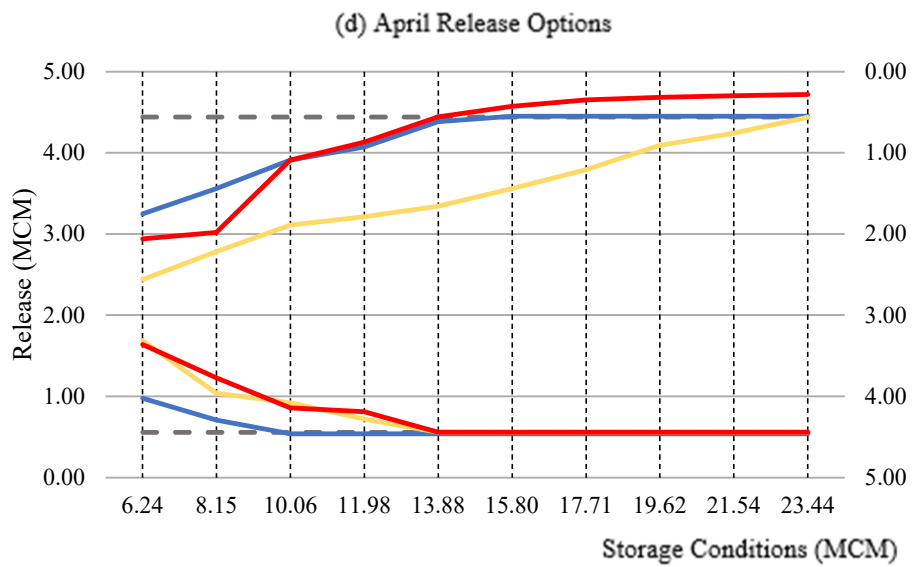
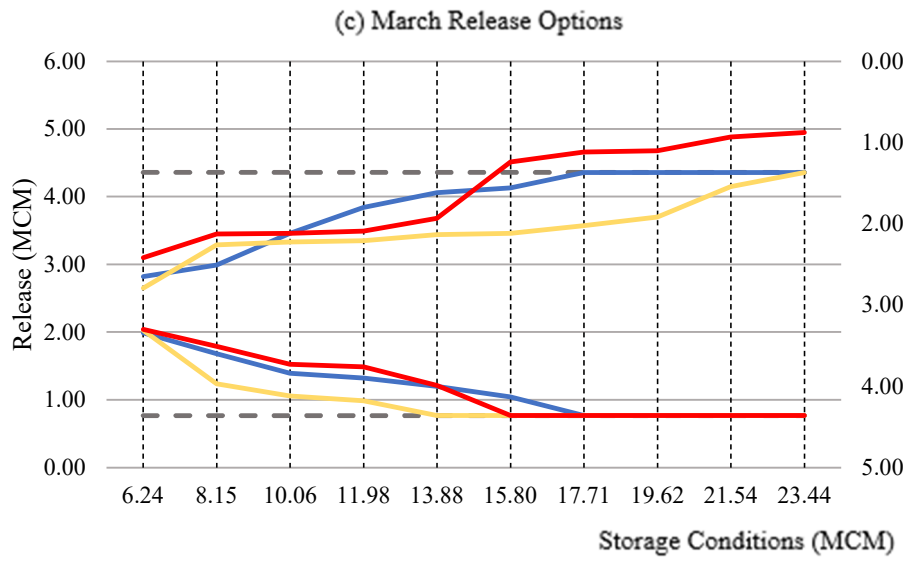
MHAs	Assesments	High	Medium	Low
	Wastage due to excess release(%)	7.46	14.47	0
	Meeting demand (%)	14.47	39.91	3.95
WOA	Shortage index	0.00007	0.00024	0.00005
	Vulnerability	0.49	0.35	2.74
	Resiliency	-	3.26	1.29
	Wastage due to excess release(%)	6.58	12.72	0
	Meeting demand (%)	15.35	42.54	2.63
LFWOA	Shortage index	0.00003	0.00033	0
	Vulnerability	0.55	0.44	0.12
	Resiliency	-	3.60	0.55

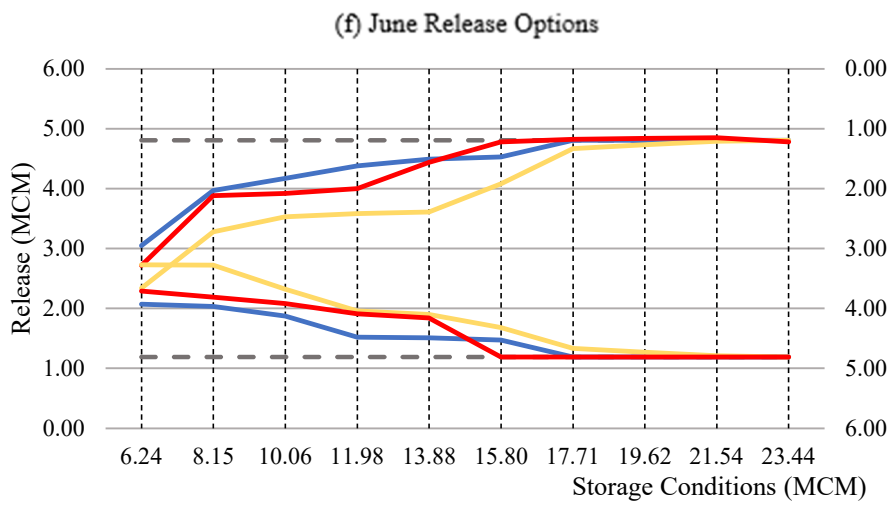
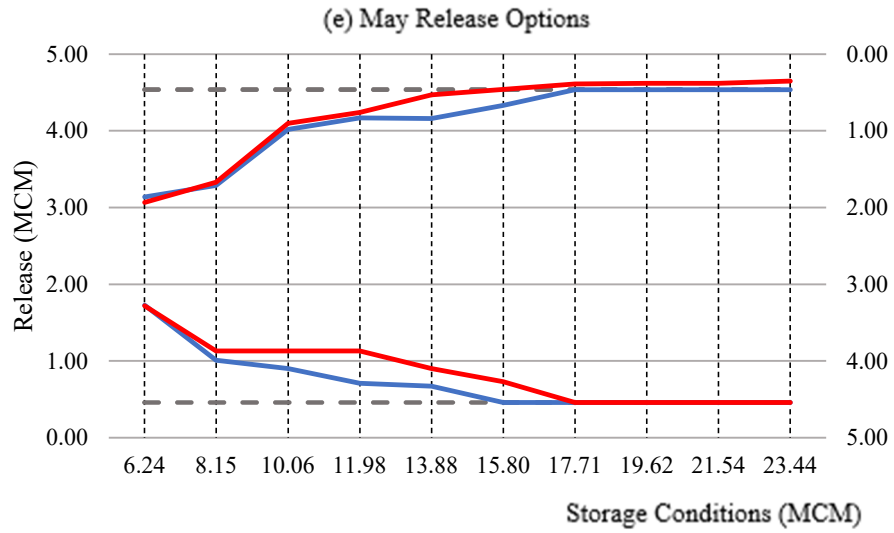
4.3.4 Monthly Release Curves Correspond with Inflow Categories by Utilising HHO versus OBL-HHO

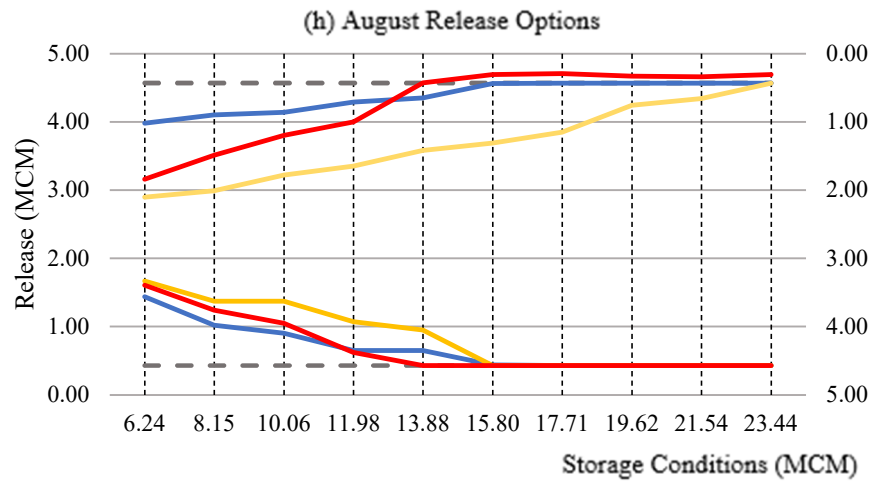
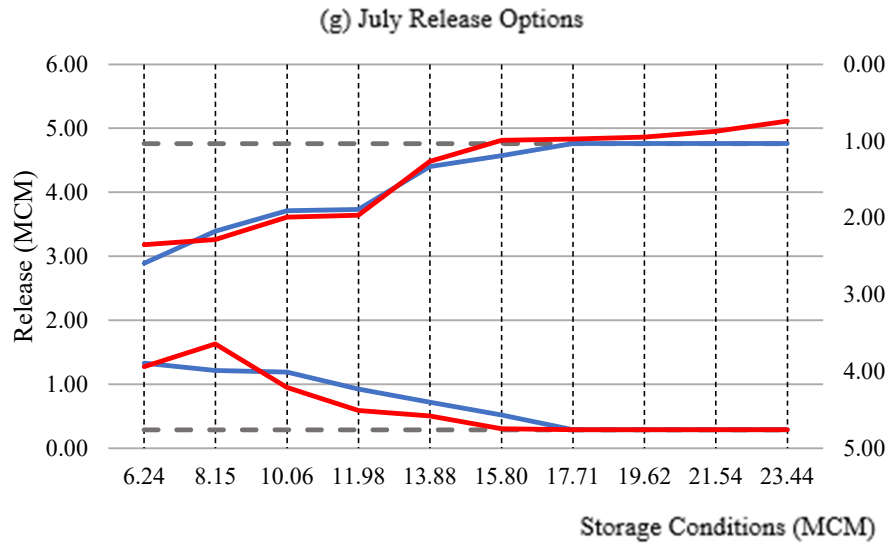
Figure 4.10 (a) - (l) depict the release curves of the HHO and OBL-HHO under different storage condition limits from January to December. Figure 4.10 (a) and (b) display the monthly release curves for January and February, respectively. The releases have performed an escalate pattern approaching to the demand lines for both months. As there was no major high inflow for February, only low and medium inflows are depicted on the graph. As shown in Figure 4.10 (a) for the the HHO and its enhancement model, respectively, the algorithms executed and produced the optimal water release curves in supplying minimum deficit and no excessive release occurred during these months in comparison to Figure 4.10 (a) and (b) implemented via the WOA and LFWOA. As shown in Figure 4.10 (c) and (d) for March and April, an oversupplied scenario occurred in March due to the utilisation of the WOA at the storage boundary of 15.80 MCM for the high inflow category, resulting in a waste condition. In addition, as depicted in Figure 4.10 (d) during the month of April, the WOA exhibited an excessive water release at the storage level of 15.80 MCM, whereas the LFWOA did not demonstrate an excess loss of water. In Figure 4.10 (e),(g),(i), and (k)-(l) during the months of May, July, September, November, and December, there were no low inflow category. Figure 4.10 (f) depicts a scenario where both release curves intersect at a storage level between 6.24 MCM and 8.15 MCM, demonstrating that there is still sufficient reservoir storage to fill the reservoir and satisfy demand. Figure 4.10 (g)-(l), which illustrates the plots of the release curves for the low and medium inflow categories, reveals that the releases have

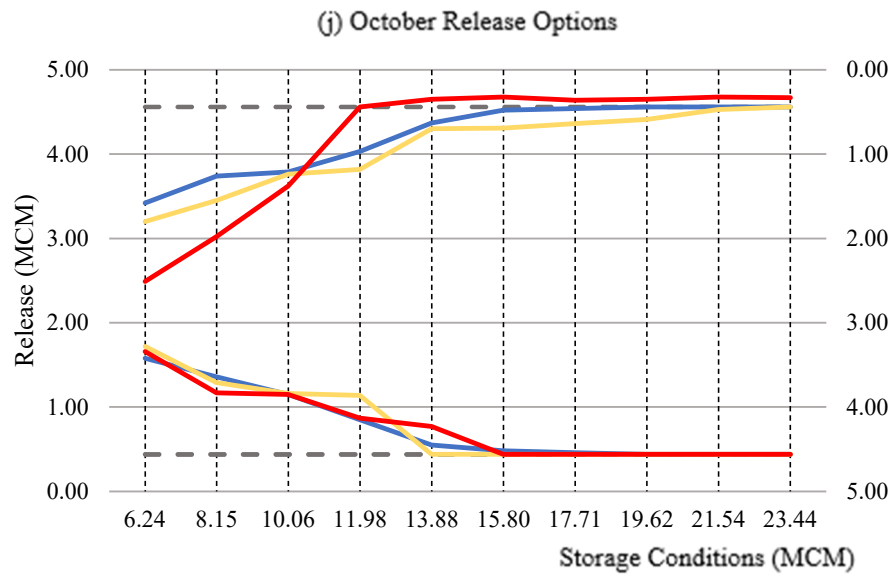
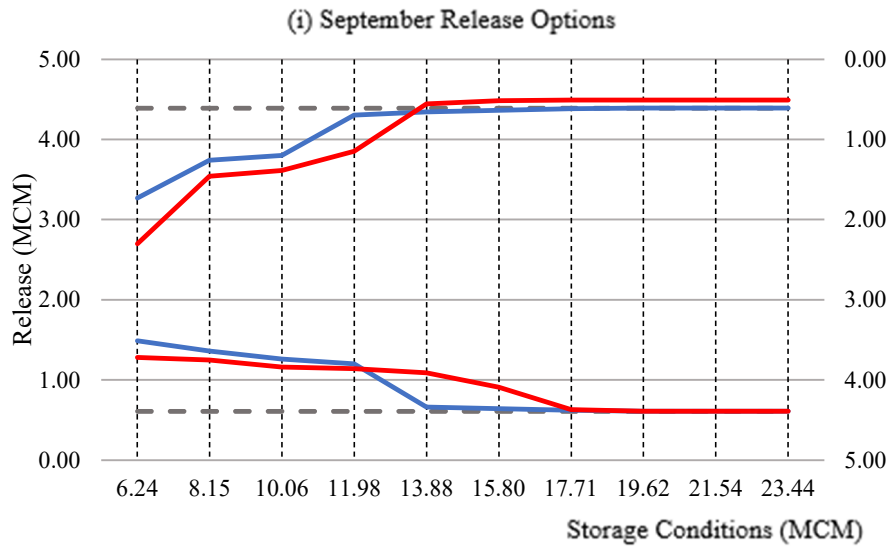
been increasing toward the demand lines. Most plots in these figures showed that water surplus or overflow often occurred in the high inflow category, resulting in excessive water discharge back into the river or sea, as illustrated in Figure 4.10 (g)- (k)











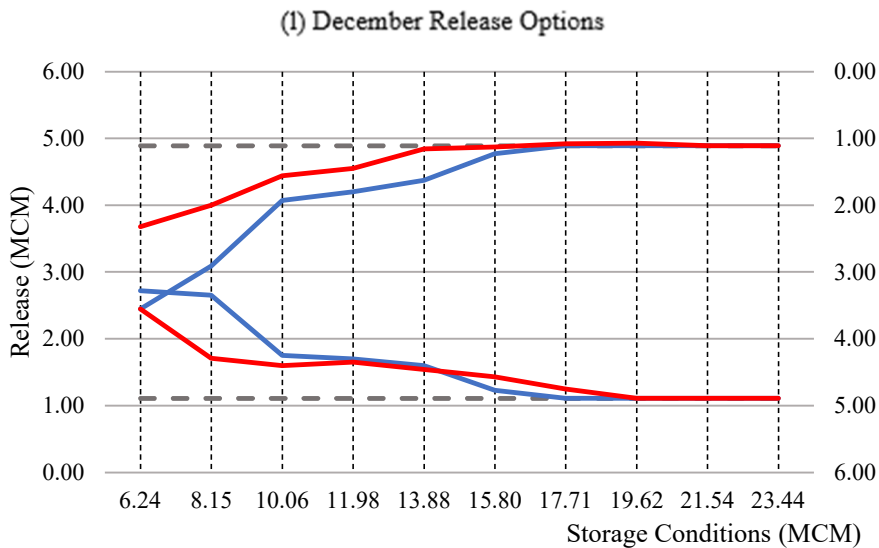
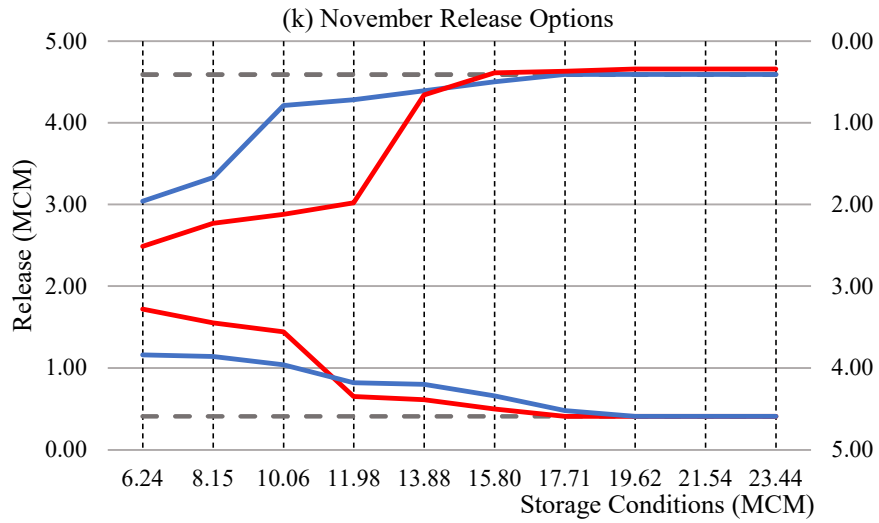


Figure 4.10 : (a) January release curve - (l) December release curve by utilising HHO and OBL-HHO

4.3.5 Reservoir Risk Assessment for HHO and OBL-HHO

Table 4.6 presents a comparative analysis of the periodic reliability of HHO and OBL-HHO. Between 2001 and 2019, a total of 228 outcomes were generated by the HHO and its enhancement model utilising three different input categories. The high inflow category does not have a specified shortage period for optimisation purposes, as the inflow is deemed adequate to satisfy demand. The HHO system experienced surplus periods, which exceeded the water demand, on 21 times, accounting for 9.21% of the total observations. On the other hand, the OBL-HHO system had 28 surplus periods, representing 12.28% of the total observations. At times of high inflows, the HHO was able to satisfy demand on 30 times, which corresponds to 13.16% of the total, while the OBL-HHO met demand 21 times, equivalent to 9.21%. The HHO convened on 88 times, which accounted for 38.60% of the medium inflow demand. In contrast, the OBL-HHO convened on 47 times, representing 20.61% of the demand, which is 1.87 times lower than the HHO. During the surplus period, the HHO gained 15.35% (35 times) and OBL-HHO generated 27.19% (62 times). During the period of scarcity with a medium inflow, the HHO was observed to have a delivery rate of 16.67%, which amounted to 38 times. On the other hand, the OBL-HHO was found to have an acquisition rate of 23.68%, which equated to 54 times. Within the low inflow category, the HHO and its enhancement model exhibited a frequency of 3.95% (9 times) and 4.39% (10 times), respectively. With respect to the specific criteria for the low inflow categories, it was observed that the HHO and enhancement of its model met on 3.07% (7 times) and 2.63% (6 times), respectively.

Table 4.6: Periodic Reliability performance via HHO and OBL-HHO

Inflow categories	Surplus period	Exact period	Shortage period
HHO (times, %)			
High	21, (9.21%)	30, (13.16%)	0, (0%)
Medium	35, (15.35%)	88, (38.60%)	38, (16.67%)
Low	0, (0%)	7, (3.07%)	9, (3.95%)
Total no. of release	56, (24.56%)	125, (54.83%)	47, (20.61%)
OBL-HHO (times, %)			
High	28, (12.28%)	21, (9.21%)	0, (0%)
Medium	62, (27.19%)	47, (20.61%)	54, (23.68%)
Low	0, (0%)	6, (2.63%)	10, (4.39%)
Total no. of release	49, (21.49%)	163, (71.49%)	16, (7.02%)

Table 4.7 provides a summary of the KGD performances via HHO and enhancement of its model. The reliability of the model is evidenced by its success and failure rates. Based on the criteria used in the shortage index evaluation, the disparity between high and low inflow for the HHO was not found to be statistically significant. However, for the OBL-HHO, the respective values were determined to be 0.00008 and 0.00004. Nonetheless, the HHO and OBL-HHO systems garnered the highest scarcity for medium inflow, suggesting that water scarcity may be a potential challenge for the system in the times ahead. Hence, it is imperative to assess the system's capacity to recuperate from a

breakdown. The HHO model showed resilience in the face of medium and low inflow events, however, it exhibited an inability to recover during high inflow events, leading to a breach of the storage constraint. The resilience-based criterion for the occurrence of OBL-HHO was analogous to that of HHO. Hence, it may be imperative for us to heighten our vigilance towards this unfavourable phenomenon. In a more dependable manner, the vulnerability index showed the lowest value. The series exhibiting the minimum values for the HHO initiates with medium inflows, 0.34; high inflows, 0.63; and low inflows, 1.23. In contrast, the OBL-HHO exhibits values for medium inflows, 0.20; high inflows, 0.49; and low inflows, 0.96, as observed in the series. The findings of this study on reservoir risk assessment indicate that the OBL-HHO model exhibits greater resistance compared to the HHO model across all three inflow categories. During the analysis period from 2001 to 2019, the HHO model outperformed the OBL-HHO model in terms of periodic reliability performance, and the system was better able to "bounce back" after a failure.

Table 4.7: Reservoir Risk Assessment

MHAs	Assessments	High	Medium	Low
	Wastage due to excess release(%)	9.21	15.35	0
HHO	Meeting demand (%)	13.16	38.60	3.07
	Shortage index	0.00007	0.00024	0.00005
	Vulnerability	0.63	0.34	1.23
	Resiliency	-	3.24	0.78

Table 4.7(continued): Reservoir Risk Assessment

MHAs	Assessments	High	Medium	Low
	Wastage due to excess release(%)	12.28	27.19	0
OBL-	Meeting demand (%)	9.21	20.61	2.63
HHO	Shortage index	0.00008	0.000021	0.00004
	Vulnerability	0.49	0.20	0.96
	Resiliency	-	2.02	0.60

4.4 Execution and Validation of Reservoir Risk Assessment for year 1987 - 2008

The proposed MHAs were implemented in these observed period datasets of years 1987-2008 and the findings will be discussed. The proposed MHAs are compared to previous reservoir periodic reliability and risk analysis assessment studies.

Table 4.8 presents an overview of the performance of various meta-heuristic algorithms in the context of the KGD. The investigation spanned a total of 264 months and yielded findings indicating that the HHO and enhancement of its model produced periodic reliability that satisfied downstream demand (i.e., exact period) at rates of 63.26% and 56.44%, respectively. In contrast, the WOA and LFWOA algorithms provided rates of 56.06% and 69.70%, respectively. Subsequently, a comparison was made between the aforementioned findings and the previous research conducted by Hossain in 2013. Hossain (2013) reported that the ABC outcomes met the demand by 61.36%, PSO (59.47%), real-coded

GA (55.68%), and lastly binary GA (23.5%). The results indicate that the LFWOA, HHO, ABC, PSO, OBL-HHO, WOA, GA (real coded), and GA (binary) exhibit the highest levels of periodic reliability, in descending order. During the surplus period, where excess release leads to wastage, the HHO showed a yield of 12.88%. Similarly, the OBL-HHO and WOA exhibited a comparable percentage of 15.91% in excess of the expected yield. The ABC and PSO both have shown a similar level of reliability, achieving a yield of 12.1%. The binary GA exhibited the highest level of wastage at 28.4%, whereas the real-coded GA resulted in a wastage of 14.4%. The LFWOA exhibited the lowest percentage of excess release, measuring at 8.71%. The study delineates the succession of the scarcity phase in the optimal release strategy, commencing with the placement of minimal efficacy. The placements were evaluated using various optimisation algorithms, including binary GA, real-coded GA, PSO, WOA, OBL-HHO, ABC, HHO, and LFWOA. The results indicate that LFWOA had the highest percentage at 48.10%, followed by HHO at 29.92%, and ABC at 26.54%. The lowest percentage was recorded for OBL-HHO at 21.59%.

Table 4.8: Comparison of the Periodic Reliability performance

Optimisation	Surplus period	Exact Period	Shortage Period	Total no. of release
WOA	42 times (15.91%)	148 times (56.06%)	74 times (28.03%)	264
LFWOA	23 times (8.71%)	184 times (69.70%)	57 times (21.59%)	264

Table 4.8 (continued): Comparison of the Periodic Reliability performance

Optimisation	Surplus period	Exact Period	Shortage Period	Total no. of release
HHO	34 times (12.88%)	167 times (63.26%)	63 times (23.86%)	264
OBL-HHO	42 times (15.91%)	149 times (56.44%)	73 times (27.65%)	264
ABC	32 times (12.1%)	162 times (61.36%)	70 times (26.54%)	264
PSO	32 times (12.1%)	157 times (59.47%)	75 times (28.41%)	264
GA (real coded)	38 times (14.4%)	147 times (55.68%)	79 times (29.92%)	264
GA (binary)	75 times (28.4%)	62 times (23.5%)	127 times (48.1%)	264

Table 4.9 shows the reservoir risk analysis performance from 1987 to 2008. The lowest vulnerability index demonstrated the robustness of the model. The vulnerability index value that the HHO achieved was 160.10. The algorithm with the lowest vulnerability index was the Binary-GA, which scored 136.91. Additionally, it was noted that there was no statistically significant difference between the Binary-GA and OBL-HHO in respect of vulnerability indices, which had values of 136.91 and 137.83, respectively. The highest vulnerability index was that provided by the ABC, with a score of 220.94, followed by LFWOA, which obtained 197.60, the PSO, real coded-GA, and WOA,

attained values of 149.66 and 203.27, respectively. The findings of the shortage index are also tabulated in Table 4.9. The algorithms suggested in this study, the WOA, LFWOA, HHO, and OBL-HHO, had the least index, each with a value of 0.01, according to the results of the shortage index. The values obtained for the ABC, PSO, and real coded-GA are 0.68, 0.67, and 0.67, respectively, and do not exhibit significant differences. The binary-GA, with a value of 0.73, was the system with the highest potential for failure at the time. As a result, the following resilience evaluation is critical to understanding how quickly the algorithms recover from failure. With values of 1.88 and 1.56, respectively, the LFWOA and HHO algorithms have the highest ability to recover from system failure. The OBL-HHO and WOA, which generated values of 1.01 and 0.62, respectively, and the ABC algorithm, which provided a value of 0.16, were the subsequent robust models in terms of resilience factor. Following values were that, PSO (0.15) and the real coded -GA (0.14). The Binary-GA algorithm exhibited the lowest efficacy in system recovery, as indicated by its score of 0.09.

Table 4.9: Comparison of the Reservoir Risk Assessments

Algorithm	Vulnerability (MG)	Shortage Index	Resiliency
WOA	149.66	0.01	0.62
LFWOA	197.6	0.01	1.88
HHO	160.10	0.01	1.56
OBL-HHO	137.83	0.01	1.01
ABC	220.94	0.68	0.16
PSO	203.27	0.67	0.15
GA			
(real coded)	199.15	0.67	0.14
GA			
(binary)	136.91	0.73	0.09

4.5 Statistical Model Performances for Investigation of Future Climate Change Impact under Climatic Scenarios

In this sub-section, the statistical model performances for the predictants, water demand and evaporation, are described.

4.5.1 For the Predictants

This sub-section evaluated the KGD reservoir under the CMIP5 climate scenarios RCP 2.6, RCO 4.5, and RCP 8.5, respectively. From 1991 to 2005, Table 4.10 presents the summary of the base period statistical performances

between the predictants and predictors variables for the downscaling procedure. The SVR-Poly Kernel function (PKF) obtained the highest coefficient of 0.62, followed by the ANN which attained 0.49, and the SVR-RBF Kernel function gained the lowest coefficient with 0.28 for the training of the *Pr* predictant variable. In addition, for the Temperature predictants, the PKF attained the highest correlation at 0.57, 0.69, and 0.60, respectively for the Mean, Maximum, and Minimum Temperature. In contrast, the ANN revealed the best correlation for the Solar Radiation predictants during model training yet the PKF served as the aim of validation, and it attained the least error. In short, throughout the statistical downscaling process and assessments it was revealed that the downscaling strategy via the PKF delivered more convincing output due to the results obtained for the testing, which obtained the lowest error of RMSE and MAE. Thus, PKF was selected to downscale the climatic scenarios.

Table 4.11 illustrates the summary of the climatic scenarios for the statistical performance of the PKF for year 2020-2099. The downscaling statistical output acquired during training and testing periods had an average R value of more than 0.70, while the RMSE and MAE averaged 0.50.

Table 4.10: Summary of the Base Period Statistical Performance for the Predictants - Predictors

Training									
Statistical Performance/ Predictants	R	ANN		R	SVR-PKF		R	SVR-RBF	
		MAE	RMSE		MAE	RMSE		MAE	RMSE
Pr	0.49	0.47	0.59	0.62	0.27	0.44	0.28	0.44	0.55
Ta	0.50	0.71	0.86	0.57	0.56	0.82	0.28	0.77	0.95
Tas_Max	0.60	0.73	0.91	0.69	0.47	0.72	0.32	0.75	0.95
Tas_Min	0.22	0.82	1.01	0.60	0.53	0.79	0.31	0.76	0.95
Solar Radiation	0.81	0.53	0.67	0.53	0.45	0.85	0.29	0.56	0.96
Testing									
Pr	0.40	0.47	0.56	0.39	0.48	0.60	0.19	0.48	0.61
Ta	0.23	0.91	1.13	0.26	0.82	1.00	0.26	0.82	1.00
Tas_Max	0.30	0.85	1.04	0.30	0.92	1.14	0.03	0.90	1.10
Tas_Min	0.21	0.94	1.12	-0.03	1.13	1.38	0.14	0.92	1.11
Solar Radiation	0.26	0.96	1.27	0.37	0.72	1.08	0.27	0.62	1.11

Table 4.11: Summary of the Climatic Scenarios for the Statistical Performance for year 2020 - 2099 (Poly Kernel Functions)

Statistical Performance/ Predictants	Training								
	RCP2.6			RCP4.5			RCP8.5		
	R	MAE	RMSE	R	MAE	RMSE	R	MAE	RMSE
Precipitation	0.8119	0.2493	0.3921	0.7583	0.1883	0.2519	0.909	0.2188	0.2895
Mean Temperature	0.74088	0.7433	0.9683	0.7112	0.218	0.2941	0.8802	0.2722	0.3498
Max. Temperature	0.8436	0.1539	0.2017	0.5538	0.1759	0.2332	0.7046	0.1996	0.2558
Min. Temperature	0.697	0.4053	0.5242	0.847	0.3376	0.4501	0.909	0.1168	0.1531
Solar Radiation	0.6957	0.2419	0.3416	0.6671	0.2399	0.3551	0.6935	0.2384	0.3468
Testing									
Precipitation	0.9243	0.0462	0.0597	0.6923	0.222	0.2777	0.8709	0.264	0.3423
Mean Temperature	0.6799	0.8379	1.0777	0.6777	0.2491	0.3181	0.8597	0.3102	0.3877
Max. Temperature	0.7773	0.1913	0.2459	0.4072	0.2147	0.2715	0.5927	0.2404	0.3016
Min. Temperature	0.5741	0.5117	0.6329	0.8091	0.4164	0.5218	0.8852	0.1347	0.1727
Solar Radiation	0.4286	0.5257	0.6681	0.5307	0.313	0.4495	0.4358	0.3584	0.491

Tan et al. (2014) revealed that a group of GCMs could produced more competent results for the future planning of water management. This is in contrast to a previous study by Nourani et al. (2020), which only conducted a single GCM. As a result, in this study it was conducted by utislng four ensembles of GCMs. Table 4.12 illustrates the average proportion (%) of predictants corresponded to RCPs and base period. Based on the table, precipitation generally showing the highest proportion with 11.88% under RCP 2.6 giving that the inflow to the KGD is the major contributing element when compared to the other predictant factors. Even the next contributing element is, mean temperature, which is estimated to have a moderate impact on water demand forecasting. In addition, the highest average proportion and contributing predictant under RCP4.5 to the base period was minimum temperature gained 4.39 %, and the mean temperature obtained 2.26% followed by the least proportion at 2.12% which is precipitation. Lastly, the highest average proportion under the RCP 8.5 was precipitation which has attained the highest percentage of 7.87% and 3.52% for mean temperature. In short, the precipitation and mean temperature were exerting the greatest influence on the future KGD optimisation operation under RCP 2.6 and RCP 8.5.

Table 4.12: Average Proportion (%) of Predictants Corresponded to RCPs and Base Period

RCP	Precipitation	Maximum Temperature	Minimum Temperature	Mean Temperature
2.6	11.88	0.037	3.73	8.02
4.5	2.12	1.23	4.39	2.26
8.5	7.87	1.79	0.70	3.52

Figure 4.11 illustrates the monthly mean inflow (MCM) corresponded to RCPs and Base Period, while Figure 4.12 illustrates the inflow variance corresponded to RCPs and Mean Base Period (MCM).

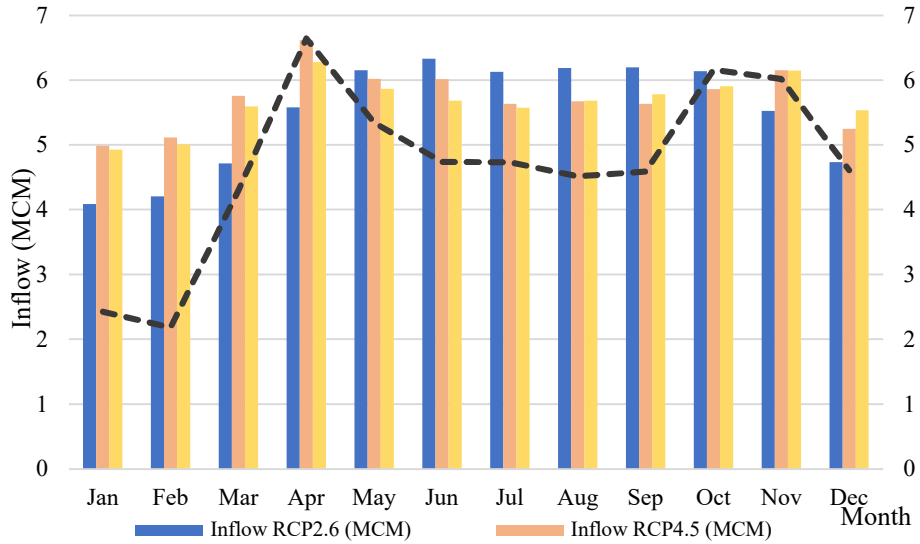


Figure 4.11: Monthly mean inflow (MCM) corresponded to RCPs and Base Period

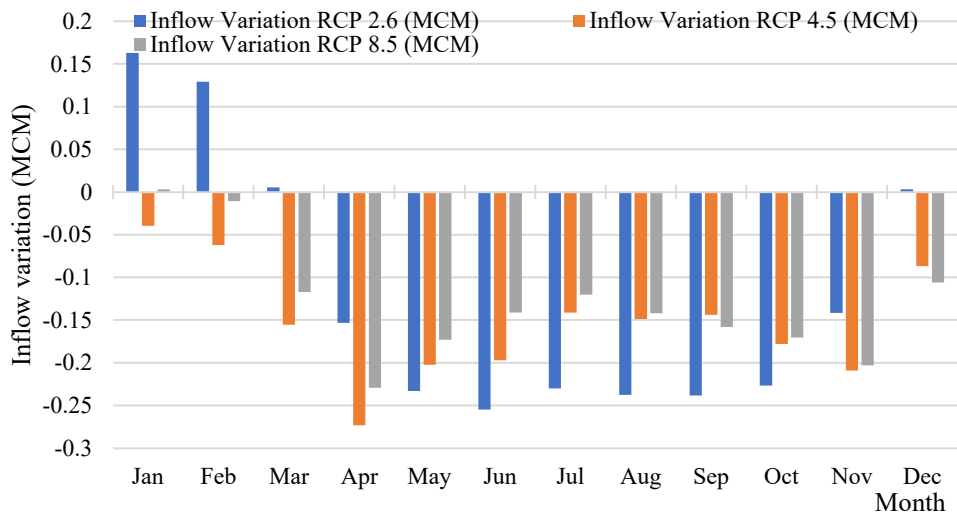


Figure 4.12: Inflow variation corresponded to RCPs and Mean Base Period (MCM)

4.5.2 For the Estimation of Water Demand

Table 4.13 displays the performance of the statistical model for predicting future water demand based on the Eqns. (3.9) - (3.11) by employing the ANN under various RCPs. In summary, the statistical performance under RCP 2.6, RCP 4.5, and RCP 8.5 provided an acceptable range of R, with the majority with ability to perform more than 0.55 on average. As a result, the future KGD optimisation operation can rely on the predicted water demand based on the temperature factor provided by the ANN.

Table 4.13: Statistical model performance for predicted of future water demand based on temperature factor under climate change scenarios

Predicted future water demand based on temperature factor via ANN									
Statistical test	Maximum Temperature			Mean Temperature			Minimum Temperature		
	RCP2.6	RCP4.5	RCP8.5	RCP2.6	RCP4.5	RCP8.5	RCP2.6	RCP4.5	RCP8.5
Training									
R	0.808	0.608	0.940	0.766	0.576	0.887	0.763	0.744	0.929
MAE	0.096	0.134	0.051	0.113	0.147	0.093	0.126	0.115	0.055
RMSE	0.14	0.182	0.078	0.165	0.188	0.123	0.178	0.157	0.085
Testing									
R	0.811	0.574	0.941	0.766	0.536	0.859	0.751	0.731	0.930
MAE	0.092	0.160	0.058	0.112	0.170	0.113	0.143	0.124	0.061
RMSE	0.14	0.201	0.084	0.154	0.208	0.144	0.176	0.169	0.091

4.5.3 For the Estimation of Evaporation

The performance of the statistical models for the estimation of evaporation under climatic scenarios via empirical methods and the prediction-based method (SVR) are shown in Table 4.14(a) and (b).

Even though the *Kharuffa* method had achieved the highest R results, as shown in Table 4.14(a), this method was not chosen because the MAE attained the highest error compared to others. Moreover, the *Kharuffa* method was primarily employed in dry locations, while the Malaysia condition is wet and tropical area (Poyen et al., 2018). Next, evaporation under future RCPs scenarios was studied using the *Turc* method. In the training phase, the *Turc* method had the greatest coefficient, 0.8453, compared to *Kharuffa* methods, 0.7408. Under RCP 4.5, the *Turc* method achieved a consistent R coefficient of 0.8468 with minimal variation in the training process. Additionally, the prediction based SVR methods were employed to validate the *Kharuffa* and *Turc* methods which are presented in Table 4.14(b). According to Tukimat et al. (2012), Muniandy et al. (2016) and Muhammad et al. (2019), the *Turc* method is more reliable than temperature-based methods especially for the study area at Peninsular Malaysia. Furthermore, prior research has shown that the *Turc* method is better for use in Malaysia since it is more reliable to be applied in moist and wet region (Jensen et al., 1990; Tukimat et al., 2012; Goh et al., 2021), and sub-humid region (Birara et al., 2021). As a result, in this study, the future KGD optimisation operation will use the *Turc* method to estimate evaporation under various climate change scenarios.

Table 4.14: (a) Performance of statistical tests for empirical methods

Statistical test	Empirical Methods					
	<i>Kharuffa</i> method (Temperature based)			<i>Turc</i> method (Radiation based)		
	RCP2.6	RCP4.5	RCP8.5	RCP2.6	RCP4.5	RCP8.5
	Training					
R	0.7408	0.7112	0.8802	0.739	0.8453	0.9528
MAE	0.7433	0.218	0.2722	0.3584	0.2804	0.158
RMSE	0.9683	0.2941	0.3498	0.4722	0.377	0.2137
	Testing					
R	0.6799	0.6777	0.8597	0.6807	0.8468	0.9465
MAE	0.8376	0.2491	0.3102	0.4056	0.3053	0.1761
RMSE	1.0777	0.3181	0.3877	0.5272	0.3873	0.2299

Table 4.14 : (b) Performance of statistical tests for prediction-based methods

Statistical test	Prediction-based Methods					
	SVR Prediction (in respect to Temperature)			SVR Prediction (in respect to Temperature and Radiation)		
	RCP 2.6	RCP 4.5	RCP 8.5	RCP 2.6	RCP 4.5	RCP 8.5
	Training					
R	0.5525	0.5767	0.7505	0.5984	0.5761	0.7386
MAE	0.3352	0.3435	0.2684	0.3213	0.3383	0.2951
RMSE	0.4179	0.4111	0.3407	0.4032	0.41	0.3479
	Testing					
R	0.5944	0.5732	0.6865	0.6244	0.5731	0.6846
MAE	0.3354	0.3582	0.3078	0.3231	0.3503	0.3096
RMSE	0.411	0.424	0.3836	0.3985	0.4214	0.3882

4.6 Climate Change Impact on Future Water Demand Based on Temperature Factor

In section 2.3 the justifications has been given for the climatic change impacts reservoir discharge activity, and the impact ultimately also affect the trend of the rainfall-runoff indirectly, thus affecting the river input as well as temperature factor. Hence, the motivation for capturing the temperature factor in the future water demand is pertinent to investigate in order to close up the gap between water supply and demand for future scenarios. In section 3.5.3, a mention was made on the estimation of the future water demand based on temperature factor via ANN. The statistical results of the training and testing were then discussed in section 4.5.2 under different climate scenarios. In order to investigate the potential impact of climate change on the future operations of the KGD, the estimation of the future water demand associated with three distinct temperature factors including the maximum, mean, and minimum temperatures, are thus anticipated to be developed and analysed with different climate change scenarios. Hence, the outcomes of the future climate change impact based on temperature factor of the future water demand for the years 2020-2099 are discussed in the subsequent sections and the arrangement begins with Scenario 1: base period (demand similar as observed period); Scenario 2: maximum temperature of water demand; Scenario 3: mean temperature of water demand; and lastly, Scenario 4: minimum temperature of water demand. The purpose of execution of the base period was to understand how the proposed algorithms behaved in observed period during simulation and simulation-optimisation compared with future timeline.

4.6.1 Scenario 1: Base Period

This sub-section describes the outcome obtained for Scenario 1. According to Figure 4.13, simulation vs simulation-optimisation comparisons were conducted for the base period of 1991 to 2005. The proposed algorithms exhibit the same optimal release trend line for the base period. Comparing simulation vs simulation-optimisation, Table 4.15 presents the reservoir risk analysis assessment for the base period. In comparison to simulation-optimisation, the periodic reliability of simulation attained a much lower percentage. In addition, the shortage index for the proposed MHAs outperformed the simulation release by a small margin.

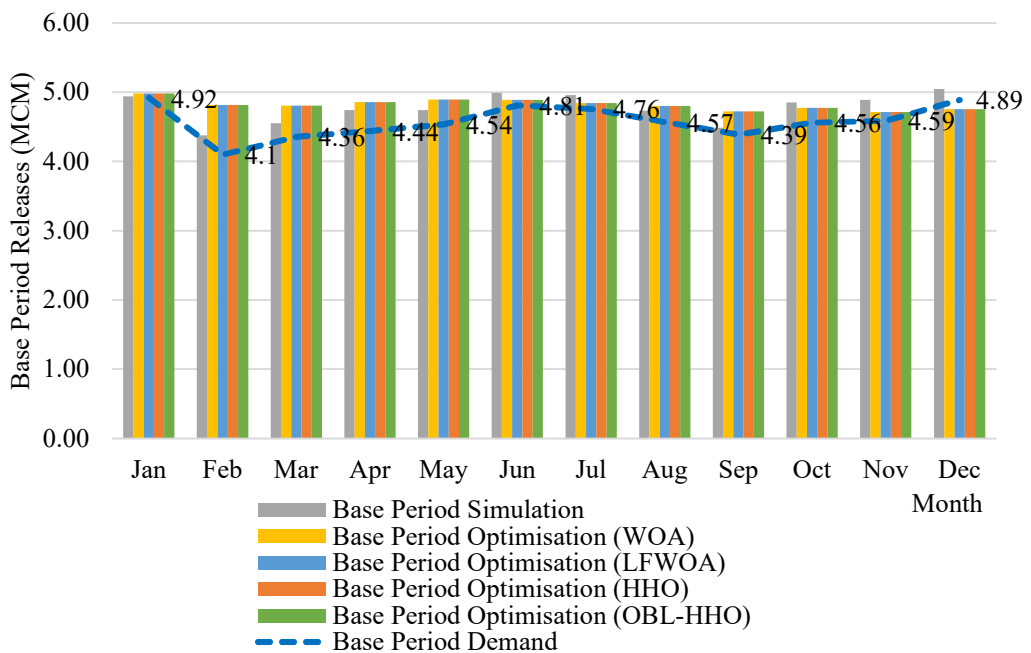


Figure 4.13: Comparison of base period releases (1991-2005)

Table 4.15: Comparison between simulation vs simulation-optimisation for reservoir risk analysis evaluation in base period

Algorithms/ Reservoir risk analysis evaluation	Simulation	Optimisation			
		WOA	LFWOA	HHO	OBL-HHO
Periodic Reliability	8.89% (15 times)	22.22% (40 times)	22.22% (40 times)	22.22% (40 times)	22.22% (40 times)
Vulnerability	0.2175	0.3142	0.3142	0.3142	0.3142
Shortage Index	0.000468	0.000713	0.000713	0.000713	0.000713
Resiliency	6.09	4.77	4.77	4.77	4.77

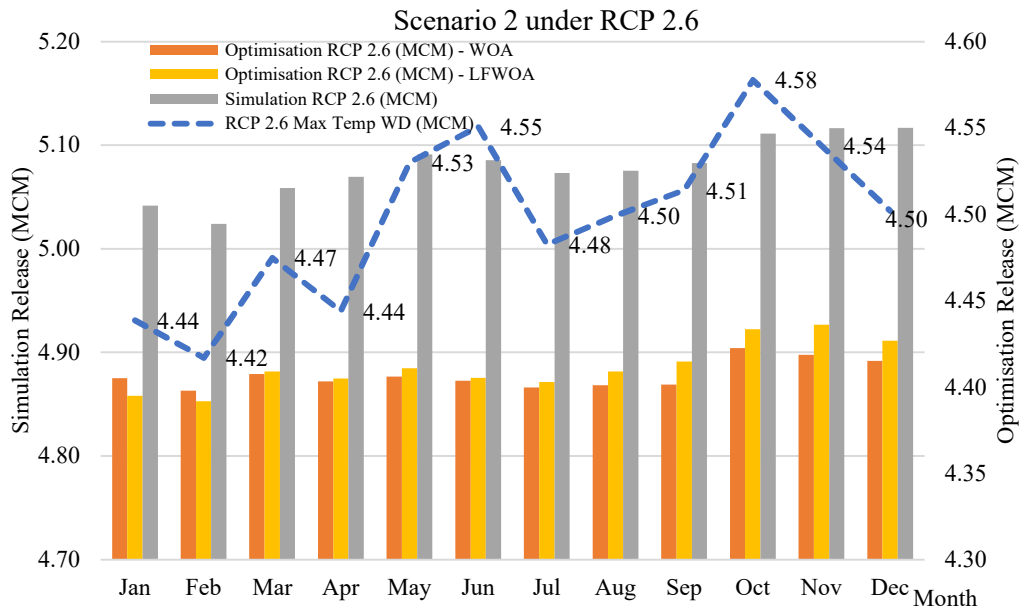
4.6.2 Scenario 2: Maximum Temperature

In this section, the findings of proposed MHAs are described. This comprise a reservoir risk analysis assessment, optimal monthly release curves, and optimal storage capacity.

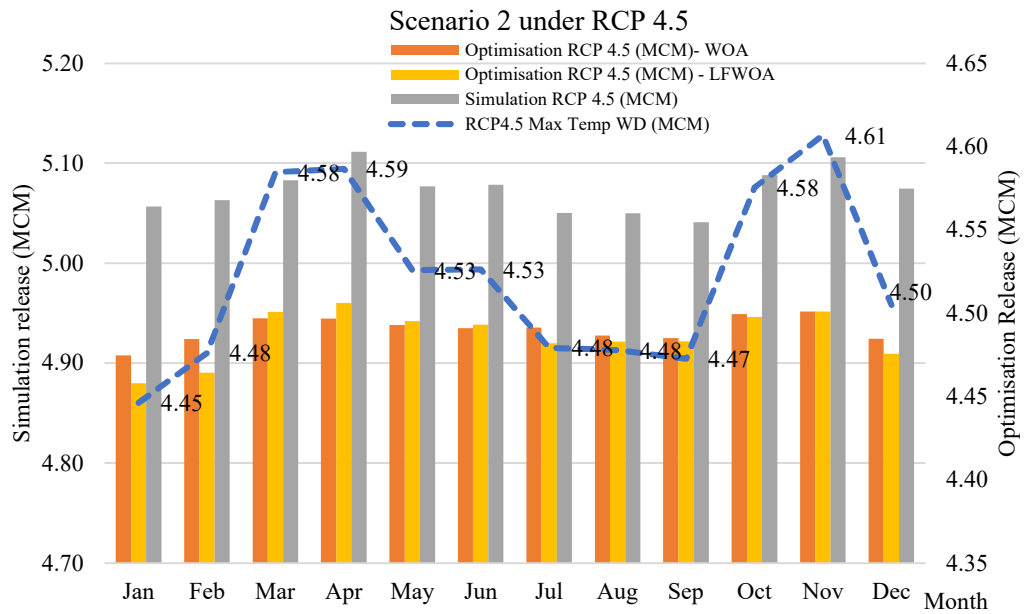
(a) Reservoir release operation under various RCPs

Figure 4.14 (a) – (c) illustrates the monthly release curves derived from the WOA and LFWOA. According to the observation, neither the the WOA nor the LFWOA release curves exhibit excessive release scenarios. In Scenario 2, according to RCP 2.6, the periodic reliability of the WOA and LFWOA to meet exact demand was 37.60% and 37.40%, respectively. The monthly release curves for Scenario 2 under RCP 4.5 indicated that the simulation was incapable of meeting the exact demand line while simultaneously generating an excess release. Consequently, the WOA and LFWOA in Scenario 2 under RCP 4.5 are capable of meeting the water demand for July to September with periodic reliability of 30.0% for both algorithms. Nevertheless, based on the graphs, a policy of excessive release might emerge in Scenario 2 under RCP 8.5, as the WOA and LFWOA were unable to achieve a minimal deficit state for several months (the algorithms go beyond the water demand line).

(a) RCP 2.6



(b) RCP 4.5



(c) RCP 8.5

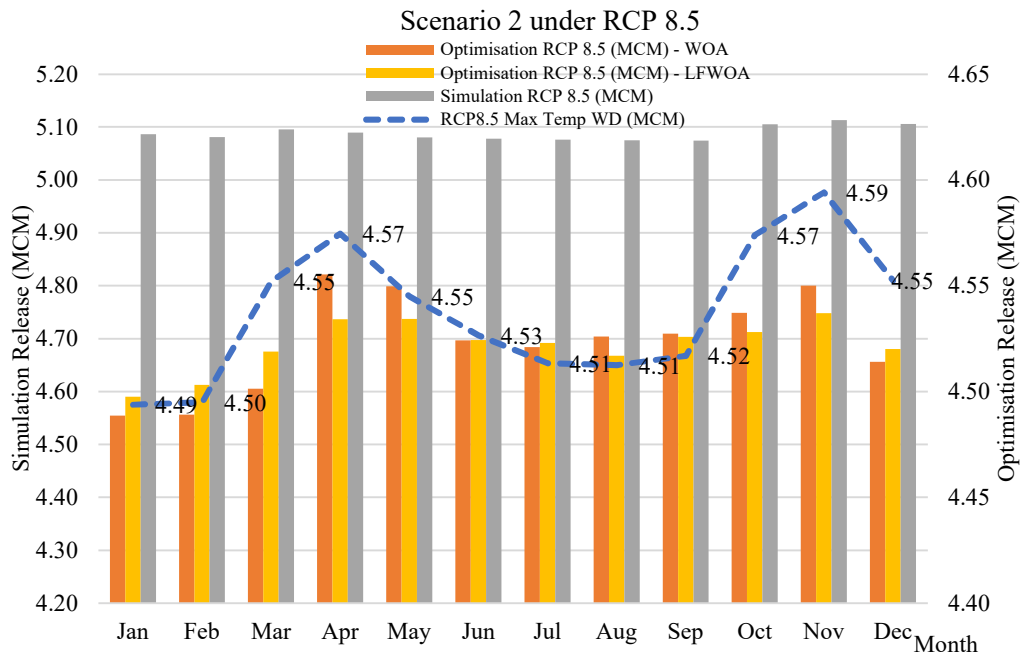
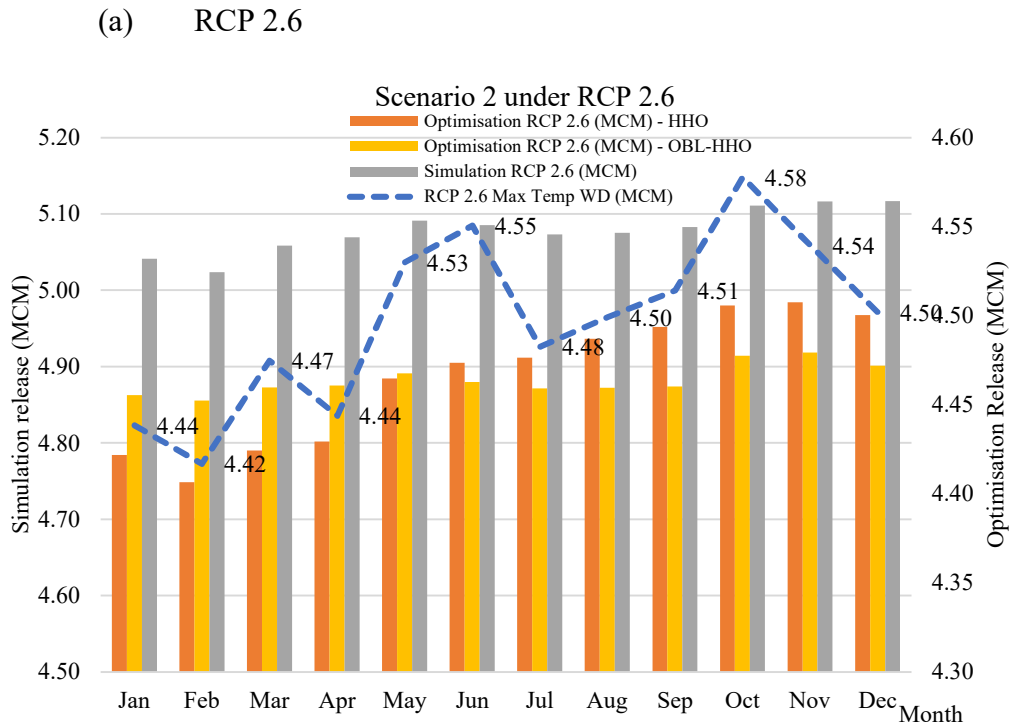


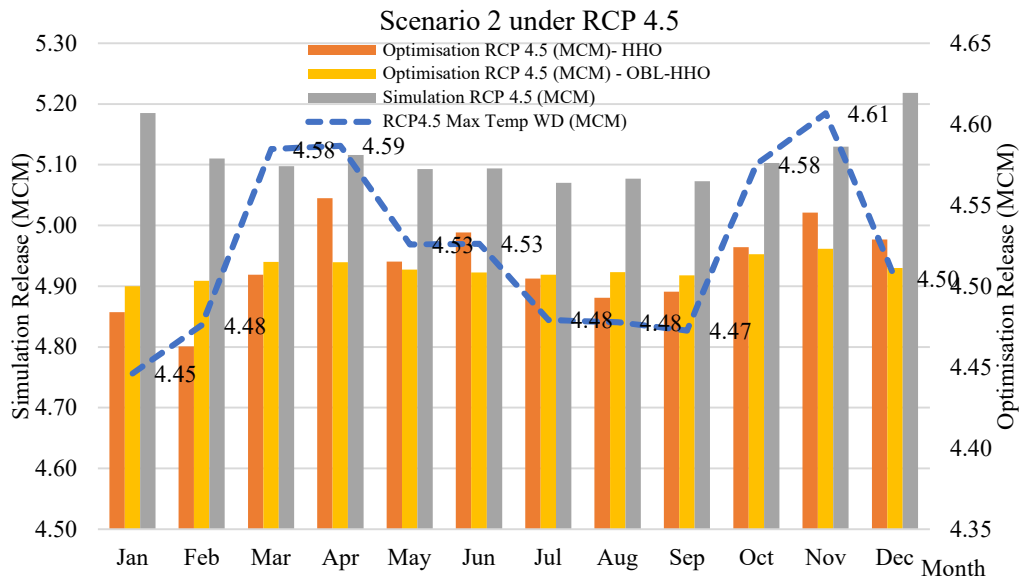
Figure 4.14: WOA vs LFWOA for the comparison of simulation vs simulation-optimisation of optimal reservoir releases in Scenario 2 (a) RCP 2.6, (b) RCP 4.5 and (c) RCP 8.5

Figure 4.15 (a) – (c) illustrates the monthly release curves for Scenario 2 under the HHO and OBL-HHO for RCP 2.6, RCP 4.5, and RCP 8.5. Using the HHO and OBL-HHO in accordance with RCP2.6 resulted in an excessive release in Scenario 2. In Scenario 2, under RCP 2.6, the periodic reliability of the HHO and its enhancement model to meet exact demand was 22.23% and 27.8 %, respectively. Comparing the HHO and its enhancement model to the WOA and LFWOA, the percentage of periodic reliability under RCP 2.6 dropped. The monthly release curves for Scenario 2 under RCP 4.5 revealed that the simulation was unable to match the exact demand line, leading to the exceed reservoir release policy. In comparison, the HHO and OBL-HHO in Scenario 2 under RCP 4.5 with similar release graphs in the WOA and LFWOA, achieved 13.96% and

29.90%, respectively, as shown in Figure 4.15 (a). Due to the inability of the HHO and its enhancement model to establish a minimal deficit state for Scenario 2 under RCP 8.5, the graphs reveal that an excessive release policy may be found in various months (January, February, July to September).



(b) RCP 4.5



(c) RCP 8.5

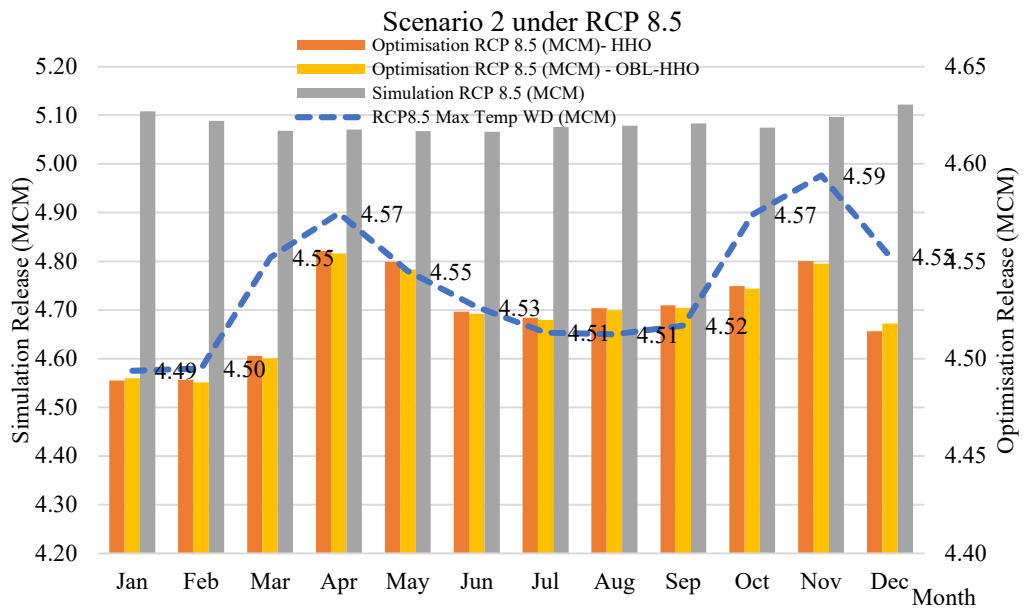
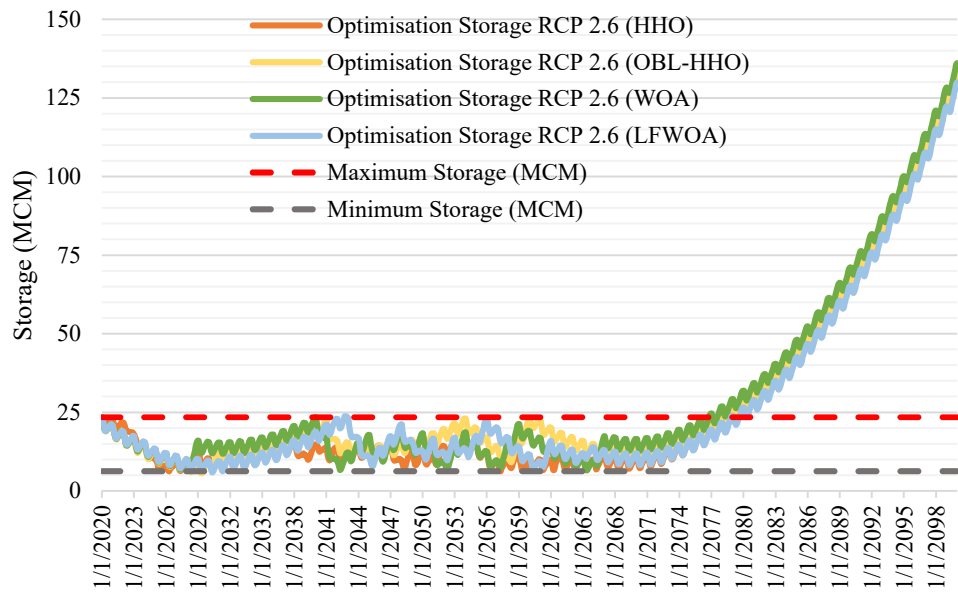


Figure 4.15: HHO vs OBL-HHO for the comparison of simulation vs simulation-optimisation of optimal reservoir releases in Scenario 2 (a) RCP 2.6, (b) RCP 4.5 and (c) RCP 8.5

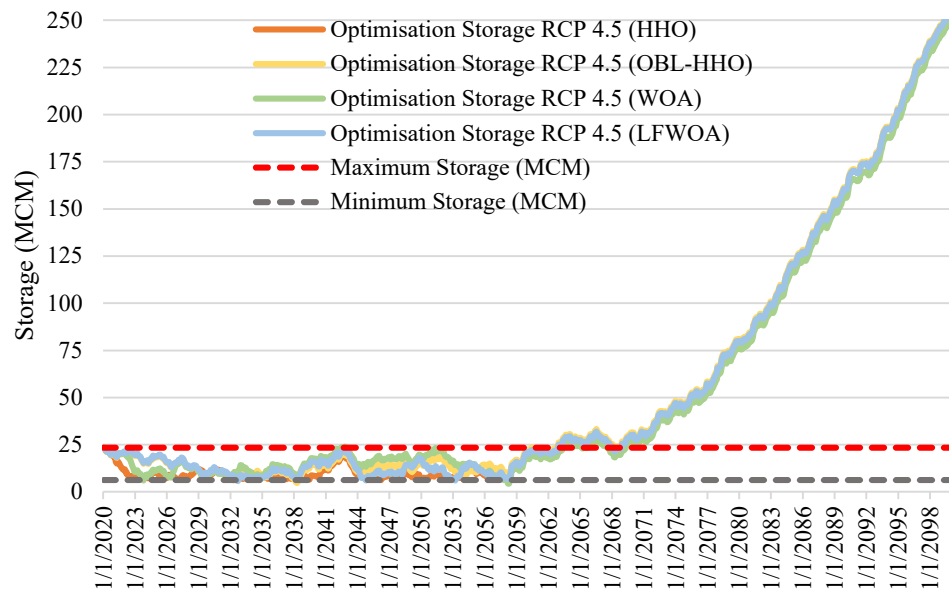
(b) Monthly Reservoir Storage Capacity under various RCPs

Figure 4.16 (a) illustrates the monthly storage capacity at the KGD under RCP 2.6 for Scenario 2 that could maintain its safety levels till the Mid-Future (2050-2079). In this Figure 4.14 (a) the WOA encountered a storage breach of 24.18 MCM approximately in the year 2077 and onwards, whereas the HHO, OBL-HHO, and LFWOA experienced a storage failure approximately in the year 2079 and onwards at level 25.35 MCM, 25.63 MCM, and 23.97 MCM, respectively. On the other hand, Figure 4.16 (b) presents the monthly storage capacity under RCP 4.5 for Scenario 2. In contrast to RCP 2.6, in which the storage failure occurred in 2062 (Mid Future), it occurred 10 years earlier under this scenario. The OBL-HHO at level 24.04 MCM was the first MHA to encounter a storage failure, followed by the LFWOA at level 24.99 MCM, HHO at level 24.72 MCM, and the WOA at level 24.35 MCM. However, Figure 4.16 (c) shows the monthly storage capacity under RCP 8.5 for Scenario 2, demonstrating that the same storage failure occurred in the Mid Future, nearly in the year 2075 and onwards at a storage level of 23.86 MCM, which had a similar situation under RCP 2.6. In terms of the monthly storage capacity, the proposed MHAs do not exhibit consistency under Scenario 2. This will be further elaborated until all the MHAs have described the outcomes of the optimal monthly storage capacity for Scenario 3 and Scenario 4.

(a) For Maximum Temperature Scenario (Scenario 2) under RCP 2.6



(b) For Maximum Temperature Scenario (Scenario 2) under RCP 4.5



(c) For Maximum Temperature Scenario (Scenario 2) under RCP 8.5

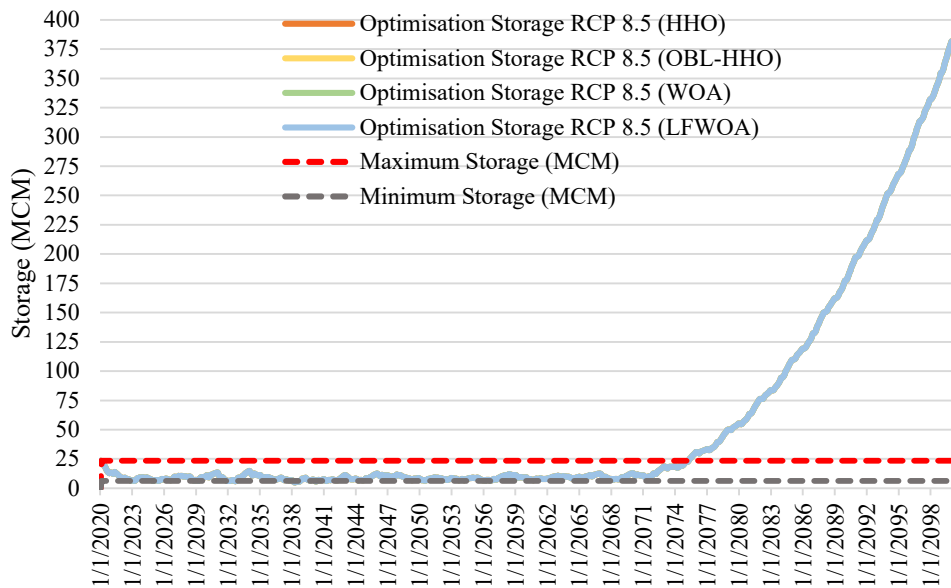


Figure 4.16: Monthly storage capacity (MCM) for Scenario 2 (a) RCP 2.6, (b) RCP 4.5 and (c) RCP 8.5

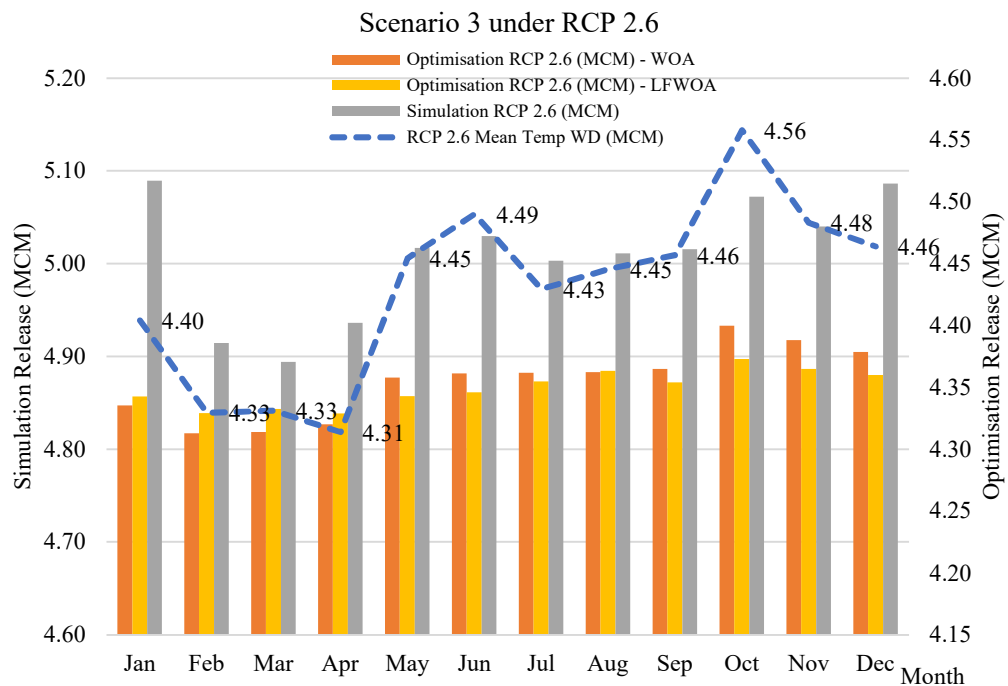
4.6.3 Scenario 3: Mean Temperature

(a) Reservoir Simulation vs Reservoir Simulation-Optimisation of the reservoir release operation under various RCPs

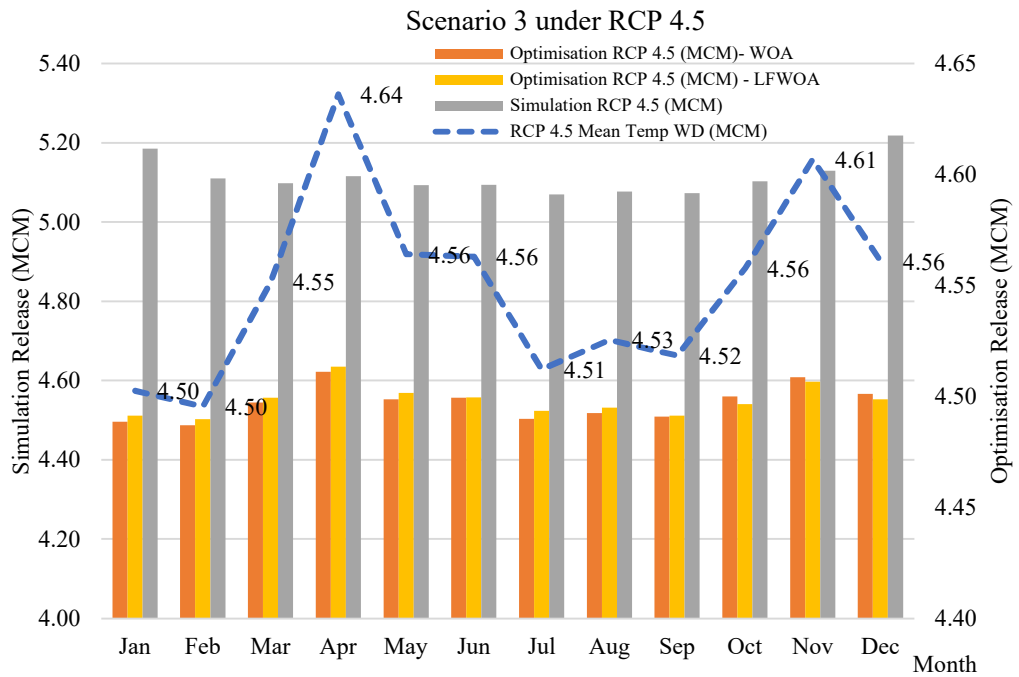
Figure 4.17 (a) – (c) depicts the monthly release curves by utilising the WOA and LFWOA. According to the observation, the WOA and LFWOA were able to meet the exact demand in this section scenario under RCP 2.6 from February to April. Followed by in the months of May through January of the following year, the monthly release curves in Scenario 3 under RCP 2.6 were inadequate to fulfil the water demand; after all, there was no excessive release by leveraging on the WOA and LFWOA compared to the simulation. In Scenario 3, under RCP 2.6, the

periodic reliability for the WOA and LFWOA to satisfy exact demand was 36.15% and 33.13 %, respectively. The monthly release curves for Scenario 3 under RCP 4.5 revealed once more that the simulation was unable to satisfy the exact demand line while simultaneously generating an excessive release. Consequently, the WOA and LFWOA in Scenario 3 under RCP 4.5 attained the optimal monthly release policy without surpassing the downstream water demand, achieving 94.69% and 87.81%, respectively. However, based on the graphs an excessive release policy could occur in Scenario 3 under RCP 8.5 as the WOA and LFWOA were unable to achieve a minimal deficit state.

(a) RCP 2.6



(b) RCP 4.5



(c) RCP 8.5

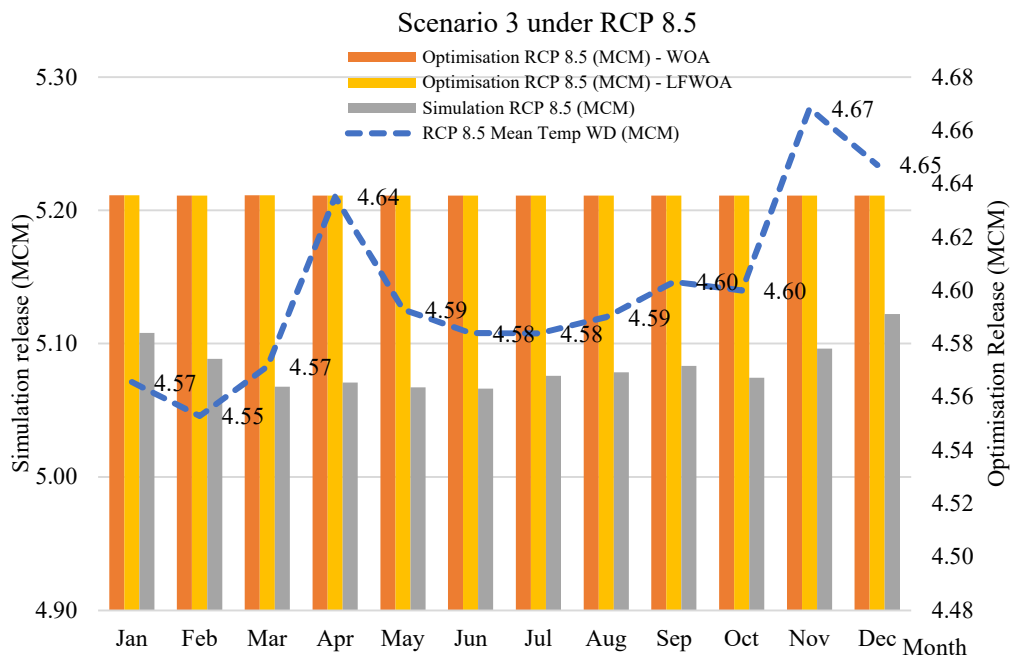
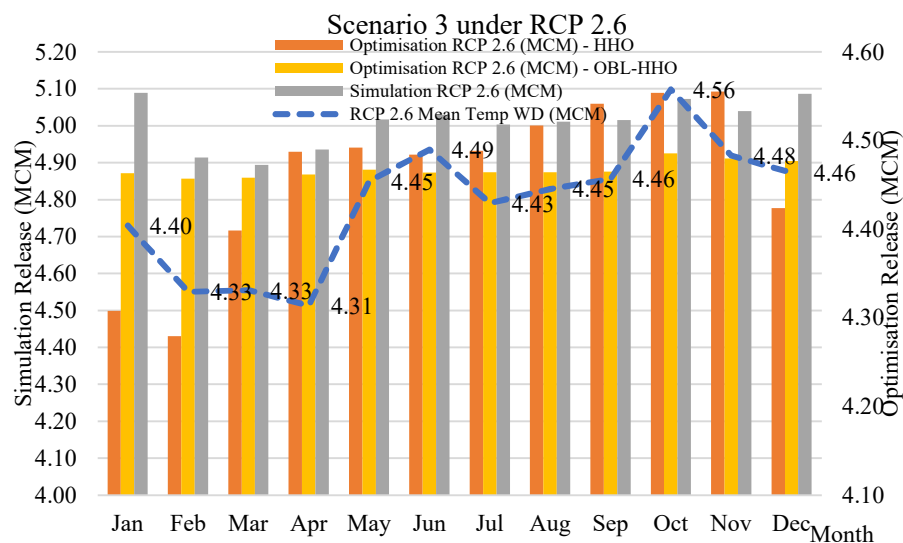


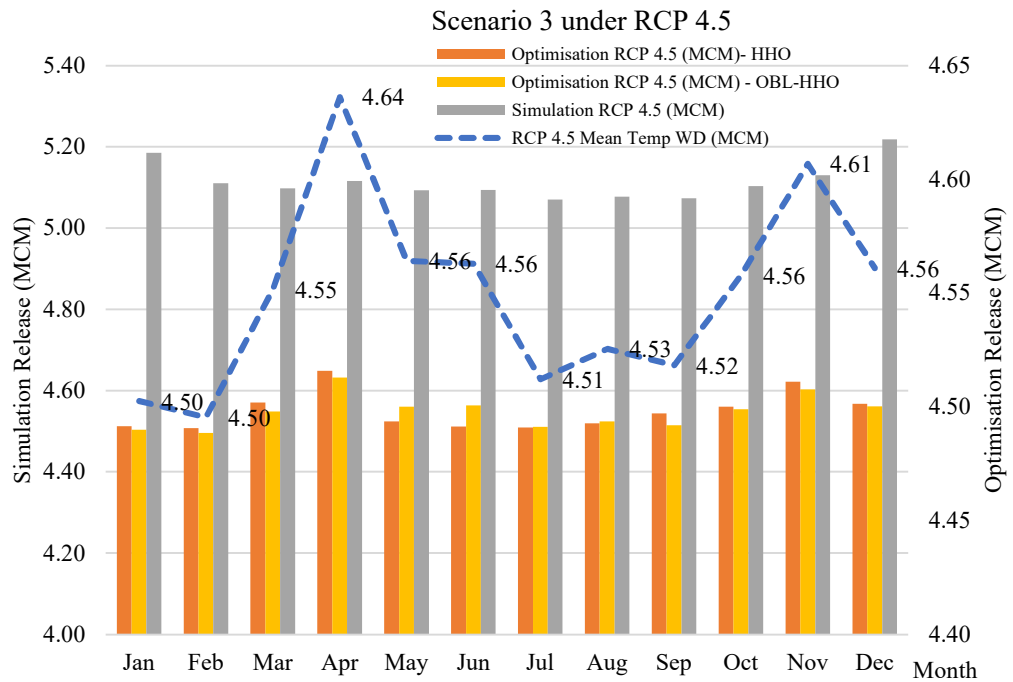
Figure 4.17: WOA vs LFWOA and for the comparison of simulation vs simulation-optimisation of optimal reservoir releases in Scenario 3 (a) RCP 2.6, (b) RCP 4.5 and (c) RCP 8.5

Figure 4.18 (a) – (c) depicts the monthly release curves for Scenario 3 applying the HHO and enhancement of its model for RCP 2.6, RCP 4.5, and RCP 8.5. Scenario 3 involving the use of HHO and OBL-HHO in accordance with RCP2.6 resulted in an excessive release. In Scenario 3, under RCP 2.6, the periodic reliability of the HHO and enhancement of its model to meet exact demand was 18.54 % and 29.04 %, respectively. In comparison to the WOA, the percentage of periodic reliability under RCP 2.6 for the HHO and enhancement of its model had decreased by half. The monthly release curves for Scenario 3 under RCP 4.5 have shown that the simulation could not meet the exact demand line, resulting in the exceeding of reservoir release policy. In contrast, the HHO and enhancement of its model in Scenario 3 under RCP 4.5 met the ideal monthly release policy without exceeding the downstream water demand, attaining 93.4% and 96.25%, respectively. The graphs show that an excessive release policy may be performed because the HHO and enhancement of its model were unable to generate a minimal deficit state for Scenario 3 under RCP 8.5.

(a) RCP 2.6



(b) RCP 4.5



(c) RCP 8.5

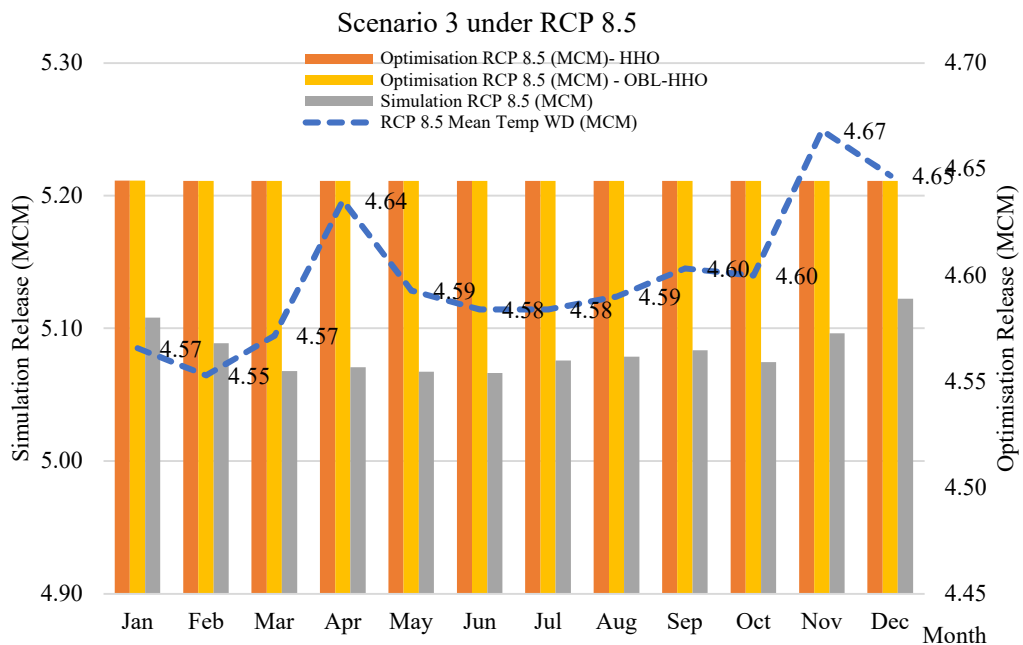
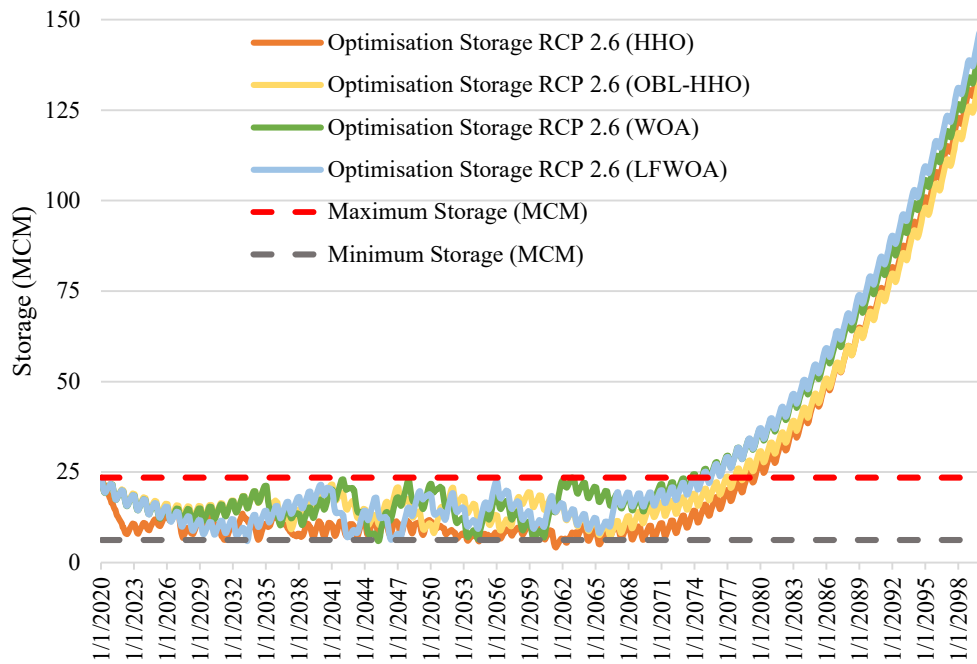


Figure 4.18: HHO vs OBL-HHO for the comparison of simulation vs simulation-optimisation of optimal reservoir releases in Scenario 3 (a) RCP 2.6, (b) RCP 4.5 and (c) RCP 8.5

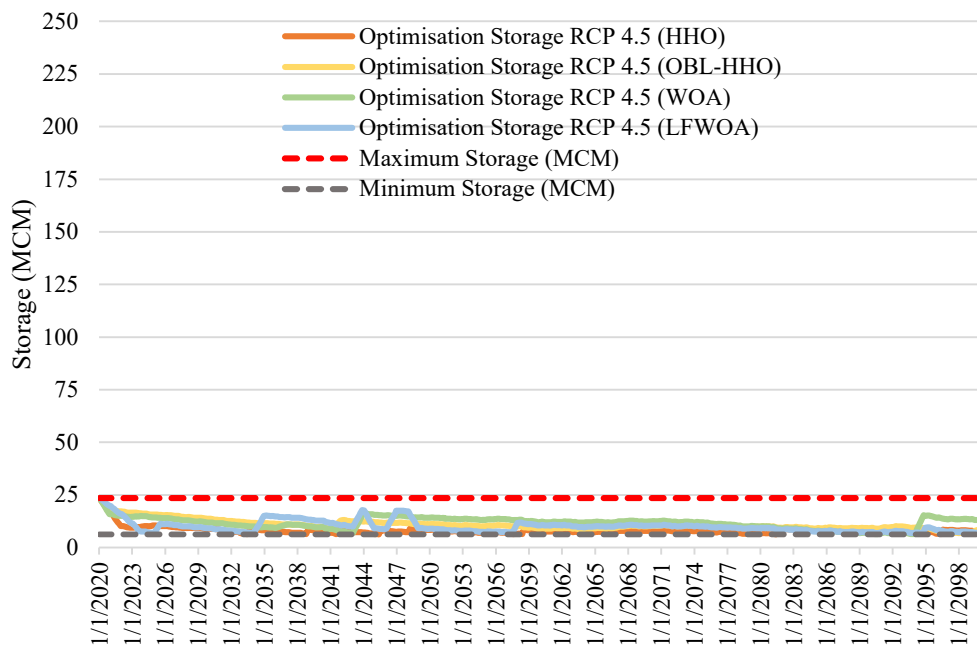
(b) Monthly Reservoir Storage Capacity under various RCPs

Figure 4.19 (a) – (c) depicts the monthly storage capacity at the KGD for Scenario 3 under RCP 2.6 that could maintain its safety levels until the mid-future safety levels (2050-2072). In this Figure 4.19 (a), the WOA and LFWOA experienced a storage failure of 24.16 MCM in year 2074 onwards, while the HHO and OBL-HHO experienced storage failures in year 2075 onwards at levels of 24.53 MCM and 23.91 MCM, respectively. In contrast to Scenario 2 of RCP 4.5, which is depicted in Figure 4.19 (b), Scenario 3 of RCP 4.5 revealed a highly significant outcome in which no MHAs encountered storage failure events. This was due to the fact that both future water demand scenarios had different temperatures, with Scenario 2 having the maximum temperature and Scenario 3 having the mean temperature. Figure 4.19 (c) displayed the monthly storage capacity under RCP 8.5 for Scenario 3, indicating that the initial phase of storage failure occurred in the near future onwards. However, this overestimation of the mitigation plan under RCP 8.5 for Scenario 3 has yet to occur at the current KGD reservoir operation and can be attributed to the current climate change at KGD, which relates to the RCPs in CMIP5 (AR5).

(a) For Mean Temperature Scenario (Scenario 3) under RCP 2.6



(b) For Mean Temperature Scenario (Scenario 3) under RCP 4.5



(c) For Mean Temperature Scenario (Scenario 3) under RCP 8.5

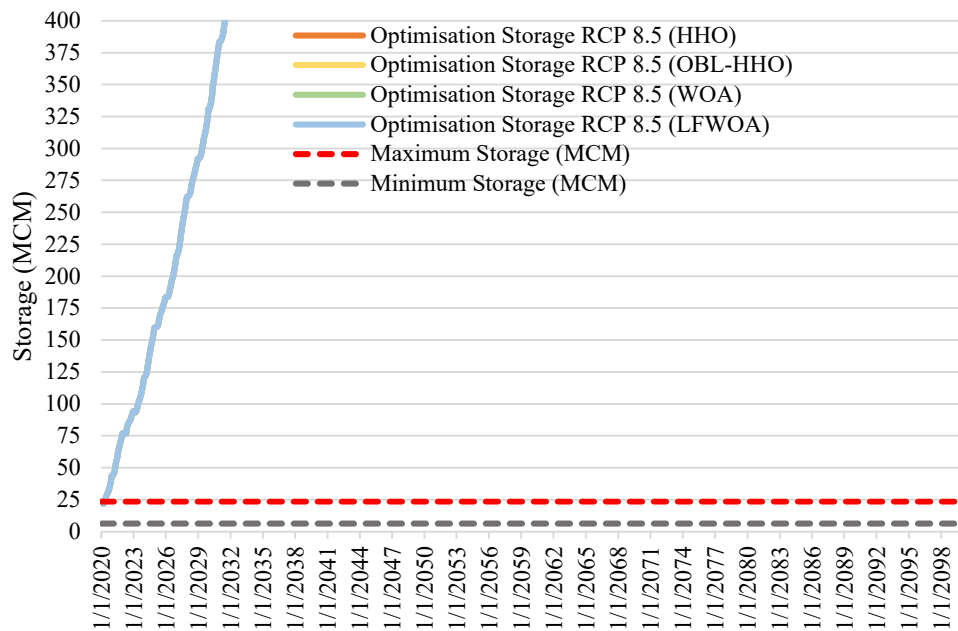


Figure 4.19: Average monthly storage capacity (MCM) for Scenario 3 (a) RCP 2.6, (b) RCP 4.5 and (c) RCP 8.5

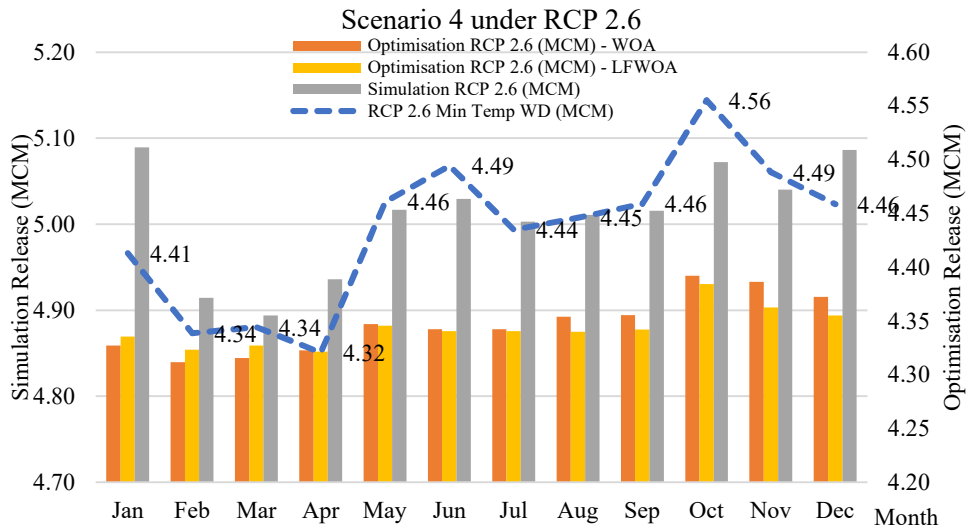
4.6.4 Scenario 4: Minimum Temperature

(a) Reservoir Simulation vs Reservoir Simulation-Optimisation of the reservoir release operation under various RCPs

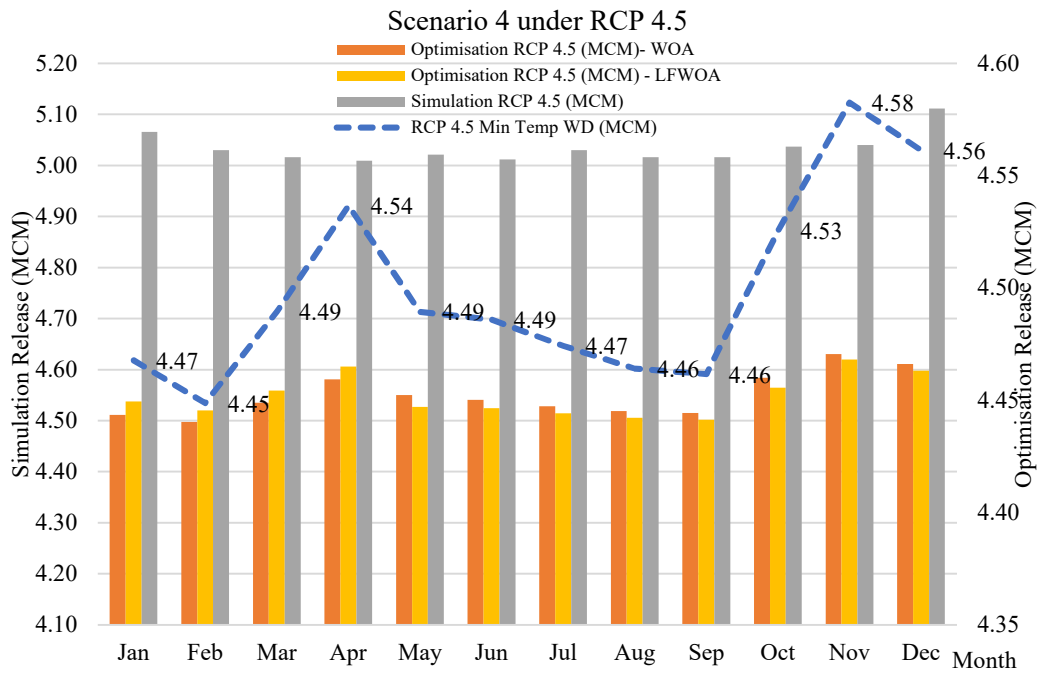
Figure 4.20 (a) – (c) depicts the monthly release curves for Scenario 4 (Minimum Temperature of Water Demand) using the WOA and LFWOA for RCP 2.6, RCP 4.5, and RCP 8.5. According to the observation, from the months of February to April, the WOA and LFWOA were capable of meeting the exact demand in this scenario under RCP 2.6. Followed by in the months of May through January of the following year, the monthly release curves in Scenario 4 under RCP

2.6 were inadequate to meet the water demand. The periodic reliability to meet exact water demand at downstream for the WOA and LFWOA were 34.69% and 38.11 %, respectively under RCP 2.6. Based on the observation made in Scenario 4 under RCP 2.6, the simulation illustrated the excessive release to the downstream that resulted in the release flow returning to the river/sea. The monthly release curves for Scenario 4 under RCP 4.5 have shown that the simulation was unable to satisfy the exact demand line and yet produced the situation of exceeding release to the reservoir policy. As a result, the WOA and LFWOA in Scenario 4 under RCP 4.5 obtained the optimal monthly release policy without exceeding the downstream water demand and obtained 91.15% and 96.67 %, respectively. For Scenario 4 under RCP 8.5, the WOA and LFWOA were unable to produce a minimal deficit state, and based on the graphs, an excessive release policy could emerge. As a result, Scenario 4 under RCP 8.5 is regarded as a critical state, and additional recommendations are detailed in Chapter 5.

(a) RCP 2.6



(b) RCP 4.5



(b) RCP 8.5

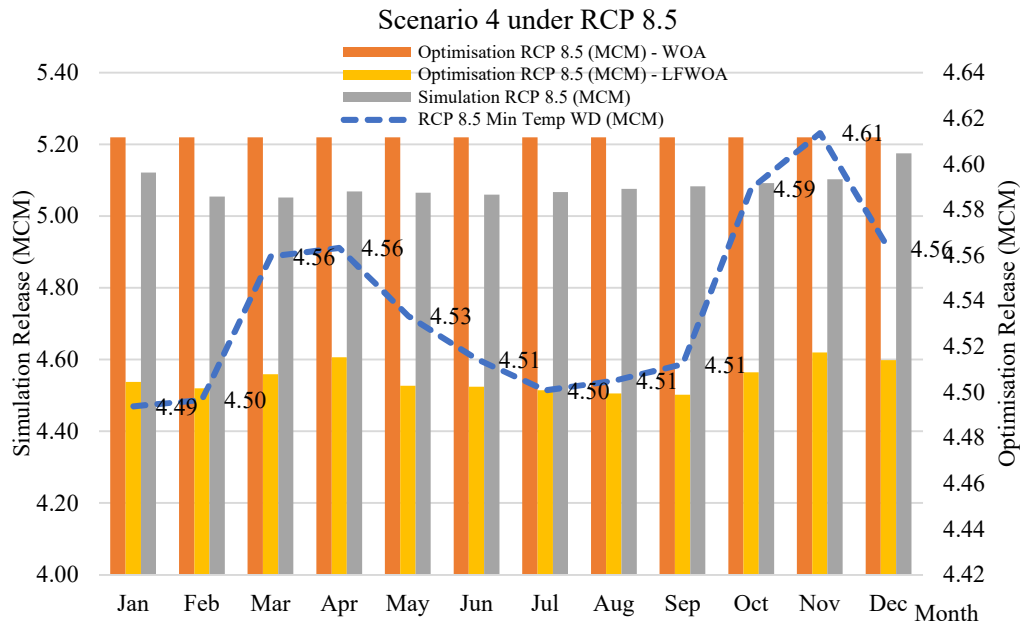
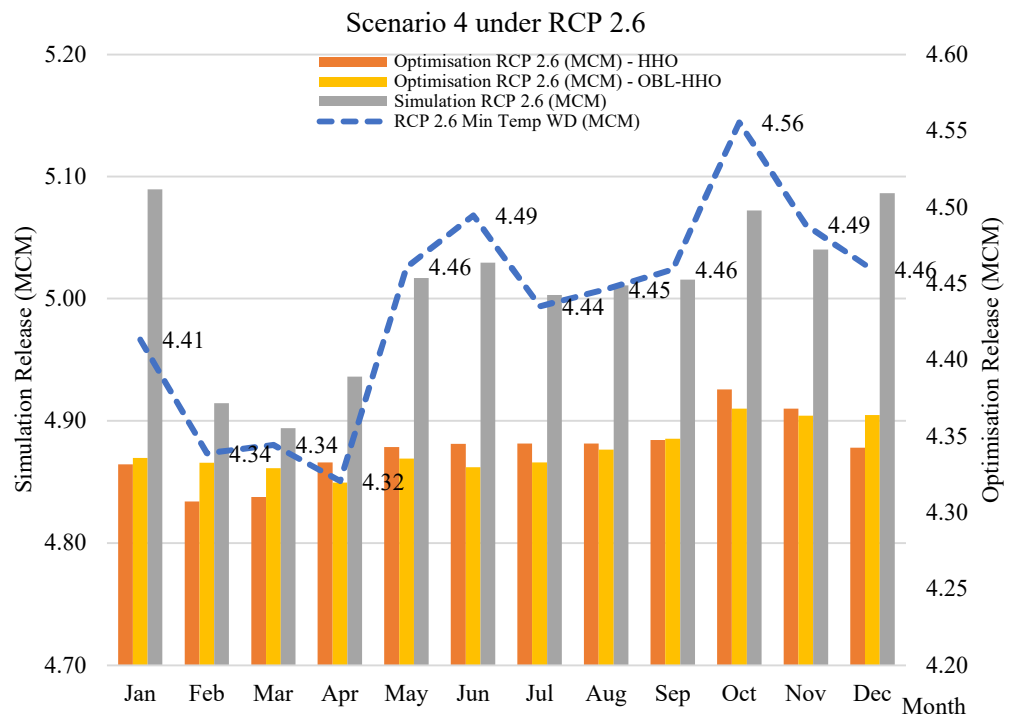


Figure 4.20: WOA vs LFWOA for the comparison of simulation vs simulation-optimisation of optimal reservoir releases in Scenario 4 (a) RCP 2.6, (b) RCP 4.5 and (c) RCP 8.5

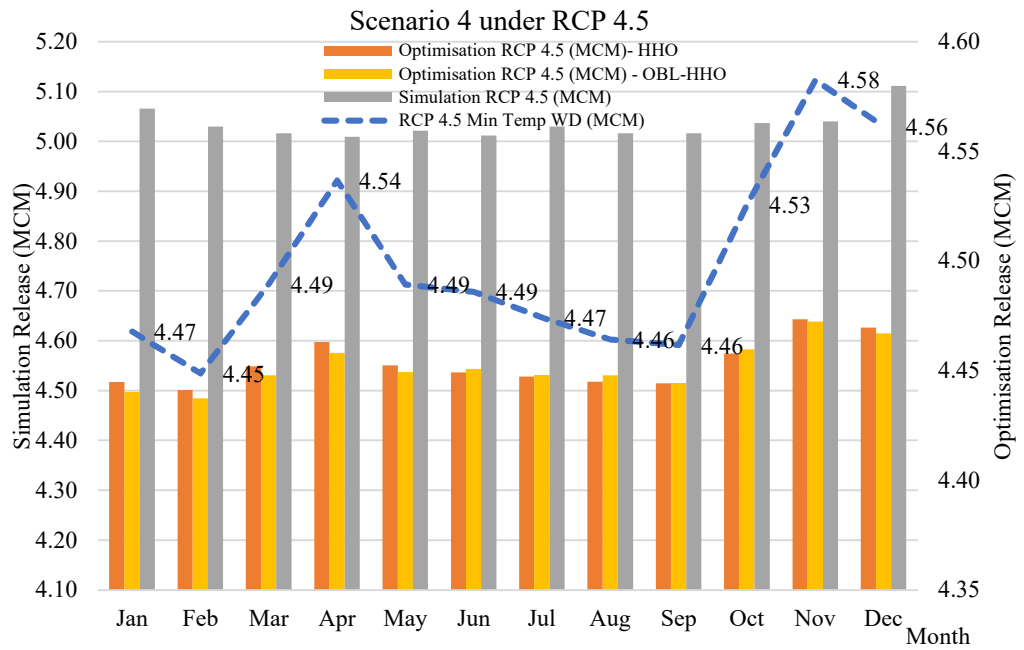
The monthly release curves for Scenario 4 utilising the HHO and OBL-HHO for RCP 2.6, RCP 4.5, and RCP 8.5 are depicted in Figure 4.21 (a) – (c). From February to April, the HHO and enhancement of its model were able to supply the water demand in the WOA and LFWOA in Scenario 4 under RCP 2.6, based on observations. Followed by the months of May through January of the following year, the monthly release curves in Scenario 4 under RCP 2.6 were insufficient to meet water demand. As a result, the release flow returned to the river and then the sea. In Scenario 4, under RCP 2.6, the periodic reliability for the HHO and enhancement of its model to satisfy exact demand was 37.92% and 20.5%, respectively. Compared to the WOA, the percentage of periodic

reliability for the HHO was slightly higher. The monthly release curves for Scenario 4 under RCP 4.5 indicated that the simulation was unable to satisfy the exact demand line and generated the exceed release to reservoir policy, which is comparable to the HHO level of 37.92%. In contrast, the OBL-HHO in Scenario 4 under RCP 4.5 reached the optimal monthly release policy without exceeding downstream water demand, achieving 92.40 %. The HHO and enhancement of its model were unable to establish a minimal deficit state for Scenario 4 under RCP 8.5, and based on the graphs, an excessive release policy could occur.

(a) RCP 2.6



(b) RCP 4.5



(c) RCP 8.5

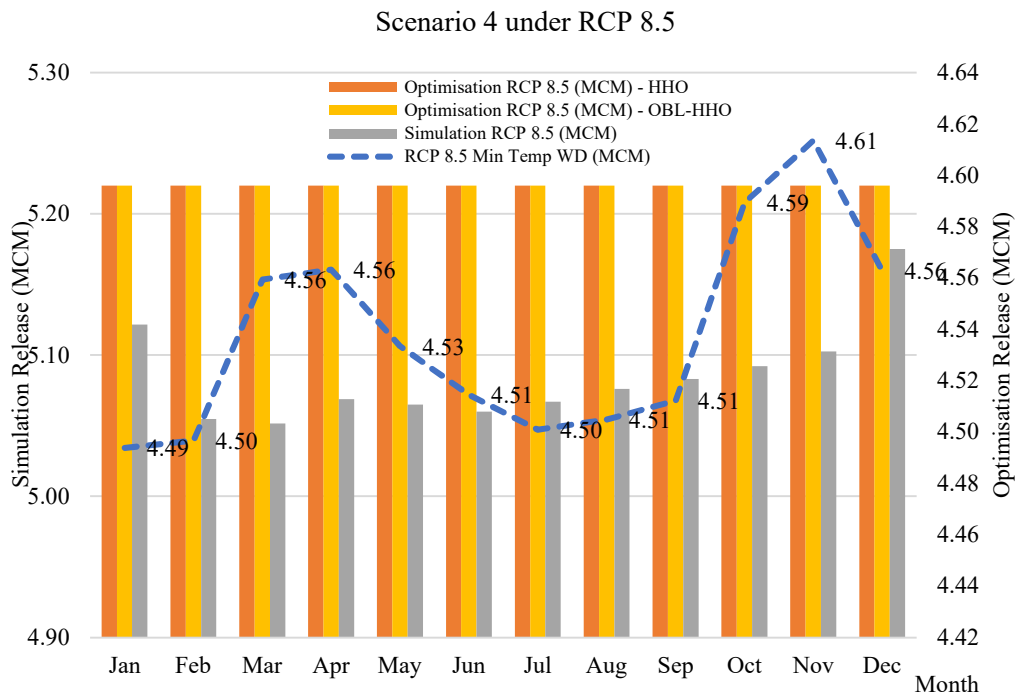
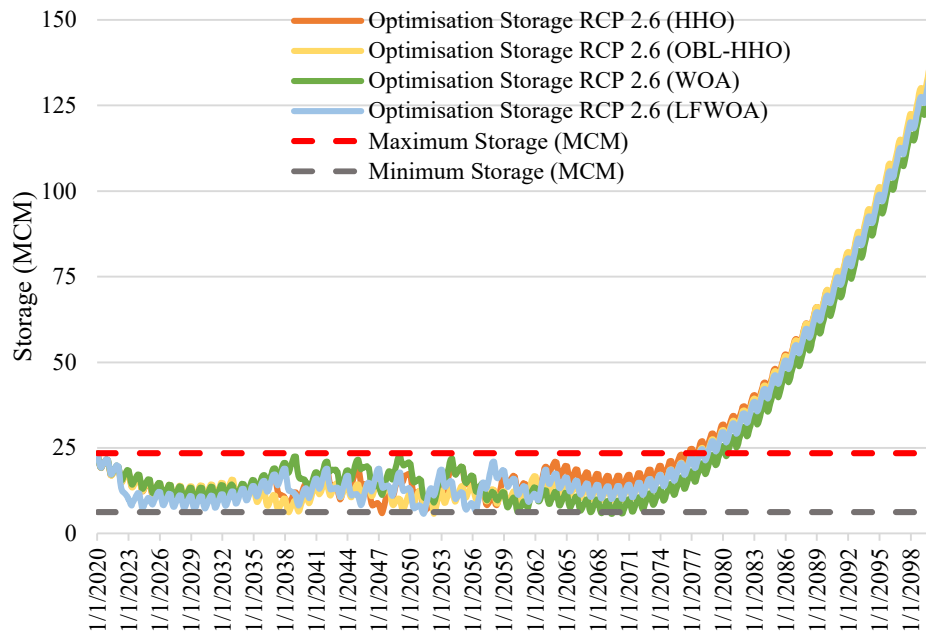


Figure 4.21: HHO vs OBL-HHO for the comparison of simulation vs simulation-optimisation of optimal reservoir releases in Scenario 4 (a) RCP 2.6, (b) RCP 4.5 and (c) RCP 8.5

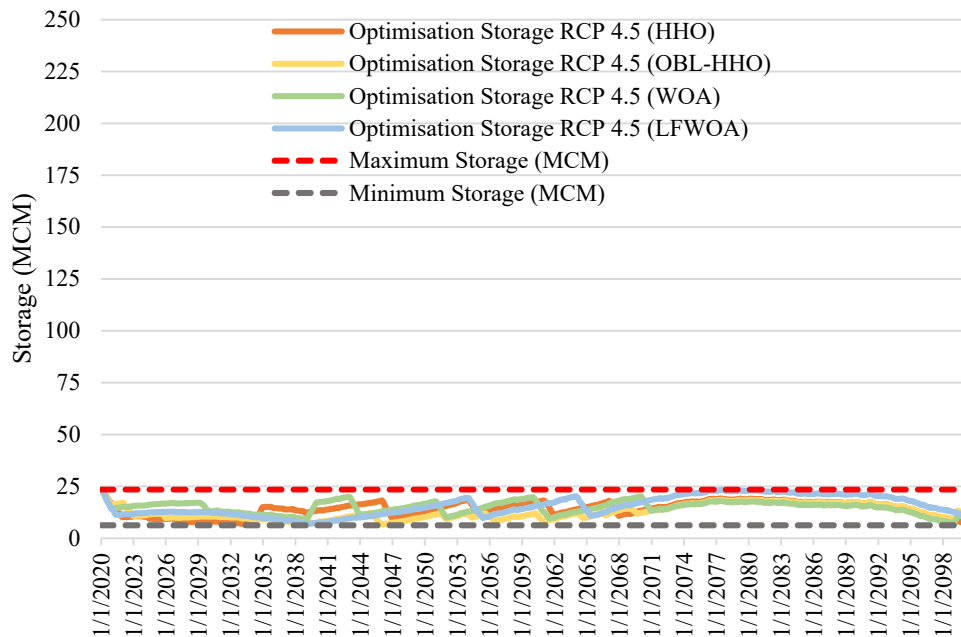
(b) Monthly Reservoir Storage Capacity under various RCPs

From 2050 to 2076, Figure 4.22 (a) demonstrates the average monthly storage capacity in KGD for Scenario 4 under RCP 2.6 to balance the storage capacity of the KGD between its maximum and minimum. However, the HHO encountered storage failure in the year 2076 onwards at the level of 23.87 MCM, followed by the OBL-HHO and LFWOA in the year 2077 onwards at the storage levels of 26 MCM and 23.62 MCM, respectively, and then WOA, which faced failure later than the other three algorithms, in the year 2079 onwards at the level of 23.66 MCM. Similar to Scenario 2 and Scenario 3 of RCP 4.5, Scenario 4 of RCP 4.5 presumed a highly significant outcome in which no MHAs experienced a storage failure event which depicts in Figure 4.22 (b). Figure 4.22 (c) represents the average monthly storage capacity for Scenario 4 under RCP 8.5, revealing the initial phase of storage failure occurred in the near future which had a similar storage event failure to Scenario 3.

(a) For Minimum Temperature Scenario (Scenario 4) under RCP 2.6



(b) For Minimum Temperature Scenario (Scenario 4) under RCP 4.5



(c) For Minimum Temperature Scenario (Scenario 4) under RCP 8.5

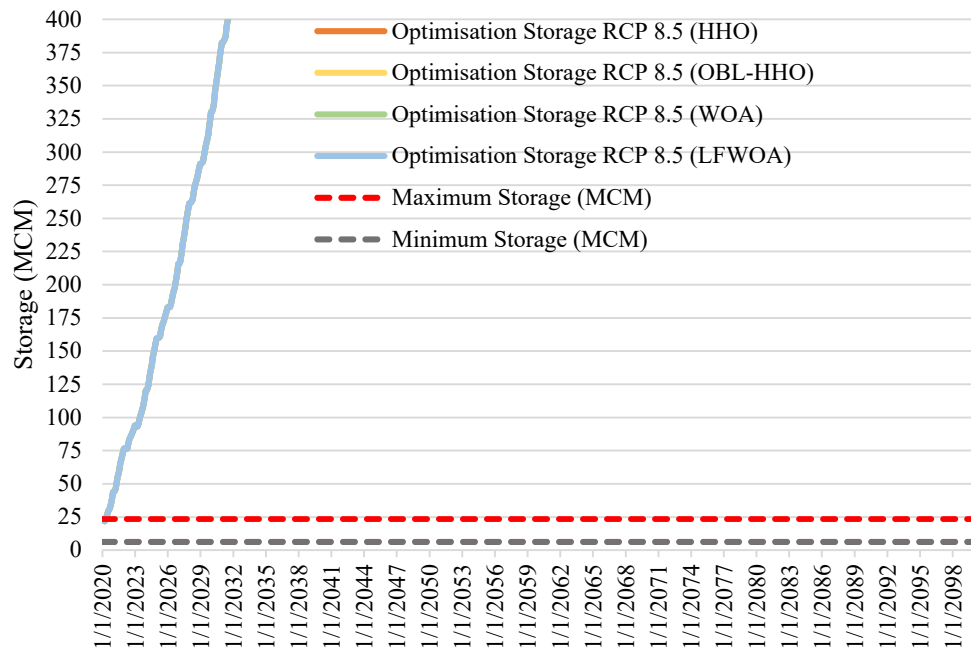


Figure 4.22: Average monthly storage capacity (MCM) for Scenario 4 (a) RCP 2.6, (b) RCP 4.5 and (c) RCP 8.5

4.6.5 Reservoir Risk Assessment for all Scenarios

Tables 4.16 - 4.19 present the maximum, mean, and minimum water demand temperatures under RCPs as Scenarios 2, Scenario 3, and Scenario 4, respectively, for the WOA, LFWOA, HHO and OBL-HHO. 960 future releases are anticipated from year 2020-2099. In Scenario 2, it showed no substantial difference for the overflow period under RCP2.6 and RCP4.5 with the proportion of 71.88% and 76.46%, respectively. The surplus event fraction in RCP 8.5 decreased to 61.15 %. Based on the Tables 4.16 - 4.19, the results depicted suboptimal condition especially under RCP 4.5 for Scenario 2, when the WOA and HHO accomplished just 13.96%, whereas the LFWOA attained 30% and OBL-HHO obtained 29.9%.

In Scenario 3, there is no evidence whether increase or decline trend was achieved for the shortage period, especially under RCP 8.5, as there does not show any proportion in reaching the exact water demand. Tables 4.16 - 4.19 depict an overflow period under RCP 8.5 reaching the maximum proportion for Scenario 3 and Scenario 4, respectively. This denotes the KGD received more inflows than in Scenario 3 and Scenario 4. Consequently, if this circumstances occurs, Scenario 3 and Scenario 4 requires additional consideration, particularly under RCP 8.5. Based on Tables 4.16 - 4.19, the WOA, LFWOA, HHO, and OBL-HHO under RCP 2.6 allocated a surplus event weighting of 63.13%, 71.77%, 71.77 % and 69.69%, respectively in Scenario 3. Besides, the surplus event under RCP 4.5 for WOA, LFWOA, HHO, and OBL-HHO generated 1.35%, 6.88%, 3.54%, and 1.25%, respectively in Scenario 3.

According to Tables 4.16 - 4.19, there were few shortage events under RCP 2.6 and RCP 4.5 of Scenario 4, with averages of 0.42% and 0.83%, respectively. However, there was a significant variation between the surplus events in Scenario 4 under RCP2.6 and RCP 4.5 with the weightage of 6.56% and 66.77 %, respectively. Overall, the periodic reliability obtained under Scenario 3 and Scenario 4 were in average of 90%, respectively. In order to be well-prepared and reduce the possibility of losses in terms of lives and assets, decision-makers at KGD should be cognizant of these scenarios, especially the Scenarios 2 and Scenario 3 under all RCPs that could occur in the future.

Table 4.16: Periodic Reliability by utilising WOA

Periodic Reliability/RCPs	RCP2.6	RCP4.5	RCP8.5
Maximum Temperature-Scenario 2, (% , times)			
Surplus Period	61.25%; (588)	76.46%; (734)	61.15% ;(587)
Exact Period	37.60% ;(361)	13.96%; (134)	17.50% ; (168)
Shortage Period	1.15% ; (11)	9.58% ; (92)	21.35% ; (205)
Mean Temperature-Scenario 3, (% , times)			
Surplus Period	63.13%; (606)	1.35%; (13)	100%; (960)
Exact Period	36.15%; (347)	94.69%; (909)	0
Shortage Period	0.73%; (7)	3.96%; (38)	0
Minimum Temperature-Scenario 4, (% , times)			
Surplus Period	65.00%; (624)	6.77%; (65)	100%; (960)
Exact Period	34.69%; (333)	91.15%; (875)	0
Shortage Period	0.31%; (3)	2.08%; (20)	0

Table 4.17: Periodic Reliability by utilising LFWOA

Periodic Reliability/RCPs	RCP2.6	RCP4.5	RCP8.5
Maximum Temperature-Scenario 2, (% , times)			
Surplus Period	61.46%; (590)	66.25%; (636)	58.02% ;(557)
Exact Period	37.40% ;(359)	30.00%; (288)	25.83% ; (248)
Shortage Period	1.15% ; (11)	3.75% ; (36)	16.15% ; (155)
Mean Temperature-Scenario 3, (% , times)			
Surplus Period	71.77%; (689)	6.88%; (66)	100%; (960)
Exact Period	18.54%; (178)	87.81%; (843)	0
Shortage Period	9.69%; (93)	5.31%; (51)	0
Minimum Temperature-Scenario 4, (% , times)			
Surplus Period	61.04%; (586)	3.33%; (32)	100%; (960)
Exact Period	38.13%; (366)	96.67%; (928)	0
Shortage Period	0.83%; (8)	0	0

Table 4.18: Periodic Reliability by utilising HHO

Periodic Reliability/RCPs	RCP2.6	RCP4.5	RCP8.5
Maximum Temperature-Scenario 2, (% , times)			
Surplus Period	71.88%; (690)	76.46%; (734)	61.15% ;(587)
Exact Period	23.23% ;(223)	13.96%; (134)	17.50% ; (168)
Shortage Period	4.90% ; (47)	9.58% ; (92)	21.35% ; (205)
Mean Temperature-Scenario 3, (% , times)			
Surplus Period	71.77%; (689)	3.54%; (34)	100%; (960)
Exact Period	18.54%; (178)	93.54%; (898)	0
Shortage Period	9.69%; (93)	2.92%; (28)	0
Minimum Temperature-Scenario 4, (% , times)			
Surplus Period	61.88%; (594)	8.54%; (82)	100%; (960)
Exact Period	37.92%; (364)	90.21%; (866)	0
Shortage Period	0.21%; (2)	1.25%; (12)	0

Table 4.19: Periodic Reliability by utilising OBL-HHO

Periodic Reliability/RCPs	RCP2.6	RCP4.5	RCP8.5
Maximum Temperature-Scenario 2, (% , times)			
Surplus Period	71.67%; (688)	66.35%; (637)	61.15% ;(587)
Exact Period	27.81% ;(267)	29.90%; (287)	17.40% ; (167)
Shortage Period	0.52% ; (5)	3.75% ; (36)	21.46% ; (206)
Mean Temperature-Scenario 3, (% , times)			
Surplus Period	69.69%; (669)	1.25%; (12)	100%; (960)
Exact Period	29.06%; (279)	96.25%; (924)	0
Shortage Period	1.25%; (12)	2.50%; (24)	0
Minimum Temperature-Scenario 4, (% , times)			
Surplus Period	79.17%; (760)	7.60%; (73)	100%; (960)
Exact Period	20.52%; (197)	92.40%; (887)	0
Shortage Period	0.31%; (3)	0	0

According to Table 4.20 and Table 4.21, the reservoir risk assessment was conducted using the proposed MHAs to investigate the impact of climate change on the future KGD operations under RCP 2.6, RCP 4.5, and RCP 8.5, with distinctive future water demand based on temperature factor. As shown in Table 4.20, the LFWOA performed marginally better than the WOA in Scenario 2 in terms of resiliency, as the higher value indicates the system's ability to recover from a failed operation. In addition, there was no significant variance between the WOA and LFWOA in terms of vulnerability. In Scenario 3, the WOA have shown improved risk analysis assessment ability. Under RCP 8.5, however, both algorithms produced pessimistic results, rendering the system incapable of recovering from the failure. Then comes Scenario 4, wherein the LFWOA is more resilient than the WOA under RCP 2.6. However, the LFWOA revealed pessimistic results at RCP 4.5 and RCP 8.5 since the resiliency criteria could not be evaluated.

According to Table 4.21, there are no significant differences between the HHO and enhancement of its model in terms of vulnerability criteria for Scenario 2. However, the OBL-HHO performed admirably for RCP 2.6 and RCP 4.5 in Scenario 2. In Scenario 3, the HHO showed the lowest vulnerability in comparison to the OBL-HHO. Under RCP 8.5, the pessimistic outcome occurred, and both algorithms were incapable of examining the resiliency. In Scenario 4, the HHO and OBL-HHO under RCP 4.5 and RCP 8.5, respectively, were unable to assess the resiliency criterion based on the pessimistic results obtained, which are identical to Table 4.20. As a result, an extensive assessment was conducted on the average water storage resilience indicator (WSR_{avg}) to examine the

resilience criterion, particularly for the worst-case scenarios, as tabulated in Table 4.22. The negative value of the (WSR_{avg}) indicated the reservoir system may be a violate in certain period, as illustrated in the aforementioned optimal reservoir release curves via proposed MHAs.

Table 4.20: WOA vs LFWOA comparison of the reservoir risk assessment under various RCPs based on temperature water demand

Temperature Based	Maximum Temperature, Scenario 2			Mean Temperature ,Scenario 3			Minimum Temperature, Scenario 4		
Water Demand (WD)/									
Reservoir risk analysis	RCP 2.6	RCP 4.5	RCP 8.5	RCP 2.6	RCP 4.5	RCP 8.5	RCP 2.6	RCP 4.5	RCP 8.5
WOA									
Vulnerability	0.6093	0.4782	0.1907	0.6933	0.1176	0.61146	0.6890	0.5764	0.6833
Shortage Index	0.001787	0.002070	0.0003	0.002497	4.72E-07	0.0044	0.002574	3.22E-05	0.005671
Resiliency	8.82	1.46	0.82	29.43	15.79	-	56	6	-
LFWOA									
Vulnerability	0.6006	0.5804	0.2022	0.6511	0.008547	0.61146	0.7189	1.4688	0.6833
Shortage Index	0.001866	0.002018	0.0002731	0.002415	1.32E-08	0.004418	0.002515	2.96E-05	0.005671
Resiliency	32.64	8	1.60	6.18	8.63	-	112	-	-

Table 4.21: HHO vs OBL-HHO comparison of the reservoir risk assessments under various RCPs based on temperature water demand

Temperature Based	Maximum Temperature, Scenario 2			Mean Temperature, Scenario 3			Minimum Temperature, Scenario 4		
Water Demand (WD)/	RCP 2.6	RCP 4.5	RCP 8.5	RCP 2.6	RCP 4.5	RCP 8.5	RCP 2.6	RCP 4.5	RCP 8.5
Reservoir risk analysis									
HHO									
Vulnerability	0.5074	0.4782	0.1907	0.5345	0.001774	0.6115	0.7131	0.5638	0.6833
Shortage Index	0.001876	0.002070	0.00030	0.002415	1.56E-10	0.004418	0.002491	3.76E-05	0.005671
Resiliency	4.74	1.46	0.82	1.52	32.07	-	103	14	-
OBL-HHO									
Vulnerability	0.5325	0.5795	0.1866	0.6358	0.05556	0.61146	0.5570	0.6438	0.6833
Shortage Index	0.001826	0.002018	0.00030	0.002592	5.24E-08	0.004418	0.002491	2.96E-05	0.005671
Resiliency	24	4	0.14	17	10.50	-	8.33	-	-

Table 4.22: Extensive assessment in terms average water storage resilience (WSR_{avg}) indicator under various RCPs based on temperature water demand

Temperature Based Water Demand (WD)/ Extensive assessment	Maximum Temperature, Scenario 2			Mean Temperature, Scenario 3			Minimum Temperature ,Scenario 4		
	RCP 2.6	RCP 4.5	RCP 8.5	RCP 2.6	RCP 4.5	RCP 8.5	RCP 2.6	RCP 4.5	RCP 8.5
WOA									
WSR_{avg}	-0.98	-0.97	-0.97	-0.98	-0.99	0.30	-0.98	-0.99	0.32
LFWOA									
WSR_{avg}	-0.98	-0.97	-0.98	-0.98	-0.99	0.30	-0.99	-0.99	0.32
HHO									
WSR_{avg}	-0.98	-0.97	-0.97	-0.98	-0.99	0.30	-0.98	-0.99	0.32
OBL-HHO									
WSR_{avg}	-0.98	-0.97	-0.97	-0.98	-0.99	0.30	-0.98	-0.99	0.32

4.7 Execution of Future Climate Change Impact Based on Forecasted Population Growth

The results of the investigation into the effects of climate change based on forecasted population growth and future water demand using the suggested MHAs are described in this sub-section. In the subsequent sub-sections, the impact on the monthly release operation and monthly storage capacity will be described.

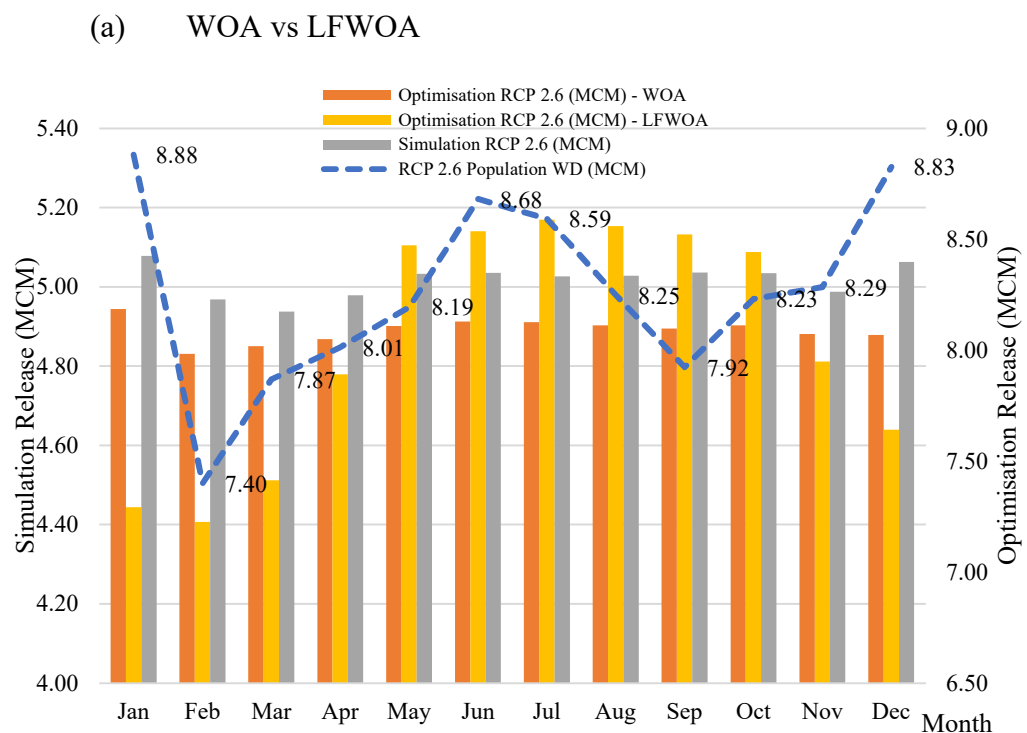
4.7.1 Monthly Release Operation under various RCPs

As depicted in Figure 4.23(a) – (c), the simulation vs simulation-optimisation utilising the WOA versus LFWOA and the HHO versus OBL-HHO under RCP 2.6, RCP 4.5, and RCP 8.5 of the anticipated population growth of water demand is given. For Figure 4.23 (a) at RCP 2.6, the LFWOA achieved 7.81% periodic reliability but the WOA only achieved 4.17 %. Both algorithms are incapable of optimising reservoir release. In addition, for the simulated bar chart (shown in grey) that occurred under RCP 2.6, it was unable to achieve the ideal reservoir release in accordance with the forecasted population growth of the water demand line and only achieved 2.6% in periodic reliability using the ANN.

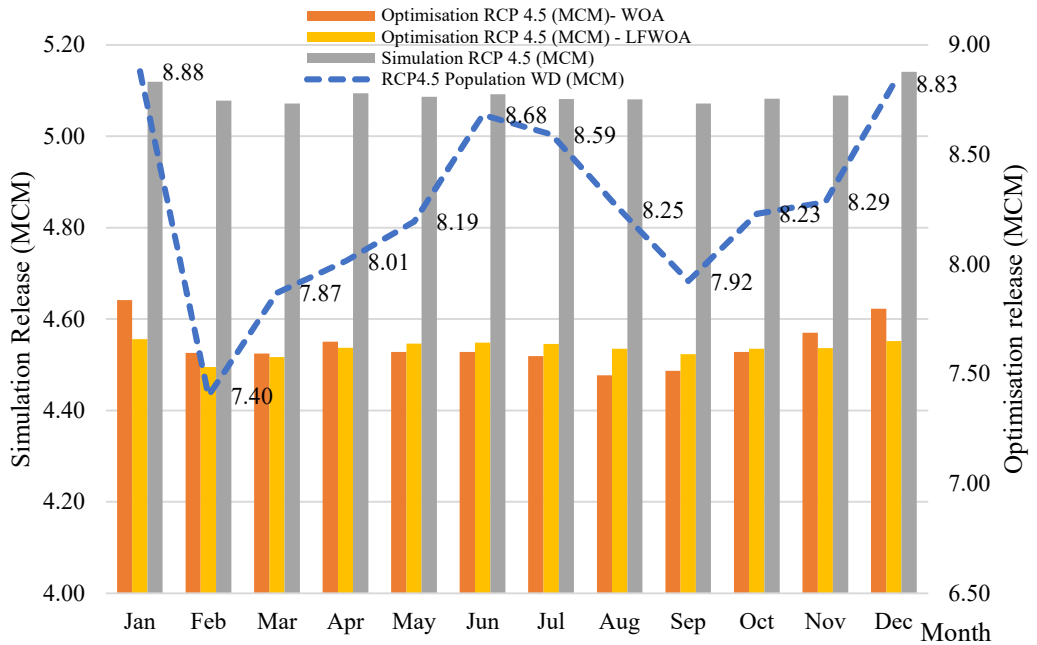
In addition, the WOA and LFWOA were tasked with examining the appropriate release policy under RCP 4.5 for the anticipated increase in water demand due to population growth. Figure 4.23 (b) under RCP 4.5 shows that the

WOA under RCP 4.5 increased by 6.88% to meet water demand, however the LFWOA under RCP 4.5 decreased by 6.77% compared to RCP 2.6. With an ANN result of 15.94%, the simulated release met the exact water demand far more precisely.

The next step is to evaluate the appropriate release curves using the WOA and LFWOA under RCP 8.5. However, the obtained results were incapable of producing a minimum deficit state. This is the weakness of the algorithms in the critical scenario state. Therefore, recommendations for future research are required for this case.



(b) RCP 4.5



(c) RCP 8.5

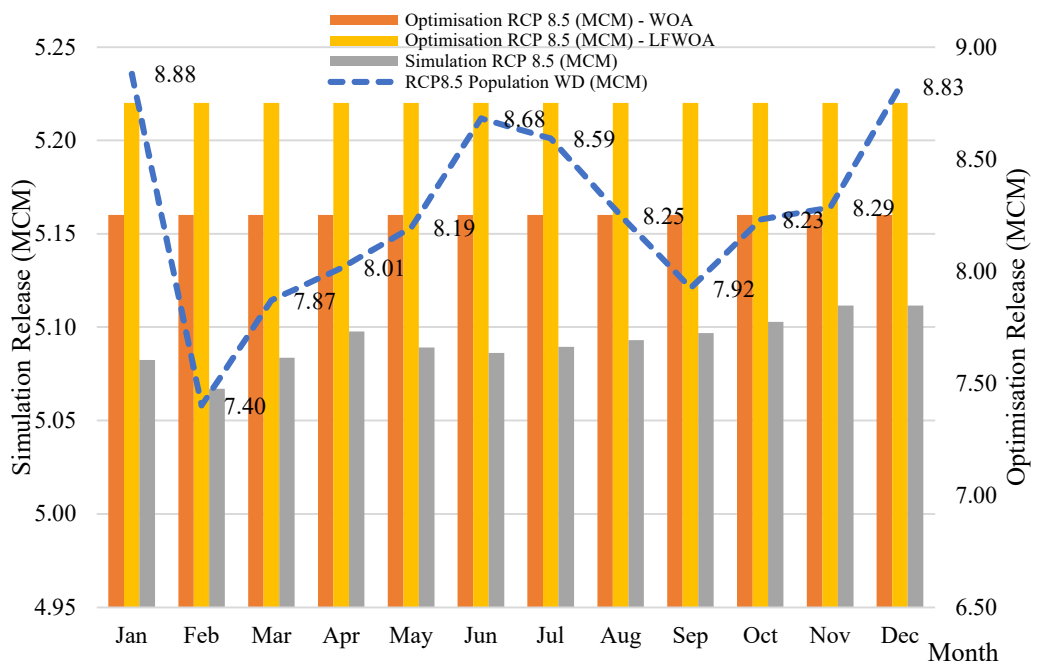
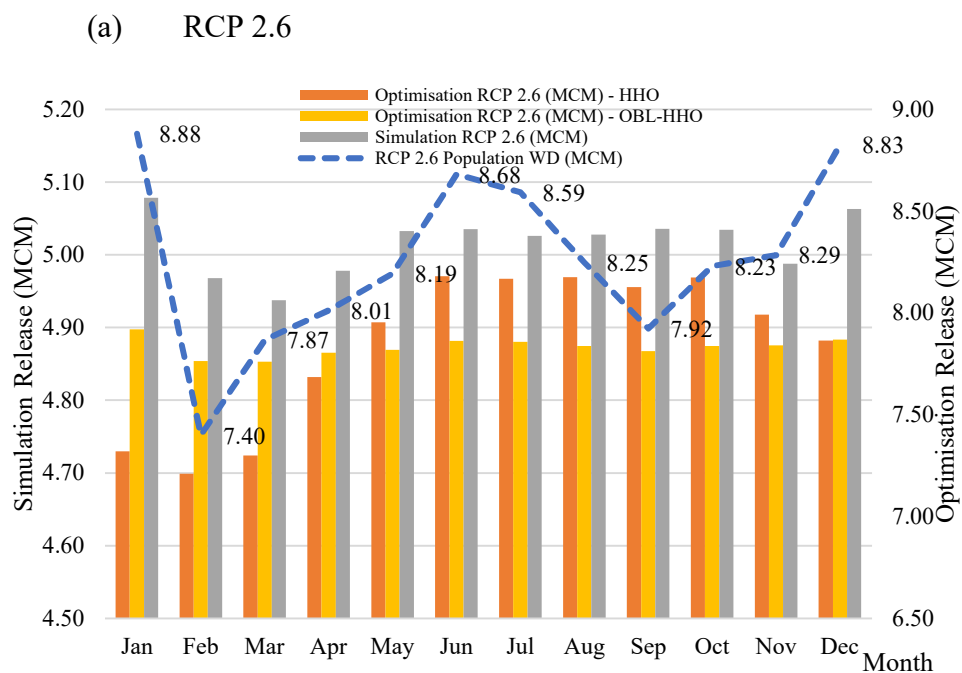
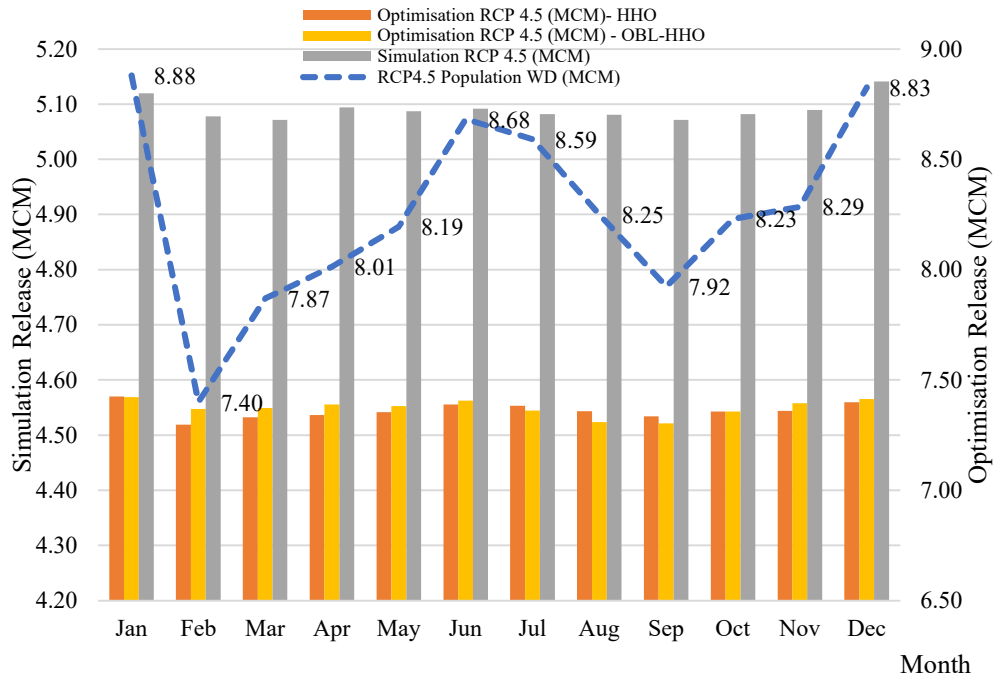


Figure 4.23: WOA vs LFWOA for the comparison of simulation vs simulation-optimisation of optimal reservoir releases in forecasted population growth factor (a) RCP 2.6, (b) RCP 4.5, and (c) RCP 8.5

For Figure 4.24 (a) – (c) at RCP 2.6, the HHO attained a periodic reliability of 4.58% whereas the OBL-HHO achieved just 3.02%. Neither algorithm is able to optimise reservoir release. In addition, the HHO and enhancement of its model were engaged in analysing the optimal RCP 4.5 release policy for the forecasted water demand owing to population growth. Figure 4.23 (b) demonstrates that the HHO under RCP 4.5 surged by 5.31 % to meet water demand, however, the OBL-HHO under RCP 4.5 did not change significantly from RCP 2.6 and reached 3.44 %. According to RCP 8.5, neither the HHO nor OBL-HHO could produce a minimum deficit state. The LFWOA, HHO, WOA, and OBL-HHO, in that order, achieved the highest periodic reliability when comparing these proposed algorithms for the forecasted population growth of water demand under RCP 2.6. The sequence for getting the optimum periodic reliability under RCP 4.5 is then followed by the WOA, LFWOA, HHO, and finally OBL-HHO. For RCP 8.5, no algorithm is able to supply the water demand satisfactorily.



(b) RCP 4.5



(c) RCP 8.5

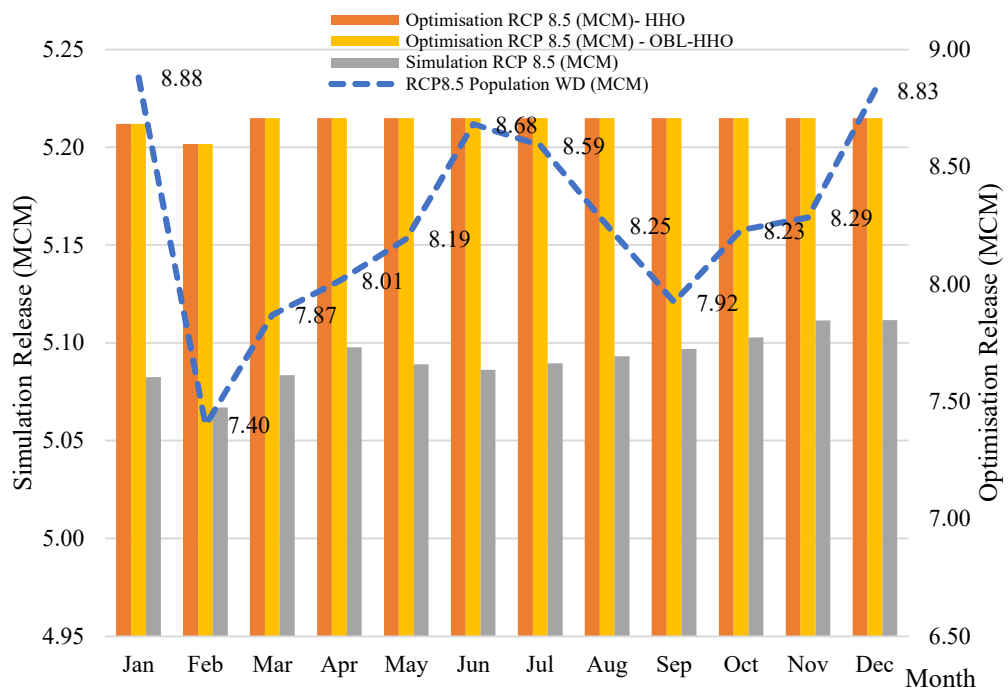
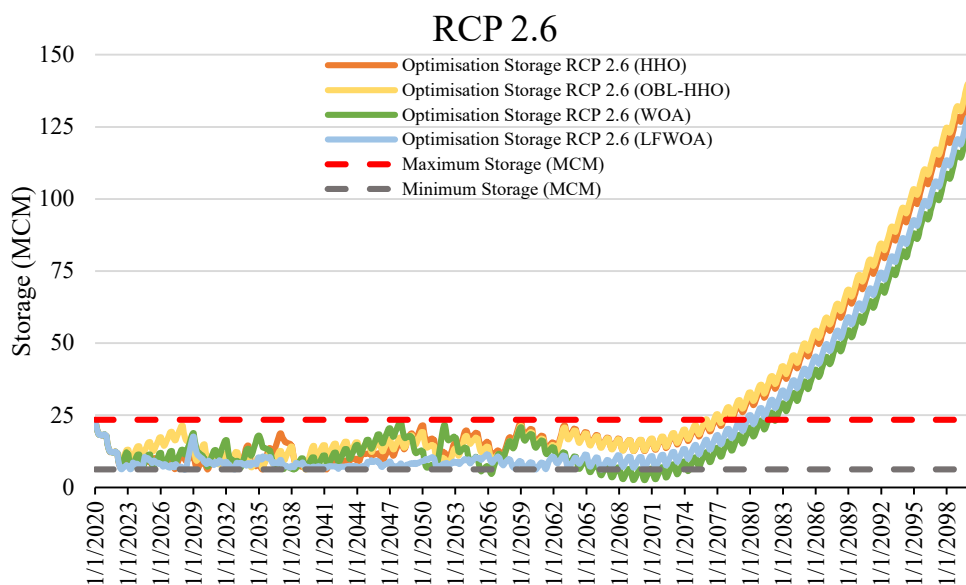


Figure 4.24: HHO vs OBL-HHO for the comparison of simulation vs simulation-optimisation of optimal reservoir releases in forecasted population growth factor (a) RCP 2.6, (b) RCP 4.5, and RCP 8.5

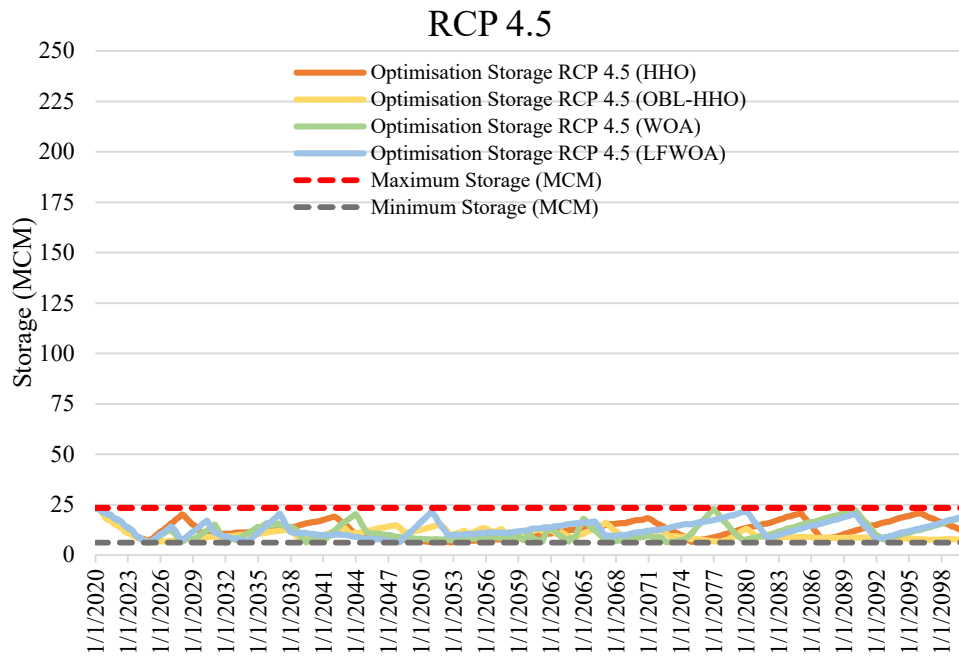
4.7.2 Monthly Reservoir Storage Capacity under various RCPs

Figure 4.25 (a) depicts the average monthly storage capacity at the KGD for future population growth and water demand projections under RCP 2.6. The HHO and OBL-HHO experienced storage failure in the year 2077 at the level of 24.02 MCM and 25.08 MCM, respectively, followed by the LFWOA in the year 2079 at the level of 24.09 MCM, and finally the WOA, which encountered storage failure later than the other three algorithms, in the year 2082 at the level of 23.96 MCM. Figure 4.25 (b) demonstrates a similar outcome to Scenario 3 and Scenario 4 of RCP 4.5, in which no MHAs had a storage failure event. Figure 4.25 (c) depicts the average monthly storage capacity for Scenario 4 under RCP 8.5, indicating that the initial phase of storage failure has occurred in the Near Future, which experienced a storage event failure identical to Scenario 3 and Scenario 4.

(a) Storage for Forecasted Population Growth under RCP 2.6



(b) Storage for Forecasted Population Growth under RCP 4.5



(c) Storage for Forecasted Population Growth under RCP 8.5

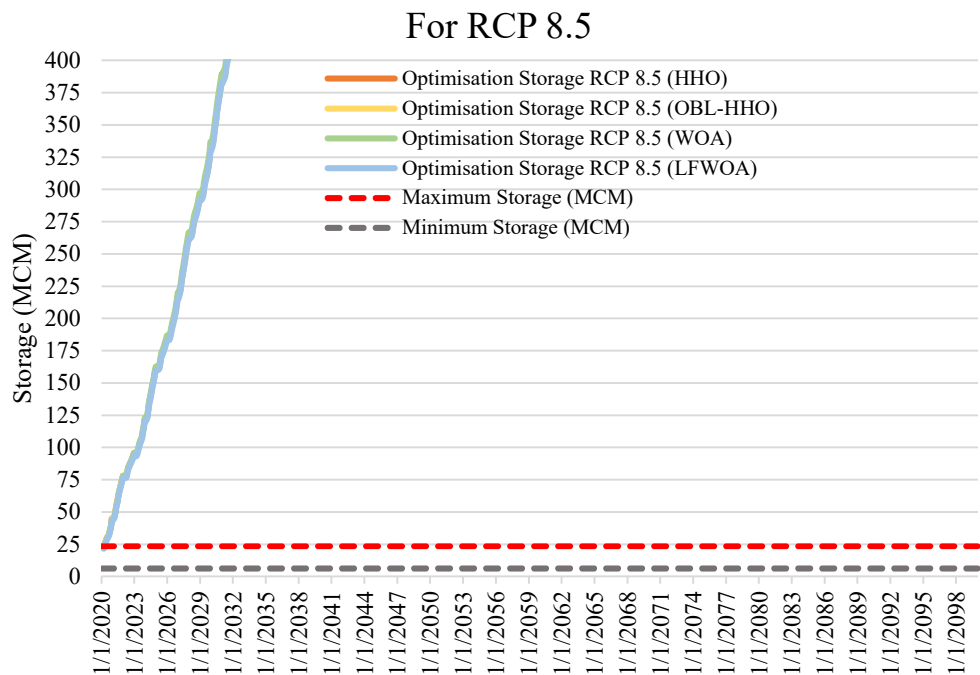


Figure 4.25: Average monthly storage capacity (MCM) for forecasted population growth of water demand (a) RCP 2.6, (b) RCP 4.5, and (c) RCP 8.5

4.7.3 Reservoir Risk Assessment

According to Tables 4.23 and 4.24, the outcomes of the reservoir optimisation operation at the KGD were determined by comparing the proposed algorithms with the execution of water demand based on population growth/land use land cover change. As presented in Table 4.23, the majority of the scarcity periods occurred under RCP2.6 and RCP4.5, with an average of 95.08% and 94.12%, respectively. In addition, the surplus period under RCP 8.5 reached 100 %. Overall, based on population growth and land use land cover changed, most proposed algorithms are unable to meet the water demand under all RCPs scenarios by only achieving between 3.02 and 7.8 %.

Based on Table 4.24, the reservoir risk analysis performance based on the population growth of water demand yielded a pessimistic result in which the vulnerability attained was much higher than resiliency, which elevates this scenario and requires additional recommendations to improve the study in this context. In addition, the novelty of this study is to highlight the investigation of climate change's impact on future reservoir operations at KGD and to provide valuable knowledge to the reservoir's decision-maker, whose actions and management of the reservoir in response to this matter should be more focus due to the erratic in order to mitigate or dissuade any disaster event.

Table 4.23: Comparison of Periodic Reliability under several RCPs

Algorithms	Periodic Reliability/RCPs	RCP2.6	RCP4.5	RCP8.5
WOA	Surplus Period	0	0	100% ;(960 times)
	Exact Period	4.17% ;(40 times)	6.88% ; (66 times)	0
	Shortage Period	95.83% ; (920 times)	93.13% ; (894 times)	0
LFWOA	Surplus Period	0% ; (0 time)	0% ; (0 times)	100% ; (960 times)
	Exact Period	7.81% ; (75 times)	6.77% ; (65 times)	0
	Shortage Period	92.19% ; (885 times)	93.23% ; (895 times)	0
HHO	Surplus Period	0.10% ; (1 time)	0.21% ; (2 times)	100% ; (960 times)
	Exact Period	4.58% ; (44 times)	5.31% ; (51 times)	0
	Shortage Period	95.31% ; (915 times)	94.48% ; (907 times)	0
OBL-HHO	Surplus Period	0	0.94% ; (9 times)	100% ; (960 times)
	Exact Period	3.02% ;(29 times)	3.44% ; (33 times)	0
	Shortage Period	96.98% ; (931 times)	95.63% ; (918 times)	0

Table 4.24: Comparison of the Reservoir Risk Assessments under various RCPs

Algorithm	RCP 2.6	RCP 4.5	RCP 8.5
WOA			
Vulnerability	3.52	4.00	3.10
Shortage Index	0.04160	0.05069	0.03523
Resiliency	0.03	0.06	-
LFWOA			
Vulnerability	3.69	4.00	3.04
Shortage Index	0.04228	0.05089	0.03390
Resiliency	0.03	0.06	-
HHO			
Vulnerability	3.55	3.93	3.06
Shortage Index	0.0420	0.05064	0.03404
Resiliency	0.01	0.05	-
OBL-HHO			
Vulnerability	3.50	3.85	3.10
Shortage Index	0.04207	0.05050	0.03404
Resiliency	0.02	0.04	-

4.8 Summary

In this sub-section, the model performances of the respective MHAs are explained briefly and discussed in relation to the observed and climate period reservoir risk analysis assessments and the monthly storage capacity. All the optimisation of the reservoir policy was done by setting up a slightly tolerance to the objective function which also known as penalty function in order to achieve the trade-off of the KGD optimisation operation policy.

4.8.1 Relationship between Reservoir Risk Assessment and MHAs for Observed Period Assessments

This paragraph focuses mostly on a summary of the observed period evaluation for the years 1987-2008. Based on Table 4.25, each algorithm revealed its advantages and disadvantages when subjected to the reservoir optimisation analysis. This table provides alternatives for the dam operator or stakeholder to choose between reliability and resilience to optimise the operation of the KGD. For instance, based on the results acquired from 1987 to 2008, the sequence with the lowest reliability was the GA binary, but at the same time, it had the highest resilience sequence, demonstrating its ability to recover from reservoir operation failure. In addition, the ABC showed the most vulnerability and sensitivity in terms of data interpretation, particularly when coping with the absence of partially observed datasets. In view of the two examples provided for the years 1987 and 2008, the advice to the dam operator or stakeholder is to avoid choosing these algorithms to conduct the optimisation operation policy

due to the inconsistent effectiveness of the algorithms and the limitations of these modern evolutionary algorithms (without the strategy of exploration and exploitation simultaneously). In contrast, the overall findings obtained by utilising the MHAs for the years 1987-2008 indicated an optimistic conclusion for the dam operator to evaluate based on the priority of the trade-off between reliability and resilience or other possible combinations of reservoir risk indices.

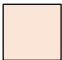







In contrast, this paragraph elaborates mostly on the observed assessments for the years 2001-2019. The algorithms exhibited variation in the order of reservoir risk analysis assessments for all inflow categories. These observed period datasets for years 2001-2019 served as the base period scenario and also were utilised for the climate assessment to generate the future variables such as rainfall, temperature, evaporation, and demand. With these inputs that were incorporated with the observed period datasets, the proposed MHAs were executed and had the reservoir risk assessment performed in order to investigate the climate assessment for the future KGD operation management and planning. Furthermore, the dam operator or stakeholder can decide which algorithm is suited for the current KGD operation strategy based on the reservoir risk indices and inflow conditions that are most important to them. For instance, during the high inflow category condition, the dam operator or stakeholder can look for the OBL-HHO algorithm to execute the KGD operation policy in order to fulfil the objective functions of KGD without violating the storage condition and, at the same time, meeting the exact demand period in the downstream by placing the highest priority between reliability and vulnerability. However, for the resilience index of high inflow, the final outcome showed all identical ranking due to being

unable to recover from the system if facing any failure event. Table 4.25 provides the dam operator or stakeholder with an option for constructing their policy based on their prioritised reservoir risk assessments.

Table 4.25: Comparison of the Reservoir Risk Assessment for the Observed Period for year 2001-2019 and for year 1987-2008

Ranking	Reliability, R_p			Vulnerability, V_{ul}			Resilience, R_s			$Max\ Deficit_{annual}$						
	1987-2008	2001-2019			1987-2008	2001-2019			1987-2008	2001-2019						
		High Flow	Medium Flow	Low Flow		High Flow	Medium Flow	Low Flow		High Flow	Medium Flow	Low Flow	High Flow	Medium Flow	Low Flow	
1	WOA	OBL-HHO	LFWO	WOA	GA-binary	OBL-HHO	OBL-HHO	LFWO	WOA	All identical	LFWO	WOA	OBL-HHO	OBL-HHO		
2	HHO	HHO	WOA	HHO	OBL-HHO	HHO	HHO	OBL-HHO	HHO		WOA	WOA	HHO	HHO	LFWO	
3	ABC	WOA	HHO	LFWO	WOA	LFWO	WOA	HHO	OBL-HHO		HHO	OBL-HHO	OBL-HHO	LFWO	WOA	
4	PSO	LFWO	OBL-HHO	OBL-HHO	HHO	HHO	LFWO	WOA	WOA		OBL-HHO	WOA	HHO	WOA	HHO	
5	OBL-HHO				WOA				ABC				GA-real coded			
6	WOA				GA-real coded				PSO				PSO			
7	GA-real coded				PSO				GA-real coded				ABC			
8	GA-binary				ABC				GA-binary				GA-binary			

Legend:

 WOA	 HHO	 ABC	 GA-real coded
 LFWO	 OBL-HHO	 PSO	 GA-binary

4.8.2 Relationship between Reservoir Risk Climate Assessments and Monthly Storage Capacity via MHAs under various RCPs Based on Temperature and Forecasted Population Growth Factors

This paragraph focuses primarily on RCP 2.6. This emission pathway, commonly referred to as "Low emissions" or too optimistic future event is an example of a scenario that would result in very low concentrations of greenhouse gases (GHGs). The future in this scenario is low energy intensity, CO₂ emissions remain at current levels until 2020, then drop and turn negative in 2100, with a world population of 9 billion people, reducing fossil fuel use, and a 40% reduction in methane emissions (Van Vuuren et al., 2011). Table 4.26 compares the ranking of the respective algorithms in terms of individual reservoir risk assessment in accordance with RCP 2.6 of Scenario 2, Scenario 3, Scenario 4, and the forecasted population growth of future water demand. The findings were then further analysed and simultaneously interpreted with reference to Figure 4.16(a), Figure 4.19(a), Figure 4.22(a), and Figure 4.25(a). Since the vulnerability indices of the WOA fall in the lowest sequence number for Scenario 2 and Scenario 3 of RCP 2.6 compared to other algorithms, this indicates that the WOA is extremely vulnerable and sensitive to climatic datasets. This may be observed in Figure 4.16(a) which demonstrates that the monthly storage capacity has failed roughly from year 2077 onwards which is much earlier than the other three algorithms happened roughly after two years for Scenario 2. Consequently, the LFWOA was utilised in this study to alleviate the limitations of WOA in order to increase the efficacy of the algorithms by providing a more accurate monthly storage capacity and reservoir risk analysis

assessment in terms of resilience and vulnerability for Scenario 2 of RCP 2.6. In addition, Figure 4.19 (a) depicts the monthly storage capacity has failed approximately in year later 2074 for the WOA and LFWOA for Scenario 3 of RCP 2.6. This can be seen in Table 4.26, where the WOA attained the lowest sequence for Scenario 2 and Scenario 3 in terms vulnerability indices. However, in terms of resilience indices, the WOA has the competence to recover from the storage failure as is shown in Table 4.26 for Scenario 3. In contrast to Scenario 2 and Scenario 3, the lowest sequence of the vulnerability in Scenario 4 showed that the LFWOA was the most vulnerable and sensitive based on Table 4.26. This may be observed in Figure 4.22 (a) which demonstrates the LFWOA has failed monthly storage capacity roughly in year 2077, but it is capable of rebounding back from the storage failure as indicated in Table 4.26 in which the resilience indices generated the confidence level by achieving the second highest sequence. Besides, the WOA performed in forecasted population growth of future water demand happened an odd event in which the storage capacity goes beyond the minimum storage capacity during 2067 to 2073 as depicted in Figure 4.25 (a). Even though the WOA occurred in this odd event, resilience indices for the forecasted population growth of future water demand scenario showed the highest capability to recover from the failure as shown in Table 4.26. In a similar scenario of future water demand, the LFWOA attained the lowest sequence of the vulnerability indices as tabulated in Table 4.26, which indicates the algorithm was the most vulnerable and sensitive to the dataset, yet the resilience indices showed the competency to recuperate from the storage failure.

This paragraph focuses primarily on RCP 4.5. The future occurrence in this scenario, called as an "intermediate emission" is compatible with reducing grassland and agricultural use because of productivity gains and dietary changes, constant methane emissions, and a slight increase in CO₂ emissions before the reduction begins about 2040. Scenario 3, Scenario 4, and forecasted population growth of future water demand as represented in Figure 4.19 (b), Figure 4.22 (b), and Figure 4.25 (b) did not experience any monthly storage failures. Yet, to keep the balance of the trade-offs at the KGD operation, the optimal decision of the reservoir operation shall be aware as there is a possibility of facing the storage failure event when an extreme event occurs. However, the LFWOA was the algorithm with the lowest sequence of vulnerability for Scenario 2. As shown in Table 4.26, the monthly storage failure in the year 2062 and beyond (mid-future) for Scenario 2.

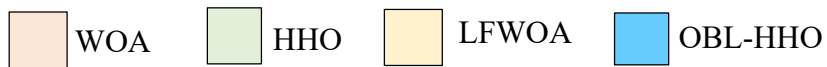
In conclusion, this paragraph focuses on RCP 8.5. This scenario is referred to as "High emissions" or an overly pessimistic future event because it is compatible, an escalating event of the methane emissions, a massive reliance on fossil fuels, a high energy intensity with a world population of 12 billion by 2100, and an increase in croplands and grasslands caused by a growth in population. The monthly storage failure occurred too quickly at the beginning of the near future for Scenario 3, Scenario 4, and forecasted population growth of future water demand which are displayed in Figure 4.19 (c), Figure 4.22 (c) and Figure 4.25 (c). Besides, the lowest sequence of vulnerability was the LFWOA for Scenario 2, which according to Figure 4.16 (c) and Table 4.26 occurred in year 2062 onwards. Referring to the reservoir risk analysis assessment indices

of vulnerability and resilience yields a convincing and reliable conclusion regarding the respective scenario events corresponding to the MHAs effectiveness. The ranking that showed all identical indicates that all the proposed MHAs do not show any significant difference and obtained in overall similar final outcome.

Table 4.26: Comparison of Reservoir Risk Assessments under various RCPs Based on Temperature and Forecasted Population Growth

Ranking	Reliability, R_p									Vulnerability, Vul														
	Max.Temp. Scenario			Mean Temp. Scenario			Min.Temp. Scenario			Forecasted Population			Max.Temp. Scenario			Mean Temp. Scenario			Min.Temp. Scenario			Forecasted Population		
	RCP2.6	RCP4.5	RCP8.5	RCP2.6	RCP4.5	RCP8.5	RCP2.6	RCP4.5	RCP8.5	RCP2.6	RCP4.5	RCP8.5	RCP2.6	RCP4.5	RCP8.5	RCP2.6	RCP4.5	RCP8.5	RCP2.6	RCP4.5	RCP8.5	RCP2.6	RCP4.5	RCP8.5
1	WOA	LFWOA	All identical	WOA	OBL-HHO	All identical	LFWOA	LFWOA	All identical	LFWOA	WOA	All identical	LFWOA	LFWOA	All identical	LFWOA	LFWOA	All identical	LFWOA	LFWOA	All identical	LFWOA	LFWOA	All identical
2	LFWOA	OBL-HHO	All identical	OBL-HHO	WOA	All identical	LFWOA	WOA	All identical	LFWOA	LFWOA	All identical	LFWOA	WOA	All identical	LFWOA	WOA	All identical	LFWOA	LFWOA	All identical	LFWOA	LFWOA	All identical
3	OBL-HHO	WOA	All identical	LFWOA	LFWOA	All identical	WOA	OBL-HHO	All identical	WOA	LFWOA	All identical	LFWOA	OBL-HHO	All identical	LFWOA	OBL-HHO	All identical	LFWOA	LFWOA	All identical	LFWOA	LFWOA	All identical
4	LFWOA	LFWOA	OBL-HHO	LFWOA	LFWOA	All identical	OBL-HHO	LFWOA	All identical	OBL-HHO	OBL-HHO	All identical	WOA	LFWOA	All identical	WOA	LFWOA	All identical	WOA	LFWOA	All identical	WOA	LFWOA	All identical
Ranking	Resilience, R_s									Max Deficit _{annual}														
1	LFWOA	LFWOA	WOA	WOA	LFWOA	All identical	LFWOA	LFWOA	All identical	LFWOA	LFWOA	All identical	WOA	LFWOA	LFWOA	LFWOA	LFWOA	All identical	LFWOA	LFWOA	All identical	WOA	OBL-HHO	LFWOA
2	OBL-HHO	OBL-HHO	LFWOA	LFWOA	OBL-HHO	All identical	LFWOA	WOA	All identical	WOA	WOA	All identical	OBL-HHO	OBL-HHO	OBL-HHO	LFWOA	OBL-HHO	All identical	OBL-HHO	WOA	All identical	LFWOA	LFWOA	OBL-HHO
3	WOA	WOA	LFWOA	LFWOA	LFWOA	All identical	OBL-HHO	LFWOA	All identical	OBL-HHO	LFWOA	All identical	LFWOA	LFWOA	WOA	LFWOA	OBL-HHO	All identical	LFWOA	OBL-HHO	All identical	OBL-HHO	WOA	LFWOA
4	LFWOA	LFWOA	OBL-HHO	OBL-HHO	WOA	All identical	WOA	OBL-HHO	All identical	LFWOA	OBL-HHO	All identical	LFWOA	LFWOA	OBL-HHO	LFWOA	LFWOA	All identical	WOA	LFWOA	All identical	WOA	LFWOA	WOA

Legend:



CHAPTER 5

CONCLUSIONS AND RECOMMENDATIONS

5.1 Conclusions

In this study, the meta-heuristic algorithms (MHAs) such as the WOA, LFWOA, HHO, and OBL-HHO, were proposed for computing and simulating the initial model's response using the observed datasets by generating the current reservoir release operation (Objective 1). It was then further taken to optimise the current reservoir release operation for the observed periods until they attained the ideal objective functions (Objective 2). Carrying it further along, the objective functions, decision variables, constraints, and penalty functions of the reservoir optimisation procedure were determined and established to evaluate the reservoir risk analysis for the observed period assessment and climate assessment (Objective 3).

The final outcomes for the evaluation assessment for year 2001-2019 were described. The LFWOA had the highest periodic reliability in the high inflow category for meeting exact demand, at 15.35%, followed by the WOA (14.47%), HHO (13.16%), and the OBL-HHO (9.21%). For the vulnerability in the high inflow category, it was shown that the HHO was still persuaded to conduct the reservoir optimisation operation, as it achieved the highest sequence; this showed that the model was robust and imbued with efficacy. However, the

resilience metric for high inflow categories did not produce any optimistic results; this indicating that the system may not be able to recover from any reservoir failure event. As a result, the stakeholder or policymaker should be more concerned and vigilant. Some recommendations on this have been provided in the final paragraph in this section. The LFWOA has the highest percentage of periodic reliability for the medium inflow category to meet exact demand, at 42.54 %, followed by the WOA (39.91 %), HHO (38.60 %), and OBL-HHO (20.54 %). The resilience metric for the medium inflow category which achieved the performances in the same sequence to the periodic reliability. In terms of medium inflow category for the vulnerability metric, the algorithms OBL-HHO, HHO, WOA, and LFWOA have shown to be the most robust.

A reservoir risk analysis was performed and compared to validate the proposed MHAs and other heuristic algorithms developed in the prior work in terms of their efficacy performances for the years 1987-2008. The LFWOA exhibited the highest percentage of periodic reliability at 69.70%, with the HHO followed closely at 63.26%. The ABC and PSO algorithms showed periodic reliability percentages of 61.36% and 59.47%, respectively. The OBL-HHO and WOA algorithms exhibited periodic reliability percentages of 56.44% and 56.06%, respectively. The GA-RC algorithm showed a periodic reliability percentage of 55.65%, while the GA algorithm exhibited the lowest periodic reliability percentage at 23.5%. However, the proposed MHAs were incapable of reaching the lowest vulnerability. In respect of shortage index and resilience, however the algorithms results have shown that they have outperformed those in previous prior studies conducted.

Even though there was inconsistency among the MHAs in respect of reservoir risk assessments for both observed periods (1987-2008 and 2001-2019), the outcome of this sub-section of the observed periods were used to enhance the understanding of water resources management by implementing reservoir optimisation into the KGD operation in order to maximise the benefits and simultaneously satisfy the objective functions of KGD. Consequently, the dam operator or stakeholder can control the indices of the reservoir risk analysis for the current KGD operation by prioritising current climate events. By preserving the equilibrium between the proposed MHAs and reservoir risk analysis indices, the stakeholder can select the optimal KGD operation by referring to the summary of findings for the observed period assessments. For instance, to select the optimal algorithm between reliability and vulnerability, etc.

Even if greenhouse gas emissions were to be stopped, many parts of climate change and its accompanying effects will persist for millennia. As global warming intensifies, the likelihood of abrupt or irreversible consequences increases. Thus, the continuing investigation of the optimisation of the future reservoir operation under various climatic scenarios was conducted by leveraging the proposed MHAs (Objective 4). The comparison between the reservoir simulation (ANN) and reservoir simulation-optimisation (MHAs) were carried out in terms of examined the reservoir risk analysis evaluation for climate assessments as well as the monthly storage capacity. In addition, a few scenarios of the future water demand were developed and predicted based on a close proximity of real condition: (i) Temperature Scenarios and (ii) Forecasted

Population Growth. Scenario 1 was developed for the base period investigation and the water demand was identical to the observed period assessment. Apart from that, the temperature scenarios of future water demand were segregated into three scenarios: (a) Scenario 2: Maximum Temperature; (b) Scenario 3: Mean Temperature and lastly (c) Scenario 4: Minimum Temperature.

This sub-section under climate assessments provide a summary of the temperature scenarios for future water demand incorporated with RCPs events (Objective 4). There were no monthly storage failures in any of the scenarios examined under RCP 4.5. However, the results of all RCP 2.6 scenarios indicated that monthly storage capacity failures occurred from the Mid-Future decade onwards into the Far Future. According to the vulnerability indices, the WOA was the most vulnerable in this event; nevertheless, the resilience indices revealed the ability of the WOA managed to recover from the storage capacity failure. In addition, some worst-case scenarios were identified under RCP 8.5 in Scenario 3 and Scenario 4, respectively, for the temperature scenarios of future water demand, which showed that the proposed MHAs were unable to achieve the minimal deficit state due to the high precipitation, resulting in a high inflow into the KGD. Moreover, the high emissions event of an escalating methane emissions and a massive reliance on fossil fuels contributed to the breakdown of the monthly storage capacity in Scenario 3 and Scenario 4 under RCP 8.5 in the earliest stages of the Near Future. Yet, under RCP 8.5 of Scenario 2 there was supposedly, a similar storage capacity breakdown beginning in 2062, way later than Scenario 3 and Scenario 4 which demonstrates that the suggested MHAs

operated adequately with the Scenario 2's datasets as compared to Scenario 3 and Scenario 4.

Next, the proposed MHAs were implemented to accommodate the forecasted population growth of future water demand incorporated with the RCPs events (Objective 4). Due to an increase in croplands and grasslands caused by population growth (LULCC maps), the current reservoir release operation policy was unable to supply the minimal deficit state in order to meet the forecasted population growth of future water demand. Thus, in the following section, a few recommendations have been highlighted. According to RCP 4.5, there were no monthly storage failures in terms of monthly storage capacity for the forecasted population growth of future water demand. However, there was an uncommon occurrence where the monthly storage capacity goes beyond the minimum storage capacity from year 2067 to 2073 under RCP 2.6. Lastly, the monthly storage failure dropped significantly under RCP 8.5 in the near future time.

In summary, this study has accomplished the four objectives established in Chapter 1, and it is believed that the research gaps and issues raised and discussed in Chapters 1 and 2 earlier have been adequately addressed. The research gaps of the the previous studies conducted at KGD had not included any investigation of the impact of climate change. As such, the ensembled GCMs have been applied in this study for the investigation of the the climate impact at KGD operation in future timeline. Furthermore, a near approximation of realistic circumstances which were based on the temperature factors and forecasted

population growth for future water demand have been developed to investigate and optimise the future KGD operations. Lastly, the proposed MHAs in this study were seek for the development and enhancement from the drawbacks of the algorithms that used in previous studies (e.g., GA, PSO and ABC) by applying the strategy of exploitation and exploration simultaneously.

5.2 Limitations and Recommendations

Some limitations of this study have been identified during the execution of the KGD optimisation operation for the observed period and investigation of the impact of climate change on KGD operation. First, the sedimentation variable, which may impact the reservoir's storage capacity, was not taken into account because the historical data are either inaccessible or unavailable. Followed by the next limitation was the investigation of climate change impact under the various RCPs. Due to a shortage of CMIP 5 data for this study region, the predictors variables for RCP 6.0 were insufficient for inclusion in this study, as by executing an unfair possible combination of predictants-predictor variables it would have resulted in a greater degree of uncertainty regarding the final outcome. As a result, the investigation of the future KGD operation was limited to three RCPs except RCP 6.0. Additionally, there was inconsistency among the MHAs in respect of reservoir risk assessments for both observed periods. Hence, the pitfall of the proposed MHAs can be further enhance in the following paragraph.

With the limitations arising, hence, a few future recommendations have suggested in this paragraph to improve this research which includes two subdivisions that relate to the proposed MHAs in connection to the observed period and climatic assessments. Firstly, a technical execution approach by integrating (hybridisation) or utilising other algorithms (with a similar nature of strategy of exploitation and exploration) to further examine the critical events obtained in this study, particularly under the RCP 4.5 of Scenario 3 and Scenario 4 for the monthly optimal release operation. The monthly storage capacity failure and optimal release operation at KGD under RCP 8.5 of Scenario 2, Scenario 3, and Scenario 4 can be improved by adopting hedging rules in order to have the highest possibilities of meeting the demand by minimising the reliability period and simultaneously reduce scarcity during failure periods (vulnerability). Secondly, the investigation could be expanded by implementing the most recent GCMs of CMIP 6 to analyse and compare the impact of climate change on the future reservoir optimisation operation findings with those of the current studies conducted at KGD using ensembles GCMs of CMIP 5.

Finally, this study has provided a new insights of the reservoir policy for the stakeholder or policymakers at KGD to cope the extreme events which was influenced by the climate change to the future optimal KGD operation and at the same time to satisfy the forecasted population growth of future water demand at the KGD. Nevertheless, this would necessitate increasing the KGD storage capacity, implementing a new release policy, relocating or constructing of a new structure either in the upper stream of the KGD or an underground dam, which was not within the control of the scholars or researchers of this topic, but the new

implementation of the policy shall be created by policymakers. However, scholars can further investigate to enhance the current study as mentioned in previous paragraph. In short, the outcome of this study is to provide the options of the proposed MHAs for the dam operator or policymaker to prioritise which indices of the reservoir risk assessments correlate to the present climate event to be adopted to meet the optimal KGD release operations.

REFERENCES

- Abdulla, F., 2020. 21st Century Climate Change Projections of Precipitation and Temperature in Jordan. *In: Procedia Manufacturing*, 40, pp. 197-204.
- Abera, F.F., Asfaw, D.H., Engida, A.N. and Melesse, A.M., 2018. Optimal operation of hydropower reservoirs under climate change: The case of Tekeze reservoir, Eastern Nile. *Water (Switzerland)*, 10(3), p. 273.
- Adnan, R.M., Heddad, S., Yaseen, Z.M., Shahid, S., Kisi, O. and Li, B., 2021. Prediction of Potential Evapotranspiration Using Temperature-Based Heuristic Approaches. *Sustainability*, 13(1), p. 297.
- Afshar, A., Shafii, M. and Haddad, O.B., 2011. Optimizing multi-reservoir operation rules: An improved HBMO approach. *Journal of Hydroinformatics*, 13(1), pp.121-139.
- Ahmadi, M., Bozorg Haddad, O. and Mariño, M.A., 2014. Extraction of Flexible Multi-Objective Real-Time Reservoir Operation Rules. *Water Resources Management*, 28(1), pp.131–147.
- Ahmadi, M., Haddad, O.B. and Loáiciga, H.A., 2014. Adaptive Reservoir Operation Rules Under Climatic Change. *Water Resources Management*, 29(4), pp.1247–1266.
- Ahmadianfar, I., Kheyrandish, A., Jamei, M. and Gharabaghi, B., 2020. Optimizing operating rules for multi-reservoir hydropower generation systems: An adaptive hybrid differential evolution algorithm. *Renewable Energy*, 167, pp.774-790.
- Ahmadianfar, I. and Zamani, R., 2020. Assessment of the hedging policy on reservoir operation for future drought conditions under climate change. *Climatic Change*, 159(2), pp.253–268.
- Ahmadzadeh Araji, H., Wayayok, A., Massah Bavani, A., Amiri, E., Abdullah, A.F., Daneshian, J. and Teh, C.B.S., 2018. Impacts of climate change on soybean production under different treatments of field experiments considering the uncertainty of general circulation models. *Agricultural Water Management*, 205, pp.63–71.
- Ahmed, K., Shahid, S., Haroon, S. Bin and Wang, X.J., 2015. Multilayer perceptron neural network for downscaling rainfall in arid region: A case

- study of Baluchistan, Pakistan. *Journal of Earth System Science*, 124, pp.1325-1341.
- Akbary, P., Ghiasi, M., Pourkheranjani, M.R.R., Alipour, H. and Ghadimi, N., 2019. Extracting Appropriate Nodal Marginal Prices for All Types of Committed Reserve. *Computational Economics*, 53, pp. 1-26.
- Al-Aqeeli, Y.H. and Mahmood Agha, O.M.A., 2020. Optimal Operation of Multi-reservoir System for Hydropower Production Using Particle Swarm Optimization Algorithm. *Water Resources Management*, 34(10), pp.3099–3112.
- Al-Najar, H. and Ashour, E.K., 2013. The impact of climate change and soil salinity in irrigation water demand on the Gaza Strip. *Journal of Water and Climate Change*, 4(2), pp. 118-130.
- Al-Zubari, W.K., El-Sadek, A.A., Al-Aradi, M.J. and Al-Mahal, H.A., 2018. Impacts of climate change on the municipal water management system in the Kingdom of Bahrain: Vulnerability assessment and adaptation options. *Climate Risk Management*, 20, pp. 95-110.
- Ali Khan, M.M., Shaari, N., Nahar, A., Baten, M.A., and Nazaruddin, D.A., 2014. Flood Impact Assessment in Kota Bharu, Malaysia: A Statistical Analysis. *World Applied Sciences Journal*, 32(4), pp. 626-634.
- Allawi, M.F., Jaafar, O., Mohamad Hamzah, F., Abdullah, S.M.S. and El-shafie, A., 2018. Review on applications of artificial intelligence methods for dam and reservoir-hydro-environment models. *Environmental Science and Pollution Research*, 25(14), pp.13446–13469.
- Allawi, M.F., Jaafar, O., Mohamad Hamzah, F. and El-Shafie, A., 2019a. Novel reservoir system simulation procedure for gap minimization between water supply and demand. *Journal of Cleaner Production*, 206, pp.928–943.
- Allawi, M.F., Jaafar, O., Mohamad Hamzah, F., Koting, S.B., Mohd, N.S.B. and El-Shafie, A., 2019b. Forecasting hydrological parameters for reservoir system utilizing artificial intelligent models and exploring their influence on operation performance. *Knowledge-Based Systems*, 163, pp.907–926.
- Allen, R.G., 1998. FAO Irrigation and Drainage Paper Crop by. Irrigation and Drainage, 300(56).

- Amarasinghe, P.A.G.M., Abeygunawardana, N.S., Jayasekara, T.N., Edirisinghe, E.A.J.P. and Abeygunawardane, S.K., 2020. Ensemble models for solar power forecasting-a weather classification approach. *AIMS Energy*, 8(2), pp. 252-271.
- Anang, Z., Padli, J., Kamaludin, M. and Sathasivam, S., 2017. The Effect of Climate Change on Water Resources Using Panel Approach: The Case of Malaysia. *International Journal of Academic Research in Business and Social Sciences*, 7(11), pp. 141-152.
- Asadieh, B. and Afshar, A., 2019. Optimization of water-supply and hydropower reservoir operation using the Charged System Search algorithm. *Hydrology*, 6(1), p.5.
- Ashofteh, P.-S., Bozorg-Haddad, O. and Loáiciga, H.A., 2017. Development of Adaptive Strategies for Irrigation Water Demand Management under Climate Change. *Journal of Irrigation and Drainage Engineering*, 143(2), p.04016077.
- Ashofteh, P.-S., Bozorg-Haddad, O. and Mariño, M.A., 2016. Performance Evaluation of a Developed Hybrid AOGCM Model under Climate Change. *Journal of Irrigation and Drainage Engineering*, 142(12), p.04016068.
- Ashofteh, P.-S., Haddad, O.B., Akbari-Alashti, H. and Mariño, M.A., 2015. Determination of Irrigation Allocation Policy under Climate Change by Genetic Programming. *Journal of Irrigation and Drainage Engineering*, 141(4), p.04014059.
- Ashofteh, P.S., Haddad, O.B. and A. Mariño, M., 2013. Climate Change Impact on Reservoir Performance Indexes in Agricultural Water Supply. *Journal of Irrigation and Drainage Engineering*, 139(2), pp.85–97.
- Atmaja, B.T. and Akagi, M., 2021. Evaluation of error- And correlation-based loss functions for multitask learning dimensional speech emotion recognition. *In: Journal of Physics: Conference Series*, 1896, p.012004.
- Aydilek, İ.B., 2018. A hybrid firefly and particle swarm optimization algorithm for computationally expensive numerical problems. *Applied Soft Computing Journal*, 66, pp.232–249
- Bai, T., Kan, Y. bin, Chang, J. xia, Huang, Q. and Chang, F.J., 2017. Fusing

- feasible search space into PSO for multi-objective cascade reservoir optimization. *Applied Soft Computing Journal*, 51, pp.328–340.
- Bai, T., Wei, J., Chang, F.J., Yang, W. and Huang, Q., 2019. Optimize multi-objective transformation rules of water-sediment regulation for cascade reservoirs in the Upper Yellow River of China. *Journal of Hydrology*, 577, p.123987.
- Bao, J., Feng, J. and Wang, Y., 2015. Dynamical downscaling simulation and future projection of precipitation over China. *Journal of Geophysical Research*, 120(16), pp. 8227-8243.
- Bates, B.C., Kundzewicz, Z.W., Wu, S. and Palutikof, J.P., 2008. Climate Change and Water. Technical Paper of the Intergovernmental Panel on Climate Change (IPCC), *IPCC Secretariat, Geneva*, pp. 210.
- Bates, B.C., Walker, K., Beare, S. and Page, S., 2010. Incorporating climate change in water allocation planning. *Waterlines Report Series No 28*, p.76.
- Begou, J.C., Jomaa, S., Benabdallah, S., Bazie, P., Afouda, A. and Rode, M., 2016. Multi-site validation of the SWAT model on the Bani catchment: Model performance and predictive uncertainty. *Water (Switzerland)*, 8(5), p.178.
- Benli, B. and Kodal, S., 2003. A non-linear model for farm optimization with adequate and limited water supplies Application to the South-east Anatolian Project (GAP) Region. *Agricultural Water Management*, 62(3), pp.187-203.
- Bhatt, R. and Hossain, A., 2019. Concept and Consequence of Evapotranspiration for Sustainable Crop Production in the Era of Climate Change. In: *Advanced Evapotranspiration Methods and Applications*. DOI: 10.5772/intechopen.73720.
- Birara, H., Mishra, S.K. and Pandey, R.P., 2021. Comparison of Methods for Evapotranspiration Computation in the Tana Basin, *Ethiopia*, 97, pp. 405-422.
- Blaney, H.F., 2017. Determining Water Requirements in Irrigated Areas From Climatological and Irrigation Data.
- Blaney, H.F. and Criddle, W.D., 1950. Determining water requirements in

- irrigated areas from climatological and irrigation data. [Washington, D.C.]: U.S. Soil Conservation Service.
- Bozorg-Haddad, O., Janbaz, M. and Loáiciga, H.A., 2016. Application of the gravity search algorithm to multi-reservoir operation optimization. *Advances in Water Resources*, 98, pp.173-185.
- Campozano, L., Tenelanda, D., Sanchez, E., Samaniego, E. and Feyen, J., 2016. Comparison of Statistical Downscaling Methods for Monthly Total Precipitation: Case Study for the Paute River Basin in Southern Ecuador. *Advances in Meteorology*, 13, pp. 1-13..
- Carini, M., Maiolo, M., Pantusa, D., Chiaravalloti, F. and Capano, G., 2018. Modelling and optimization of least-cost water distribution networks with multiple supply sources and users. *Ricerche di Matematica*, 67, pp.465-479.
- Celeste, A.B., 2016. Managing spills in reservoir design optimisation models. *Proceedings of the Institution of Civil Engineers: Water Management*, 169(5), pp. 1-8.
- Celeste, A.B. and Billib, M., 2009. Evaluation of stochastic reservoir operation optimization models. *Advances in Water Resources*, 32(9), pp. 1429-1443.
- Chan, N.W., Ghani, A.A., Samat, N., Roy, R., Tan, M.L. and Rahman, H.A., 2021. Addressing Water Resources Shortfalls Due to Climate Change in Penang, Malaysia. *Water Security in Asia*. In: *Springer Water*, pp. 239-249.
- Chaves, P., Tsukatani, T. and Kojiri, T., 2004. Operation of storage reservoir for water quality by using optimization and artificial intelligence techniques. In: *Mathematics and Computers in Simulation*, 67(4-5), pp. 419-432.
- Chebbi, A., Kebaili Bargaoui, Z., Abid, N. and da Conceição Cunha, M., 2017. Optimization of a hydrometric network extension using specific flow, kriging and simulated annealing. *Journal of Hydrology*, 555, pp. 971-982.
- Chen, D., Ding, C., Ma, X., Yuan, P. and Ba, D., 2013. Nonlinear dynamical analysis of hydro-turbine governing system with a surge tank. *Applied Mathematical Modelling*, 37(14-15), pp. 7611-7623.
- Chen, H. tao, Wang, W. chuan, Chen, X. nan and Qiu, L., 2020. Multi-objective

- reservoir operation using particle swarm optimization with adaptive random inertia weights. *Water Science and Engineering*, 13(2), pp.136–144.
- Chen, J., Chen, H. and Guo, S., 2018. Multi-site precipitation downscaling using a stochastic weather generator. *Climate Dynamics*, 50(5–6), pp. 1975–1992.
- Chishugi, D.U., Sonwa, D.J., Kahindo, J.-M., Itunda, D., Chishugi, J.B., Félix, F.L. and Sahani, M., 2021. How Climate Change and Land Use/Land Cover Change Affect Domestic Water Vulnerability in Yangambi Watersheds (D. R. Congo). *Land*, 10(2), p.165.
- Chong, K.L., Lai, S.H., Ahmed, A.N., Wan Jaafar, W.Z. and El-Shafie, A., 2021. Optimization of hydropower reservoir operation based on hedging policy using Jaya algorithm. *Applied Soft Computing*, 106, p.107325.
- Chu, J.T., Xia, J., Xu, C.Y. and Singh, V.P., 2010. Statistical downscaling of daily mean temperature, pan evaporation and precipitation for climate change scenarios in Haihe River, China. *Theoretical and Applied Climatology*, 99(1–2), pp.149-161.
- Cioffi, F. and Gallerano, F., 2012. Multi-objective analysis of dam release flows in rivers downstream from hydropower reservoirs. *Applied Mathematical Modelling*, 36(7), pp. 2868-2889.
- Coelho, G.B.A., Entradas Silva, H. and Henriques, F.M.A., 2020. Impact of climate change in cultural heritage: from energy consumption to artefacts' conservation and building rehabilitation. *Energy and Buildings*, 224, p.110250.
- Colette, A., Vautard, R. and Vrac, M., 2012. Regional climate downscaling with prior statistical correction of the global climate forcing. *Geophysical Research Letters*, 39(13), p.13707.
- Da Conceição Cunha, M. and Ribeiro, L., 2004. Tabu search algorithms for water network optimization. *European Journal of Operational Research*, 157(3), pp.746-758.
- Dai, A., Rasmussen, R.M., Ikeda, K. and Liu, C., 2020. A new approach to construct representative future forcing data for dynamic downscaling. *Climate Dynamics*, 55(1–2), pp.313-323.

- Danandeh Mehr, A., Nourani, V., Karimi Khosrowshahi, V. and Ghorbani, M.A., 2019. A hybrid support vector regression–firefly model for monthly rainfall forecasting. *International Journal of Environmental Science and Technology*, 16(1), pp.335-346.
- Daniell, T.M., 1991. Neural networks. Applications in hydrology and water resources engineering. In: *National Conference Publication - Institution of Engineers, Australia*.
- Deb, K., Pratap, A., Agarwal, S. and Meyarivan, T., 2002. A fast and elitist multiobjective genetic algorithm: NSGA-II. *IEEE Transactions on Evolutionary Computation*, 6(2), pp.182-197.
- Dehghani, M., Riahi-Madvar, H., Hooshyaripor, F., Mosavi, A., Shamshirband, S., Zavadskas, E.K. and Chau, K. wing, 2019. Prediction of hydropower generation using Grey wolf optimization adaptive neuro-fuzzy inference system. *Energies*, 12(2), pp.1–20.
- Demory, M.E., Berthou, S., Fernández, J., Sørland, S.L., Brogli, R., Roberts, M.J., Beyerle, U., Seddon, J., Haarsma, R., Schär, C., Buonomo, E., Christensen, O.B., Ciarlo, J.M., Fealy, R., Nikulin, G., Peano, D., Putrasahan, D., Roberts, C.D., Senan, R., Steger, C., Teichmann, C. and Vautard, R., 2020. European daily precipitation according to EURO-CORDEX regional climate models (RCMs) and high-resolution global climate models (GCMs) from the High-Resolution Model Intercomparison Project (HighResMIP). *Geoscientific Model Development*, 13(11), pp. 5485-5506.
- Derepasko, D., Guillaume, J.H.A., Horne, A.C. and Volk, M., 2021. Considering scale within optimization procedures for water management decisions: Balancing environmental flows and human needs. *Environmental Modelling and Software*, 139, p. 104991.
- Desiree, T., Cara, W. and Kellie, V., 2020. Reservoir Operational Performance Subject to Climate and Management Changes in the Willamette River Basin, Oregon. *Journal of Water Resources Planning and Management*, 146(10), p.5020021.
- Dias, V. de S., da Luz, M.P., Medero, G.M. and Nascimento, D.T.F., 2018. An overview of hydropower reservoirs in Brazil: Current situation, future

- perspectives and impacts of climate change. *Water (Switzerland)*, 10(5), p.592.
- Dobson, B., Wagener, T. and Pianosi, F., 2019. An argument-driven classification and comparison of reservoir operation optimization methods. *Advances in Water Resources*, 128, pp.74–86.
- Douglas, E.M., Vogel, R.M. and Kroll, C.N., 2002. Impact of Streamflow Persistence on Hydrologic Design. *Journal of Hydrologic Engineering*, 7(3), pp.220-227.
- Du, P., Xu, M. and Li, R., 2021. Impacts of climate change on water resources in the major countries along the Belt and Road. *PeerJ*, 9, p.12201.
- Durumin Iya, S., 2014. Floods In Malaysia Historical Reviews, Causes, Effects and Mitigations Approach. *International Journal of Interdisciplinary Research and Innovations*, 2, pp. 59-65.
- Ehteram, M., El-Shafie, A.H., Hin, L.S., Othman, F., Koting, S., Karami, H., Mousavi, S.F., Farzin, S., Ahmed, A.N., Zawawi, M.H.B., Hossain, M.S., Mohd, N.S., Afan, H.A. and El-Shafie, A., 2019. Toward bridging future irrigation deficits utilizing the shark algorithm integrated with a climate change model. *Applied Sciences (Switzerland)*, 9(19), p.3960.
- Ehteram, M., Karami, H., Mousavi, S.F., El-Shafie, A. and Amini, Z., 2017a. Optimizing dam and reservoirs operation based model utilizing shark algorithm approach. *Knowledge-Based Systems*, 122, pp.26–38.
- Ehteram, M., Mousavi, S.F., Karami, H., Farzin, S., Emami, M., Binti Othman, F., Amini, Z., Kisi, O. and El-Shafie, A., 2017b. Fast convergence optimization model for single and multi-purposes reservoirs using hybrid algorithm. *Advanced Engineering Informatics*, 32, pp.287-298.
- Elhoseiny, M., Huang, S. and Elgammal, A., 2015. Weather classification with deep convolutional neural networks. In: *Proceedings - International Conference on Image Processing, ICIP, Quebec City, QC, Canada*, pp. 3349-3353.
- El Ghamrawy, S.M. and Hassanien, A.E., 2020. Diagnosis and Prediction Model for COVID19 Patients Response to Treatment based on Convolutional Neural Networks and Whale Optimization Algorithm Using CT Images. *MedRxiv*.

- Emami, M., Nazif, S., Mousavi, S.F., Karami, H. and Daccache, A., 2021. A hybrid constrained coral reefs optimization algorithm with machine learning for optimizing multi-reservoir systems operation. *Journal of Environmental Management*, 286, p.112250.
- Fallah-Mehdipour, E., Bozorg-Haddad, O. and Loáiciga, H.A., 2020. Climate-environment-water: integrated and non-integrated approaches to reservoir operation. *Environmental Monitoring and Assessment*, 192(1), p.60.
- Faris, H., Aljarah, I., Mirjalili, S., Castillo, P.A. and Merelo, J.J., 2016. EvoloPy: An open-source nature-inspired optimization framework in python. In: *Proceedings of the 8th International Joint Conference on Computational Intelligence (IJCCI 2016)*, 1, pp. 171-177.
- Feng, Z. kai, Niu, W. jing and Cheng, C. tian, 2018a. Optimization of hydropower reservoirs operation balancing generation benefit and ecological requirement with parallel multi-objective genetic algorithm. *Energy*, 153, pp.706-718.
- Feng, Z. kai, Niu, W. jing and Cheng, C. tian, 2018b. Optimizing electrical power production of hydropower system by uniform progressive optimality algorithm based on two-stage search mechanism and uniform design. *Journal of Cleaner Production*, 190, pp. 432-442.
- Feng, Z. kai, Niu, W. jing, Zhang, R., Wang, S. and Cheng, C. tian, 2019. Operation rule derivation of hydropower reservoir by k-means clustering method and extreme learning machine based on particle swarm optimization. *Journal of Hydrology*, 576, pp.229–238.
- Feng, Z. kai, Liu, S., Niu, W. jing, Li, B. jian, Wang, W. chuan, Luo, B. and Miao, S. min, 2020a. A modified sine cosine algorithm for accurate global optimization of numerical functions and multiple hydropower reservoirs operation. *Knowledge-Based Systems*, 208, p.106461.
- Feng, Z. kai, Niu, W. jing, Cheng, X., Wang, J. yang, Wang, S. and Song, Z. guo, 2020b. An effective three-stage hybrid optimization method for source-network-load power generation of cascade hydropower reservoirs serving multiple interconnected power grids. *Journal of Cleaner Production*, 246, p.119035.

- Ferreiro-Ferreiro, A.M., García-Rodríguez, J.A., López-Salas, J.G., Escalante, C. and Castro, M.J., 2020. Global optimization for data assimilation in landslide tsunami models. *Journal of Computational Physics*, 403, p. 109069.
- Field, C.B., Barros, V.R., Dokken, D.J., Mach, K.J., Mastrandrea, M.D., Bilir, T.E., Chatterjee, M., Ebi, K.L., Estrada, Y.O., Genova, R.C., Girma, B., Kissel, E.S., Levy, A.N., MacCracken, S., Mastrandrea, P.R. and White, L.L., 2014. Climate change 2014 impacts, adaptation and vulnerability: Part A: Global and sectoral aspects: Working group II contribution to the fifth assessment report of the intergovernmental panel on climate change.
- Fowler, H.J., Blenkinsop, S. and Tebaldi, C., 2007. Linking climate change modelling to impacts studies: Recent advances in downscaling techniques for hydrological modelling. *International Journal of Climatology*, 27(12), pp. 1547-1578.
- Fu, X., Li, A., Wang, L. and Ji, C., 2011. Short-term scheduling of cascade reservoirs using an immune algorithm-based particle swarm optimization. *Computers and Mathematics with Applications*, 62(6), pp. 2463-2471.
- George H. Hargreaves and Zohrab A. Samani, 1985. Reference Crop Evapotranspiration from Temperature. *Applied Engineering in Agriculture*, 1(2).
- Glover, F. and Laguna, M., 2013. TABU SEARCH: Effective Strategies for Hard Problems in Analytics and Computational Science. *Handbook of Combinatorial Optimization*, XXI, pp. 3261-3362.
- Goh, E.H., Ng, J.L., Huang, Y.F. and Yong, S.L.S., 2021. Performance of potential evapotranspiration models in Peninsular Malaysia. *Journal of Water and Climate Change*, 12(7), pp. 3170-3186.
- Guo, D. and Wang, H., 2016. Comparison of a very-fine-resolution GCM with RCM dynamical downscaling in simulating climate in China. *Advances in Atmospheric Sciences*, 33(5), pp. 559-570.
- Haddad, O.B., Adams, B.J. and Mariño, M.A., 2008. Optimum rehabilitation strategy of water distribution systems using the HBMO algorithm. *Journal of Water Supply: Research and Technology - AQUA*, 57(5), pp. 337-350.

- Haddad, O.B., Moradi-Jalal, M. and Mariño, M.A., 2011. Design-operation optimisation of run-of-river power plants. *Proceedings of the Institution of Civil Engineers: Water Management*, 164(9), pp. 463-475.
- Hashimoto, T., Stedinger, J.R. and Loucks, D.P., 1982. Reliability, resiliency, and vulnerability criteria for water resource system performance evaluation. *Water Resources Research*, 18(1).
- Hazen, A., 1914. Storage to be Provided in Impounding Municipal Water Supply. *Transactions of the American Society of Civil Engineers*, 77(1).
- He, Y., Xu, Q., Yang, S. and Liao, L., 2014. Reservoir flood control operation based on chaotic particle swarm optimization algorithm. *Applied Mathematical Modelling*, 38(17-18), pp. 448-4492.
- Heidari-Rarani, M., Ezati, N., Sadeghi, P. and Badrossamay, M.R., 2020. Optimization of FDM process parameters for tensile properties of polylactic acid specimens using Taguchi design of experiment method. *Journal of Thermoplastic Composite Materials*, 35(12), pp. 2435-2452.
- Heidari, A.A., Mirjalili, S., Faris, H., Aljarah, I., Mafarja, M. and Chen, H., 2019. Harris hawks optimization: Algorithm and applications. *Future Generation Computer Systems*, 97, pp.849–872.
- Holland, D.E., Olesen, R.J. and Bevins, J.E., 2021. Multi-objective genetic algorithm optimization of a directionally sensitive radiation detection system using a surrogate transport model. *Engineering Applications of Artificial Intelligence*, 104, p. 104357.
- Holland, G.J., Done, J., Bruyere, C., Cooper, C. and Suzuki-Parker, A., 2010. Model investigations of the effects of climate variability and change on future gulf of Mexico tropical cyclone activity. In: *Proceedings of the Annual Offshore Technology Conference*, 2, p. 20690.
- Holland, J.H., 1992. Genetic algorithms. *Scientific American*.
- Hossain, M.S., 2013. Adopting Artificial Intelligences In Optimizing Reservoir Operation Policy. PhD. Universiti Kebangsaan Malaysia.
- Hossain, M.S. and El-Shafie, A., 2014a. Evolutionary techniques versus swarm intelligences: Application in reservoir release optimization. *Neural Computing and Applications*, 24(7–8), pp.1583–1594.
- Hossain, M.S. and El-shafie, A., 2014b. Performance analysis of artificial bee

- colony (ABC) algorithm in optimizing release policy of Aswan High Dam. *Neural Computing and Applications*, 24(5), pp.1199–1206.
- Hossain, M.S., Mohd Sidek, L.B., Marufuzzaman, M. and Zawawi, M.H., 2018. Passive congregation theory for particle swarm optimization (PSO): An application in reservoir system operation. *International Journal of Engineering and Technology(UAE)*, 7(4), pp.383–387.
- Houck, M.H., Cohon, J.L. and ReVelle, C.S., 1980. Linear decision rule in reservoir design and management: 6. Incorporation of economic efficiency benefits and hydroelectric energy generation. *Water Resources Research*, 16(1), pp. 196-200.
- Houssein, E.H., Saad, M.R., Hashim, F.A., Shaban, H. and Hassaballah, M., 2020. Lévy flight distribution: A new metaheuristic algorithm for solving engineering optimization problems. *Engineering Applications of Artificial Intelligence*, 94, p. 103731.
- Huang, Z., Hejazi, M., Li, X., Tang, Q., Vernon, C., Leng, G., Liu, Y., Döll, P., Eisner, S., Gerten, D., Hanasaki, N. and Wada, Y., 2018. Reconstruction of global gridded monthly sectoral water withdrawals for 1971-2010 and analysis of their spatiotemporal patterns. *Hydrology and Earth System Sciences*, 22(4), pp. 2117-2133.
- Huangpeng, Q., Huang, W. and Gholinia, F., 2021. Forecast of the hydropower generation under influence of climate change based on RCPs and Developed Crow Search Optimization Algorithm. *Energy Reports*, 7, pp. 385-397.
- Hui, R., Lund, J., Zhao, J. and Zhao, T., 2016. Optimal Pre-storm Flood Hedging Releases for a Single Reservoir. *Water Resources Management*, 30(14), pp. 5113-5129.
- Hussain, M., Yusof, K.W., Mustafa, M.R.U., Mahmood, R. and Jia, S., 2018. Evaluation of CMIP5 models for projection of future precipitation change in Bornean tropical rainforests. *Theoretical and Applied Climatology*, 134, pp. 1–2.
- Hwang, S.H., Kim, K.B. and Han, D., 2020. Comparison of methods to estimate areal means of short duration rainfalls in small catchments, using rain gauge and radar data. *Journal of Hydrology*, 588, p.125084.

- Ibrahim, K.S.M.H., Huang, Y.F., Ahmed, A.N., Koo, C.H. and El-Shafie, A., 2021. A review of the hybrid artificial intelligence and optimization modelling of hydrological streamflow forecasting. *Alexandria Engineering Journal*, 61(1), pp. 279-303.
- Islam, M.Z., Wahab, N.I.A., Veerasamy, V., Hizam, H., Mailah, N.F., Guerrero, J.M. and Mohd Nasir, M.N., 2020. A Harris Hawks optimization based singleand multi-objective optimal power flow considering environmental emission. *Sustainability (Switzerland)*, 12(13), p. 5248.
- Jahandideh-Tehrani, M., Bozorg Haddad, O. and Loáiciga, H.A., 2014. Hydropower Reservoir Management Under Climate Change: The Karoon Reservoir System. *Water Resources Management*, 29(3), pp.749–770.
- Jaiswal, R.K., Lohani, A.K. and Tiwari, H.L., 2021. A decision support system framework for strategic water resources planning and management under projected climate scenarios for a reservoir complex. *Journal of Hydrology*, 603(c), p. 127051.
- Jakob Themeßl, M., Gobiet, A. and Leuprecht, A., 2011. Empirical-statistical downscaling and error correction of daily precipitation from regional climate models. *International Journal of Climatology*, 31(10), pp. 1530-1544.
- Jensen, M.E. and Allen, R.G., 2016. Evaporation, evapotranspiration, and irrigation water requirements.
- Jensen, M.E., Burmann, R.D. and Allen, R.G., 1990. Evaporation and irrigation water requirements. *ASCE manual and reports on engineering practice*, p.360.
- Jourdain, N.C., Gupta, A. Sen, Taschetto, A.S., Ummenhofer, C.C., Moise, A.F. and Ashok, K., 2013. The Indo-Australian monsoon and its relationship to ENSO and IOD in reanalysis data and the CMIP3/CMIP5 simulations. *Climate Dynamics*, 41, pp. 11–12.
- Kamaruzaman, A.F., Zain, A.M., Yusuf, S.M. and Udin, A., 2013. Levy flight algorithm for optimization problems - A literature review. In: *Applied Mechanics and Materials*, 421, pp. 496-501.
- Kang, M. and Park, S., 2014. Modeling water flows in a serial irrigation reservoir

- system considering irrigation return flows and reservoir operations. *Agricultural Water Management*, 143, pp. 131-141.
- Katellaris, C.H., 2021. Climate Change and Extreme Weather Events in Australia: Impact on Allergic Diseases. *Immunology and Allergy Clinics of North America*, 41(1), pp. 53-62.
- Kelidari, M. and Hamidzadeh, J., 2020. Feature selection by using chaotic cuckoo optimization algorithm with levy flight, opposition-based learning and disruption operator. *Soft Computing*, 25, pp. 2911-2933.
- Kevin E . Lansey, Larry W. Mays, 1989. Optimization Model for Water Distribution System Design. *Journal of Hydraulic Engineering*, 115(10), pp. 1401-1418.
- Khan, T.A. and Ling, S.H., 2021. A novel hybrid gravitational search particle swarm optimization algorithm. *Engineering Applications of Artificial Intelligence*, 102, p. 104263.
- Kharrufa, N.S. 1985. Simplified equation for evapotranspiration in arid regions. *Beiträge zur Hydrologie. Sonderheft*, 5(1), pp. 39–47.
- Khurma, R.A., Aljarah, I., Sharieh, A. and Mirjalili, S., 2020. EvoloPy-FS: An Open-Source Nature-Inspired Optimization Framework in Python for Feature Selection, *Evolutionary Machine Learning Techniques*, pp. 131-173.
- Kisi, O. and Heddam, S., 2019. Evaporation modelling by heuristic regression approaches using only temperature data. *Hydrological Sciences Journal*, 64(6), pp. 653-672.
- Kurek, W. and Ostfeld, A., 2013. Multi-objective optimization of water quality, pumps operation, and storage sizing of water distribution systems. *Journal of Environmental Management*, 115, pp. 189-197.
- Labadie, J.W., 2004. Optimal Operation of Multireservoir Systems: State-of-the-Art Review. *Journal of Water Resources Planning and Management*, 130(2), pp. 89-183.
- Lai, V., Huang, Y.F., Koo, C.H., Ahmed, A.N. and El-Shafie, A., 2021. Optimization of reservoir operation at Klang Gate Dam utilizing a whale optimization algorithm and a Lévy flight and distribution enhancement technique. *Engineering Applications of Computational Fluid Mechanics*,

15(1), pp.1682–1702.

- Lang, D., Zheng, J., Shi, J., Liao, F., Ma, X., Wang, W., Chen, X. and Zhang, M., 2017. A comparative study of potential evapotranspiration estimation by eight methods with FAO Penman–Monteith method in southwestern China. *Water (Switzerland)*, 9(10), p. 734.
- Latif, S.D., Ahmed, A.N., Sherif, M., Sefelnasr, A., and El-Shafie, A., 2020. Reservoir water balance simulation model utilizing machine learning algorithm. *Alexandria Engineering Journal*, 60(1), pp.1365-1378.
- Latif, S.D., Marhain, S., Hossain, M.S., Ahmed, A.N., Sherif, M., Sefelnasr, A. and El-shafie, A., 2021. Optimizing the operation release policy using charged system search algorithm: A Case Study of Klang Gates Dam, Malaysia. *Sustainability (Switzerland)*, 13(11), p. 5900.
- Lee, I.M., Maass, A., Hufschmidt, M.M., Dorfman, R., Thomas, H.A., Marglin, S.A. and Fair, G.M., 1963. Design of Water-Resource Systems. *Journal of Farm Economics*, 45(2).
- Li, D., Yin, B., Feng, J., Dosio, A., Geyer, B., Qi, J.F., Shi, H. and Xu, Z., 2018. Present climate evaluation and added value analysis of dynamically downscaled simulations of CORDEX-East Asia. *Journal of Applied Meteorology and Climatology*, 57(10), pp. 2317-2341.
- Li, F.F. and Qiu, J., 2016. Multi-objective optimization for integrated hydro-photovoltaic power system. *Applied Energy*, 167, pp. 377-384.
- Li, X. and Babovic, V., 2019a. A new scheme for multivariate, multisite weather generator with inter-variable, inter-site dependence and inter-annual variability based on empirical copula approach. *Climate Dynamics*, 52(3–4), pp. 2247-2267.
- Li, X. and Babovic, V., 2019b. Multi-site multivariate downscaling of global climate model outputs: an integrated framework combining quantile mapping, stochastic weather generator and Empirical Copula approaches. *Climate Dynamics*, 52(9–10), pp. 5775-5799.
- Li, X., Liu, P., Gui, Z., Ming, B., Yang, Z., Xie, K. and Zhang, X., 2020. Reducing lake water-level decline by optimizing reservoir operating rule curves: A case study of the Three Gorges Reservoir and the Dongting Lake. *Journal of Cleaner Production*, 264, p. 121676.

- Li, Y., Li, N., Gong, G. and Yan, J., 2021. A novel design of experiment algorithm using improved evolutionary multi-objective optimization strategy. *Engineering Applications of Artificial Intelligence*, 102, p. 104283.
- Li, Z., Shi, X. and Li, J., 2017. Multisite and multivariate GCM downscaling using a distribution-free shuffle procedure for correlation reconstruction. *Climate Research*, 72(2), pp. 141-151.
- Liang, X.Z., Sun, C., Zheng, X., Dai, Y., Xu, M., Choi, H.I., Ling, T., Qiao, F., Kong, X., Bi, X., Song, L. and Wang, F., 2019. CWRP performance at downscaling China climate characteristics. *Climate Dynamics*, 52(3–4), pp. 2159-2184.
- Liao, H. Te, Shie, J.R. and Yang, Y.K., 2008. Applications of Taguchi and design of experiments methods in optimization of chemical mechanical polishing process parameters. *International Journal of Advanced Manufacturing Technology*, 38(7–8), pp. 674-682.
- Liu, D., Huang, Q., Yang, Y., Liu, D. and Wei, X., 2020a. Bi-objective algorithm based on NSGA-II framework to optimize reservoirs operation. *Journal of Hydrology*, 585, p.124830.
- Liu, J., Li, D., Wu, Y. and Liu, D., 2020b. Lion swarm optimization algorithm for comparative study with application to optimal dispatch of cascade hydropower stations. *Applied Soft Computing Journal*, 87, p. 105974.
- Liu, J., Zhang, Q., Zhang, Y., Chen, X., Li, J. and Aryal, S.K., 2017. Deducing Climatic Elasticity to Assess Projected Climate Change Impacts on Streamflow Change across China. *Journal of Geophysical Research: Atmospheres*, 122(19), pp. 10.228-10.245.
- Liu, P., Li, L., Chen, G. and Rheinheimer, D.E., 2014. Parameter uncertainty analysis of reservoir operating rules based on implicit stochastic optimization. *Journal of Hydrology*, 514, pp. 102-113.
- Liu, P., Li, L., Guo, S., Xiong, L., Zhang, W., Zhang, J. and Xu, C.Y., 2015. Optimal design of seasonal flood limited water levels and its application for the Three Gorges Reservoir. *Journal of Hydrology*, 527, pp. 1045-1053.
- Liu, X. and Luo, J., 2019. A dynamic multi-objective optimization model with

- interactivity and uncertainty for real-time reservoir flood control operation. *Applied Mathematical Modelling*, 74, pp.606–620.
- Loucks, D.P., 1969. Erratum for “Computer Models for Reservoir Regulation”. *Journal of the Sanitary Engineering Division*, 95(4).
- Loucks, D.P. and Van Beek, E., 2017. Water resource systems planning and management: An introduction to methods, models, and applications.
- Loucks, D.P. and Sigvaldason, O.T., 1982. Multiple- reservoir operation in North America. *International Institute for Applied Systems Analysis, Collaborative Publication*, (CP-82-S3).
- Lu, C., Lin, D., Jia, J. and Tang, C.K., 2017. Two-Class Weather Classification. *IEEE Transactions on Pattern Analysis and Machine Intelligence*, 39(12), pp. 2510-2524.
- Lu, Q., Zhong, P. an, Xu, B., Zhu, F., Huang, X., Wang, H. and Ma, Y., 2021. Stochastic programming for floodwater utilization of a complex multi-reservoir system considering risk constraints. *Journal of Hydrology*, 599, p. 126388.
- Lund, J.R. and Guzman, J., 1999. Derived Operating Rules for Reservoirs in Series or in Parallel. *Journal of Water Resources Planning and Management*, 125(3), pp. 143-153.
- Luo, J., Qi, Y., Xie, J. and Zhang, X., 2015. A hybrid multi-objective PSO-EDA algorithm for reservoir flood control operation. *Applied Soft Computing Journal*, 34, pp.526–538.
- Macêdo, J.E.S. de, De Azevedo, J.R.G. and de Marques Bezerra, S.T., 2021. Hybrid particle swarm optimization and tabu search for the design of large-scale water distribution networks. *Revista Brasileira de Recursos Hidricos*, 26, p.e11.
- Makkink, G.F., 1957. Testing the Penman formula by means of lysimeters. *Journal of the Institution of Water Engineers.*, 11, pp. 277-288.
- Mandal, S., Arunkumar, R., Breach, P.A. and Simonovic, S.P., 2019. Reservoir Operations under Changing Climate Conditions: Hydropower-Production Perspective. *Journal of Water Resources Planning and Management*, 145(5), p. 04019016.
- Manzanas, R., Fiwa, L., Vanya, C., Kanamaru, H. and Gutiérrez, J.M., 2020.

- Statistical downscaling or bias adjustment? A case study involving implausible climate change projections of precipitation in Malawi. *Climatic Change*, 162, pp. 1437-1453.
- Marotzke, J., Jakob, C., Bony, S., Dirmeyer, P.A., O’Gorman, P.A., Hawkins, E., Perkins-Kirkpatrick, S., Quéré, C. Le, Nowicki, S., Paulavets, K., Seneviratne, S.I., Stevens, B. and Tuma, M., 2017. Climate research must sharpen its view. *Nature Climate Change*, 7, pp. 89-91.
- Mayowa, O.O., Pour, S.H., Shahid, S., Mohsenipour, M., Harun, S. Bin, Heryansyah, A. and Ismail, T., 2015. Trends in rainfall and rainfall-related extremes in the east coast of peninsular Malaysia. *Journal of Earth System Science*, 124(8), pp. 1609-1622.
- Meinshausen, M., Smith, S.J., Calvin, K., Daniel, J.S., Kainuma, M.L.T., Lamarque, J., Matsumoto, K., Montzka, S.A., Raper, S.C.B., Riahi, K., Thomson, A., Velders, G.J.M. and van Vuuren, D.P.P., 2011. The RCP greenhouse gas concentrations and their extensions from 1765 to 2300. *Climatic Change*, 109(1), p. 213.
- Meng, X., Chang, J., Wang, X. and Wang, Y., 2019. Multi-objective hydropower station operation using an improved cuckoo search algorithm. *Energy*, 168, pp.425–439.
- Meyer, J.D.D. and Jin, J., 2016. Bias correction of the CCSM4 for improved regional climate modeling of the North American monsoon. *Climate Dynamics*, 46(9–10), pp. 2961-2976.
- Middelkoop, H., Daamen, K., Gellens, D., Grabs, W., Kwadijk, J.C.J., Lang, H., Parmet, B.W.A.H., Schädler, B., Schulla, J. and Wilke, K., 2001. Impact of climate change on hydrological regimes and water resources management in the Rhine basin. *Climatic Change*, 49(1–2), pp. 105-128.
- Ming, B., Liu, P., Bai, T., Tang, R. and Feng, M., 2017. Improving Optimization Efficiency for Reservoir Operation Using a Search Space Reduction Method. *Water Resources Management*, 31(4), pp. 1173-1190.
- Mirjalili, S., 2015. Moth-flame optimization algorithm: A novel nature-inspired heuristic paradigm. *Knowledge-Based Systems*, 89, pp. 228-249.
- Mirjalili, S. and Lewis, A., 2016. The Whale Optimization Algorithm. *Advances in Engineering Software*, 95, pp. 51-67.

- Moazenzadeh, R., Mohammadi, B., Shamsirband, S. and Chau, K.W., 2018. Coupling a firefly algorithm with support vector regression to predict evaporation in northern iran. *Engineering Applications of Computational Fluid Mechanics*, 12(1), pp. 584-597.
- Moeini, R. and Babaei, M., 2020. Hybrid SVM-CIPSO methods for optimal operation of reservoir considering unknown future condition. *Applied Soft Computing Journal*, 95, p. 106572.
- Moeini, R., Soltani-nezhad, M. and Daei, M., 2017. Constrained gravitational search algorithm for large scale reservoir operation optimization problem. *Engineering Applications of Artificial Intelligence*, 62, pp. 222-233.
- Mohamad, N.D., Hanan, Z., Izzati, N. and Kamal, A., 2020. Water Demand Estimation Based On Land Use In Urban City. *International Journal of Scientific & Technology Research*, 9(6), pp. 545-550.
- Moise, A., Wilson, L., Grose, M., Whetton, P., Watterson, I., Bhend, J., Bathols, J., Hanson, L., Erwin, T., Bedin, T., Heady, C. and Rafter, T., 2015. Evaluation of CMIP3 and CMIP5 Models over the Australian Region to Inform Confidence in Projections. *Australian Meteorological and Oceanographic Journal*, 65(1), pp. 19-53.
- Muhammad, M.K.I., Nashwan, M.S., Shahid, S., Ismail, T. bin, Song, Y.H. and Chung, E.S., 2019. Evaluation of empirical reference evapotranspiration models using compromise programming: A case study of Peninsular Malaysia. *Sustainability (Switzerland)*, 11(16), p. 4267.
- Muhammad, M.K.I., Shahid, S., Ismail, T., Harun, S., Kisi, O. and Yaseen, Z.M., 2021. The development of evolutionary computing model for simulating reference evapotranspiration over Peninsular Malaysia. *Theoretical and Applied Climatology*, 144(3-4), pp. 1419-1434.
- Muniandy, J.M., Yusop, Z. and Askari, M., 2016. Evaluation of reference evapotranspiration models and determination of crop coefficient for *Momordica charantia* and *Capsicum annum*. *Agricultural Water Management*, 169, pp. 77-89.
- Myers, T.A., 2011. Goodbye, Listwise Deletion: Presenting Hot Deck Imputation as an Easy and Effective Tool for Handling Missing Data. *Communication Methods and Measures*, 5(4), pp. 297-310.

- Näschen, K., Diekkrüger, B., Evers, M., Höllermann, B., Steinbach, S. and Thonfeld, F., 2019. The Impact of Land Use/Land Cover Change (LULCC) on Water Resources in a Tropical Catchment in Tanzania under Different Climate Change Scenarios. *Sustainability (Switzerland)*, 11(24), p. 7083.
- Nguyen-Thuy, H., Ngo-Duc, T., Trinh-Tuan, L., Tangang, F., Cruz, F., Phan-Van, T., Juneng, L., Narisma, G. and Santisirisomboon, J., 2021. Time of emergence of climate signals over Vietnam detected from the CORDEX-SEA experiments. *International Journal of Climatology*, 41(3), pp. 1599-1618.
- Ning, L. and Bradley, R.S., 2016. NAO and PNA influences on winter temperature and precipitation over the eastern United States in CMIP5 GCMs. *Climate Dynamics*, 46(3–4), pp. 1257-1276.
- Niu, W., Feng, Z., Cheng, C. and Zhou, J., 2018a. Forecasting Daily Runoff by Extreme Learning Machine Based on Quantum-Behaved Particle Swarm Optimization. *Journal of Hydrologic Engineering*, 23(3), p. 04018002.
- Niu, W. jing, Feng, Z. kai, Cheng, C. tian and Wu, X. yu, 2018b. A parallel multi-objective particle swarm optimization for cascade hydropower reservoir operation in southwest China. *Applied Soft Computing Journal*, 70, pp. 562-575.
- Niu, W. jing, Feng, Z. kai and Liu, S., 2021. Multi-strategy gravitational search algorithm for constrained global optimization in coordinative operation of multiple hydropower reservoirs and solar photovoltaic power plants. *Applied Soft Computing*, 107, p. 107315.
- Nourani, V., Baghanam, A.H., Adamowski, J. and Gebremichael, M., 2013. Using self-organizing maps and wavelet transforms for space-time pre-processing of satellite precipitation and runoff data in neural network based rainfall-runoff modeling. *Journal of Hydrology*, 476, pp. 228-243.
- Nourani, V., Hosseini Baghanam, A., Adamowski, J. and Kisi, O., 2014. Applications of hybrid wavelet-Artificial Intelligence models in hydrology: A review. *Journal of Hydrology*, 514, pp. 358-377.
- Nourani, V., Rouzegari, N., Molajou, A. and Hosseini Baghanam, A., 2020. An integrated simulation-optimization framework to optimize the reservoir

- operation adapted to climate change scenarios. *Journal of Hydrology*, 587, p. 125018.
- Olofintoye, O., Otieno, F. and Adeyemo, J., 2016. Real-time optimal water allocation for daily hydropower generation from the Vanderkloof dam, South Africa. *Applied Soft Computing Journal*, 47, pp. 119-129.
- Pang, R., Xu, B., Kong, X. and Zou, D., 2018. Seismic fragility for high CFRDs based on deformation and damage index through incremental dynamic analysis. *Soil Dynamics and Earthquake Engineering*, 104, pp. 432-436.
- Payus, C., Huey, L.A., Adnan, F., Rimba, A.B., Mohan, G., Chapagain, S.K., Roder, G., Gasparatos, A. and Fukushi, K., 2020. Impact of extreme drought climate on water security in North Borneo: Case study of Sabah. *Water (Switzerland)*, 12(4), pp.1–19.
- Peel, M.C. and McMahon, T.A., 2020. Historical development of rainfall-runoff modeling. *Wiley Interdisciplinary Reviews: Water*, 7(5), p. e1471.
- Pokhrel, Y., Burbano, M., Roush, J., Kang, H., Sridhar, V. and Hyndman, D.W., 2018. A review of the integrated effects of changing climate, land use, and dams on Mekong river hydrology. *Water (Switzerland)*, 10(3), p. 266.
- Poonia, V. and Tiwari, H.L., 2020. Rainfall-runoff modeling for the Hoshangabad Basin of Narmada River using artificial neural network. *Arabian Journal of Geosciences*, 13(18), p. 944.
- Priestley, C.H.B. and Taylor, R.J., 1972. On the Assessment of Surface Heat Flux and Evaporation Using Large-Scale Parameters. *Monthly Weather Review*, 100(2), pp. 81-92.
- Qaddoura, R., Faris, H., Aljarah, I. and Castillo, P.A., 2020. EvoCluster: An Open-Source Nature-Inspired Optimization Clustering Framework in Python. In: *Applications of Evolutionary Computation. EvoApplications 2020. Lecture Notes in Computer Science*, 12104, pp. 20-36.
- Rana, G. and Katerji, N., 2000. Measurement and estimation of actual evapotranspiration in the field under Mediterranean climate: A review. In: *European Journal of Agronomy*, 13(2-3), pp. 125-153.
- Rao, S.S., 2019. Engineering optimization: Theory and practice. *John Wiley & Sons, Inc.*
- Ren, K., Huang, S., Huang, Q., Wang, H., Leng, G., Cheng, L., Fang, W. and Li,

- P., 2019. A nature-based reservoir optimization model for resolving the conflict in human water demand and riverine ecosystem protection. *Journal of Cleaner Production*, 231, pp. 406-418.
- Rippl, W., 1883. The Capacity Of Storage-Reservoirs For Water-Supply. (Including Plate). *Minutes of the Proceedings of the Institution of Civil Engineers*, 71(1883), pp. 270-278.
- Rocheta, E., Evans, J.P. and Sharma, A., 2017. Can Bias correction of regional climate model lateral boundary conditions improve low-frequency rainfall variability? *Journal of Climate*, 30(24), pp. 9785-9806.
- Rogelj, J., Meinshausen, M. and Knutti, R., 2012. Global warming under old and new scenarios using IPCC climate sensitivity range estimates. *Nature Climate Change*, 2(4), pp. 248-253.
- Rowell, D.P., 2006. A demonstration of the uncertainty in projections of UK climate change resulting from regional model formulation. *Climatic Change*, 79(3-4), pp. 243-257.
- Roy, R.K., 2010. A primer on the Taguchi method. *Society of Manufacturing Engineers*.
- Sachindra, D.A., Ahmed, K., Rashid, M.M., Shahid, S. and Perera, B.J.C., 2018b. Statistical downscaling of precipitation using machine learning techniques. *Atmospheric Research*, 212, pp. 240-258.
- Sachindra, D.A., Ahmed, K., Shahid, S. and Perera, B.J.C., 2018a. Cautionary note on the use of genetic programming in statistical downscaling. *International Journal of Climatology*, 38(8), pp. 3449-3465.
- Sachindra, D.A., Huang, F., Barton, A. and Perera, B.J.C., 2013. Least square support vector and multi-linear regression for statistically downscaling general circulation model outputs to catchment streamflows. *International Journal of Climatology*, 33(5), pp. 1087-1106.
- Sachindra, D.A., Huang, F., Barton, A. and Perera, B.J.C., 2014. Statistical downscaling of general circulation model outputs to precipitation-part 1: calibration and validation. *International Journal of Climatology*, 34(11), pp. 3264-3281.
- Safari, M.J.S., Rahimzadeh Arashloo, S. and Danandeh Mehr, A., 2020. Rainfall-runoff modeling through regression in the reproducing kernel

- Hilbert space algorithm. *Journal of Hydrology*, 587, p. 125014.
- Sample, J.E., Duncan, N., Ferguson, M. and Cooksley, S., 2015. Scotland's hydropower: Current capacity, future potential and the possible impacts of climate change. *Renewable and Sustainable Energy Reviews*, 52, pp. 111-122.
- Schafer, J.L., 1997. Analysis of Incomplete Multivariate Data. *Chapman and Hall/CRC*.
- Schoof, J.T., 2013. Statistical downscaling in climatology. *Geography Compass*, 7(4), pp. 249-265.
- Sedki, A. and Ouazar, D., 2012. Hybrid particle swarm optimization and differential evolution for optimal design of water distribution systems. *Advanced Engineering Informatics*, 26(3), pp. 582-591.
- Semenov, M.A. and Barrow, E.M., 1997. Use of a stochastic weather generator in the development of climate change scenarios. *Climatic Change*, 35(4), pp. 397-414.
- Shahid, S., 2011. Impact of climate change on irrigation water demand of dry season Boro rice in northwest Bangladesh. *Climatic Change*, 105(3-4), pp. 433-453.
- Shiri, J., 2017. Evaluation of FAO56-PM, empirical, semi-empirical and gene expression programming approaches for estimating daily reference evapotranspiration in hyper-arid regions of Iran. *Agricultural Water Management*, 188, pp. 101-114.
- Shukla, R., Khare, D. and Deo, R., 2016. Statistical downscaling of climate change scenarios of rainfall and temperature over Indira Sagar canal command area in Madhya Pradesh, India. In: *Proceedings - 2015 IEEE 14th International Conference on Machine Learning and Applications, ICMLA 2015*, pp. 313-317.
- Smith, A.E. and Coit, D.W., 1997. Constraint handling techniques: penalty functions. In: *Handbook of Evolutionary Computation*.
- Solomon, S., D., Qin, M., Manning, Z., Chen, M., Marquis, K.B., Averyt, M.T., Miller HL, Solomon, S., Qin, D., Manning, M., Chen, Z., Marquis, M., Averyt, K.B., Tignor, M. and Miller, H.L., 2007. Summary for Policymakers. In: *Climate Change 2007: The Physical Science Basis*.

Contribution of Working Group I to the Fourth Assessment Report of the Intergovernmental Panel on Climate Change. *D Qin M Manning Z Chen M Marquis K Averyt M Tignor and HL Miller New York Cambridge University Press pp*, Geneva.

- Sperber, K.R., Annamalai, H., Kang, I.S., Kitoh, A., Moise, A., Turner, A., Wang, B. and Zhou, T., 2013. The Asian summer monsoon: An intercomparison of CMIP5 vs. CMIP3 simulations of the late 20th century. *Climate Dynamics*, 41(9–10), pp. 2711-2744.
- Srivastav, R.K., Srinivasan, K. and Sudheer, K.P., 2011. Simulation-optimization framework for multi-season hybrid stochastic models. *Journal of Hydrology*, 404(3–4), pp. 209-225.
- Stocker, T.F., Qin, D., Plattner, G.-K., Tignor, M., Allen, S.K., Boschung, J., Nauels, A., Xia, Y., Bex, V. and Midgley, P.M., 2013. IPCC, 2013: Climate Change 2013: The Physical Science Basis. Contribution of Working Group I to the Fifth Assessment Report of the Intergovernmental Panel on Climate Change. *IPCC, AR5*.
- Stuhlmacher, A. and Mathieu, J.L., 2020a. Chance-Constrained Water Pumping to Manage Water and Power Demand Uncertainty in Distribution Networks. *Proceedings of the IEEE*, 108(9), pp. 1640-1655.
- Stuhlmacher, A. and Mathieu, J.L., 2020b. Water distribution networks as flexible loads: A chance-constrained programming approach. *Electric Power Systems Research*, 188, p. 106570.
- Sui, X., Wu, S.N., Liao, W.G., Jia, L., Jin, T.T. and Zhang, X., 2013. Optimized operation of cascade reservoirs on Wujiang River during 2009-2010 drought in southwest China. *Water Science and Engineering*, 6(3), pp. 308-316.
- Sun, J., Lei, X., Tian, Y., Liao, W. and Wang, Y., 2013. Hydrological impacts of climate change in the upper reaches of the Yangtze River Basin. *Quaternary International*, 304, pp. 62-74.
- Sunil, A., Deepthi, B., Mirajkar, A.B. and Adarsh, S., 2021. Modeling future irrigation water demands in the context of climate change: a case study of Jayakwadi command area, India. *Modeling Earth Systems and Environment*, 7(3), pp. 1963-1977.

- Tan, M.L., Ficklin, D.L., Ibrahim, A.L. and Yusop, Z., 2014. Impacts and uncertainties of climate change on streamflow of the johor River Basin, Malaysia using a cmip5 general circulation model ensemble. *Journal of Water and Climate Change*, 5(4), pp. 676-695.
- Tan, M.L., Ibrahim, A.L., Yusop, Z., Chua, V.P. and Chan, N.W., 2017. Climate change impacts under CMIP5 RCP scenarios on water resources of the Kelantan River Basin, Malaysia. *Atmospheric Research*, 189, pp. 1-10.
- Tanco, M., Viles, E. and Pozueta, L., 2009. Comparing different approaches for design of experiments (DoE). In: *Lecture Notes in Electrical Engineering*, 39, pp. 611-621.
- Tangang, F., Chung, J.X., Juneng, L., Supari, Salimun, E., Ngai, S.T., Jamaluddin, A.F., Mohd, M.S.F., Cruz, F., Narisma, G., Santisirisomboon, J., Ngo-Duc, T., Van Tan, P., Singhruck, P., Gunawan, D., Aldrian, E., Sopaheluwakan, A., Grigory, N., Remedio, A.R.C., Sein, D. V., Hein-Griggs, D., McGregor, J.L., Yang, H., Sasaki, H. and Kumar, P., 2020. Projected future changes in rainfall in Southeast Asia based on CORDEX–SEA multi-model simulations. *Climate Dynamics*, 55(5–6), pp. 1247-1267.
- Tao, H., Diop, L., Bodian, A., Djaman, K., Ndiaye, P.M. and Yaseen, Z.M., 2018. Reference evapotranspiration prediction using hybridized fuzzy model with firefly algorithm: Regional case study in Burkina Faso. *Agricultural Water Management*, 208, pp. 140-151.
- Taylor, K.E., Stouffer, R.J. and Meehl, G. a, 2012. An Overview of the CMIP5 Experiment Design. *Bulletin of the American Meteorological Society*, 93, pp. 485-498.
- Tegegne, G. and Kim, Y.O., 2020. Representing inflow uncertainty for the development of monthly reservoir operations using genetic algorithms. *Journal of Hydrology*, 586, p. 124876.
- Terzi, V.G. and Manolis, G.D., 2020. Model reduction for structural health monitoring accounting for soil-structure-interaction. *Structure and Infrastructure Engineering*, 17(6), pp. 779-791.
- Teutschbein, C. and Seibert, J., 2010. Regional climate models for hydrological impact studies at the catchment scale: A review of recent modeling

- strategies. *Geography Compass*, 4(7), pp. 834-860.
- Thomas, T., Ghosh, N.C. and Sudheer, K.P., 2021. Optimal reservoir operation – A climate change adaptation strategy for Narmada basin in central India. *Journal of Hydrology*, 598, p. 126238.
- Thongwan, T., Kangrang, A. and Prasanchum, H., 2019. Multi-objective future rule curves using conditional tabu search algorithm and conditional genetic algorithm for reservoir operation. *Heliyon*, 5(9), p. e02401.
- Thorntwaite, C.W., 1948. An Approach toward a Rational Classification of Climate. *Geographical Review*, 38(1), pp.55–94.
- Tikhamarine, Y., Souag-Gamane, D., Ahmed, A.N., Sammen, S.S., Kisi, O., Huang, Y.F. and El-Shafie, A., 2020. Rainfall-runoff modelling using improved machine learning methods: Harris hawks optimizer vs. particle swarm optimization. *Journal of Hydrology*, 589, p. 125133.
- Tinoco, V., Willems, P., Wyseure, G. and Cisneros, F., 2016. Evaluation of reservoir operation strategies for irrigation in the Macul Basin, Ecuador. *Journal of Hydrology: Regional Studies*, 5, pp. 213-225.
- Trisurat, Y., Shirakawa, H. and Johnston, J.M., 2019. Land-use/land-cover change from socio-economic drivers and their impact on biodiversity in Nan Province, Thailand. *Sustainability (Switzerland)*, 11(3), p. 649.
- Tukimat, N.N.A., Harun, S. and Shahid, S., 2012. Comparison of different methods in estimating potential évapotranspiration at Muda Irrigation Scheme of Malaysia. *Journal of Agriculture and Rural Development in the Tropics and Subtropics*, 113(1), pp. 77-85.
- Turgut, M.S., Turgut, O.E., Afan, H.A. and El-Shafie, A., 2019. A novel Master–Slave optimization algorithm for generating an optimal release policy in case of reservoir operation. *Journal of Hydrology*, 577, p. 123959.
- Valiantzas, J.D., 2018. Temperature-and humidity-based simplified Penman’s ET0 formulae. Comparisons with temperature-based Hargreaves-Samani and other methodologies. *Agricultural Water Management*, 208, pp. 326-334.
- Villarreal Guerra, J.C., Khanam, Z., Ehsan, S., Stolkin, R. and McDonald-Maier, K., 2018. Weather Classification: A new multi-class dataset, data augmentation approach and comprehensive evaluations of Convolutional

- Neural Networks. In: *2018 NASA/ESA Conference on Adaptive Hardware and Systems, Adaptive Hardware and Systems*, 2018, pp. 305-310.
- Vogel, R.M. and Stedinger, J.R., 1987. Generalized storage-reliability-yield relationships. *Journal of Hydrology*, 89(3-4), pp. 303-327
- Vogel, R.M. and Stedinger, J.R., 1988. The value of stochastic streamflow models in overyear reservoir design applications. *Water Resources Research*, 24(9), pp. 1483-1490.
- Van Vuuren, D.P., Edmonds, J., Kainuma, M., Riahi, K., Thomson, A., Hibbard, K., Hurtt, G.C., Kram, T., Krey, V., Lamarque, J.F., Masui, T., Meinshausen, M., Nakicenovic, N., Smith, S.J. and Rose, S.K., 2011. The representative concentration pathways: An overview. *Climatic Change*, 109(1), p. 5.
- Wada, Y., Wisser, D., Eisner, S., Flörke, M., Gerten, D., Haddeland, I., Hanasaki, N., Masaki, Y., Portmann, F.T., Stacke, T., Tessler, Z. and Schewe, J., 2013. Multimodel projections and uncertainties of irrigation water demand under climate change. *Geophysical Research Letters*, 40(17), pp. 4626-4632.
- Wan Ismail, W.N. and Wan Zin @ Wan Ibrahim, W.Z., 2017. Estimation of rainfall and stream flow missing data for Terengganu, Malaysia by using interpolation technique methods. *Malaysian Journal of Fundamental and Applied Sciences*, 13(3), pp. 213-217.
- Wan, W., Guo, X., Lei, X., Jiang, Y. and Wang, H., 2018. A Novel Optimization Method for Multi-Reservoir Operation Policy Derivation in Complex Inter-Basin Water Transfer System. *Water Resources Management*, 32, pp. 31-51.
- Wang, C., Liang, J. and Hodges, K.I., 2017. Projections of tropical cyclones affecting Vietnam under climate change: downscaled HadGEM2-ES using PRECIS 2.1. *Quarterly Journal of the Royal Meteorological Society*, 143(705), pp. 1844-1859.
- Wang, H., Lei, X., Yan, D., Wang, X., Wu, S., Yin, Z. and Wan, W., 2018a. An Ecologically Oriented Operation Strategy for a Multi-Reservoir System: A Case Study of the Middle and Lower Han River Basin, China.

- Engineering*, 4(5), pp. 627-634.
- Wang, K.W., Chang, L.C. and Chang, F.J., 2011. Multi-tier interactive genetic algorithms for the optimization of long-term reservoir operation. *Advances in Water Resources*, 34(10), pp. 1343-1351.
- Wang, W., Lee, X., Xiao, W., Liu, S., Schultz, N., Wang, Y., Zhang, M. and Zhao, L., 2018b. Global lake evaporation accelerated by changes in surface energy allocation in a warmer climate. *Nature Geoscience*, 11(6), pp. 410-414.
- Wang, W.C., Chau, K.W., Cheng, C.T. and Qiu, L., 2009. A comparison of performance of several artificial intelligence methods for forecasting monthly discharge time series. *Journal of Hydrology*, 374(3-4), pp. 294-306.
- Wang, X. jun, Zhang, J. yun, Yang, Z. feng, Shahid, S., He, R. min, Xia, X. hui and Liu, H. wei, 2015. Historic water consumptions and future management strategies for Haihe River basin of Northern China. *Mitigation and Adaptation Strategies for Global Change*, 20(3), pp. 371-387.
- White, R.H. and Toumi, R., 2013. The limitations of bias correcting regional climate model inputs. *Geophysical Research Letters*, 40(12), pp. 2907-2912.
- Wilby, R.L., Dawson, C.W. and Barrow, E.M., 2002. SDSM - A decision support tool for the assessment of regional climate change impacts. *Environmental Modelling and Software*, 17(2), pp. 145-157.
- Wilby, R.L., Troni, J., Biot, Y., Tedd, L., Hewitson, B.C., Smith, D.M. and Sutton, R.T., 2009. A review of climate risk information for adaptation and development planning. *International Journal of Climatology*, 29(9), pp. 1193-1215.
- Wilby, R.L. and Wigley, T.M.L., 1997. Downscaling general circulation model output: A review of methods and limitations. *Progress in Physical Geography*, 21(4), pp. 530-548.
- Wu, X., Cheng, C., Lund, J.R., Niu, W. and Miao, S., 2018. Stochastic dynamic programming for hydropower reservoir operations with multiple local optima. *Journal of Hydrology*, 564, pp.712–722.

- Xiao-jun, W., Jian-yun, Z., Jian-hua, W., Rui-min, H., ElMahdi, A., Jin-hua, L., Xin-gong, W., King, D. and Shahid, S., 2014. Climate change and water resources management in Tuwei river basin of Northwest China. *Mitigation and Adaptation Strategies for Global Change*, 19(1), pp. 107-120.
- Xie, A., Liu, P., Guo, S., Zhang, X., Jiang, H. and Yang, G., 2018. Optimal Design of Seasonal Flood Limited Water Levels by Jointing Operation of the Reservoir and Floodplains. *Water Resources Management*, 32(1), pp. 179-193.
- Xu, B., Pang, R. and Zhou, Y., 2020. Verification of stochastic seismic analysis method and seismic performance evaluation based on multi-indices for high CFRDs. *Engineering Geology*, 264, p. 105412.
- Xu, B., Zhong, P. an, Lu, Q., Zhu, F., Huang, X., Ma, Y. and Fu, J., 2020. Multiobjective stochastic programming with recourses for real-time flood water conservation of a multireservoir system under uncertain forecasts. *Journal of Hydrology*, 590, p. 125513.
- Xu, C., Kohler, T.A., Lenton, T.M., Svenning, J.C. and Scheffer, M., 2020. Future of the human climate niche. *Proceedings of the National Academy of Sciences of the United States of America*, 117(21), pp. 11350-11355.
- Xu, C.Y. and Singh, V.P., 2001. Evaluation and generalization of temperature-based methods for calculating evaporation. *Hydrological Processes*, 15(2), pp. 305-319.
- Xu, R., Chen, N., Chen, Y. and Chen, Z., 2020. Downscaling and Projection of Multi-CMIP5 Precipitation Using Machine Learning Methods in the Upper Han River Basin. *Advances in Meteorology*, 2020, p.17.
- Xu, Z., Han, Y. and Yang, Z., 2019. Dynamical downscaling of regional climate: A review of methods and limitations. *Science China Earth Sciences*, 62, pp. 365-375.
- Xu, Z. and Yang, Z.L., 2012. An improved dynamical downscaling method with GCM bias corrections and its validation with 30 years of climate simulations. *Journal of Climate*, 25(18), pp. 6271-6286.
- Xu, Z. and Yang, Z.L., 2015. A new dynamical downscaling approach with GCM bias corrections and spectral nudging. *Journal of Geophysical*

Research, 120(8), pp. 3063-3084.

- Yaghoubi, B., Hosseini, S.A., Nazif, S. and Daghighi, A., 2020. Development of reservoir's optimum operation rules considering water quality issues and climatic change data analysis. *Sustainable Cities and Society*, 63, p. 102467.
- Yakowitz, S., 1982. Dynamic programming applications in water resources. *Water Resources Research*, 18(4), pp. 673-696.
- Yalew, S.G., van Vliet, M.T.H., Gernaat, D.E.H.J., Ludwig, F., Miara, A., Park, C., Byers, E., De Cian, E., Piontek, F., Iyer, G., Mouratiadou, I., Glynn, J., Hejazi, M., Dessens, O., Rochedo, P., Pietzcker, R., Schaeffer, R., Fujimori, S., Dasgupta, S., Mima, S., da Silva, S.R.S., Chaturvedi, V., Vautard, R. and van Vuuren, D.P., 2020. Impacts of climate change on energy systems in global and regional scenarios. *Nature Energy*, 5, pp. 794-802.
- Yan, D., Zhuang, K., Xu, B., Chen, D., Mei, R., Wu, C. and Wang, X., 2017. Excitation Current Analysis of a Hydropower Station Model Considering Complex Water Diversion Pipes. *Journal of Energy Engineering*.
- Yan, Z., Wang, S., Ma, D., Liu, B., Lin, H. and Li, S., 2019. Meteorological factors affecting pan evaporation in the Haihe River Basin, China. *Water (Switzerland)*, 11(2), pp.1–18.
- Yang, T., Asanjan, A.A., Welles, E., Gao, X., Sorooshian, S. and Liu, X., 2017. Developing reservoir monthly inflow forecasts using artificial intelligence and climate phenomenon information. *Water Resources Research*, 53(4), pp. 2786-2812.
- Yang, T., Gao, X., Sellars, S.L. and Sorooshian, S., 2015. Improving the multi-objective evolutionary optimization algorithm for hydropower reservoir operations in the California Oroville-Thermalito complex. *Environmental Modelling and Software*, 69, pp. 262-279.
- Yang, T., Gao, X., Sorooshian, S. and Li, X., 2016. Simulating California reservoir operation using the classification and regression-tree algorithm combined with a shuffled cross-validation scheme. *Water Resources Research*, 52(3), pp. 1626-1651.
- Yang, X.S. and Deb, S., 2009. Cuckoo search via Lévy flights. In: *2009 World*

Congress on Nature and Biologically Inspired Computing, Nature & Biologically Inspired Computing- Proceedings, pp. 210-214.

- Yaseen, Z.M., Allawi, M.F., Karami, H., Ehteram, M., Farzin, S., Ahmed, A.N., Koting, S.B., Mohd, N.S., Jaafar, W.Z.B., Afan, H.A. and El-Shafie, A., 2019. A hybrid bat–swarm algorithm for optimizing dam and reservoir operation. *Neural Computing and Applications*, 31(12), pp.8807–8821.
- Yazdi, J. and Moridi, A., 2018. Multi-Objective Differential Evolution for Design of Cascade Hydropower Reservoir Systems. *Water Resources Management*, 32(14), pp. 4779-4791.
- Yuan, W., Wang, X., Su, C., Cheng, C., Liu, Z. and Wu, Z., 2021. Stochastic optimization model for the short-term joint operation of photovoltaic power and hydropower plants based on chance-constrained programming. *Energy*, 222, p.119996.
- Zaman, M., Anjum, M.N., Usman, M., Ahmad, I., Saifullah, M., Yuan, S. and Liu, S., 2018. Enumerating the effects of climate change on water resources using GCM scenarios at the Xin’anjiang Watershed, China. *Water (Switzerland)*, 10, p. 1296.
- Zamani, R., Akhond-Ali, A.M., Ahmadianfar, I. and Elagib, N.A., 2017. Optimal Reservoir Operation under Climate Change Based on a Probabilistic Approach. *Journal of Hydrologic Engineering*, 22(10), p.05017019.
- Zeng, X., Hu, T., Cai, X., Zhou, Y. and Wang, X., 2019. Improved dynamic programming for parallel reservoir system operation optimization. *Advances in Water Resources*, 131, p.103373.
- Zhang, C., Li, Y., Chu, J., Fu, G., Tang, R. and Qi, W., 2017. Use of Many-Objective Visual Analytics to Analyze Water Supply Objective Trade-Offs with Water Transfer. *Journal of Water Resources Planning and Management*, 143(8), p. 05017006.
- Zhang, F., Wang, M. and Yang, M., 2021. Successful application of the Taguchi method to simulated soil erosion experiments at the slope scale under various conditions. *Catena*, 196, p. 104835.
- Zhang, L.E.I., Xu, Y., Meng, C., Li, X., Liu, H. and Wang, C., 2020. Comparison of statistical and dynamic downscaling techniques in generating high-

- resolution temperatures in China from CMIP5 GCMs. *Journal of Applied Meteorology and Climatology*, 59(2), pp. 207-235.
- Zhang, R., Zhou, J., Ouyang, S., Wang, X. and Zhang, H., 2013. Optimal operation of multi-reservoir system by multi-elite guide particle swarm optimization. *International Journal of Electrical Power and Energy Systems*, 48(1), pp. 58-68.
- Zhang, W., Liu, P., Wang, H., Lei, X. and Feng, M., 2017. Operating rules of irrigation reservoir under climate change and its application for the Dongwushi Reservoir in China. *Journal of Hydro-Environment Research*, 16, pp. 34-44.
- Zhang, Z., Qin, H., Yao, L., Liu, Y., Jiang, Z., Feng, Z. and Ouyang, S., 2020. Improved Multi-objective Moth-flame Optimization Algorithm based on R-domination for cascade reservoirs operation. *Journal of Hydrology*, 581, p.124431.
- Zhao, T., Wang, Q.J., Bennett, J.C., Robertson, D.E., Shao, Q. and Zhao, J., 2015. Quantifying predictive uncertainty of streamflow forecasts based on a Bayesian joint probability model. *Journal of Hydrology*, 528, pp. 329-340.
- Zhao, X., Zhang, W.H. and Wang, M.X., 2015. An Analysis and Comparison of Areal Precipitation Estimation. *Applied Mechanics and Materials*, 737, pp. 737-740.
- Zheng, F., Zecchin, A.C., Newman, J.P., Maier, H.R. and Dandy, G.C., 2017. An adaptive convergence-trajectory controlled ant colony optimization algorithm with application to water distribution system design problems. *IEEE Transactions on Evolutionary Computation*, 21(5), pp. 773-791.
- Zhou, Y., Ling, Y. and Luo, Q., 2018. Lévy flight trajectory-based whale optimization algorithm for engineering optimization. *Engineering Computations (Swansea, Wales)*, 35(7), pp. 2406-2428.
- Zubaidi, S.L., Ortega-Martorell, S., Al-Bugharbee, H., Olier, I., Hashim, K.S., Gharghan, S.K., Kot, P. and Al-Khaddar, R., 2020. Urban water demand prediction for a city that suffers from climate change and population growth: Gauteng province case study. *Water (Switzerland)*, 12(7), p. 1885.

LIST OF PUBLICATION

Lai, V., Huang, Y.F., Koo, C.H., Ahmed, A.N. and El-Shafie, A., 2021. Optimization of reservoir operation at Klang Gate Dam utilizing a whale optimization algorithm and a Lévy flight and distribution enhancement technique. *Engineering Applications of Computational Fluid Mechanics*, 15(1), pp.1682–1702. (Q1; IF: 8.39)

Lai, V., Huang, Y.F., Koo, C.H., Ahmed, A.N. and El-Shafie, A., 2022. A Review of Reservoir Operation Optimisations: from Traditional Models to Metaheuristic Algorithms. *Archives of Computational Methods in Engineering*, 29, pp. 3435- 3457. (Q1; IF: 7.302)

Lai, V., Huang, Y.F., Koo, C.H., Najah Ahmed, A. and El-Shafie, A., 2022. Conceptual Sim-Heuristic Optimization Algorithm to Evaluate the Climate Impact on Reservoir Operations. *Journal of Hydrology*, 614, p. 128530 (Q1; IF:6.708)

Lai, V., Huang, Y.F., Koo, C.H., Najah Ahmed, A., Sherif. M., and El-Shafie, A., 2023. Optimal water supply reservoir operation by leveraging the meta-heuristic Harris Hawks algorithms and opposite based learning technique. *Scientific Reports*, 13, p.6966 (Q1; IF:4.996)

Accepted:

1. “Application of the Whale Optimisation Algorithm (WOA) in Reservoir Optimisation Operation under Investigation of Climate Change Impact: A Case Study at Klang Gate Dam, Malaysia”, *7th Asia Conference on Environment and Sustainable Development (ACESD 2022)*, November 4-6, 2022, Kyoto, Japan. (SCOPUS database)